UNIVERSITY OF BOTSWANA

FACULTY OF SCIENCE

Department of Chemistry

INVESTIGATION OF INTERACTION, HYSTERESIS AND REACTIONS OF MIXED LANGMUIR MONOLAYERS OVER AIR/AQUEOUS INTERFACE

Ph.D. Thesis

BY

SIJI SUDHEESH

ID NO: 201108209

A PROJECT SUBMITTED IN PARTIAL FULFILLMENT OF THE REQUIREMENTS FOR DOCTOR OF PHILOSOPHY IN CHEMISTRY AT THE UNIVERSITY OF BOTSWANA

SEPTEMBER 2015

SUPERVISOR: PROFESSOR JAMIL AHMAD

Certification

The undersigned certify that they have read and hereby recommend for the acceptance by the Department of Chemistry, University of Botswana, a Thesis entitled **" INVESTIGATION OF INTERACTION, HYSTERESIS AND REACTIONS OF MIXED LANGMUIR MONOLAYERS OVER AIR/AQUEOUS INTERFACE "** as part of the work recommended in fulfillment of the requirements for a Ph.D. degree in chemistry at the University of Botswana.

…… ……

Prof. Jamil Ahmad

Project Supervisor Internal Examiner

Date: Date:

……

External Examiner

Date:

Declaration

"I hereby declare that this thesis submitted for the award of Doctor of Philosophy to the University of Botswana is my original work and has not been previously submitted to any other institution, except for the purpose of publication to the journals which have been listed in page IV. Any work quoted in here is indicated and acknowledged by means of a comprehensive list of references".

……

Siji Sudheesh

Date:

Acknowledgement

I would like to express my deepest gratitude to my supervisor Professor J. Ahmad for his tireless supervision, guidance, support and encouragement during this research work. I am grateful to Professor G.S. Singh for his helpful skills in the synthesis of the compounds and their NMR spectra interpretation. I thank the University Library interlibrary loan (ILL) department for their help in out-sourcing the journals. My appreciation goes to my research supervisory committee members Dr. M.S.T. Nadiye, Dr. F. Mbaiwa, and Dr. G. Kumar for their valuable suggestions and assistance during my project work. Let me take this opportunity to thank the post graduate students for their encouragement and also thank the technicians for their help. My special thanks go to my family for the encouragement and being an inspiration.

Publications

A part of the work presented here has been published in refereed journals as follows

1. Siji Sudheesh and Jamil Ahmad; Effect of Wilhelmy Plate Material on Hysteresis of Langmuir Film Isotherms, Asian Journal of Chemistry, 25 (7), (2013), 3535.

2. Siji Sudheesh, Jamil Ahmad, and Girija S. Singh; Hysteresis of Isotherms of Mixed Monolayers of N-Octadecyl-N'- Phenylthiourea and Stearic Acid at Air/Water Interface, ISRN Physical Chemistry, 2012, Article ID 835397.

3. Siji Sudheesh, Jamil Ahmad, and Girija S. Singh; Hysteresis of Mixed Monolayers of 2-[(Octadecylimino)methyl]phenol and Octadecylamine, Current Physical Chemistry, 4(3), (2014).

TABLE OF CONTENTS

List of Figures

List of Tables

List of Abbreviations

SA	Stearic acid
ODA	Octadecylamine
ODT	Octadecanethiol
OPT	*N*-octadecyl-*N'*-phenylthiourea
ODIMP	2-[(Octadecylimino)methyl]phenol
MODIMP	2-methoxy-6-[(octadecylimino)methyl]phenol

Abstract

Mixed Langmuir films of *N*-octadecyl-*N'*-phenylthiourea/stearic acid (OPT/SA), 2-[(octadecylimino)methyl]phenol/octadecylamine (ODIMP/ODA) and 2-methoxy-6-[(octadecylimino)methyl]phenol/stearic acid (MODIMP/SA) over air/water interface have been investigated for their pressure-area isotherms and the hysteresis behaviour of the isotherms. Likewise films of OPT over copper ions containing aqueous subphase were investigated. Calculations of the areas/molecules of films formed by spreading pre-mixed solutions of various ratios reveals that a 1:1 complex is formed between OPT and SA. When pre-mixed solutions of ODIMP and ODA are spread homogeneous monolayers result, but when the components are spread individually, the monolayers formed are non-homogeneous. For homogeneous MODIMP/SA film, the calculated excess areas exhibited negative deviation from the ideal values at all compositions for lower surface pressures. Gibbs free energies of mixing had been calculated and the most stable state of the mixed monolayer was found to be one having the mole fraction of SA between 0.5 and 0.6. The study of OPT over copper ions reveals that the interaction between thiourea and copper ions could be controlled by the addition of protons. The mechanism of this reaction is based on the intermolecular shift of two electrons from the thiolates to Cu (II) atoms to form the disulfides, and the corresponding reduction of the Cu^{2+} to Cu^{+} and the formation of Cu (I)-disulfide complexes.

CHAPTER 1
INTRODUCTION

1.1 Surfactants

It has long been recognized that many substances with the general formula $C_nH_{2n+1}X$ (amphiphiles), where X denotes a polar group, are characterized by their surface activity [1]. Amphiphiles contain two dissimilar parts, a polar head group which is attracted to water and a hydrophobic tail group [2]. When these substances are dissolved in an appropriate volatile organic solvent and placed on the free water surface, they spread and cover the entire surface [1]. The polar groups tend to confer water solubility, while the hydrophobic part prevents it; the balance between them helps the amphiphile to adopt a preferred orientation at the air/water interface, in such a way that the polar head group is immersed in the water and that the long hydrocarbon chain is pointing towards air. A one-molecule thin film is thus formed provided that the area of the surface is sufficient enough to accommodate all the molecules deposited on the surface. This monomolecular insoluble film on the surface of water is called a Langmuir monolayer (Figure 1.1.1) [3]. The monolayer forming abilities of the amphiphiles is dependent on the balance between the hydrophilic and the hydrophobic parts which are determined by the size of the hydrophobic tail group (the alkyl chain length) and the strength of the hydrophilic head group (its size, polarity, charge and hydration capacity). If the hydrocarbon chains are too short, and the polar group too strong, the material would simply “dissolve” in the subphase and could not form a stable monolayer and some of it will adsorb from the bulk solution to form Gibbs monolayer [4].

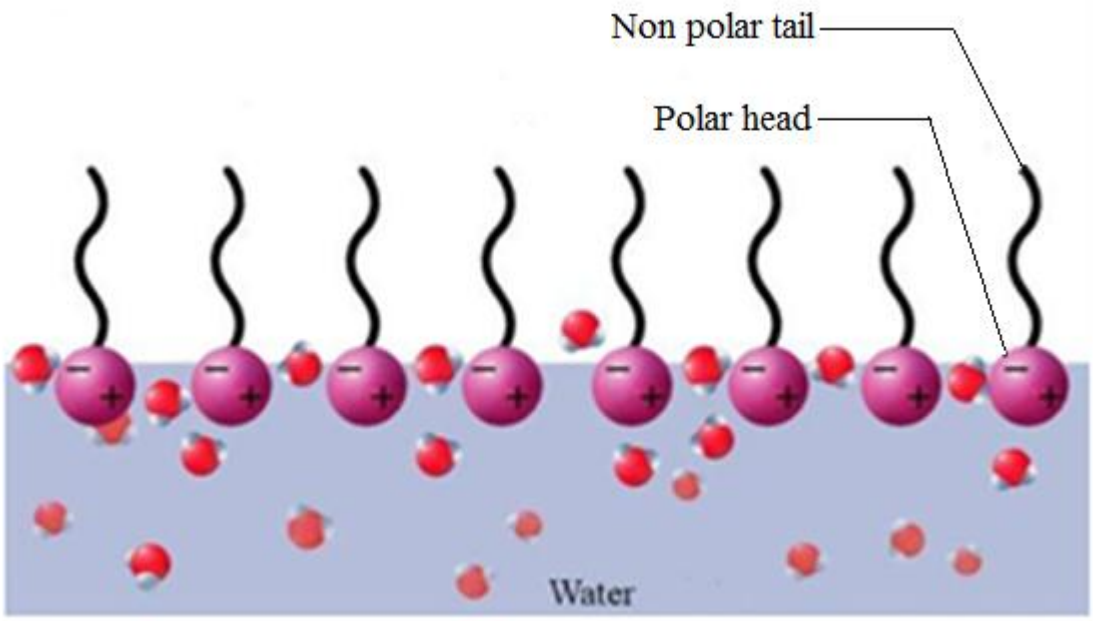

Figure 1.1.1: Schematic representation of a Langmuir monolayer: The spherical beads represent the head groups and the tails represent a chain of hydrocarbon molecules [3].

An amphiphile molecule containing more than 12 carbon atoms in its hydrocarbon chain is able to form a monolayer on air/aqueous interface. Conversely, if the hydrophobic part is dominant (chain length very long for instance) these amphiphiles tend to crystallize on the water surface and they do not form a monolayer at the interface. It is difficult to determine the optimal length for the hydrocarbon chain because the film-forming ability is also dependent on the polar part of the amphiphile, and for the spreading to occur that molecules of the organic substance must be attracted to water more than they can attract each other. Furthermore, the amphiphile has to be soluble in some organic solvent which is highly volatile and water insoluble (chloroform or hexane are commonly used). Mainly long chain fatty acids, phospholipids and alcohols are used for monolayer fabrication, of which octadecanoic acid (stearic acid) is the most common one. Properties of Langmuir monolayers are in general dependent upon the physicochemical nature of constituent molecules.

1.2 Historical background

Calming effect of oil spread on rough sea was observed in ancient times by sailors and was described by Plutarch, Aristotle and Plinius. In 1774, Benjamin Franklin made the observation more quantitative by remarking that a teaspoon of oil sufficed to calm a half-acre surface of a pond [1]. Then in 1890, Lord Rayleigh reported [5] that a 16 Å thick oleic acid film is enough to stop the erratic movements of camphor on a water surface. About this time, Fraulein Agnes Pockels, a German pioneer in surface chemistry, described a method for manipulating oil films on water, which laid the foundation for a generation of fruitful research [6]. Pockels confined the films by means of barriers and found little change in the surface tension of fatty acid films until they were confined to an area corresponding to about 20 $Å^2$ (Pockels point) per molecule.

This system was a precursor to the Langmuir trough. Within ten years, Rayleigh commented on Pockels point, that at this area (20 $Å^2$) the molecules of the surface material were just touching each other [5]. Devaux reported [7] that the films behaved sometimes as solids and sometimes as fluids. Hardy found [8] that oils that do not contain polar functional groups do not spread in the same way as the animal and vegetable oils, which have the polar ester groups. Finally, in 1917, Irving Langmuir [9] gave a great impetus to the study of monomolecular films by developing the technique used by Pockels. Langmuir confined the film with a rigid but adjustable barrier on one side and with a floating one on the other. The actual force on the barrier was then measured directly to give π, the film pressure. As had been observed by Pockels, he found that one could sweep a film off the surface quite cleanly by moving the sliding barrier, always keeping it in contact with the surface. As it was moved along, a fresh surface of clean water would form behind it. The floating barrier was connected to a knife-edge suspension by means of which the force on the barrier could be determined. The barriers were constructed of paper coated with paraffin so as not to be wet by the water. His experimental and theoretical concepts underlie our modern understanding of the behaviour of molecules in insoluble monolayers [10]. For this insightful and novel work, Langmuir received a Nobel Prize in 1933.

Many experimental studies have revealed that the orientation of the amphiphilic surfactant molecules at the surface of liquid is significantly different from the bulk solution where most molecules are randomly and isotropically distributed [11; 12; 13]. Several techniques are employed to study monolayer films on an aqueous surface, such as determination of π-A isotherms, grazing incidence X-ray diffraction (GIXRD), Brewster angle microscopy (BAM), Fluorescence imaging microscopy (FIM), Ultra Violet-visible (UV-vis) spectroscopy and Fourier

Transform Infrared (FT-IR) spectroscopy [14; 15; 16]. Π-A isotherms give the information about molecular area, monolayer phases, collapse behaviour, monolayer stability, interaction of the monolayer with subphase and miscibility of the mixed monolayers. Grazing incidence X-ray diffraction provides information about microscopic structure (lattice parameters and molecular tilt) of the phases in a monolayer. A Brewster angle microscope (BAM) enables the visualization of Langmuir monolayers. This also provides morphological features, domain formation, aggregation, monolayer phases, phase-coexistence and collapse behaviour. The technique of fluorescence microscopy enables imaging of domain formation, phases and their coexistence. UV-vis spectroscopy is used to detect the presence of chromophores, aggregation and inter-molecular interaction in Langmuir films. FT-IR technique reveals the presence of functional groups, orientation of head/tail groups and H-bonding in monolayers. Among these π-A isotherm is the basic and most widely used technique to characterize Langmuir monolayers. It is a plot of surface pressure (a measure of the decrease in surface tension), as a function of the area available per molecule on the surface. In a liquid, the molecules have a certain degree of attraction to each other, called cohesion. In water, hydrogen bonding forces tend to set up well ordered networks. In bulk, a molecule is surrounded on all sides by other liquid molecules, balancing the forces experience by it. On the other hand, a molecule at the interface does not have symmetric surroundings so it experiences unsymmetrical forces exerted on it by other molecules. This difference in the cohesive forces is responsible for surface tension. The surface tension of water is 72.8 mN/m at 20 °C and atmospheric pressure. This is an exceptionally high value compared to most other liquids and consequently makes water a suitable subphase for monolayer studies. Air/water interface has been found to be ideal for study of monolayers of fatty acids [17], fatty amines [18] and proteins [19].

1.3 Surface tension

The formation of an amphiphile monolayer is a result of the peculiar thermodynamic properties of the air/liquid interface. The surface of a liquid has excess free energy due to the difference in environment between the surface molecules and those in the bulk liquid. Due to the difference in the cohesive forces among water molecules, a net attractive force directed towards the bulk, and an air/water interface will spontaneously tend to have a minimum area. Extending a liquid surface requires work to overcome this attractive force and consequently produces an increase in the free energy of the system. For a liquid, the free energy per unit area is equivalent to force per unit length and is called surface tension (γ), as in Eq. (1):

$$\gamma = G^s/A \qquad \text{Equation 1}$$

Where, G^s refers to the surface excess free energy.

Surface tension is usually expressed in mN/m, since energy is usually expressed in J = N.m and surface area in m^2. In other words, it can also be defined as force per unit length in terms of the cohesive energy present at an interface. It is also important to note that surface tension is dependent on temperature. The general trend is that surface tension decreases with increase of temperature.

1.4 Surface pressure

The presence of a monolayer on an aqueous surface will lower the surface tension of the liquid. The amphiphile molecules on the surface disrupt the forces between the adjacent water

molecules and create an interaction between the hydrophilic polar group of the amphiphile and the water surface molecules. The resulting effect is the reduction of the surface tension. When the area of surface available to the interfacial film is large and the amount of surfactants sufficiently low to limit the interactions between adjacent water molecules, the monolayer has a minimal effect on the liquid surface tension. If the surface area available to the monolayer is reduced by a compression system through the use of mobile barriers, the intermolecular distance decreases and the surface tension is lowered. This reduction in the surface tension can be thought of as a 2-dimensional force exerted on any adjoining water surface of pure water. The force exerted by the film per unit length, corresponding to a two-dimensional analogue of a pressure, is called surface pressure (π). This being equal to the reduction of the pure liquid surface tension by the presence of the interfacial film, and can be represented by the Eq (2):

$$\pi = \gamma^0 - \gamma \qquad \text{Equation 2}$$

Here, γ^0 is the surface tension of the pure liquid and γ is the surface tension of the film-covered surface.

1.5 Surface pressure measurement - Theoretical background

Two different approaches can be used to measure the surface pressure in the interfacial film during the monolayer compression: the Langmuir balance method and the Wilhelmy plate method. In the Langmuir balance method, two dimensional force exerted along the surface is measured directly while in the second surface tension is sensed by a Wilhelmy plate. In this study the Wilhelmy plate method is used. It is a well-established and widely used technique to characterize the physical state of an adsorbed Langmuir monolayer. The basic instrumentation consists of a Langmuir trough made of a hydrophobic material like PTFE (Teflon), two movable

barriers and a Wilhelmy plate attached to a very sensitive electro-balance. The trough is filled to the brim with subphase. The most commonly used subphase is ultrapure water, because of its high surface tension value.

In a typical experiment, a known amount of solution of a film-forming compound is spread on the surface of water between two surface barriers using a micro syringe. The solvent is allowed to evaporate and one of the barriers is moved towards the other, decreasing the area available to the monolayer. The surface tension is measured using a tensiometer with the Wilhelmy plate partially immersed in the aqueous phase (Figure 1.5.1). The barrier position and hence the available area and the surface tensions are recorded. The process is continued till the monolayer collapses.

The measurement is first performed on a clean surface and subsequently on the same surface covered by the monolayer. The variation due to the alteration in the surface tension is then converted into surface pressure with the help of the dimensions of the plate. Indeed, the forces acting on the plate consists of downward forces, such as gravity and surface tension, and upward force, such as buoyancy due to the displacement of water. For a rectangular plate of dimensions length (l), width (w), and thickness (t), of material density (ρ_p), immersed to a depth (h) in a liquid of density (ρ_L), the net downward force, F_0, in the absence of a monolayer, is given by Eq. (3):

$$F_0 = \rho_p glwt - \rho_l ghwt + 2\gamma^0(t+w)\cos\theta_0 \qquad \text{Equation 3}$$

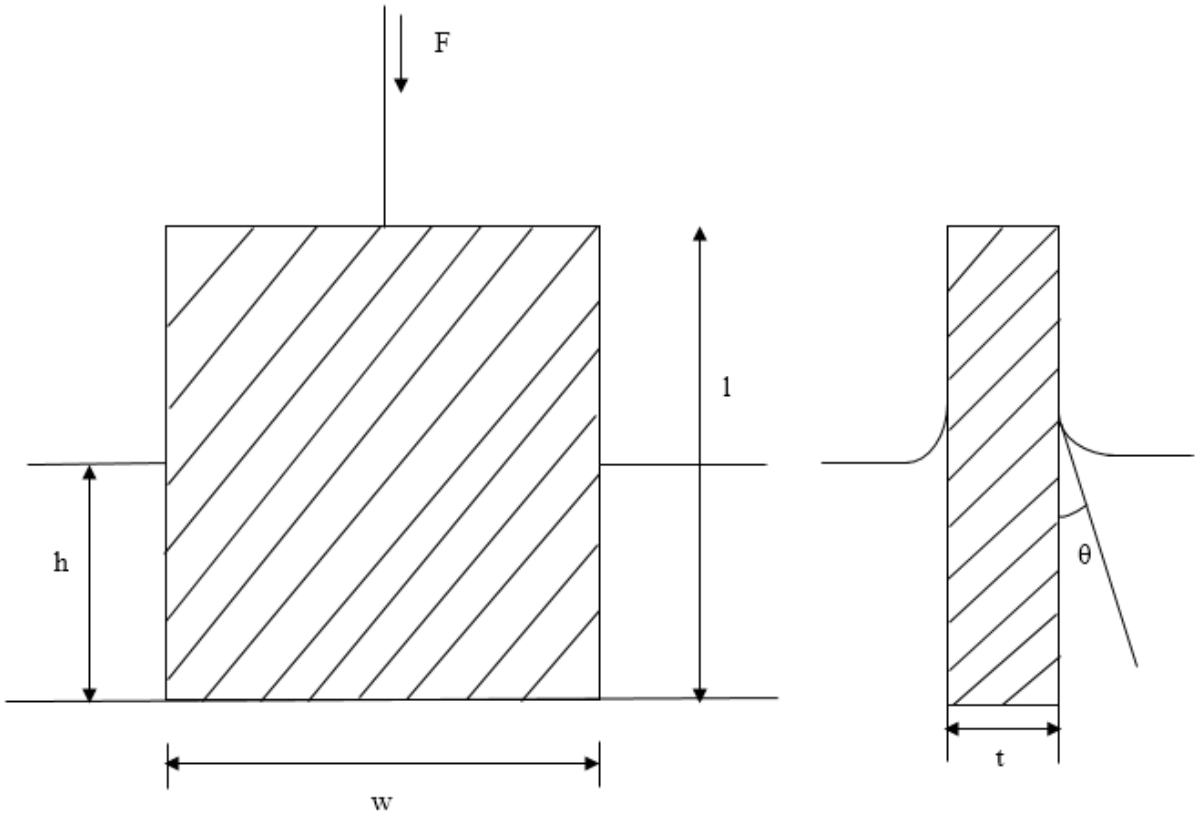

Figure 1.5.1: A Wilhelmy plate partially immersed in water.

Where ρ_p and ρ_l are the densities of the plate and the liquid respectively. γ^0 is the liquid surface tension, θ_0 is the contact angle of the liquid on the solid plate and *g* is the acceleration due to gravity.

With a monolayer-covered surface, the expression of the force, F_m, exerted on the plate is described by Eq. (4):

$$F_m = \rho_p glwt - \rho_l ghwt + 2\gamma\,(t+w)\cos\theta_m \qquad \text{Equation 4}$$

Here, θ_m is the contact angle of the liquid covered by the monolayer on the solid plate.

The measurement of the change in the force exerted in the presence of the monolayer on a stationary plate (h maintained constant) is related to the change in surface tension by Eq. (5):

$$\Delta F = F_m - F_0 = 2(t+w)(\gamma\cos\theta_m - \gamma^0\cos\theta_0) \qquad \text{Equation 5}$$

If the plate is completely wetted by the liquid, the contact angles equal zero, and if it is thin enough so that $t << w$, then the change in force can be expressed as in Eq. (6):

$$\Delta F = 2(\gamma^0 - \gamma)\, w = 2\pi w \qquad \text{Equation 6}$$

During an experiment, w is constant, so the force measured is proportional to the surface pressure and through a calibration procedure its value can be changed to surface pressure. In case the contact angle, θ, has a value other than zero, the measured force will not give the correct value of the surface pressure.

The formation of a monolayer at the air/water interface is usually monitored by recording the surface pressure (π) – area (A) isotherm diagram.

1.6 Surface pressure (π)-area (A) isotherm

The surface pressure – Area isotherm is a plot of the surface pressure as a function of the area available per molecule on the aqueous subphase surface. This isotherm is the most common indicator of the monolayer formation and monolayer properties of an amphiphilic material. The isotherm is measured by continuously compressing the monolayer while monitoring the surface pressure.

As the film is compressed by reducing the area available to it, the molecules self-organize and the monolayer undergoes several phase transformations analogous to three-dimensional gaseous, liquid, and solid states to finally form a perfectly ordered floating monolayer at the liquid surface. During this process, the hydrophilic and hydrophobic ends of the molecule ensure that the individual molecules are aligned in the same way. A typical surface pressure-area (π–A) isotherm is obtained by recording the surface pressure as the motorized barrier is moved to decrease the area available to the monolayer.

Figure 1.6.1 [20] depicts a schematic π-A isotherm classically recorded for stearic acid (lipid with one alkyl chain, left) and phospholipid (natural membrane lipid presenting two alkyl chains, right). It must be stressed here that the shape of the isotherm greatly depends on temperature, hydrocarbon chain length and also on the presence of unsaturated acyl chains, which results in a disruption of the packing of the chains. Generally π-A isotherms provide information on the monolayer stability at the air/water interface, the reorientation of the molecules in the two-dimensional system, and the existence of phase transitions and conformational transformations [21].

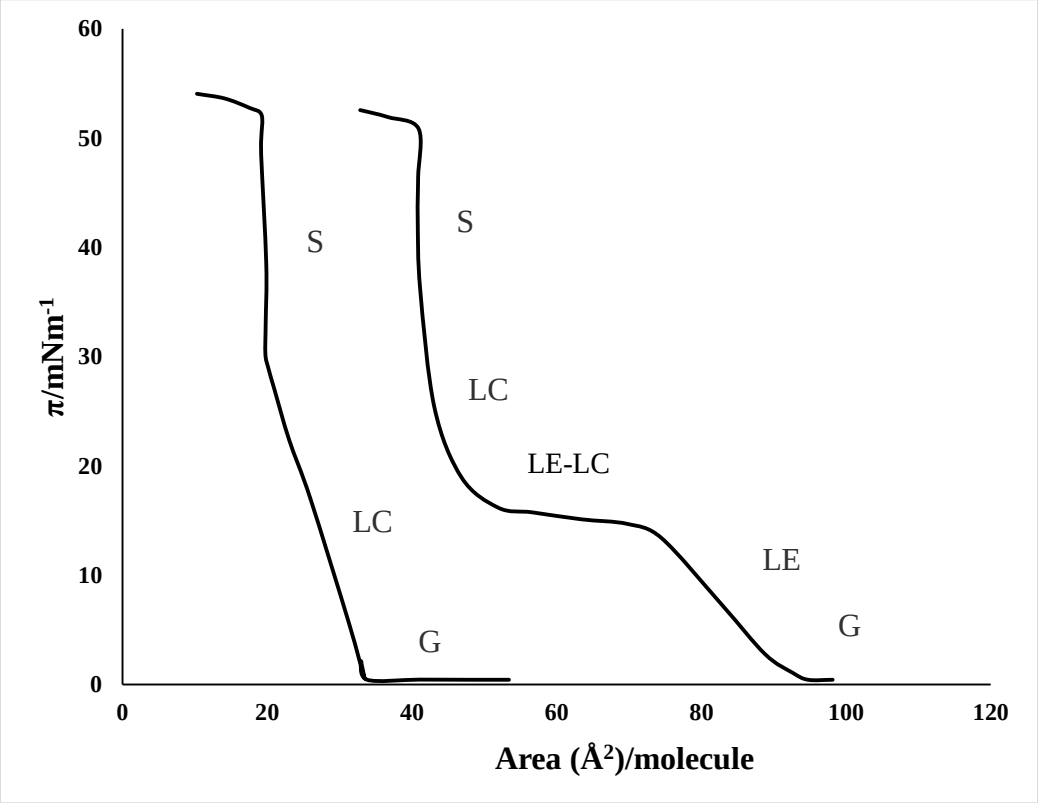

Figure 1.6.1: Schematic surface pressure-area isotherms of fatty acids (left) and phospholipids (right) [20].

1.7 Monolayer states

Henri Devaux [10], shortly after 1900, pointed out that molecules in monolayers could exist in different states, more or less analogous to three-dimensional liquids, solids, or gases. Although a large variety of mesophases have been found to date, the generally accepted phase diagram of two dimensional (2D) monolayers consists of four phases (Figure 1.6.1) [22]. These are gaseous (G), liquid expanded (LE), liquid condensed (LC), and solid (S) phases. The phase transitions G–LC, G–LE, and LE–LC all are of first order [23; 24]. The G–LE phase transition occurs at very low surface pressure, whereas the LE–LC phase transition takes place at relatively high surface pressure.

1.7.1 Gaseous phase

In the 'gaseous' state, the molecules are far apart and are believed not to interact with each other. The free energy of the aqueous subphase and therefore the surface tension remain unchanged. The film obeys the equation of state of a more or less perfect two-dimensional gas.

1.7.2 Liquid phase

The film is coherent in this state and some degree of cooperative interaction is present. It appears to be fluid and its π-A plot extrapolates to zero π at areas larger (up to several times larger) than that corresponding to a molecular cross section so that some looseness in the structure is indicated. The two indistinguishable types of liquid phases are explained below.

1.7.2.1 Liquid expanded phase

In the liquid expanded phase, the monolayer becomes coherent, but the molecules still possess some degrees of freedom. The area per molecule varies considerably with the surface pressure and no relation between the observed molecular area and the dimensions of the constituent molecules is apparent: the area per molecule is larger than the area associated with the cross-section of cylindrical alkyl chains (≈0.19 nm^2 per unit). Under further compression, a second first-order thermodynamic transition from the liquid expanded phase to the condensed states can occur in the monolayer and is characterized by a second constant pressure region in the isotherm which occurs at area per molecule around 0.6 to 0.8 nm^2/molecule.

1.7.2.2 Liquid condensed phase

In the condensed phases, the monolayer presents a strong lateral cohesion and is relatively closely packed. The hydrocarbon chains are more uniformly oriented in comparison with the liquid expanded state. The area per molecule is approaching that of the molecular cross-section (≈ 0.2 $nm^2/molecule^{-1}$ for fatty acids and ≈ 0.4 – 0.5 $nm^2/molecule^{-1}$ for phospho- and glycolipid molecules), thus confirming the interpretation of the condensed monolayers as a two-dimensional solid.

1.7.3 Solid phase

In solid phase, molecules are highly ordered and packed as tightly together as possible. The limiting area per molecule permits no free movement within the dense, rigid film.

Finally, if compression is further applied to the monolayer, the phenomenon of collapse occurs at smaller surface areas. It is due to mechanical instability at very high surface pressures and molecules are forced out of the interfacial film. The monolayer loses its integrity. Molecular layers are riding on top of each other and disordered multilayers are being formed (Figure 1.6.1). The onset of collapse depends on many factors including the rate at which the monolayer is being compressed.

As seen from Figure 1.6.1, the isotherm of stearic acid (left) consists of three regions, gas (region G) liquid (region LC) and solid (region S). For fatty acid monolayers, the transition between the different condensed phases are characterized by a decrease of tilt angle of the alkyl chains from the normal to the interface, the chain axes being vertically oriented at the highest surface pressures. The isotherm for the phospholipid (right) shows an additional liquid state (LE) and an almost horizontal transition phase (liquid expanded-liquid condensed, region LE-LC) between the two different liquid phases. A first order transition from the gas phase to the liquid expanded phase is shown by a change in slope of the π-A isotherm. This transition is very common for phospholipids, while in the isotherm of the stearic acid the liquid expanded state does not exist; rather a direct transition from the gas to the condensed phase takes place. This is because in fatty acids with a long hydrocarbon chain, van der Waals forces between the hydrocarbon chains are largely responsible for the phase transitions, without much influence from the hydrophilic head group. For the phospholipid molecules, which contain two hydrocarbon chains per molecule, the size of the hydrophilic headgroup influences the hydrocarbon chain packing, and consequently, the molecular aggregation state in the condensed monolayer. In generally, because of their polarity, size, shape, interaction with water and/or the neighbouring headgroups, many polar groups strongly influence the arrangement of the hydrocarbon chains and hence the

characteristics of the π-A isotherm. The position of the LE-LC phase is very temperature dependent. As the temperature is increased the surface pressure value at which the horizontal transition phase occurs will increase and vice versa. This is because reducing the temperature or lengthening the chain both enhance the intermolecular (chain–chain) interactions, tending to make the film more coherent and ordered (extension of the LC phase with a clear fading of the LE–LC transition). Hence, an increase (or a reduction) in the saturated chain length can, to some extent, be traded for a reduction (or an increase) in temperature [25; 26].

1.7.4 Mixed monolayers

Monolayers containing more than one chemical compound are of considerable interest because of their vast range of properties and applications compared to a pure component. The interactions between the components in a mixed film can be studied from the point of view of miscibility and stability, based on an analysis of π-A isotherms. By comparing the π-A isotherms of mixed and single-component monolayers, one is able to assess the miscibility and interactions between monolayer components. Another approach is the study of the thermodynamic behaviour of a mixed monolayer.

In the miscibility treatment of mixed monolayers, the surface phase is considered to be a mixture of two film-forming components and is based on simple additivity relations. According to Costin and Barnes [27], when a mixed monolayer shows properties that do not depend linearly on the monolayer composition, and a maximum or minimum occurs in its isotherm, it is said to be non-ideal. This behaviour is caused by significant molecular interactions between the components of the mixed film.

The miscibility of a mixed monolayer can be examined by quantitative analysis of the excess area (A_{ex}) of the mixed monolayer at the air/water interface. The excess area can be obtained by comparing the average area per molecule of a mixed monolayer consisting of components 1 and 2 (A_{12}) with that of an ideal mixed monolayer (A_{id}) [Eq. (7)]:

$$A_{ex} = A_{12} - A_{id} = A_{12} - (X_1A_1 + X_2A_2) \quad \text{Equation 7}$$

where X_1 and X_2 are the mole fractions of components 1 and 2, respectively, in the mixed monolayer and A_1 and A_2 are the respective areas per molecule of the pure monolayers at the same surface pressure. If the mixture is ideal or when the components in the mixed monolayer are immiscible, the excess area will be zero and A_{12} will be linear in X_1 and deviations from these conditions indicate miscibility or non-ideality.

Similarly, deviations from ideality can also be tested based on the following additivity relation [1] which is analogous to the Raoult's law for bulk mixtures [Eq. (8)]:

$$\pi_{12} = \pi_1X_1 + \pi_2X_2 \quad \text{Equation 8}$$

wherein π_{12} is the surface pressure of mixed monolayer and $\pi_1(\pi_2)$ is the surface pressure of a single component monolayer, all measured at the same molecular area, A. The deviation from the linearity of the function $\pi_{12} = f(X_i)$ indicates the existence of interactions while the linearity proves either an ideal 2-dimensional mixture or complete immiscibility.

A relationship between the value of collapse pressure and the molecular interactions has been suggested. The enhanced π^c (collapse pressure) in the mixed film indicates the existence of stronger interaction in comparison to an ideal 2-D mixture. Several authors used this method to indicate excess interactions in mixed monolayers [28; 29].

Another method for examining the existence of molecular interaction is based on an analysis of the stability of surface pressure. It has been suggested by Crisp [30] that a mixed film of completely miscible components exhibits enhanced surface pressure stability i.e., the mixed film showed a drift in surface pressure with time under constant area when a monolayer is compressed to a given value of surface pressure which is higher than its equilibrium spreading pressure but lower than the collapse pressure [31].

1.7.4.1 Thermodynamics of mixed monolayers

Quantitatively, molecular interactions are expressed as an excess of some thermodynamic functions, e.g. entropy, enthalpy, free energy or in terms of surface activity coefficients. Among these, free energy of mixing, (ΔG_{mix}), is commonly used because of the convenience of measurement. To calculate other excess thermodynamic functions, as excess entropy and excess enthalpy, temperature dependence of π-A isotherms are needed.

The excess of free energy of mixing, ΔG_{exc}, can be treated as an indication of interactions and of the stability of the mixed monolayer. The value of ΔG_{exc} can be obtained directly from the surface pressure-area isotherms using the following equation [Eq. (9)]:

$$\Delta G_{exc} = \int_0^{\pi} [A_{12} - (X_1 A_1 + X_2 A_2)] d\pi \qquad \text{Equation 9}$$

The negative sign of ΔG_{exc} is considered as a criterion of monolayer's stability while a positive value can suggest phase separation in the monolayer [32]. The total free energy of mixing, ΔG_{mix}, which can be determined by Eq. (10):

$$\Delta G_{mix} = \Delta G_{exc} + \Delta G_{id} \qquad \text{Equation 10}$$

Where ΔG_{id} is the ideal free energy of mixing.

$$\Delta G_{id} = RT (X_1 \ln X_1 + X_2 \ln X_2) \quad \text{Equation 11}$$

where R is the gas constant and T is the absolute temperature.

The negative value of the total energy of mixing, ΔG_{mix}, proves that the 2-dimensional mixed state is thermodynamically more stable than the corresponding unmixed state [33].

1.8 Detailed study of monolayers

Among the amphiphiles commonly studied are octadecanoic acid, octadecylamine, octadecanamide, octadecylurea, arachidic acid, palmitic acid, myristic acid and octadecanethiol [1]. However, in recent times a large number of semi-amphiphilic and non-amphiphilic molecules, with or without derivatisation with long alkyl chains, have also been employed, including polymers [34; 35; 36] C_{60} derivatives [37; 38; 39] organometallic compounds mechanically-threaded pseudorotaxanes [40; 41; 42], amphiphilic dendrimers [43; 44] and sheet-shaped multialkyne amphiphiles [44].

The study of octadecanoic acid or stearic acid (SA) monolayer has been known since the eighteen century and has been the subject of scientific research for over 100 years [45]. Langmuir [9] proposed that the hydrophilic group such as carboxylic head group in SA is immersed in the water surface while the alkyl tails remain above the surface. However, at that time it was difficult to characterize and directly observe the surface because of its ultra-thickness. Recently, some studies [28; 46] have reported direct observation of monolayers. Munden and coworkers [47] studied the influence of compression rate on SA monolayer and the effect of compression-expansion cycles on the surface area of stearic acid. The surface pressure-area isotherm of stearic acid has also been theoretically studied by Okamura and coworkers [48]. In another study, Moller and coworkers [49] investigated the structure and dynamics of a

Langmuir-Blodgett (LB) film of stearic acid, physisorbed on graphite. A Langmuir-Blodgett film is formed by transferring a monolayer to a glass slide by dipping in and removing the slide from the water over which the monolayer is spread [10]. The model predicts that the molecules of this system are normal to the surface at head group areas below 21 $Å^2$, but tilted away from the normal at head group areas above 21 $Å^2$, and that this change occurs over a very small range in head group area. The formation and stability of SA film were investigated on Artificial Sea Water (ASW) [50], which is a solution of slats that simulates sea water. The composition of the subphase solution was varied via dilution (1, 10 and 100 times) and adjustment of the pH (3, 7, and 10). It was found that SA monolayers can lose stability on these aqueous subphases in three ways, via dissolution into the sub-phase, via 3-dimensional (3D) solid formation at the air/water interface and via fracture of the monolayer. Formation of 3D solid phase occurs mainly under acidic conditions (pH 3) where the SA molecules are uncharged. Dissolution can occur under basic conditions (pH 10), where it can be suppressed by increasing the salt concentration. Fracture (collapse) ultimately occurs upon continued compression of the monolayer. The required surface pressure generally increases with pH, while the fracture mechanism also changes, from a constant area collapse (a sudden drop of surface pressure at a fixed specific molecular area after collapse of the monolayer) at pH 3 to a predominantly constant pressure collapse (decrease of area/molecule at constant surface pressure after collapse of the monolayer) at pH 10. Increasing the salt concentration has strong effects at pH 7, where it suppresses formation of 3D solid phase. This mechanism is of relevance to various fields in science and technology (biology, food, oil recovery). The conformation and orientation of the carboxylic group of fatty acids, heptadecanoic acid (C_{17}), nonadecanoic acid (C_{19}) with octadecanoic acid (C_{18}), in a Langmuir monolayer film on water was investigated [51]. It has been found that they

are influenced by three driving forces, hydration of the polar group, chain length, and film compression. In C_{19} Langmuir films, the long chain length plays a dominant role, and the influence of the film compression is negligible. In C_{17} Langmuir films, the hydration is the key, and the film compression is not so important. C_{18} has a unique property that it is in the middle between C_{17} and C_{19}. On the other hand, in C_{18} Langmuir films, both the chain length and the film compression concertedly influence the Langmuir film property.

There are many publications that deal with octadecylamine [52; 53; 54; 55], one of the simplest monolayer forming materials. Its isotherms (Handbook of Monolayers) [56], are generally featureless, although, under conditions of different temperature or pH, broad features may be seen [55]. The normally accepted isotherm shows a very low, not easily detectable surface pressure at larger areas, followed, upon film compression, by a very sharp continuous increase in film pressure that ends in monolayer breakdown [56]. Yuh-Lang Lee has investigated the behaviour of octadecylamine (ODA) monolayers on various subphases and reported that the ODA monolayer is especially stable over alkaline solutions [57]. Albrecht and coworkers [18] found that ODA shows a transition that is very similar to the liquid-condensed to solid transition of fatty acids [58]. However, this transition pressure is low, approaches zero pressure with decrease of temperature and disappears below about 10 °C.

Thiol head group (–SH) containing amphiphiles form useful systems to study because of the importance of the thiol-disulphide reaction in biological systems [59]. But thiol group cannot be classified as a typical polar head group especially because it cannot form strong hydrogen bonds with water molecules. However, many molecules of this non-typical amphiphilic structure, including octadecanethiol, the longest commercially available thiol, have been reported to form monolayers [60; 61]. Itaya and co-authors [62] reported that the Langmuir monolayers of

octadecanethiol on pure water were quite unstable, however, on the diluted solution of barium chloride their film stability increased. Bilewicz and Majda [63] investigated mixed monolayers of octadecanethiol and stearic acid, showing that the addition of the latter profoundly increases the stability of thiol monolayers and the quality of the LB-transferred multilayers. Ahmad and Silavwe studied the behaviour of octadecanethiol monolayer over silver nitrate solution and compared with that over pure water subphase [64]. The two isotherms showed condensed behaviour at high surface pressures, while at low surface pressure, the monolayer over silver nitrate solution behaved as an expanded film. This has been interpreted as the complex formation of octadecanethiol with Ag^+ ions at low surface pressure and the squeezing out of the silver part of the complex at high surface pressure. Zhao and coworkers [65] investigated the interactions between monolayers of octadecanethiol and silver cations dissolved in the aqueous subphase, whereas Gupta and coworkers [66] reported the formation of stable octadecanethiol monolayers on ultrapure water subphase of resistivity greater than 18 MΩ cm and applied optical methods, such as Brewster Angle Microscopy (BAM) and Atomic Force Microscopy for a deeper characterization of the Langmuir monolayers and LB-transferred layers, respectively.

1.8.1 Langmuir monolayers of Schiff bases

Schiff base derivatives are important organic compounds and have many applications in various fields [67; 68; 69; 70]. A Schiff base is a compound with a C-N double bond, with N connected to an aryl or alkyl group. In recent years a number of studies on Schiff bases and their derivatives as amphiphiles have been reported for their film forming and interesting optical and electrical properties [71; 72; 73]. So far, the LB films of amphiphilic Schiff base compounds, especially for those with salicylaldehyde, have been investigated and their interesting features

revealed [74; 75; 76]. Schiff bases are well known metal ion chelators, so the main focus has been on coordination of Schiff bases with metal ions, and some organized molecular films of these derivatives have been investigated. For example, Nagel and coworkers [77] have investigated copper complexes of Schiff base compounds. Liang and co-workers have investigated the organization of Schiff base amphiphiles by spectral characterization [78; 79]. In another paper, the fabrication of the ultrathin film from the carbazole-containing Schiff base and its acidichromism is reported [80]. Jiao and coworkers have investigated [81; 82] several series of Schiff base derivatives at the air/water interface. They have found that bolaform Schiff bases, which have two hydrophilic heads linked by one or several hydrophobic chains could form coordinated complex films which showed some novel features such as molecular recognition and headgroup effect in interfacial organized films. In another paper [71] Jiao and coworkers explained the *in situ* coordination of trigonal Schiff base amphiphiles, having symmetric aromatic cores and different substituted headgroups with metal ions subphases of various pH values . They also reported the effect of substituted headgroups such as phenyl, naphthyl [83], ylidene, and anthryl moieties, in the isotherms and their supramolecular assemblies at the air/water interface [84]. Jiao and Liu also reported that the single chain Schiff base, 2-hydroxybenzaldehyde-octadecylamine (HBOA) and the bolaform Schiff base, *N,N'*-bis(salicylidene)-1,10-decanediamine (BSC10), can be spread on water surface to form stable monolayer and multilayer films respectively at air/water interface [85]. When they were spread on the subphase containing barbituric acid, *in situ* molecular recognition through the hydrogen bond occurred. As a result, a 2:1 complex was formed for the single chain Schiff base with barbituric acid, while a 1:2 complex was formed for the bolaamphiphilic Schiff base through hydrogen bonding. Besides these, the hydrogen bond formation of a trigonal Schiff base from

2,4-dihydroxybenzaldehyde with barbituric acid at air/water interface was also reported [86]. Dhathathreyan and coworkers have reported a molecule, octadecylaminodihydroxysalicyl aldehyde, with a cross sectional mismatch between the headgroup and the long alkyl chain that is capable of forming both stable monolayers at air/water interface as well as LB films. The results indicated that, to accommodate the cross-sectional mismatch between the tail and the headgroup regions, the chains become tilted, allowing the film to organize in a stable arrangement [74]. Hemakanthi and coworkers have reported the stable monolayer formation of *O*-vaniline Schiff base at the air/water interface and on a subphase containing Cu^{2+}, Ni^{2+}, and Zn^{2+} ions [87]. Surface pressure-area isotherm showed the formation of bilayer aggregates of *O*-vaniline Schiff base on water subphase. These aggregates are stable and kinetics of dissociation appears to be slow on the timescale of expansion of the film. Π-A isotherms show that the complexes of Cu^{2+}, Ni^{2+}, Zn^{2+} with *O*-Vanilline Schiff base are stable at air/solution interface. They also investigated the complexation of 2,4 dihydroxy hexadecyl benzilideneamine (HDBA) and 2,4 dihydroxy benzilidene- 4(hexadecylamino) benzylamine (HDBBA) ligands with metal ions Mn^{2+}, Cu^{2+} and Zn^{2+} at the air/water interface [88]. They found that the faster rate of formation of Cu^{2+} complex in the case of HDBA indicates the specificity of binding of Cu^{2+} ion to its monolayer. Lakshmanan and coworkers studied [89] the influence of nitro group on packing and phase transitions in Langmuir monolayers of ortho, meta and para substituted *N*-benzylidene Schiff base amphiphiles at air/water interface as a function of temperature. The results showed significant effects of intramolecular hydrogen bonds on surface and interfacial properties of the compounds. The ortho derivative shows better order than the meta or para nitro substituted compounds. In the ortho derivative the intramolecular hydrogen bonding seems to compete with

intermolecular hydrogen bonding leading to a lesser hydration-induced repulsive interactions between the head groups thereby inducing better packing.

Recently the materials used to form organized molecular films at the air/water interface have also been expanded to some nontraditional amphiphiles of Schiff bases without long alkyl chains. Cai and coworkers have reported the monolayer formation of benzimidazole-containing Schiff bases by coordination with the Ag(I) ions [90]. Guo and Liu have reported that 1-benzthiazolyliminomethyl-2-naphthol (TSN) and 1-(6'-chlorobenzthiazolyliminomethyl)-2-naphthol (ClTSN) could not form true Langmuir monolayers at air/water interface, but they can be spread as multilayer films [91]. In another report [72] they have showed that though the benzothiazole-derived Schiff bases themselves could not form films, the *in situ* coordination between the Schiff bases and metal ions such as Ag (I) and Cu (II) could lead to the film formation.

1.8.2 Mixed monolayers

The behaviour of mixtures of soluble and insoluble surfactants at air/water interface is particularly interesting. Different spreading techniques such as co-spreading, separated spreading and incorporation from the subphase have been investigated by several authors [28; 92]. In the co-spreading method, stock solutions of the separate components are premixed and then co-spread on the interface [10]. In the separated spreading, the components are separately dissolved in the spreading solvents and then individually added onto the subphase [93]. The third method is the incorporation of the water soluble surfactant from the subphase into the monolayer. In this method, the aqueous solution of the water soluble component is injected into the subphase, and the other surface active component is spread at the surface. Although co-

spreading is the most widely used and expeditious, it presents the inherent difficulty associated with the dissolution of a strongly hydrophilic surfactant in a spreading organic solvent. To overcome it, mixtures of solvents may be used. The incorporation of the water soluble surfactant from the subphase, avoiding the solvent mixture, seems easy to accomplish and is of great importance in studies of molecular recognition or interfacial chemical reactions.

The effect of spreading procedures on the formation of cationic –anionic mixed monolayers were investigated by Goncalves da Silva and coworkers [92]. The three spreading methods have been used to investigate the mixed monolayers of dioctadecyldimethylammonium bromide (DODAB) with sodium hexadecylsulfate (SHS). The results showed that the most efficient procedure is co-spreading when equimolar amounts are used. On the other hand, when the components are spread separately at the interface, or when SHS is adsorbed from the aqueous subphase, it is not possible to obtain efficiency as high as that of co-spreading, even after 5 h. The equimolar composition at the interface can also be immediately obtained after solvent evaporation when SHS is added to the subphase in large excess to DODAB (9:1); alternatively, the same composition can be obtained from smaller excesses of SHS to DODAB, but only after larger time intervals.

Mixed monolayers of stearic acid (SA) and octadecylamine (ODA) [28] were intensively studied by co-spreading and separated spreading methods. The mixing and the miscibility of SA and ODA in the mixed monolayer are affected by the spreading methods used in preparing the monolayer. In the individual spreading method, the two compounds cannot mix well via 2-D contact and phase separation exists. As a result, individual characteristics of SA and ODA are still preserved in the mixed monolayers. On the contrary, in the premixed method (mixed in the spreading solvent before being spread on the subphase), a well-mixed phase is formed for the

monolayer. The same group also reported the area relaxation behaviour of SA/ODA mixed monolayer prepared by spreading the two compounds individually onto the subphase [94]. The area relaxation of the monolayer is the measurement of area as a function of time at constant surface pressure. The monolayer is compressed to a preset surface pressure; the surface pressure was then kept constant by automatically adjusting the surface area of the film through movement of barriers. This result also showed that the two components do not mix completely if they are individually spreading.

Stosch and Cammenga [95] have investigated mixed monolayers of stearic acid with each of the three related amphiphilic compounds, octadecanamide (OMAD), octadecylamine, and octadecylurea (OU) by measuring their surface pressure-area (π–A) isotherms and also their resistances to water evaporation. It has been shown that binary systems consisting of stearic acid with OAMD, OAM, or OU are capable of forming insoluble mixed monolayers at all molar ratios and surface pressures. Weak interactions due to intermolecular hydrogen bonding were detected in SA/OMAD monolayers, whereas significant condensation effects were observed in 1:1 mixed films containing SA and ODA. This is attributed to an acid-base equilibrium followed by the formation of a well-ordered arrangement of COO^- and NH_3^+ headgroups bound to each other by electrostatic forces. OU is well known for its anomalous temperature dependence of the two-dimensional transition from a low-temperature phase (β-phase; limiting area, 25.5 $Å^2$/ molecule) to a high-temperature phase (α-phase; limiting area, 19.5 $Å^2$/ molecule). The phenomenon of area contraction with increasing temperature was postulated to arise from the disruption of a hydrogen bonded network. The addition of small amounts of SA to OU monolayer seems to transform OU into the more condensed α-phase. This behaviour indicates that SA can be regarded as the structure-determining compound without forming distinct

molecular complexes with OU [95]. Teixeira and coworkers studied the phase behaviour of stearic acid/stearonitrile (SA/SN) [96] and stearic acid/oleanolic acid (SA/OLA) [97], stearic acid/tristearin (SA/TS), stearic acid/stearyl stearate (SA/SS), tristearin/stearyl stearate(TS/SS) [98], and oleanolic acid/stearyl stearate (OLA/SS) [99] binary mixtures at air/water interface. Thermodynamic analysis indicated miscibility in the whole composition range for the systems SA/SN and SA/TS, partial miscibility for the systems SA/SS and TS/SS and immiscibility for OLA/SA and OLA/SS systems.

Kuramori and coworkers have investigated the mixing behaviour of binary monolayer of fatty acids on the basis of π-A isotherm measurements with respect to the difference in cohesive energy of each alkyl chain [100]. Palmitic acid (C_{16}) and arachidic acid (C_{20}) formed mutually miscible monolayers and so did arachidic acid (C_{20}) and linoceric acid (C_{24}). C_{16}/C_{24} monolayer is immiscible, C_{16} and C_{22} (behenic acid) were incompletely miscible as were C_{18} and C_{24}. The fact that C_{16} monolayer was miscible completely with C_{20}, was incompletely miscible with C_{22}, and totally immiscible with C_{24}, and that C_{24} was completely miscible with C_{20}, but incompletely miscible with C_{18}, shows that miscibility is determined by the difference between the numbers of methylene groups of the component molecules. This indicates that a variation of cohesive energy between the hydrophobic chains is responsible for determining miscibility.

Bhattacharjee and Hussain have studied the organized nanoscale aggregates of a coumarin derivative, 7 Hydroxy-N-Octadecyl Coumarin-3-Carboxamide (7HNO3C), at the air/water interface and in Langmuir–Blodgett films in the presence and absence of stearic acid [101]. The surface pressure-area isotherm reveals that the 7HNO3C forms stable monolayer at the air/water interface. However, the stability can be improved by mixing it with SA. The miscibility study shows that the nature of interaction is strongly dependent on the mixing ratio and surface

pressure. At a mole fraction of 0.4 of 7HNO3C in SA, the attractive and repulsive interaction between these two molecules balance each other forming a stable film with nanoscale aggregates.

Brzozowska and Duits studied the formation and stability of mixed SA/ODA and SA/PDA (12-phenyldodecanoic acid) films on aqueous sub-phases at various salt concentrations, and selected pH values [102]. Pure ODA and SA monolayers differ most strongly at pH 7, where they can dissociate into oppositely charged species. As the salt concentration is increased, SA and ODA monolayers expand, though the effect was much smaller for SA films. This difference is attributed to the effective sizes of the head groups. The head group of a bare ODA^+ cation occupies significantly less space than that of an SA^- anion, making the charge density of the fatty cation higher. As a result the counter-ions bind more strongly to the ODA^+ than to the SA^-, which in turn, results in a larger hydration shell. Hence the overall effect is that ODA, together with its hydration shell is larger than SA, occupies larger area than SA. For SA/ODA mixtures at this pH (7), surface pressure-area isotherms indicate mixing on a molecular scale. Increase of the salt concentration causes significant contraction of the layer, which is ascribed to the formation of complexes between the oppositely charged SA and ODA. In this scenario, the depletion of counter-ions and reduction of the hydration shell lead to the film contraction. As for 12-phenyldodecanoic acid (PDA), it is less amphiphilic than stearic acid, and has a higher solubility in water. Metastable mixed films of SA and PDA are formed only at high salt concentration and low pH, where the solubility of PDA into the sub-phase is the lowest. Under these conditions, SA appears to have a stabilizing effect, which is however not strong enough to prevent expulsion of PDA from the interface.

The properties of mixed monolayers composed of the cationic Gemini surfactant ($[C_{18}H_{37}(CH_3)_2N^+–(CH_2)_3–N^+(CH_3)_2C_{18}H_{37}],2Br^+$ [18-3-18,$2Br^{-1}$] and SA at the air/water interface were investigated by Rong Li and coworkers [103]. Due to the electrostatic attractive interactions between [18-3-18, $2Br^{-1}$] and SA, the excess areas indicated negative deviations from ideal mixing. Moreover, [18-3-18, $2Br^{-1}$] and SA were miscible at the air/water interface, a fact which was confirmed by atomic force microscopy (AFM) images.

There are, however, interesting alternative types of mixed films which contain at least one compound unable to form monolayers [104]. These include long chain *n*-alkanes [105; 106], halogenated alkanes, or heteroaromatic molecules which have a dominant hydrophobic character and form preferably drops or multilayers upon spreading [29; 107]. Some other ionic surfactants having strong hydrophilic character easily dissolve into the water subphase when added to the interface. When those substances are mixed with suitable film forming materials and spread at the air/water interface, they can remain at the interface by virtue of lateral interaction between the long chains, or due to interactions between both long chains and polar groups [81; 108; 109]. In most cases SA has been used to stabilize unstable components.

The interfacial properties of the spread Langmuir films of $C_{60}Br_{24}$ and SA have been studied at air/water interface by measuring their surface pressure-area isotherms [107]. $C_{60}Br_{24}$ does not form a stable film at the air/water interface. The mixed films of SA and $C_{60}Br_{24}$ were found to be immiscible and non-ideal except when the mole fraction of the latter, X $C_{60}Br_{24}$, equals 0.5, which may be the composition of greater stability when compared with its pure components. The interaction between $C_{60}Br_{24}$ and SA results in lowering of the surface pressure of SA and hence the decrease in compressibility with the increasing $X_{C60Br24}$, thereby indicating the domination of $C_{60}Br_{24}$ characteristics in the mixed monolayers. Mixed monolayer of

merocyanine 540 dye and octadecylamine (MC540/ODA) can be readily prepared on pure water subphase while MC540 alone does not form a monolayer. The strong interaction between MC540 and ODA is attributed to the formation of a stable monolayer at the air/water interface. The specific area per molecule obtained from π-A isotherm revealed that the MC540 dye molecules incorporated among the ODA molecules at the air/water interface [110]. Hussain and coworkers have investigated the monolayer characteristics of pyrene mixed with SA at the air/water interface by Langmuir-Blodgett technique [111]. It has been observed that the pure pyrene does not form stable Langmuir monolayer. However, when mixed with SA it forms self-supporting stable monolayer at the air/water interface. The area per molecule of the mixed isotherm systematically decreases with an increase in mole fraction of pyrene in the mixed films indicating successful incorporation of pyrene molecules with in the fatty acid chain. The group also reported the formation of well-organized stable Langmuir films of non-amphiphilic 2-(4-Biphenylyl)-5 phenyl-1,3,4- oxadiazole (PBD) at the air/water interface when mixed with SA as well as with inert polymer matrix poly(methyl methacrylate) (PMMA) [112]. Stable mono- and multilayer Langmuir-Blodgett films were prepared by transferring this Langmuir monolayer onto quartz substrates. Surface pressure versus area per molecule (π-A) isotherm studies reveal that the PBD moieties do not lie flat at the air/water interface but very likely stand vertically on their edges, and this arrangement allows the PBD molecules to form stacks and remain sandwiched between SA or PMMA molecules. At lower surface pressure, phase separation between PBD and matrix molecules (PMMA) occurs due to the repulsive interaction. However, at higher surface pressure, PBD molecules form aggregates.

Acharya and coworkers have prepared the LB films of nonamphiphilic benz(b)fluoranthene [B(b)F] molecules mixed with SA [113]. The (π–A) isotherm of [B(b)F] mixed with SA at different mole fraction reveals that the area per molecule decreases with increasing mole fractions of [B(b)F]. This

suggests the accommodation of [B(b)F] molecules within the SA matrix. The area per molecule versus mole fraction shows that there is positive deviation of the experimental data from the ideal behaviour. This indicates a repulsive interaction between the components that may result in aggregation of [B(b)F] molecules in the mixed films. This explains the decrease in area per molecule with increase of mole fraction of [B(b)F].

The incorporation of tetracationic meso-tetra(4-methylpyridyl)porphine (PO2) in mixed Langmuir monolayer and LB films of anionic surfactant sodium hexadecylsulfate (SHS) and SA has been investigated [114]. PO2 mixed with SHS in a 1:4 molar ratio can form expanded monolayers and LB films one layer thick. The addition of SA, enhances the stability and density of films. The stability of the monolayer and the molecular packing of PO2 vary with the surface pressure and the amount of SA in the monolayer. The two-dimensional compressibility of the condensed ternary monolayers decreases with the content of SA, approaching the value for pure SA in the solid state for the 1:4:18 molar ratio. The important role of the SA monolayer diluent is the control of the molecular orientation and packing of PO2 in Langmuir and LB films. At low surface pressures, before the transition, the Langmuir monolayers are expanded or liquid condensed and the PO2 molecules orient nearly parallel to the interface independently of the SA content. At high surface pressures, above the transition, molecular packing and aggregation of PO2 depends on the SA content. In the condensed regime of Langmuir monolayer, the global packing is governed, if not completely, by the alkyl chains, and the PO2 molecules have to adjust under a close packed monolayer of alkyl chains.

There have been extensive studies of the monolayers of phospholipids mixed with fatty acids because fatty acids are known to strongly modify the structure of biological membranes and their functions such as transport [115; 116] and enzyme adsorption [117]. Such effects can be

investigated by examining the molecular interaction of fatty acids with phospholipids in the bulk [118; 119] or in monolayers. In most of these studies SA has been used to prepare the mixed film [120], though mixed films of phospholipids with other fatty acids have been reported [121; 122].

Romao and coworkers compared the behaviour of dipalmitoylphosphatidylcholine/stearonitrile (DPPC/SN), DPPC/SA and DPPC/OD (octadecanol) at the air/water interface by (π–A) measurements and by direct visualisation of monolayers by Brewster angle microscopy (BAM) [123]. The thermodynamic analysis indicated miscibility for the three systems with negative deviations from the ideal behaviour. Mixed monolayers of DPPC/SN, DPPC/SA and DPPC/OD, reach the closest packing of aliphatic chains in the 0.4-0.6 range of mole fraction of DPPC.

Mixed monolayers of phosphatidylcholine-fatty acid or phosphatidylcholine-amine were investigated at the air/water interface by Petelska and coworkers [124]. The results showed that both the binary mixtures, phosphatidylcholine/fatty acid and phosphatidylcholine/amine, significantly deviated from the additivity rule and formed highly stable 1:1 complexes.

The miscibility of the cholesterol and its hydrophobic thiol analogue, thiocholesterol (Tch), for different compositions has been studied [125]. TCh is predominantly a hydrophobic molecule, and it does not spread at the air/water interface to form a stable Langmuir film, but when it is mixed with cholesterol molecules, it forms a stable monolayer. The mixed monolayer was stable up to 0.75 mole fraction of thiocholesterol in cholesterol. The mixed monolayer shows an initial and a final collapse. On compressing the monolayer beyond the initial collapse, the thiocholesterol molecules squeeze out irreversibly from the mixed monolayer phase. The calculation of excess area per molecule for the thiocholesterol and cholesterol mixed monolayer system indicated the attractive interaction between the component molecules.

A few studies on mixed films of polymers spread at the air/water interface have also been reported [126; 127; 128]. Some of the aromatic polymers are not classical amphiphiles and they do not spread at the air/water interface [129], but when mixed with a suitable amphiphile (a phospholipid or a fatty acid), they are able to form a Langmuir monolayer at the air/water interface. In general, the compatibility of polymer blend films spread at the air/water interface is determined by the additivity rule as explained in the case of mixed films. For instance, it has been recently reported that a polymer containing fluorenyl groups spreads well at the air/water interface when mixed with a negatively charged phospholipid [129], and it can be transferred to solid supports by using the LB technique. Polyfluorene based materials can emit light across the entire visible range [126]. Therefore, it is an attractive component in luminescent (light emitting) materials, whose emission is increased due to the molecular-level interactions among the components of the mixed film confined in a close-packed arrangement. Different reports focus on the incorporation of SA into poly(*p*-phenylene vinylene) LB films to enhance the performance of optical properties [126; 127]. In many studies, because of the low amphiphilicity of polythiophenes, SA has been chosen as assistant molecules to form high quality polythiophene monolayer and multilayer LB [130; 131; 132].

1.8.3 Hysteresis behaviour of Langmuir monolayer isotherms

If a π-A curve is measured by continuously compressing a monolayer, and if after the compression the monolayer is decompressed to its original area, in general the curves do not coincide. The term hysteresis refers to the different paths that compression and the decompression curves follow. This difference is caused by conformational changes in the surfactant film caused by compression. Hysteresis behaviour proved to be very informative in

elucidating the dynamic behaviour properties of amphiphilic systems under variable stress at the air/liquid interface. Compression-expansion cycles reveal respreading characteristics of the monolayer after compression. The absence of hysteresis, indicated by the overlap of compression and decompression curves, shows that a stable and respreadable monolayer is formed. In real situations a complete overlap of the two curves rarely occurs. If the positions of the two curves and their shapes are different, there is hysteresis. The expansion curve is usually shifted to lower area per molecule. If the monolayer is subjected to several compression-expansion cycles and successive hysteresis curves coincide, it indicates reversible behaviour. Hysteresis behaviour of monolayers indicates that most of the monolayers are reversible. But the monolayers with irreversible behaviour have also been reported.

The hysteresis behaviour of monolayer of surfactin, one of the most surface-active microbial lipopeptide produced by *Bacillus subtilis*, at different pH values was investigated by Yang Ying and coworkers [133]. The compression isotherm showed a plateau region at ~ 25 mN/m. When the monolayer is expanded at lower pressure (20 mN/m), negligible hysteresis is observed, while a larger hysteresis loop with a sharp drop in the surface pressure is observed when it is expanded at higher surface pressure (40 mN/m). The second cycle was shifted towards smaller molecular areas compared with the first one. It is suggested that the formation of three-dimensional surface aggregates at the plateau region induces a large hysteresis loop in the surfactin monolayer which can also be attributed to the submergence of molecules into the subphase.

Ke-Hsuan Wang and coworkers have studied the hysteresis behaviour of pure SA, pure ODA monolayers, mixed stearic acid/glucose oxidase (SA/GOx) and mixed ODA/GOx monolayers at air/water interface [134]. The SA monolayer demonstrates a mild hysteresis behaviour with a slight area loss after each compression-expansion cycle. The hysteresis and area loss can be

ascribed to the formation of 3-D aggregates [94]. On the contrary, the expansion curve of ODA monolayer coincides nearly completely with the compression trace, showing no hysteresis in each compression-expansion loop. However, the loop of the following cycle left-shifts slightly, indicating the loss of the monolayer material between successive cycles. This phenomenon can be ascribed to the high solubility of ODA molecules in water which had been reported in the literature [54; 94; 135]. They also investigated the effects of SA and ODA monolayers on the adsorption of GOx from the subphase for two adsorption times, 2 h and 8 h. The results show that the surface pressure-area isotherm of SA/GOx monolayer resembles that of SA monolayer, indicating that only a small amount of GOx was incorporated into the mixed film. On the contrary, the ODA/GOx monolayers are highly expandable and compressible, a property attributed to the extensive incorporation of GOx induced by the electrostatic interaction between ODA and GOx. Hysteresis behaviour of SA/GOx monolayer shows that, the expansion curves closely follow the compression curves in the early stage of expansion whereas at the late expansion stage, the surface pressure is lower than that of the compression stage, which means that GOx cannot re-adsorb fast enough in the expansion stage to compensate for the desorbed GOx in the compression stage. The slow re-adsorption rate of GOx to the SA monolayer also triggers a slightly left-shift of the hysteresis loops in the subsequent compression-expansion cycles. Hysteresis behaviour is similar for the two adsorption times. This means that increasing the adsorption time from 2 to 8 h does not lead to significant increase of adsorbed GOx. On the contrary, an ODA template possesses an electrostatic attraction to the GOx, resulting in a high adsorption rate and adsorption amount of GOx. Therefore, the mixed ODA/GOx monolayer exhibits a high compressibility and low hysteresis characteristics. The slight hysteresis behaviour of compression and expansion curves of ODA/GOx monolayer can be ascribed to the

desorption and adsorption effect of the GOx. For the mixed ODA/GOx monolayer, after 2 h of adsorption the hysteresis curve right shifts gradually in successive compression-expansion cycles. This result indicates that more GOx molecules were adsorbed continuously into the ODA monolayer during the hysteresis experiment. However, for the 8 h-adsorption the ODA/GOx monolayer demonstrated little hysteresis behaviour even as the monolayer was compressed to a surface pressure as high as 40 mN/m. The close resembling of the expansion and compression curves, as well as the successive hysteresis loops, not only indicates a fast adsorption-desorption rate of GOx during the compression-expansion process, but also the approach of an equilibrium state after 8 h adsorption.

Reversibility experiments of ATs (1-acyl-1,2,4-triazoles) have been reported [136]. The monolayers of ATs collapse due to compression to trilayers between π values of 20 and 36 mNm^{-1} and collapse finally after further compression at π values of $\sim$ 59–67mNm^{-1}. The hysteresis results show the irreversibility of the monolayers. This means the molecular arrangement formed during the first compression is so stable that it does not rearrange into a monolayer during the first expansion.

The hysteresis experiments of the mixed monolayer of DNA/ODA system show negligible hysteresis at low surface pressures (< 30 mNm^{-1}). However when pressure is increased to 45 mNm^{-1}, there is noticeable reversible hysteresis. This may be due to reversible squeezing out and reincorporation into the monolayer of the DNA molecules or the formation of reversible multilayers [137]. Similar characteristics for systems with high hysteresis have been reported in amphiphilic, large counterion Tetrakis(4-sulfonatophenyl)porphyrin/Dioctadecyl-dimethyl ammonium [138].

The hysteresis study of the Langmuir monolayer of fullerene C_{60}–oligo-*para*-phenylenevinylene (OPV) derivative with six $C_{12}H_{25}$ aliphatic chains exhibits reversibility upon successive compression/decompression cycles, as long as the collapse pressure of $\pi \approx 45$ mN m^{-1} is not exceeded [139]. This observation clearly indicates that the six aliphatic chains are capable of preventing the formation of aggregates due to strong fullerene-fullerene interactions similar to other reported amphiphilic fullerene derivatives [140].

The hysteresis behaviour of a fatty acid/protein [arachidic acid/BSA (Bovine Serum Albumin)] films has also been reported. The expansion curve of the film takes place at lower specific areas than the compression part of the curve [19]. This is due to the presence of a combined process of protein folding at the air/water interface upon compression [141] and BSA loss from the interface to the subphase. During decompression, the folded protein did not unfold as fast as it had folded by compression, resulting in lower areas per molecule. The successive hysteresis loops are reproducible and the shape of the loop after the first cycle is similar. This reproducibility is a sign that after a complete expansion, protein molecules relax back to their original state.

Pal and coworkers have investigated the hysteresis behaviour of QP (p-Quaterphenyl)/SA mixed monolayers [29]. The reproducibility of the compression-decompression cycles indicates the formation of a stable mixed monolayer and superimposition of the cycles ruled out the possibility of any significant material dissolution into the subphase. The negligible extent of hysteresis between the compression and decompression isotherms may possibly be due to the difference in the organization and disorganization process of the sample molecules on the water surface during compression and decompression, respectively.

1.8.4 Interaction of Langmuir monolayer with aqueous subphase.

Langmuir monolayers can be used to study the effect of the nature of the subphase on chemical or biochemical reactions as well as intermolecular forces between the floating molecules and the ions present in the subphase [142]. The study of surface pressure-area isotherms can shed light on the interaction between film molecules and other ions or molecules dissolved in the subphase. The interaction between the Langmuir monolayers and the ions or molecules dissolved in the subphase can be classified as simple reactions, polymerization reactions, enzymatic reactions and catalytic reactions. In most of these studies, the reactions were followed by recording variations in the area per molecule at constant pressure or changes in surface pressure at constant area per molecule with time.

1.8.4.1 Simple reactions

The study of chemical reaction between an insoluble monolayer and the subphase at varying surface pressure π (or area/molecule) is potentially a valuable tool in investigating the structure of the surface films. Ahmad and coworkers have reported [143; 144] a number of such systems which fall into two categories: those in which the state of compression of the monolayer drastically affects the rate of the reaction and the ones where rate is largely unaffected by the variation in surface pressure. A reaction belongs to one type or the other depending on how the accessibility of the reacting functionality in the molecule to the subphase is affected by surface compression. For example, the rate of acid catalyzed cyclization of the monoterpenoid alcohol, nerol [143], which takes place easily in the expanded film of nerol is disfavored at high surface pressures, since under these conditions the molecule does not have the folded conformation required for cyclization. The acid catalyzed dehydration of the tertiary alcohol 1,1-diphenyl-1-

octadecanol is slowed down dramatically as the surface pressure is increased, consistent with the fact that under these conditions the participating β-hydrogen becomes inaccessible to the subphase [144]. The oxidation of 1-octadecanethiol monolayer to dioctadecyl disulfide provided by acidified potassium hexacynoferrate in the subphase showed that the reaction was slower at high pressure as compared to lower pressure and this was ascribed to the inability of the octadecyl chain in the compressed film to form the required skewed conformation in the disulfide product [145]. On the other hand, reactions where the accessibility of the functionality is not influenced by surface compression are not greatly influenced by changes in surface pressure. Examples are the chromic acid oxidation of 1-phenyl-1-hexadecanol [146] and the hydrolysis of an octadecyl ester [147]. In both these examples, the reaction is taking place at a single carbon atom, and the geometry of the hydrophobic chain may be expected to have only a small effect on the rate of reaction. Another example is the chemical reduction of an amphiphilic ketone on aqueous subphases containing sodium borohydride reported by Gascon and coworkers [148]. Changes in the compression isotherm and in the monolayer morphology were observed when the concentration of $NaBH_4$ or the delay between spreading and compression was increased. These modifications were specific to $NaBH_4$ and suggested that a chemical reaction was taking place involving the monolayer. Analysis of the compression isotherms demonstrated that this reaction occurred for all surface pressures and therefore indicated that the ketone group was accessible to the borohydride whatever the compression state of the monolayer.

Monolayer behaviour of amphiphiles is closely related to the subphase conditions, especially when there exists an interfacial chemical reaction. This reaction often results in new products and/or different arrangement of the amphiphiles in the monolayers, such as formation of new structural molecular aggregates and polymeric network sheets, as well as nanostructural

materials [149; 150]. Kumar and Oliver studied [151] an acyl transfer reaction between a long chain thioester of an amino acid and an amphiphilic nucleophile to give an amide bond at air/water interface. This reaction was catalyzed by ribosome provided by the subphase. The kinetics of this amide bond formation was studied by ^{1}H NMR spectroscopy. The kinetics showed that while the reaction is second order in chloroform solution ($k=0.003\ M^{-1}h^{-1}$), it follows first order kinetics at the air/water interface ($k=1.58\ h^{-1}$). The influence of the nature of the subphase on the interaction between a mixed film containing diphenyl bis(octadecylamino) phophonium bromide and behenic acid has been studied [142]. The existence of strong interactions between the proton sponge (diphenyl bis(octadecylamino)phophonium bromide) and behenic acid were observed when the subphase was either pure water or a NaOH aqueous solution. A stoichiometric 1:1 reaction between the two molecules takes place at the air/water interface. The reaction has efficiency close to 100% at high surface pressures, provided the majority anion present in the subphase is OH^{-}. However, when the majority anion is another one, this complex is not formed. So this acid-base reaction is highly dependent on the protonation state of the proton sponge at the air/liquid interface that is a function of the present counterion in the subphase. It has been pointed out that monolayers of the porphyrin of MnTPyP (TPyP: tetrapyridylporphyrin) could be stabilized on the sodium tetraphenylboron and K_2PdCl_4 subphase surfaces, but not on the pure water surface [152]. MnTPyP is a kind of ionized porphyrin and can slightly dissolve into the water phase. Because of this solubility, the MnTPyP does not form a stable monolayer on the pure water surface. But when $NaB(C_6H_5)_4$ solution was used as the subphase, the large $B(C_6H_5)_4^{-}$ anionic ions could prevent the dissolution of MnTPyP and support the formation of stable MnTPyP-$B(C_6H_5)_4$ monolayer. On K_2PdCl_4 solution subphase, formation of Pd-MnTPyP multiporphyrin arrays, resulted in a stable insoluble

monomolecular layer at the air/water interface. An amphiphilic dendron, containing an azobenzene ring at the focal point and the l-glutamate peripheral groups, although without any long alkyl chains, could form a stable monolayer at the air/water interface because of favourable balance between hydrophilic and hydrophobic parts within the molecule [153]. When cyclodextrin (CyD) was added to the subphase, a host-guest reaction occurred *in situ* at the air/water interface. The inclusion of the focal azobenzene moiety into the cavity of cyclodextrin decreased the packing of the aromatic ring and also led to the diminishment of the molecular area.

Some studies have concluded that the formation of a complex Langmuir monolayer is subjected to the adsorption of the water-soluble cationic or anionic types of materials on to oppositely charged amphiphilic molecules of a preformed Langmuir monolayer [154; 155]. Such adsorption by electrostatic interaction is largely affected by the subphase temperature as well as by the concentration of amphiphile. The adsorption kinetics of a sample to a preformed monolayer can be monitored by the change in the surface pressure with time at air/water interface at fixed film area. First the monolayer forming material is spread at the air/water interface, and the surface area is reduced to form a stable monolayer. Then keeping the area constant, water soluble material is slowly injected to the aqueous subphase. Consequently interaction between the molecules occurs and the complex is formed. Since the area per molecule of the complex species is greater than that of the pure component, the area per molecule of the complex monolayer tends to increase. As the area is constant, this leads to an increase in surface pressure. Examples are the reaction kinetics of water soluble Rhodamine B (RhB) with stearic acid (SA), [156] and phospholipid 1,2-dipalmitoyl-sn-glycero-3-

phosphocholine (DPPC) [157] and the incorporation of chloroaurate ions ($AuCl_4^-$) from the subphase into the monolayers of Gemini-type amphiphiles and ODA [158; 159; 160].

1.8.4.2 Catalytic reactions

Some reactions in monolayers can be catalyzed with substances present in the monolayer or in the subphase. The oxidation of monolayers of 1-octadecanethiol to dioctadecyl disulfide over a subphase of potassium hexacyanoferrate(III) was accelerated by the presence in the monolayer of even a minute amount of octadecylamine, which acted as a catalyst [161]. As the amount of amine in the monolayer was increased, the rate of the reaction increased and finally a stage was reached at which a further increase in the catalyst concentration did not cause a commensurate increase in the rate. This has been interpreted as indicating a clumping of amine molecules in the monolayers at higher concentrations. The reaction is also catalyzed by OH^- contained in the subphase. Over both acidic and basic solutions, however, the effectiveness of the amine as a catalyst is reduced compared to its effectiveness over the neutral subphase.

The catalytic activity of a monolayer of Mn^{III}-salen complexes bearing perfluoroalkyl substituents, for the epoxidation of the cinnamyl alcohol dissolved in the subphase containing urea/hydrogen peroxide complex (UHP) as an oxygen source for the oxidation, has been reported [162]. At constant area per molecule of the catalyst, the reaction rate exhibits first-order dependence on oxidant concentration and zero-order dependence on alkene concentration, in agreement with the reaction orders reported for Mn^{III}–salen catalyzed epoxidation reactions carried out in solution. It also suggests an enhanced activity of the catalysts assembled in a Langmuir film relative to that observed in bulk reaction.

1.8.4.3 Polymerization reactions

Chemically initiated polymerizations of oriented monomers can be performed by just adding a catalyst or reagent in the subphase. Aniline derivatives [163] and vinyl monomers [164; 165] have been polymerized in this way. Zang and coworkers reported the formation of Poly(2-hexadecyloxyaniline)/selenium (Se) nanocomposite monolayer by spreading 2-hexadecyloxyaniline (2-C_{16}OAn) on selenious acid aqueous solution without additional oxidant and reductant. The formation of Se nanoparticles and the polymerization of 2-C_{16}OAn in the monolayer occurred simultaneously. The limiting area per repeat unit on selenious acid subphase was larger than that on pure water, which indicated the formation of poly(2-hexadecyloxyaniline)/Se nanocomposite monolayer at air/water interface [166]. Photopolymerizations at the air/water interface were analyzed for linoleic acid [167] octadecyl acrylate[168], acetylene derivatives [169; 170; 171] or fumarate derivatives [172]. Photopolymerization of fullerene C_{60} at air/phenol aqueous interface has also been reported.

1.8.4.4 Enzymatic reactions

For the immobilization/entrapment of protein/enzyme onto suitable substrate, Langmuir and/or Gibbs monolayer studies and subsequent monolayer transfer on solid surfaces by Langmuir Blodgett technique is the most versatile and convenient technique. To immobilize proteins depending on their net charge, an appropriate lipid having anionic, zwitterionic or cationic amphiphilic molecules may be used. The interaction of ovalbumin with an insoluble cationic ODA monolayer, zwitterionic (DPPC) and anionic (SA) monolayers have been studied [173]. The incorporation of OVA was found to be more in ODA as compared to that of DPPC and SA. It has been reported that DPPC monolayer is better to get protein lipid mixed film than SA and

ODA monolayer because unfolding of OVA is less in case of DPPC than SA and ODA. The π–A isotherm and compressibility study give the information about the different states of the protein-lipid mixed monolayer. The interaction between DPPC monolayer and the protein hemoglobin (Hb) has been studied by measuring (π-A) isotherms and the rate of change in π with time. The inclusion of Hb into the single layer of DPPC has been found to be dependent on surface pressure, concentration of Hb and their reaction/interaction time [174]. Kamilya and coworkers have studied [175] the incorporation/entrapment of water-soluble surface-active enzyme pepsin (PEP) within an insoluble cationic ODA Langmuir monolayer. The observation suggests that the incorporation of PEP is less preferable at higher surface pressure (30 mN/m). Natural biomembranes have surface pressures in the range of ~30 mN/m, so PEP is less likely to bind/penetrate to true biological membrane. The electrostatic interaction plays a significant role in the greater diffusion of PEP in cationic ODA monolayer. Compressibility studies along with Field Emission Scanning Electron Microscopy (FE-SEM) analysis indicate the squeezing out of PEP from the monolayer at higher surface pressure. The kinetic process of DNA inclusion into the ODA monolayer has also been reported [137]. The results showed that the surface pressure-area isotherms of the ODA monolayer exhibit a large expansion and lower compressibility when the DNA is present in the aqueous subphase. Moreover, this effect is highly dependent on the amount of DNA with the appearance of additional phase transitions, demonstrating the importance of the polynucleotide subphase concentration. This system is, however, highly reversible during compression-expansion cycles due to the strong interaction between the two components.

1.8.5 Reaction of monolayer with metal ions in the aqueous subphase

The properties of Langmuir films at the air/water interface are strongly affected by metal ions in the aqueous subphase, and they are often used as models of organic-inorganic interfaces. The inorganic complexes, usually metal salts, are dissolved in the aqueous subphase and allowed to interact with the weakly acidic headgroups of the organic molecules at the water surface. Generally, when ions are present in the subphase, the monolayer becomes much better ordered [176], changes its viscoelastic response [177], and transfers more easily to Langmuir-Blodgett films [178]. The inorganic minerals sometimes assemble into precise functional architectures to correspond with the structure of the organic template [179]. These systems are interesting from a fundamental as well as an applied point of view. Theoretical calculations [180] treat the organic films and ions as a two-dimensional model of an electrochemical double layer and provide analytical expressions for the electrostatic potential and ion concentration at the surface. The organic films have been used as templates for the nucleation and growth of inorganic crystals of specific morphology and crystallographic orientation, a model biomineralization process [181].

The most-studied systems are those of long chain saturated carboxylic acids (stearic, arachidic, behenic) and the divalent salts (e.g., Cd^{2+}, Ca^{2+}, Pb^{2+}, Ba^{2+}, etc.) of these acids. It is known empirically that the incorporation of these divalent cations dramatically increases the film stability and ease of deposition [182; 183]. The cations are added to the film simply by dissolving them in the subphase in sub-millimolar concentration. Since the amphiphile is acidic, however, at low pH it will not dissociate and the cations do not affect the monolayer on the water surface, nor do they become incorporated into the deposited LB film. At high pH, on the other hand, the acidic amphiphiles dissociate and are converted completely to the salt by the association of the dissolved cations. In the intermediate pH range the relative fractions of free

acid and salt are sensitive functions of pH [184; 185; 186]. (π–A) isotherms of stearic acid monolayers have been studied [187] by varying the pH of the aqueous subphase containing monovalent (Na) or divalent (Mg, Ca, Ba, Zn and Cd) cations. The lowering of the transition pressure (π_t) with increasing pH of the subphase is correlated with an increase of the headgroup dissociation of the acid monolayer. On pure water, the surface pressure drops after the collapse point (π_c) to a lower pressure value (π_l). This pressure-gap $\Delta\pi = \pi_c - \pi_l$ changes with increasing dissociation, depending upon the particular cation. After a certain pH, no pressure gap is observed and π remains constant or increases slowly after π_c. This transition from constant area collapse to constant pressure collapse of the monolayer is observed for all monovalent and divalent cations near total monolayer dissociation. Gericke and Huhnerfuss studied the interaction of SA monolayers at the air/water interface with bivalent cations Cd^{2+}, Pb^{2+}, Ca^{2+}, Ba^{2+}, Cu^{2+}, Ni^{2+}, and Zn^{2+} in aqueous subphase using the IRRAS technique [188; 189]. Wang and coworkers investigated the interaction of SA monolayer with Ag^{+}, Co^{2+}, Zn^{2+}, and Pb^{2+}-containing subphases using the same technique [190]. The results showed that Co^{2+} ions in the subphase induce a significant condensing effect on SA monolayer, but the isotherm displays a similar feature to that on pure water. In the cases of Zn^{2+} and Pb^{2+}, almost vertical condensed monolayers developed in contrast to a tilted condensed phase to vertical condensed phase transition as in the cases of pure water and Co^{2+}. On the Ag^{+} ion containing subphase, multilayers were formed. And these multilayers were composed of three monolayers, and the hydrocarbon chains in each monolayer were oriented at a tilt angle of ~ 30° away from the surface normal with their C–C–C planes almost perpendicular to the water surface. Dong June Ahn and coworkers have analyzed [191] the adsorption of metal ions onto SA Langmuir monolayers. Among bivalent ions examined (Cr^{2+}, Pb^{2+}, Cu^{2+}, Cd^{2+} Zn^{2+}, Ca^{2+}, Ni^{2+}, and Ba^{2+}),

Langmuir monolayers showed the highest selectivity to chromium ions. In addition, it was found that adsorption constants of the surface ions are quite different from binding constants of the bulk ions. Kundu and coworkers have shown that SA monolayer on pure water and in the presence of certain divalent metal ions such as Cd and Pb at pH ≈ 6.5 of the subphase water collapses at constant area, while for other divalent ions such as Mg, Co, Zn, and Mn at the same subphase pH the monolayer collapses nearly at constant pressure [192]. Ren and coworkers investigated the interaction of fatty acid monolayers at the air/water interface with bivalent cations Cd^{2+} and Ba^{2+} in the subphase using polarization modulation IRRAS (PM-IRRAS) technique [193; 194; 195]. Al-Ali and coworkers have investigated the monolayers of amphiphilic (α-amino) phosphonocarboxylic and (α-amino) phosphonic acids on Ca^{2+} and Mg^{2+} ions containing subphases [196]. The stability and the compactness of the Langmuir films are enhanced by introduction of metallic ions in the subphases. These effects are more pronounced with Ca^{2+}, because it presents a stronger affinity toward phosphorus acids and has a greater facility to form complexes than Mg^{2+}. These metal ions can form dimeric complexes with the phosphorus moieties of the surfactant polar heads and therefore bring the amphiphiles closer. The self-assembled supramolecular nanostructures of a bolaamphiphilic diacid, 1,20-octadecanedicarboxylic acid on the subphase containing Ag (I) or Eu (III) ions have been reported [197].

Besides these, a number of long chain amphiphiles modified with organic ligands such as crown ethers and analogues [198; 199; 200; 201], calixarenes [202], imidazoles [203; 204], pyridines [205] and other groups [206; 207] have been synthesized and their complex formations with the metal ions in the subphases have been investigated.

However, not much work has been reported on the monolayer properties of amphiphilic ligands spread on a subphase containing transition metal ions [208; 209; 210; 211]. Schouten and Werkamn have studied polymerisable amphiphilic ligands spread on the subphase containing transition metal ions [212]. Kesimli and coworkers have investigated the effects of different transition metal ions, metal ion concentration, complexation time, and counter ions on the complexation process on vic-dioxime monolayer [213].

1.8.6 Multilayer formation of Langmuir monolayers

Multilayers at air/water interface can be used as a well-defined model to study interactions within layers. A spontaneous multilayer film formation at the air/water interface has often been observed for molecules containing hydrogen bonding groups at both ends of the chain, as well as for pure long-chain alkanes [13]. Also, multilayer formation can be obtained by compressing a Langmuir monolayer film beyond its collapse point [214; 215; 216; 217]. There are some examples of formation of well-defined multilayer structures upon compression beyond the point of film collapse [218; 219]. Mohwald [218] called this a layering transition [220; 221; 222; 223] and a ‘‘roll-over collapse’’ was proposed as a mechanism explaining this kind of layering transitions [224; 225]. Most of them form a stable “head-to-head” bilayer on top of a monolayer (Figure 1.8.1) or a “head-to-tail” bilayer at the air/water interface. Only a few of them form “tail-to-tail” interdigitated bilayers [226], which resemble the structure of the natural membranes. Normally, because of the high energy of the hydrophilic top layer, the “tail-to-tail” bilayer exposed to air is quickly destroyed and buckles to form multilayers. However, through weak acid-base interaction between the headgroups in binary mixtures of amphiphiles [226], it is still possible to obtain “tail-to-tail” bilayers.

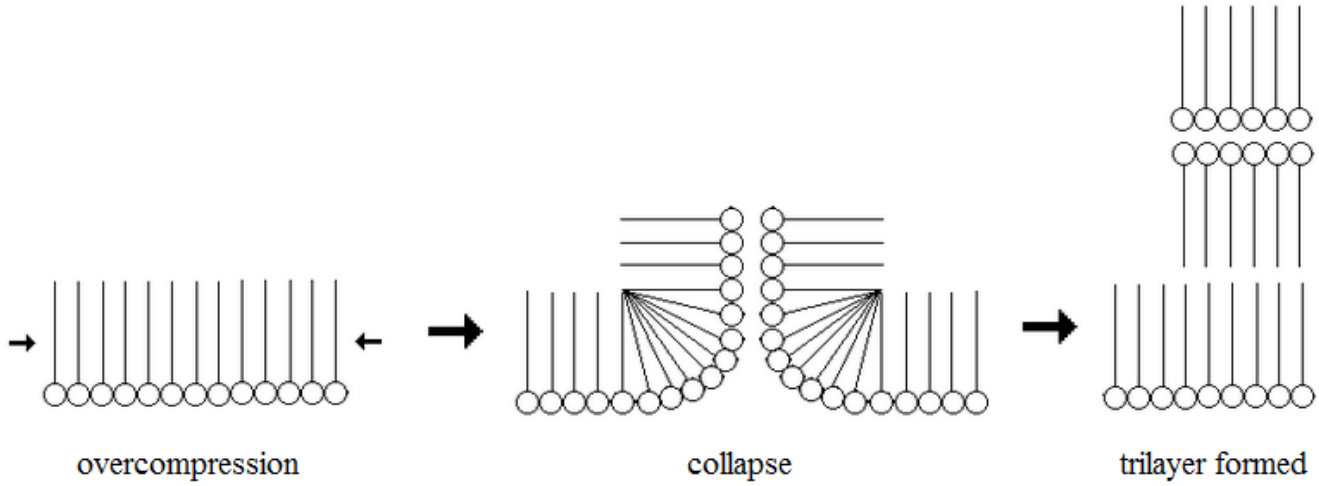

Figure 1.8.1: Schematic representation of trilayer formation in Langmuir films.

Two papers [216; 217] reported the unconventional air stable interdigitated bilayer formation at the air/water interface, in which the monolayer "collapses" through a transition to a homogeneous trilayer film composed of a monolayer plus an interdigitated bilayer. Also, the plateau observed in the π-A isotherms of aromatic carboxylic acids [227] and 2,3-disubstituted fatty acid methyl ester [217] revealed a similar behaviour (multilayer formation) to that observed for mesogenic substances [216; 228; 229]. Gourier and coworkers [230] have obtained evidence for the folding and displacement of one portion of the pentacosadiyonic acid monolayer with respect to another (sliding mechanism for collapse). By the collapse phase detected during the surface pressure-area isotherm at the air/water interface, Huo et al. [231] demonstrated the formation of a bilayer in a new nontraditional supramolecular-like Langmuir film with a urea derivative. Also, a reversible transition to a bilayer was reported by Gallani and coworkers [232] for a mesogenic compound with flexible chains at both ends of a rigid core. A reversible trilayer formation of a mixed monolayer containing a cationic lipid and an anionic porphyrin has been reported, in which the organization of the mixed ultrathin film spontaneously formed at high surface pressure corresponds to a trilayer film, where a bilayer of cationic matrix molecules, whose head polar groups retain the anionic dimer porphyrins, stand on top of a mixed monolayer with monomer porphyrins [138]. Reuter and coworkers [136] reported the trilayer formation in triazoles. The π-A isotherms exhibited a spike followed by a pseudo-plateau region. The spike is interpreted to indicate the buckling and subsequent folding of the monolayer, and the pseudo-plateau is considered as a region where a trilayer formation occurs by a roll over mechanism of the previously existent monolayer.

1.9 Applications of Langmuir monolayers

Since their discovery, Langmuir monolayers have been very widely studied using different techniques and for diverse goals. One of the initial reasons for the study of Langmuir monolayers was to characterize the thermodynamics and the molecular orientation of the bi-dimensional phases and to compare them with the corresponding bulk phases. They have considerable implications in many fields of science and technology, such as in chemistry, physics, material science and biology [233]. They serve as model systems for the simulation of several physico-chemical processes at interfaces and they range from simple saturated fatty acids to complicated networks of protein matrices. A pair of thermodynamic quantities, temperature and surface pressure, can be easily controlled; the surface pressure is varied simply by moving a barrier along the surface. Such direct mechanical control of the area, which is analogous to hydrostatic compression in 3D systems, is not available in other 2D systems and arrangements. This compression state of the monolayer offers accessibility of the reacting functionality in the molecule to the subphase. In addition to this, the interaction of molecules in the monolayer can be systematically modified by the exchange of polar and nonpolar parts of surfactant molecules using wide synthetizing possibilities of organic chemistry (e.g. the chain length can be varied in small steps) or by the change of pH or of ionic content of the subphase [234]. Langmuir monolayers have potential uses in a variety of industrial applications, and also they offer insight into several biological problems.

1.9.1 Industrial applications

The structure and dynamics of surfactant molecules at the air/liquid interface have been studied not only for their scientific properties but also for their wide industrial applications - for reducing interfacial tension, controlling wetting properties and stabilizing emulsions and foams [235].

Langmuir systems can also be used as templates for oriented growth of crystals and as a model for the nucleation phase of biomineralization [181; 236]. They provide an ideally flat organic surface with controllable chemical composition and molecular density [21]. A variety of inorganic crystals such as NaCl, $CaCO_3$, $BaSO_4$, CdS, PbS and hydroxyapatite have been successfully grown with certain crystal-axis orientations under Langmuir monolayers with various functional groups lying at the air/water interfaces serving as nucleation sites [237].

Langmuir monolayers are necessary for the fabrication of LB films, they provide a way to manipulate molecules and construct artificial structural materials for optical, electronic or sensor applications. The LB-technique enables (i) the precise control of the monolayer thickness, (ii) homogeneous deposition of the monolayer over large areas and (iii) the possibility to make multilayer structures with varying layer composition. An additional advantage of the LB technique is that monolayers can be deposited on almost any kind of solid substrate. Also, heterogeneous catalysis or electrocatalysis can take advantage of the LB technique in the preparation of modified electrodes for specific reactions [238].

1.9.2 Biological applications

The potentiality of two-dimensional molecular self-assemblies can be clearly illustrated by Langmuir monolayers of lipid molecules. Langmuir monolayers have been extensively used as

models to understand the role and the organization of biological membranes [239] and to acquire knowledge about the molecular recognition process [240; 241; 242; 243; 244], since a biological membrane can be considered as two weakly coupled monolayers (Figure 1.9.1). The advantages of utilizing Langmuir monolayers as models for biological interfaces arise primarily from the ease with which experimental variables may be manipulated. These include parameters that are not readily controlled in bulk phase such as lateral pressure, surface area, and domain size and shape of the monolayer [14]. Therefore, Langmuir film provide an environment to study biological reactions in two dimensions [234]. For example, the study of interaction of DNA with Langmuir monolayers helps to observe the molecular recognition process at the surface of lipid monolayers and as a means of modeling cellular delivery of DNA across biological membranes in gene therapy [245; 246; 247]. Similarly, the immobilization/entrapment of protein/enzyme onto suitable substrate with minimal denaturation has been found extensively crucial for their biological importance in purification of a variety of drugs, peptides, antibodies, as well as applicability in developing various biomolecular devices [248; 249; 250; 251]. Langmuir Blodgett technique is the most versatile and convenient techniques for designing ultrathin film with biological functions.

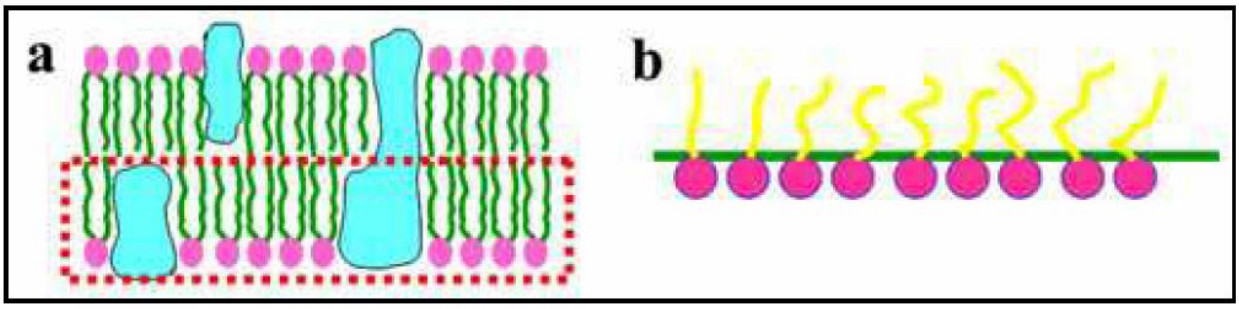

Figure 1.9.1: Schematic diagrams of a biomembrane (a) and a Langmuir monolayer (b).

1.10 Objectives

The focus of this study is divided into three parts

1. **Selection of reliable Wilhelmy plate material:** The selection of proper Wilhelmy plate material is very important in monolayer experiments, because the accurate value of surface pressure depends on the contact angle between the subphase liquid and the Wilhelmy plate material. Therefore to choose the reliable Wilhelmy plate material, the effects of different Wilhelmy plate materials, filter paper, platinum plate and glass slide on Langmuir film isotherms of stearic acid (SA), octadecylamine (ODA), and octadecanethiol (ODT) are investigated.
2. **Investigate the interactions in mixed monolayers:** Mixed monolayers have wide applications in sensors, optoelectronic devices and as models mimicking biological membranes due to the vast properties of a multicomponent system than that of pure ones. In addition to that, some substances cannot form stable monolayers by themselves but they can remain at the interface when mixed with suitable film forming materials. Thioureas constitute a well-known class of molecules with biological importance, therefore, the mechanism of interaction between thiourea and other substances within and across membranes would be of interest. So, interaction between a long-chain thiourea and a fatty acid was considered pertinent.

   Amphiphiles of Schiff base derivatives exhibit interesting optical and electrical properties. Mixed monolayers of Schiff base derivatives, 2-[(Octadecylimino)methyl] phenol (ODIMP) and 2-methoxy-6-[(octadecylimino) methyl] phenol (MODIMP) with octadecylamine and stearic acid respectively, are investigated.

3. **Study the interactions of monolayers with metal ions in the subphase:** The properties of Langmuir films at the air/water interface are strongly affected by metal ions in the aqueous subphase. Among the metal ions, copper is an essential co-factor for many enzymes and Cu-S bond is involved in many biological reactions. Thus the effect of Cu^{2+} contained in the subphase on a sulphur containing unstable amphiphile monolayer would be of interest. The effect of *N*-octadecyl-*N'*-phenylthiourea over copper containing subphase is investigated.

CHAPTER 2
EXPERIMENTAL METHODS AND MATERIALS

In-situ characterization of Langmuir monolayer at the air/water interface is always difficult because of the small amounts of substance in a single monolayer [21]. Several techniques are employed to study monolayer films on the water surface, such as π-A isotherms, grazing incidence X-ray diffraction (GIXRD), Brewster angle microscopy (BAM) and Fluorescence imaging microscopy (FIM) [14; 15; 16]. It is known that thermodynamic measurements such as π-A isotherms cannot reveal detailed microscopic information. BAM and fluorescence imaging microscopy can be employed to directly visualize the morphology of a monolayer. However, these observations are confined to macroscopic and mesoscopic scales [252] and can determine neither molecular characteristics such as conformation and packing of the alkyl chains nor structure and interaction pattern of the head groups. The GIXRD technique is a valuable tool to obtain direct structural information of crystalline films at the air/water interface on the sub nanometer scale [15; 16], but is limited by the low scattering intensity arising from the monolayers at the interface [253]. Infrared reflection-absorption spectroscopy (IRRAS) has emerged as one of the leading methods for structural analyses of monolayer at the air/water interface over the last decade [193; 254; 255]. The IRRAS technique not only allows the characterization of chain conformation and head group structure but also provides qualitative and quantitative information about molecular orientation. Among these, measurement of π-A isotherms using the Langmuir balance is the oldest and the most widely used technique to characterize Langmuir monolayers. Simple as it is, the technique still provides a wealth of information about the packing characteristics of molecules, their orientation at the interface and phase transitions, hence the use of this technique in this work.

2.1 Langmuir technique: surface film balance

Langmuir films were produced and characterized using a Langmuir trough or a Langmuir film balance. Investigations using a Langmuir trough yield information about the packing behaviour of the film, the orientation of the monolayer, the phase transitions occurring during its compressions, area per molecule in the film, its compressibility and if any reaction is taking place that might result in a change in the molecular area behaviour. In the present study a Nima Langmuir film balance was used. Nima trough is a commercially available, computer controlled, modified Langmuir film balance [256]. The instrument consists of a shallow trough made from a single slab of Teflon and has the dimensions 30 cm long, 20 cm wide and 0.5 cm deep. There are two movable Teflon barriers about 1 cm wide, which rest on the trough and which are used to adjust area enclosed between them. The barriers can be moved by electrical motors, which are controlled by computer. The two could either be moved independently so as to vary the enclosed surface area or move them simultaneously from one part of the trough to another while maintaining the enclosed area so as to transfer the monolayer between different subphases. In this study the former barrier mechanism was employed, whereby during the compression, the position of one of the barriers was kept fixed and the other moved at a controlled speed. The software displayed the surface pressure-area curve during compression on the computer screen and the data for that particular isotherm was automatically stored in the computer disk. Changes in surface tension were sensed by a Wilhelmy plate, which was attached to the pressure sensor by means of hooks.

Figure 2.1.1 shows the schematic representation of the experimental set up. Any changes in the net balance of forces on the plate are measured by a sensitive balance and displayed on the computer. The balance comprises a magnetic coil and a linear variable displacement transformer (LVDT), whose position depends on the force experienced by the Wilhelmy plate attached to it. The signal from the LVDT is displayed as weight on the computer screen. A calibration procedure allows it to be converted to the corresponding value of surface tension.

Before measurement using the Wilhelmy plate, the pressure sensor is calibrated by attaching a calibration weight to the LVDT instead. A 100 mg mass is used for the calibration, by placing it in an empty pan attached to the LVDT after zeroing the balance with the empty pan attached. The reading of the balance with the 100 mg mass should be 48.3 mNm^{-1}, a value which has been calculated using the dimensions of the Wilhelmy plate (10 mm wide and 0.15 mm thick). If the reading differs from this value, it is adjusted using the calibration button to give 48.3 mN/m. This setting is then stored in the memory. Before any measurement, the inside of the trough is cleaned thoroughly. First it is cleaned with soapy water, followed by thorough rinsing with distilled water. It was then cleaned with hexane using tissue paper. Finally it was thoroughly rinsed with copious amounts of triply distilled water. After the cleaning, the trough is filled to the brim with the desired subphase. Before spreading the monolayer, the barriers were moved toward each other thereby collecting any surface-active contaminants in the center of the trough. Next a pipet connected to a vacuum pump was used to suction off surface-active contaminants. The cleaning procedure was repeated several times. Blank runs on pure water and with spread pure solvent were made to ensure that there was no surface impurity. The movable barrier was then opened to an area of 240 cm^2, and the pressure was set to zero.

The Wilhelmy plate was attached to the pressure sensor through 'S' shaped hooks and lowered towards the subphase with one of its edges slightly immersed in the subphase. Then small aliquots of monolayer solution based on the desired initial area per molecule were slowly deposited on different locations on the subphase with a 100 μL Hamilton micro syringe. The monolayer forming solutions were prepared by dissolving the amphiphiles in appropriate volatile solvents (hexane and chloroform). Following the common practice a minimum of 5 minutes was allowed after spreading to ensure the volatile solvent, hexane/chloroform, evaporated before all measurements.

During all isotherm measurements, the surface pressure was continuously recorded by the Wilhelmy plate technique. The measurements were made at a constant temperature of 25 ºC, by allowing the substrate water to come to this temperature by storing it in a water bath.

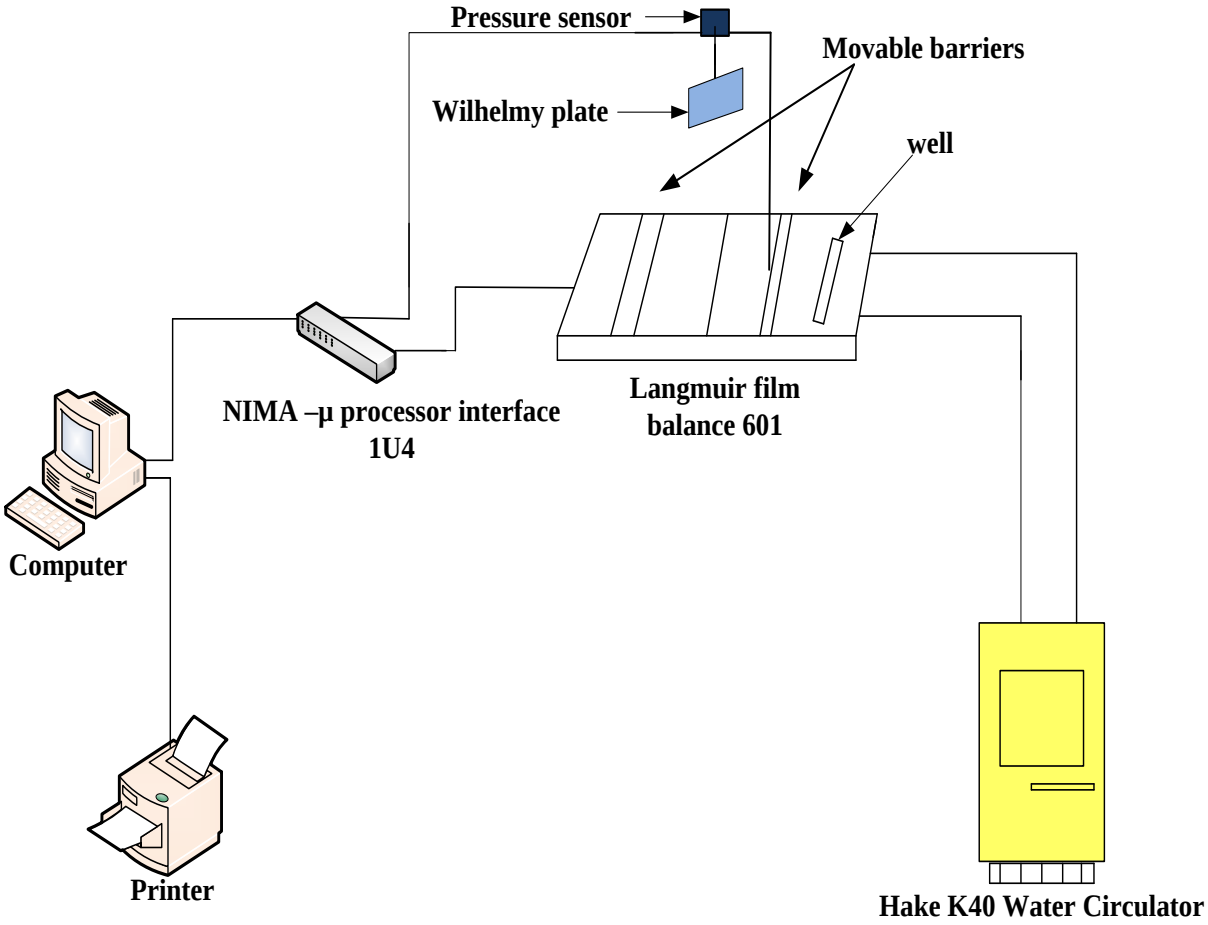

Figure 2.1.1: Schematic representation of experimental setup for study of reactions of Langmuir monolayers.

2.1.1 Surface pressure-area isotherms

After the spreading of the monolayer, the barrier was set in motion at a speed corresponding to the reduction of the area available to the monolayer of 10 cm^2/min. The screen displayed the isotherm as it was being generated in the form of the surface pressure versus the area.

2.1.2 Hysteresis loops: compression and expansion isotherms

To measure hysteresis curves, the monolayer was compressed at a speed of 10 cm^2/min and before it collapsed, the motion of the barrier was reversed to start expansion, by setting the speed on the computer to -10 cm^2/min. After the monolayer expanded fully to the point where the compression had originally started, the sign of the speed was changed back to positive to compress the monolayer to repeat the cycle. Similarly, several cycles were recorded. The hysteresis loops can be used to determine the reversibility of the π-A isotherm obtained during the compression process.

2.1.3 Surface pressure-time (π-t) measurement

Surface pressure-time curves, give the information about the accumulation of the complex species at the air/water interface and/or about the nature of the relaxations of the film forming molecules inside the film and/or about the desorption of the molecules in the bulk water subphase with time. For obtaining π-t curve, first of all a desired amount of monolayer material was spread at the air/water interface. After allowing 10 minutes for the solvent to evaporate, the barrier was moved to a different position where a different fixed target pressure was achieved, and fixed there. The surface pressure was then recorded as a function of time.

2.2 Materials

2.2.1 Wilhelmy plate materials

Platinum plate (dimensions, 10 mm × 10 mm).

Filter paper (dimensions, 10 mm × 10 mm).

Glass slide (dimensions 18 mm × 18 mm).

2.2.2 Surfactants

Surfactants used in this study are

Commercial stearic acid (SA, 90%, Saarchem, South Africa; Recrystallized from hexane) Octadecylamine (ODA, 98%, Aldrich Chemicals, UK; Recrystallized from hexane) Octadecanethiol (ODT, 98%, Aldrich Chemicals, UK; Recrystallized from hexane)

N-Octadecyl-*N'*-phenylthiourea [OPT, synthesized from phenylisothiocyanate (98%, Acros Organics, USA) and ODA]

2-[(Octadecylimino) methyl] phenol [ODIMP, synthesized from salicylaldehyde (98% from Acros Organics, USA) and ODA]

2-methoxy-6-[(octadecylimino)methyl]phenol [MODIMP, synthesized from *O*-vaniline 99%, Aldrich Chemicals, UK) and ODA]

The synthesis of OPT, ODIMP and MODIMP are described in the appropriate sections.

2.2.3 Subphases

The subphases used were triply distilled water and $CuSO_4$ (98.5%, Saarchem, South Africa) solution. The triply distilled water was prepared by taking deionized water from a milli-pore Elix 20 deionizer and redistilling it in a two-stage all-quartz still. $CuSO_4$ solution was prepared by dissolving appropriate amount of the salt in the triply distilled water.

2.2.4 Other chemicals

The other chemicals used in this study were hexane (96%, Rochelle, South Africa), ethanol (≥99.8%, Sigma-Aldrich, UK), Chloroform (99%, Rochelle chemicals, South Africa). They were used for the preparation of surfactant solutions.

2.3 Effect of Wilhelmy plate material on hysteresis of Langmuir monolayer isotherms

Commercial SA, ODA and ODT were recrystallized from hexane and their solutions were prepared. The solvents were pure hexane for SA and ODT and for ODA 5 mL of ethanol was added to the 20 mL hexane. Ethanol is added to enhance the solubility of ODA [18]. Ethanol and hexane were used as received. Pure water (triply distilled) was used as the subphase. Wilhelmy plates made of three different materials were used. They were: a platinum plate, a filter paper and a glass slide. To clean the platinum plate, it was heated in a flame to red hot to burn off any impurities. The filter paper was used without any treatment. The glass slide was cleaned with a solution of chromic acid (potassium dichromate in concentrated sulfuric acid) followed by thoroughly rinsing with copious amounts of triply distilled water.

The concentration of SA was 2.229×10^{-3} M, that of ODT was 4.174×10^{-3} M and for ODA it was 2.0248×10^{-3} M.

For monolayer preparation, 35 µL of ODA solution was spread in the case of filter paper and platinum plate and 25 µL was spread in the case of glass slide. For SA and ODT, 25 µL of solutions were spread for all three types of Wilhelmy plates.

2.4 Hysteresis of mixed monolayers of OPT and SA at air/water interface

OPT and SA are the surfactants used in this section. OPT (**3**) was synthesized by the reaction of phenylisothiocyanate (**1**) and ODA (**2**) following the reported method (Figure 2.4.1) [257]. A solution of 5.0 mmol each of phenylisothiocyanate (0.675 g) and ODA (1.345 g) in 25mL of distilled ethanol was refluxed for 30 min in a 100 mL round-bottom flask. The white solid product (OPT) obtained after allowing the solution to attain room temperature was filtered under suction and recrystallized from distilled ethanol three times. The yield obtained for OPT is 78%. The melting point was determined by using the Stuart melting point apparatus and found to be 87.3-88.1 °C. This is a new compound and has not been reported earlier in the literature.

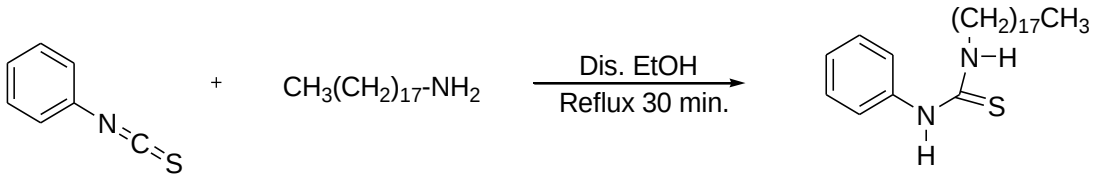

Figure 2.4.1: Synthesis of OPT.

2.4.1 Characterization of OPT

The product was characterized by satisfactory spectral data

IR (Perkin-Elmer Spectrum 100 FTIR) cm^{-1}: 3233 ν (N–H), 3054 ν (Ar C–H), 1346 ν (C=S).

^{1}H NMR (CDCl3, δ ppm): 7.77–7.65 (br, 1H, NH), 7.48 (t, 2H, arom.), 7.35 (m, 1H, arom.), 7.25 (d, 2H), 6.09 (br, 1H, NH), 3.66 (t, 2H, N–CH2), 1.60 (m, 2H, CH2), 1.30 (s, 30H, fifteen methylene protons), 0.92 (t, 3H, CH3).

^{13}C NMR (CDCl3, δ ppm): 180.7 (C=S), 136.1, 130.3, 127.4, 125.3 (Four arom. carbons), 45.7 (N–CH2), 31.9, 29.7, 29.6, 29.55, 29.5, 29.4, 29.2, 29.0, 26.9, 22.7, 14 (CH_3)].

For monolayer studies, 4.043×10^{-3} M solution of OPT was prepared in chloroform and 3.585×10^{-3} M solution of recrystallized SA was prepared in hexane. To prepare pure monolayers, 75 µL of OPT and 25 µL of SA were spread on the subphase. OPT/SA mixed monolayers in different mole fractions were prepared by mixing appropriate quantities of SA and OPT solutions and then spread on the subphase. The solvent was allowed to evaporate and the monolayer was compressed to get the surface pressure-area per molecule (π-A) isotherm. Hysteresis cycles were also recorded.

2.5 Hysteresis of mixed monolayers of ODIMP and ODA at air/water interface

ODIMP (**5**) was synthesized according to the reported method by the condensation of salicylaldehyde and ODA (Figure 2.5.1) [258]. 0.6051 g (~5 mmol) of salicylaldehyde (**4**) in 25 ml distilled ethanol and 1.3505 g (~5 mmol) of ODA (**2**) were mixed in a 100 ml round bottomed flask and the resultant solution was refluxed for 30 min. The yellow solid product was filtered under suction, and recrystallized from distilled ethanol. The yield obtained for ODIMP is 74%. Stuart melting point apparatus was used to determine the melting point and was found to

be 43.9-45.2 °C. This value is consistent with the literature data (43-44 °C) [81]. The structure of the compound was verified by IR, ^{1}H-NMR and ^{13}C NMR spectroscopy.

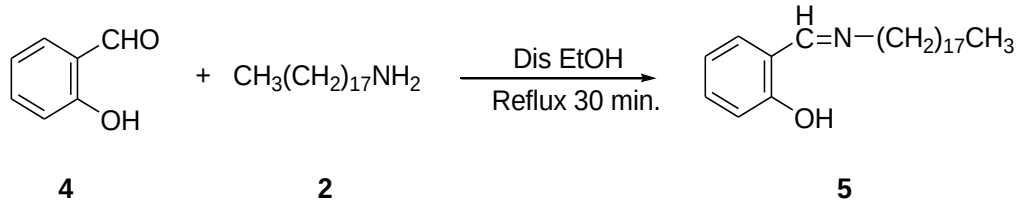

4 **2** **5**

Figure 2.5.1: Synthesis of ODIMP.

2.5.1 Characterization of ODIMP

(IR, neat, cm^{-1}): 2915, 2847, 1633, 1580.

^{1}H NMR ($CDCl_3$, δ ppm): 0.93 (t, 3H, CH_3); 1.30 (s, 30H, fifteen methylene protons); 1.74 (m, 2H, CH_2); 3.64 (t, 2H, N-CH_2); 6.91 (t, 1H, arom.), 7.01 (d, 1H, arom.), 7.32 (m, 1H, arom.), 8.38 (s, 1H, CH=N), 13.76 (br, 1H, OH).

^{13}C NMR ($CDCl_3$, δ ppm): 14.1 (CH_3); 22.7, 27.2, 29.4, 29.6, 29.7, 29.7, 30.9, 32.0 (CH_2); 59.6 (N-CH_2); 117.1, 118.4, 118.8, 131.1, 132.0 (five aromatic carbons); 164.4 (CH=N), 161.5 (C-OH).

4.274 x10^{-3} M solution of ODA was prepared in hexane with 5% ethanol and the molarity of ODIMP solution is 4.015x10^{-3} M. Pure monolayers were prepared by spreading 25 µL of ODA and ODIMP solutions on the subphase. Two different spreading methods are used to prepare the ODIMP/ODA mixed monolayer.

1 Mixed Monolayers prepared by spreading the ODIMP and ODA solutions individually

Appropriate quantities of ODIMP and ODA stock solutions were individually added onto the subphase in sequence to control the monolayer composition. Hysteresis of surface pressure-area per molecule (π-A) isotherms were recorded.

2 Mixed monolayers prepared by spreading the premixed solution of ODIMP and ODA

For this method, ODIMP and ODA were premixed in different mole fractions in chloroform and then cospread onto the subphase. Hysteresis of surface pressure-area per molecule (π-A) isotherms were recorded.

2.6 Monolayer characteristics of mixed MODIMP and SA at air/water interface

MODIMP was synthesized by the condensation of *O*-vaniline and ODA in distilled ethanol in equimolar ratio (Figure 2.6.1) [259]. 0.7858 g (~5 mmol) of *O*-vaniline (**6**) in distilled ethanol and 1.3907 g (~5 mmol) of ODA (**2**) were mixed in a 100 ml round bottomed flask and the resultant solution was refluxed for 30 min. The yellow solid product was filtered under suction, and recrystallized in distilled ethanol. The melting point was determined by Stuart melting point apparatus and found to be 71.2-73.3 °C. The yield obtained for MODIMP was 76%. This is also a new compound and has not been reported earlier. The structure of the compound was verified by IR, ^{1}H NMR and ^{13}C NMR spectroscopy.

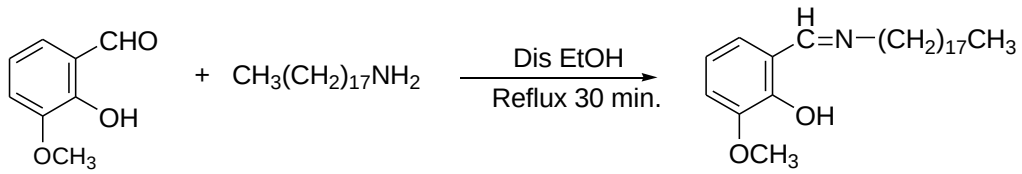

6 **2** **7**

Figure 2.6.1: Synthesis of MODIMP.

2.6.1 Characterization of MODIMP

(IR, neat, cm^{-1}): 2915, 2848, 1658, 1587, 1512.

^{1}H NMR ($CDCl_3$, δ ppm): 0.93 (t, 3H, CH_3); 1.30 (s, 30H, fifteen methylene protons); 1.73 (m, 2H, CH_2); 3.61 (t, 2H, N-CH_2); 3.93 (s, 3H, OCH_3); 4.42 (br, 1H, OH) 6.94 (d, 1H, arom.), 7.10 (dd, 1H, arom.), 7.13 (d, 1H, arom.), 7.47 (d, 1H, arom.); 8.19 (s, 1H, CH=N).

^{13}C NMR ($CDCl_3$, δ ppm): 14.1 (CH_3); 22.7, 27.4, 29.4, 29.5, 29.7, 30.0, 32.0 (CH_2); 56.0 (O-CH_3); 61.5 (N-CH_2); 108.4 114.2, 123.9, 128.9, 147.3, 148.5 (six aromatic carbons); 160.7 (CH=N).

For monolayer studies, 3.881×10^{-3} M SA and 2.180×10^{-3} M MODIMP were prepared in chloroform. To prepare the pure monolayers, 25 µL of respective solutions were spread on the subphase. Mixed monolayers were prepared by mixing the appropriate volumes of both solutions and 25 µL of the mixture was spread on the subphase.

2.7 Langmuir monolayers modulated by known chemical reactions: Behaviour of OPT over copper-containing subphase.

OPT (**3**) was synthesized by the reaction of phenylisothiocyanate (**1**) and ODA (**2**) as explained before (Figure 2.4.1). For monolayer studies, a 4.023×10^{-3} M solution of OPT was prepared in chloroform. $CuSO_4$ solution was used as the subphase. The concentration of the $CuSO_4$ solution in the subphase used for the formation of the metal complex was $5x10^{-4}$ M. The interfacial surface activity of OPT was studied by monitoring the surface pressure (π)-time (t) curves as well as the surface pressure (π)-area (A) isotherms.

CHAPTER 3
RESULTS AND DISCUSSION

3.1 Effect of Wilhelmy plate material on hysteresis of Langmuir monolayer isotherms

The selection of proper Wilhelmy plate material is very important in monolayer experiments, because the accurate value of surface pressure depends on the contact angle between the subphase liquid and the Wilhelmy plate material. Therefore to choose the reliable Wilhelmy plate material, the effects of three Wilhelmy plate materials, platinum foil, filter paper and glass slide, on Langmuir film isotherms were investigated. In these investigations three film-forming substances, having the same alkyl chain length (18 carbon atoms) and differing in the kind of a polar head group; namely, SA, ODA, and ODT were chosen. Hysteresis of surface pressure-area isotherms of these three substances were also measured.

3.1.1 Hysteresis isotherms using filter paper Wilhelmy plate

Figure 3.1.1 shows the hysteresis isotherm of ODA at air/water interface at 25 °C. When the ODA monolayer was compressed over pure water, a steep curve was obtained, indicating the highly condensed and low compressibility characteristics of the ODA monolayer. The surface pressure is nearly constant at 0 mN/m in the early compression stage. The limiting area is 21.2 $Å^2$/molecule, estimated by extrapolating the constant slope region of the isotherm to zero surface pressure. This value is consistent with the literature data, ~ 21 $Å^2$/molecule [260]. When the monolayer is expanded from 45 mN/m the curve shifted slightly to the left side, towards lower area. On recompression, the second compression curve also shifted to the left side. The first cycle is the right-most trace in the diagram. The left shifts of the expansion curve and the

subsequent cycles are negligible and indicate the loss of the monolayer material. This phenomenon can be ascribed to the solubility of ODA molecules in water which had been reported earlier [54; 94; 135].

Figure 3.1.2 shows the hysteresis isotherm of SA monolayer over air/water interface at 25 °C. When the monolayer is compressed, initially it is a smoothly rising curve with a lift off area 20.2 $Å^2$/molecule and the behaviour is that of a liquid expanded film. Around a surface pressure of 25 mN/m, the transition to a steeper portion of the curve occurred, indicating the attainment of solid phase. The area/molecule of pure SA was 20.0 $Å^2$/molecule at 25 mN/m. These values and the shape of the pure SA isotherm were in good agreement with the reported results [127; 261] . In this case also the expansion curve shifted to the left side slightly compared to the compression. In the second and third compression-expansion cycles, the compression curves follow closely the expansion traces of the previous cycles. These phenomena indicate the mild hysteresis behaviour of SA monolayer with a slight area loss after each compression-expansion cycle. According to the relaxation experiment reported in a previous work [94] the hysteresis and area loss of SA can be ascribed to the formation of 3D aggregates after compression to high surface pressures.

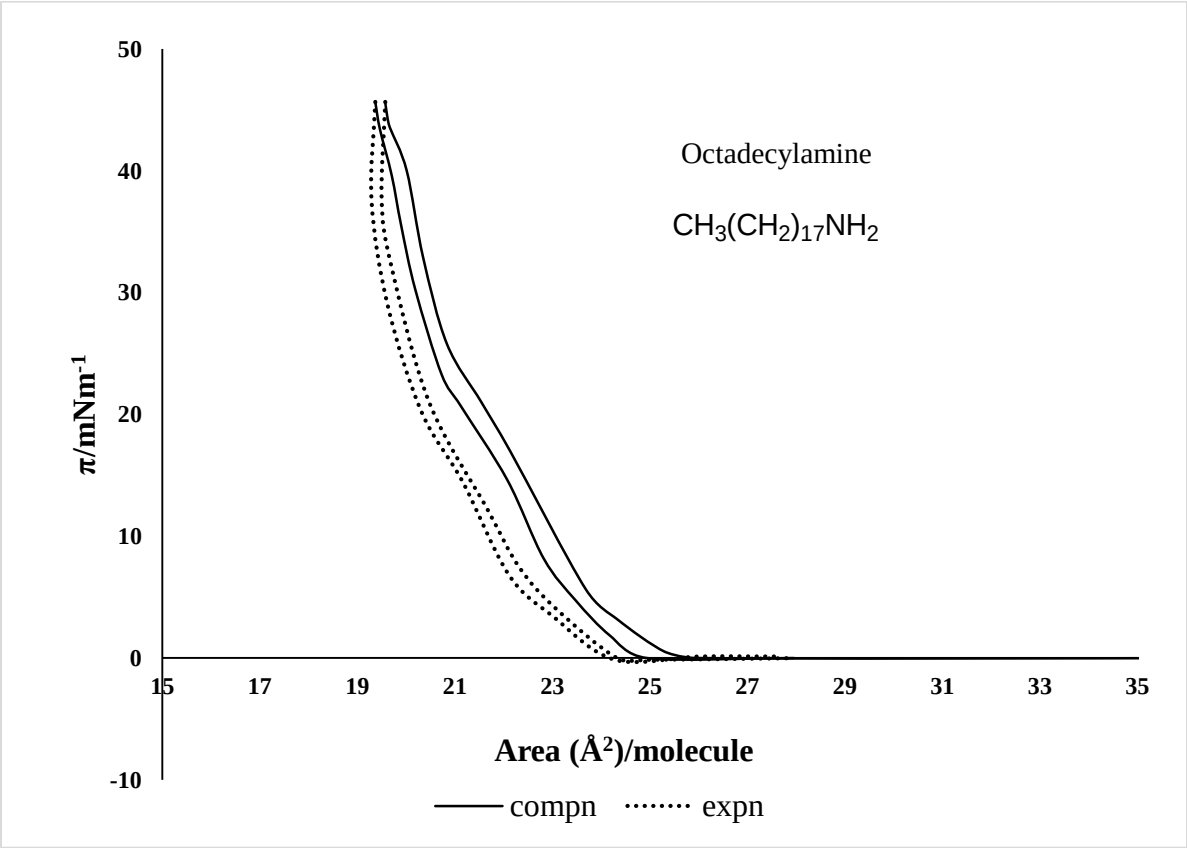

Figure 3.1.1: Surface pressure-area hysteresis isotherm of ODA monolayer over air/water interface at 25 °C using filter paper Wilhelmy plate.

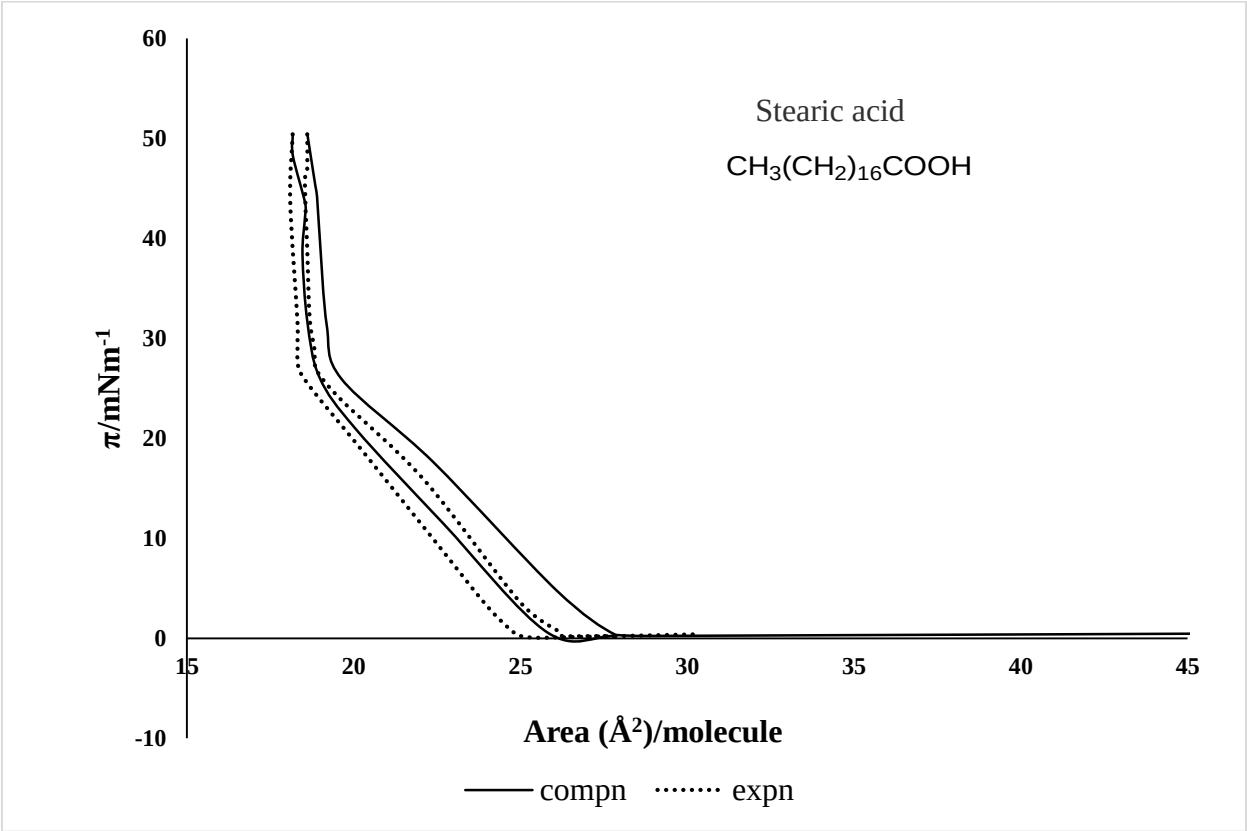

Figure 3.1.2: Surface pressure-area hysteresis isotherm of SA monolayer over air/water interface at 25 °C using filter paper Wilhelmy plate.

The hysteresis of surface pressure-area per molecule isotherm of ODT monolayer using filter paper Wilhelmy plate over pure water is shown in Figure 3.1.3. The isotherm shows the co-existence of gas and a condensed phase up to 23.6 $Å^2$/molecule, where there is a sharp change in the slope of the isotherm indicating the onset of the condensed phase. The isotherm yields a limiting area per molecule of 23.2 $Å^2$, which approximately corresponds to the cross sectional area of an alkyl chain. Hence the steep region of the isotherm may correspond to the untilted condensed phase. In this case also a narrow hysteresis loop is noticeable and the isotherms registered in subsequent compression-expansion cycles are shifted towards lower mean molecular areas. It has been reported [262] that at lower subphase temperatures the spreading of thiols can be limited and 3D aggregates can be present in the monolayers, but at higher subphase temperatures (especially higher as the bulk melting point) the degree of molecular organization decreases dramatically. Therefore the hysteresis and area loss of ODT also can be ascribed to the formation of 3D aggregates.

With the filter paper as the Wilhelmy plate, the hysteresis curves of these three substances showed that the isotherms were reversible. Except for a small amount of loss of film material, the curves were superimposable. This shows that for all the three substances, the contact angle of water with the filter paper did not change from one cycle to the next.

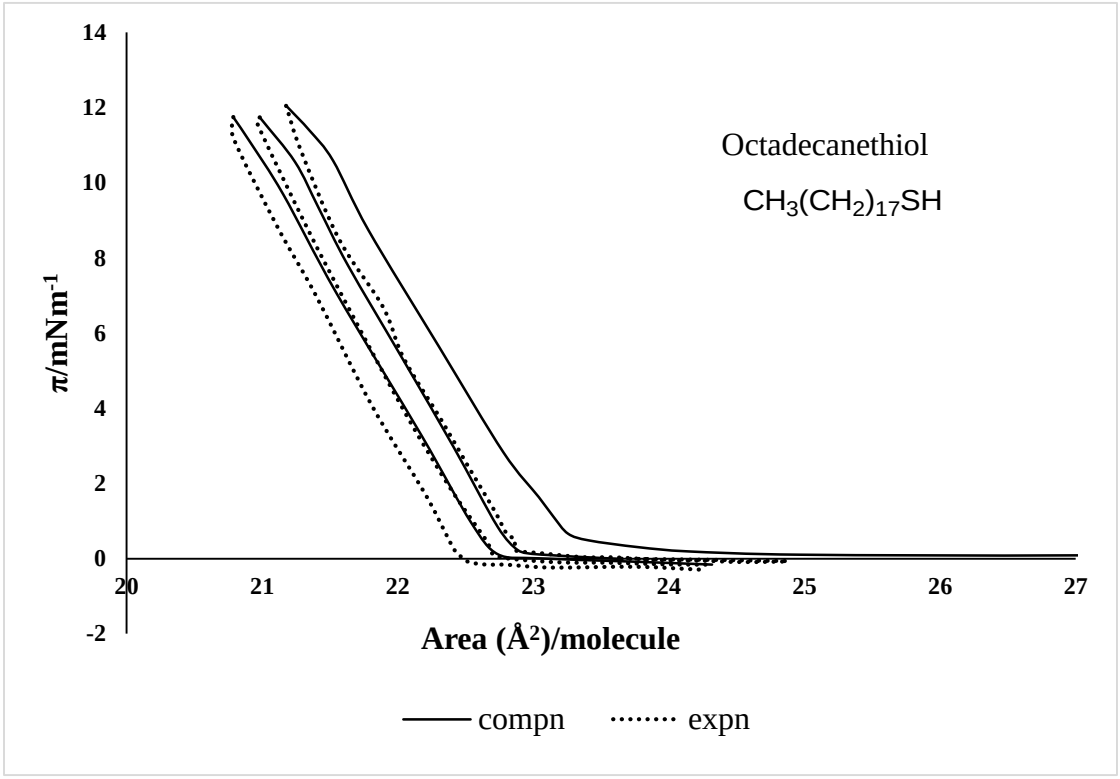

Figure 3.1.3: Surface pressure-area hysteresis isotherm of ODT monolayer over air/water interface at 25 °C using filter paper Wilhelmy plate.

3.1.2 Hysteresis isotherms using platinum Wilhelmy plate

The behaviour of the monolayers with the platinum foil contrasts markedly with filter paper, particularly for ODA. For the amine (Figure 3.1.4), instead of the isotherm beginning with a flat region as with the filter paper, the surface pressure curve continuously rises gently, before it reaches the region where it starts to increase steeply. The beginning surface pressure was ~ 5 mN/m and it starts to increase steeply at ~ 7 mN/m. The limiting area per molecule is found to be 21.1 $Å^2$/molecule. This continuous gentle increase is caused by the continuous adsorption of the amine on the Wilhelmy plate surface and this slightly modifies the contact angle of the subphase against the platinum plate, thereby altering the force on the place.

According to Young's equation, which relates interfacial tension with the contact angle, θ,

$$\cos\theta = \frac{\gamma_{SV}-\gamma_{SL}}{\gamma_{LV}} \qquad \text{Equation 12}$$

where the γ's are the interfacial tensions at the various boundaries between the solid (S), liquid (L) and vapor (V) phases as indicated in the subscripts.

For complete wetting, there is no finite contact angle, and if $\gamma_{LV} > \gamma_{SV} - \gamma_{SL,}$ $\cos\theta < 1$, and a finite equilibrium contact angle is established. By the introduction of an insoluble monolayer under a finite surface pressure the contact angle will decrease, and the complete wetting will take place. But in the presence of a soluble surface active agent, it is likely that both γ_{LV} and γ_{SL} will change, and whether θ will increase or decrease on the introduction of such a substance will depend on which tension is more affected.

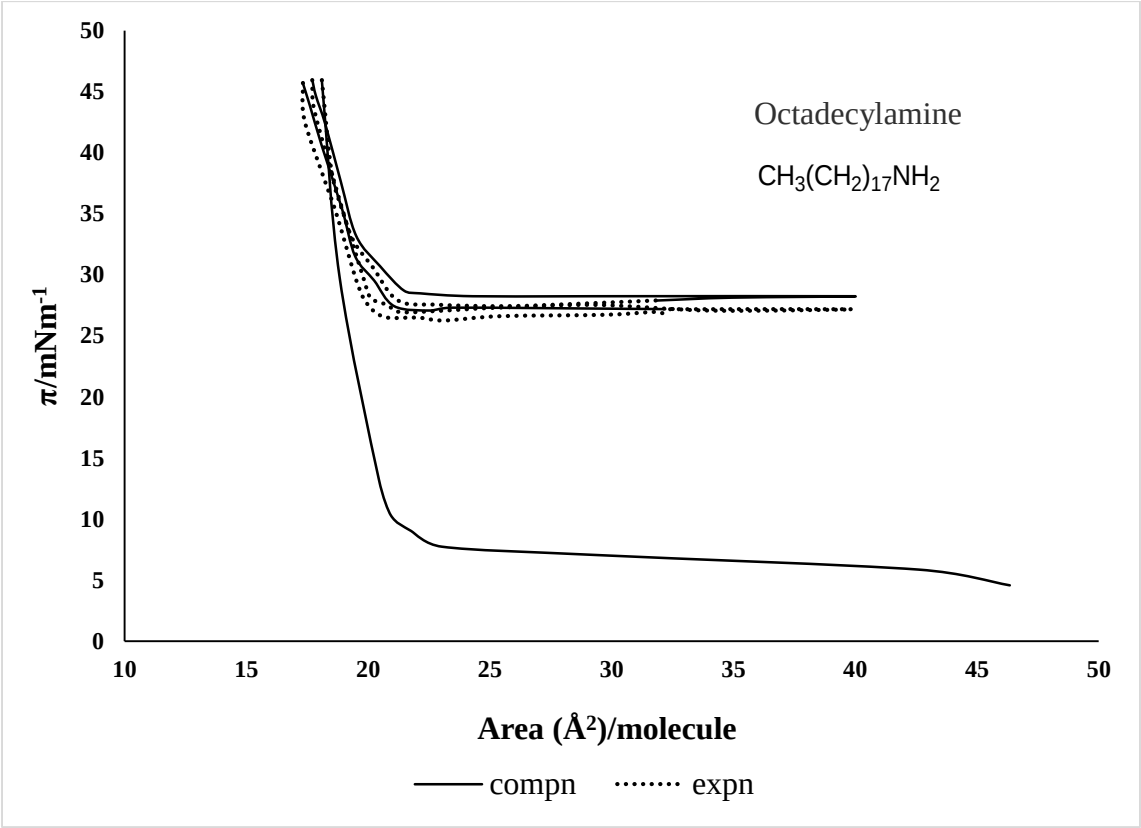

Figure 3.1.4: Surface pressure-area hysteresis isotherm of ODA monolayer over air/water interface at 25 °C using platinum Wilhelmy plate.

In the case of ODA, the higher solubility behaviour might be responsible for a high value of γ_{LV}. Therefore, $\gamma_{LV} > \gamma_{SV} - \gamma_{SL}$, so, the contact angle θ has a value other than zero, causing the measured value to be different from the true value of surface tension. This interpretation is confirmed by the hysteresis curves. During hysteresis measurements of the amine with platinum plate the baseline of the second cycle does not coincide with that of the first cycle. When the monolayer is expanded from a surface pressure of 45 mN/m, the surface pressure does not reach zero on full expansion. Instead, what should be the region of zero surface pressure (the baseline on full expansion) shows a pressure over 25 mN/m. On recompression the surface pressure increases but the beginning surface pressure of the second cycle was still 25 mN/m.

This behaviour is peculiar to ODA. When the π-A hysteresis isotherm of the ODT was measured using a platinum plate (Figure 3.1.5), the surface pressure was constant in the beginning, and the lift-off area appears at 24.8 $Å^2$/molecule. The first expansion curve closely followed the first compression curve but the baselines did not coincide, though the difference was small compared to ODA. The baselines of the subsequent cycles in hysteresis curves coincide with that of the first expansion curve. This leads to the conclusion that the contact angle of the Wilhelmy plate remains almost constant after the first cycle, which in turn implies that ODT does not get adsorbed significantly on platinum surface during the measurements.

Similarly, SA displays a small difference in isotherms measured subsequent to the first cycle (Figure 3.1.6). This indicates that the contact angle does not change significantly, which implies that SA too does not get adsorbed sufficiently on platinum surface. This is confirmed by the fact that the earlier portion of the isotherm is a straight line, with the surface pressure remaining constant before it starts rising steeply.

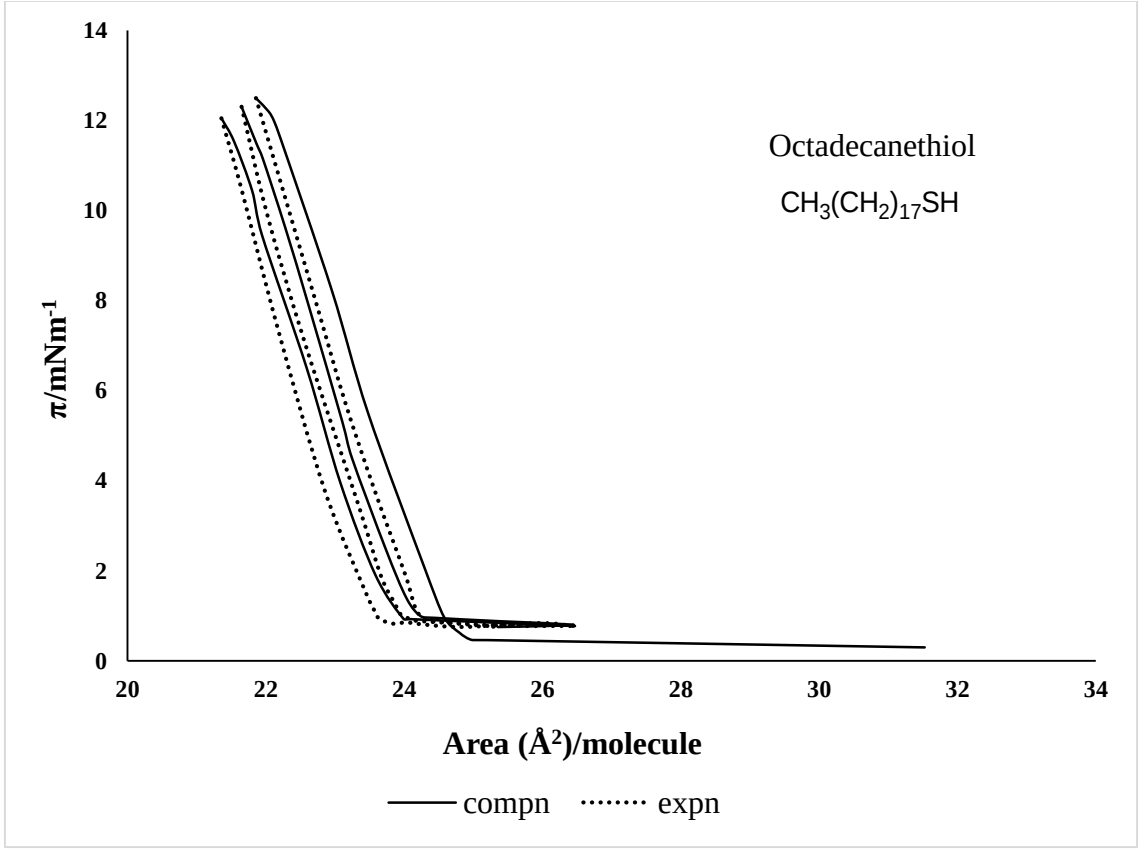

Figure 3.1.5: Surface pressure-area hysteresis isotherm of ODT monolayer over air/water interface at 25 °C using platinum Wilhelmy plate.

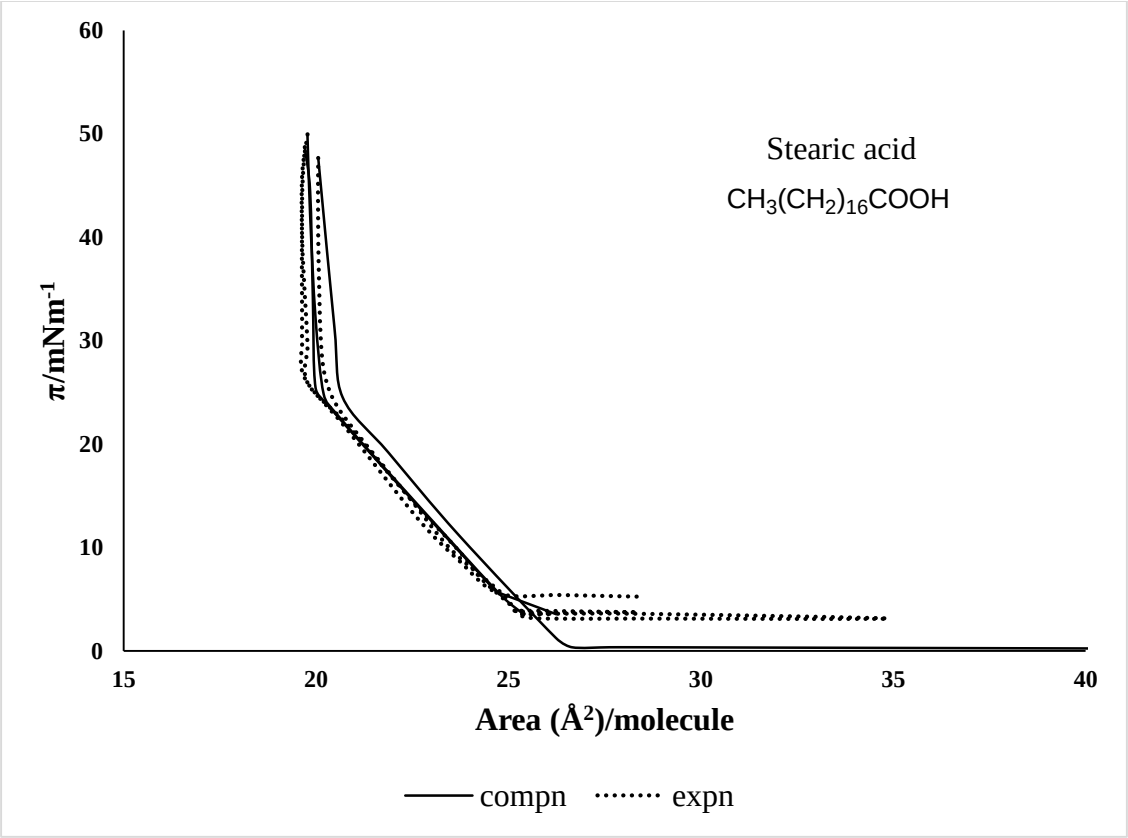

Figure 3.1.6: Surface pressure-area hysteresis isotherm of SA monolayer over air/water interface at 25 °C using platinum Wilhelmy plate.

3.1.3 Hysteresis isotherms using glass slide Wilhelmy plate

The behaviour with glass slide does not differ greatly from that of platinum foil. For amine (Figure 3.1.7) the initial surface pressure is too high, ~ 30 mN/m. Then the surface pressure curve continuously rises gently, before it reaches the region where it starts to increase steeply (35 mN/m). When the monolayer is expanded from 100 mN/m, the surface pressure does not reach zero on full expansion. Instead, it reaches only a surface pressure of ~ 80 mN/m. This indicates that the adsorption of the amine, hence the contact angle on the glass slide plate is even higher than that with the platinum plate.

For ODT, as with the platinum plate, the base line of the subsequent cycles in hysteresis curves shows a relatively small difference (Figure 3.1.8) from the first. The deviation is small, indicating that the contact angle of the Wilhelmy plate remains constant after the first cycle, which in turn implies that ODT does not get adsorbed significantly on glass slide during the measurements.

Similarly, SA also displays only a small difference in isotherms measured subsequent to the first cycle (Figure 3.1.9). In this case, the phase transition occurred at 45 mN/m, whereas both the filter paper and the glass slide, it occurred at ~ 25 mN/m.

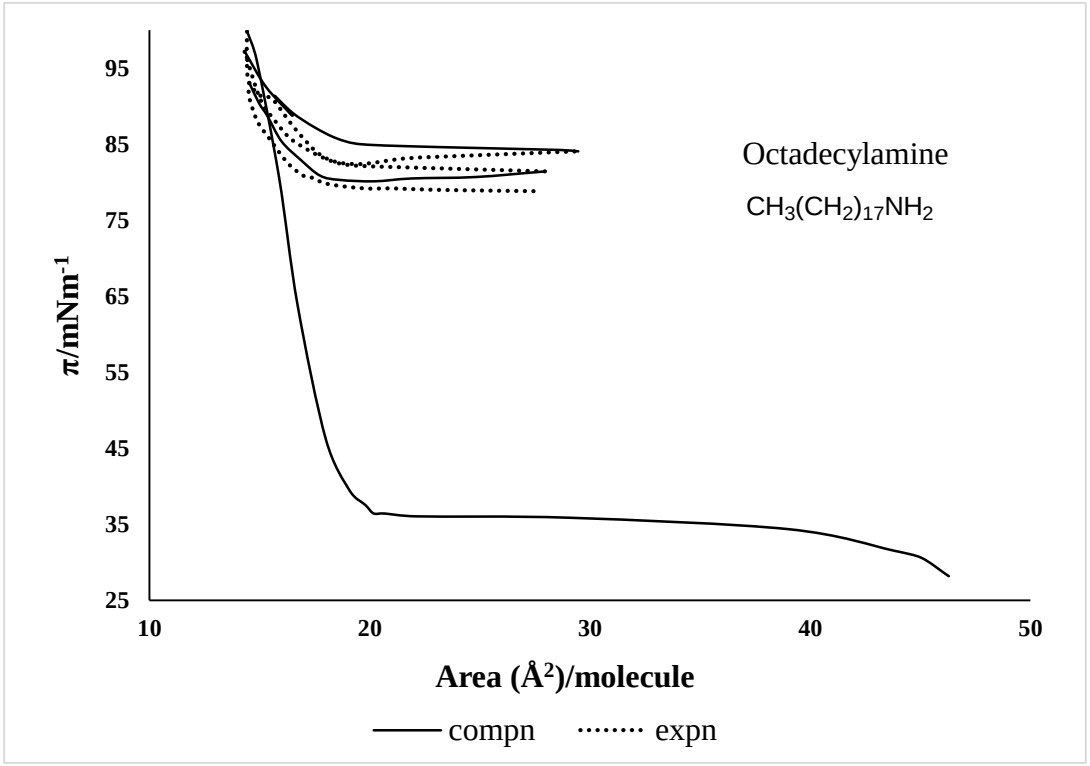

Figure 3.1.7: Surface pressure-area hysteresis isotherm of ODA monolayer over air/water interface at 25 °C using glass slide Wilhelmy plate.

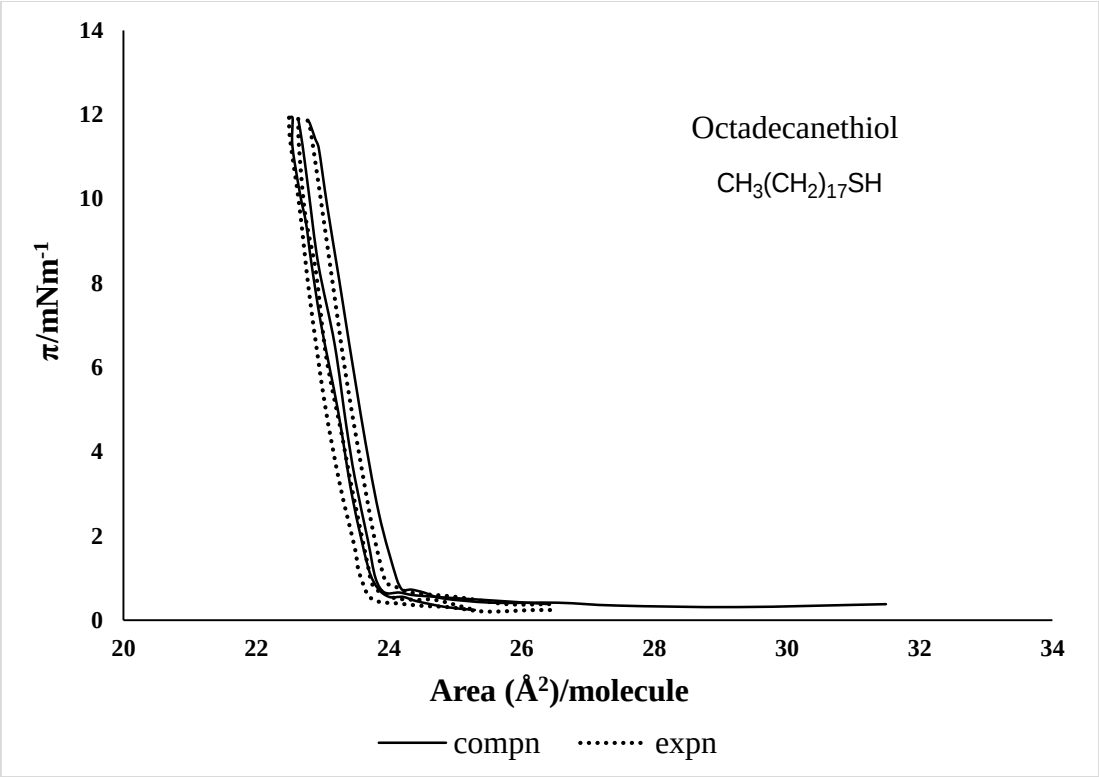

Figure 3.1.8: Surface pressure-area hysteresis isotherm of ODT monolayer over air/water at 25 °C using glass slide Wilhelmy plate.

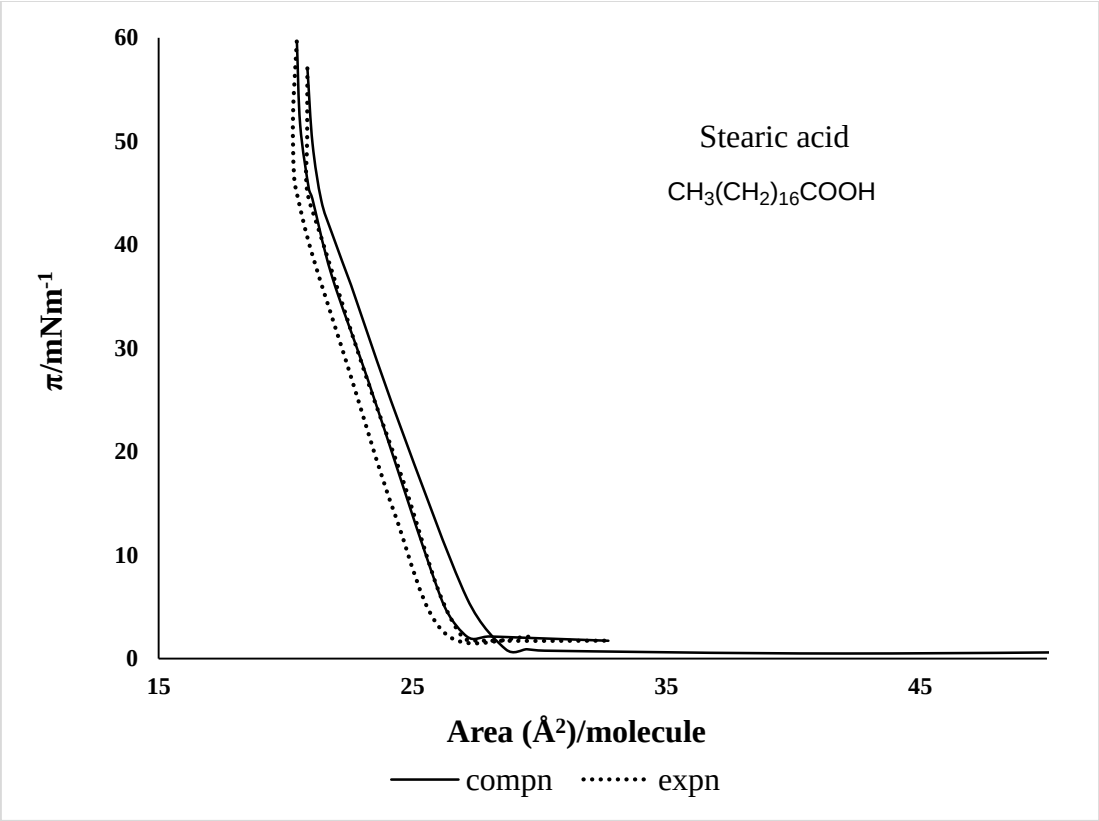

Figure 3.1.9: Surface pressure-area hysteresis isotherm of SA monolayer over air/water at 25 °C using glass slide Wilhelmy plate.

This difference in the behaviour in the case of platinum and glass plates on the one hand and filter paper on the other, points to different adsorption characteristics on the three materials. The hysteresis curves with filter paper plate show reversible behaviour for all the three substances, showing that the contact angle remains constant for all the cycles. This is as one would expect since paper is completely wetted. SA and ODT show reversible hysteresis curves on all three types of material. Adsorption on both platinum and glass is comparatively small, since subsequent isotherms differ only slightly from the first. Hysteresis shows that the loss of monolayer material during the experimental timeframe is minimal.

Therefore, the use of filter paper as the Wilhelmy plate is preferred, because of its wettability, whereby the contact angle of the subphase on the plate surface is always zero. This unique feature enables the filter paper to be reliably used to measure the surface pressure during compression and expansion of a monolayer and allows accurate control of the surface pressure [263], which is vital for proper deposition of Langmuir–Blodgett films.

3.2 Hysteresis of mixed monolayers of OPT and SA at air/water interface

In this work, the interaction between a long-chain thiourea, OPT and a fatty acid, SA has been investigated. Thioureas are important organic compounds, widely used in research and technological applications such as in the pharmaceutical industry [264; 265] and as catalysts in chemical reactions [266; 267; 268]. They possess high biological activity, act as corrosion inhibitors and antioxidants, and are important polymer components [269]. The mechanism of interaction between thiourea and other substances within and across membranes would be of interest because thioureas constitute a well-known class of molecules with biological importance [270]. Disubstituted thioureas are known to interact with several bioorganic molecules resulting in diverse types of biological activity such as anticancer activity against various types of leukemia and solid tumors [270], activity on the central nervous system [271], antimycobacterial activity [272], and antimicrobial activity [273]. They are selective analytical reagents, especially for the determination of metals in complex interfering materials [274]. Oxygen, nitrogen and sulphur donor atoms of thiourea derivatives provide a multitude of bonding possibilities [275; 276]. Hence the investigation of the interaction between a long-chain thiourea and a fatty acid was considered pertinent.

3.2.1 Surface pressure-area isotherm of OPT

To study the monolayer characteristics of pure OPT at the air/water interface, 75 µl of dilute chloroform solution of OPT (4.043×10^{-3} M) was spread at the air/water interface using a micro syringe. After allowing 5 minutes to evaporate the solvent, the barrier was compressed slowly, at a speed of 10 cm^2 /min, to record the surface pressure versus area per molecule. It was observed that the surface pressure begins to be measurable at about 8.8 $Å^2$/molecule

(Figure 3.2.1). Upon compression, the surface pressure increased linearly with diminishing area. The film has the characteristic of an expanded monolayers [26]. The area/molecule obtained by extrapolation of the linear part of the isotherm yield a value 7.5 $Å^2$/molecule. Such a small value indicates that the film is not a monolayer but a multilayer.

3.2.2 Surface pressure-area isotherm of SA

The pure SA isotherm is a smoothly rising curve with a lift off area 20.2 $Å^2$, which collapses at about 49 mN/m (Figure 3.2.2). A transition to a steeper portion of the curve occurs at about 25 mN/m indicating the formation of a solid phase. The area/molecule of pure SA was 20.0 $Å^2$ at 25 mN/m which is in agreement with the literatures [127; 261]. When the SA monolayer is compressed after the collapse point, 49 mN/m, it decreases sharply. With further compression the surface pressure essentially remains constant (Figure 3.2.3).

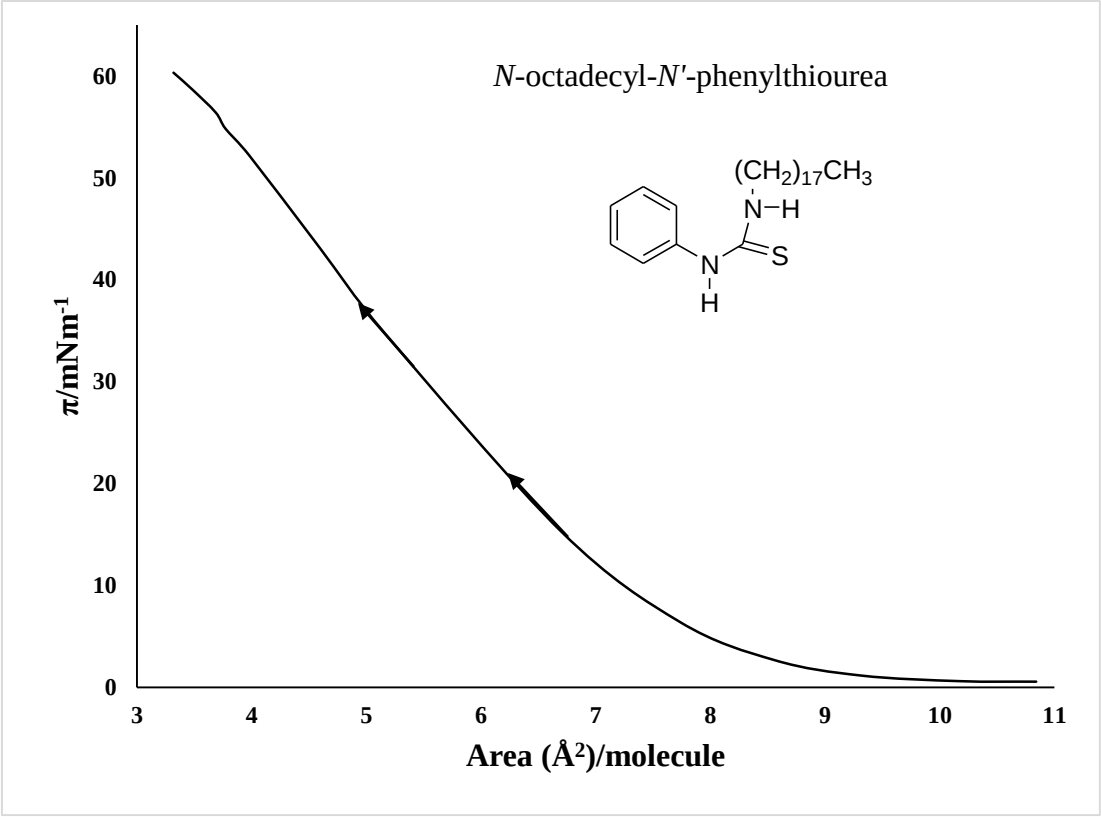

Figure 3.2.1: Surface pressure-area isotherm of OPT spread over air/water interface at 25 °C.

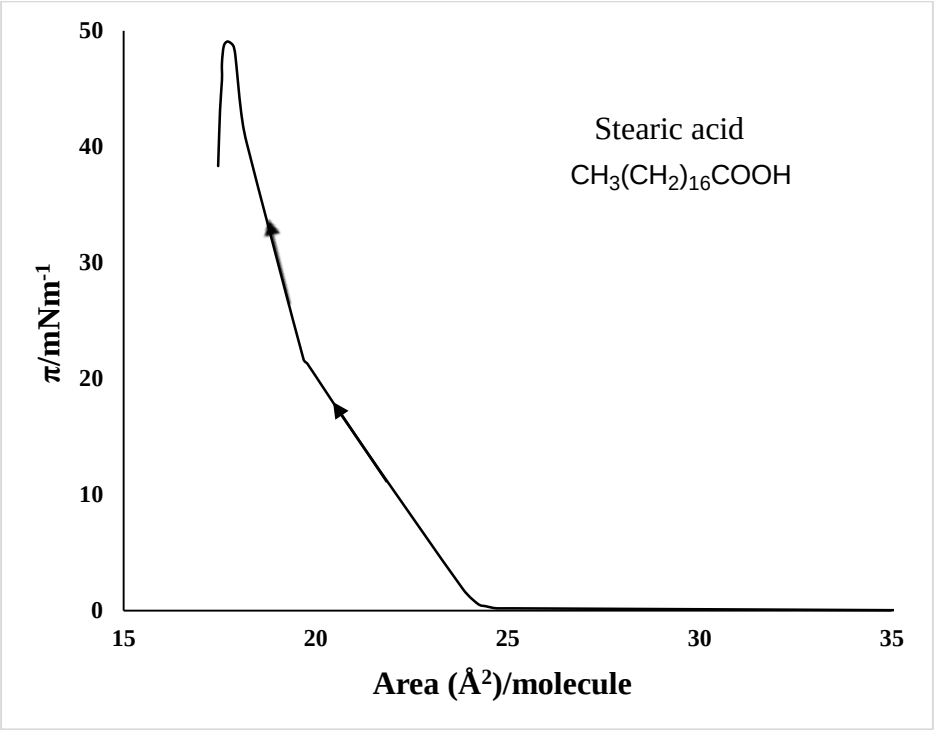

Figure 3.2.2: Surface pressure-area isotherm of SA spread over air/water interface at 25 °C.

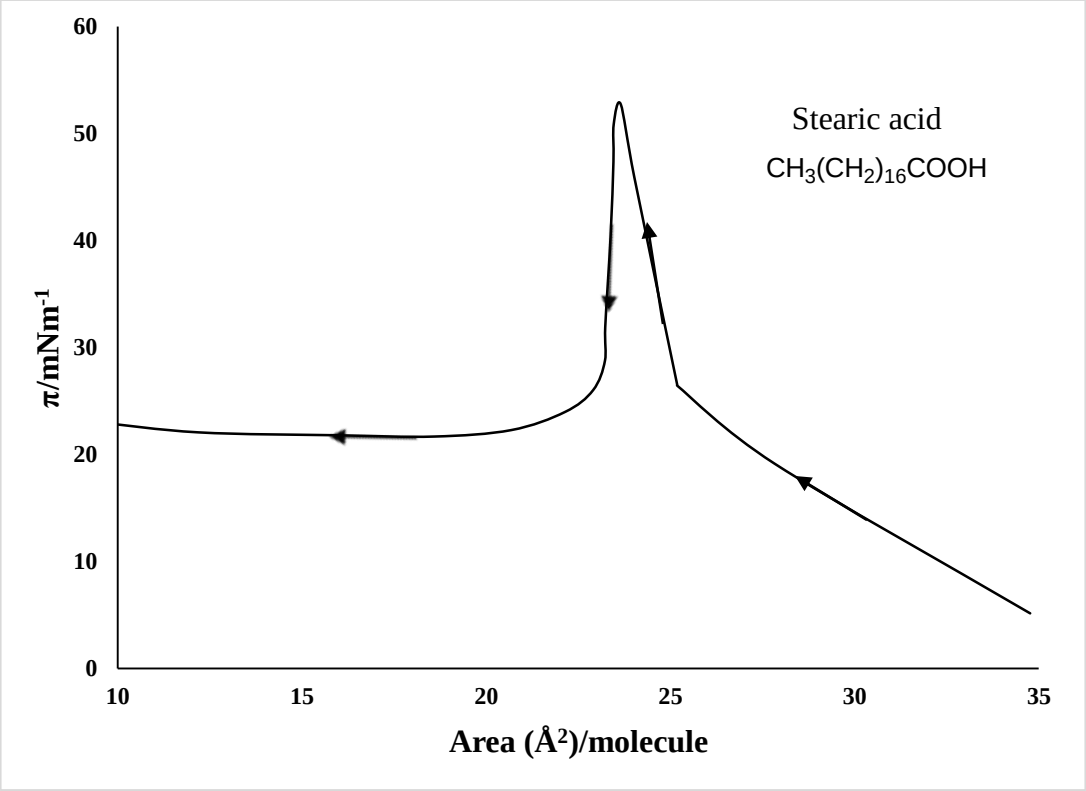

Figure 3.2.3: Surface pressure-area isotherm of SA (after collapse) spread over air/water interface at 25 °C.

3.2.3 Surface pressure-area hysteresis isotherms of mixed monolayers of OPT and SA

OPT alone does not form a stable monolayer. However, when mixed with SA, it was observed that stable and compressible films were formed. The behaviour of a monolayer formed by spreading an equimolar mixture of the two components and subjected to repeated compression-expansion cycles is shown in Figure 3.2.4. The initial compression is the right-most trace in the diagram. As the monolayer is compressed initially the behaviour is that of an expanded film. Around a surface pressure of 15 mN/m the curve starts to flatten out indicating a phase transition. As the area available to the film is decreased further, the surface pressure starts to rise steeply again. When the monolayer is expanded from a value of surface pressure of around 38 mN/m, there is a steep drop in the surface pressure to around 8 mN/m, followed by a gentler drop to about zero. On recompression the surface pressure increases but the second cycle does not retrace the curve of the first one. During the second cycle, the area per molecule is much smaller and the phase change that was pronounced during the first compression has largely disappeared. The expansion curve, however, follows the path of the first expansion. Subsequent cycles largely coincide with the second cycle indicating that it was during the first compression that changes took place in the monolayer, and the state of the monolayer was largely preserved through the subsequent compression-expansion cycles. The indication is that the film has reached a stable state and the composition of the monolayer remains unchanged during subsequent compressions and expansions.

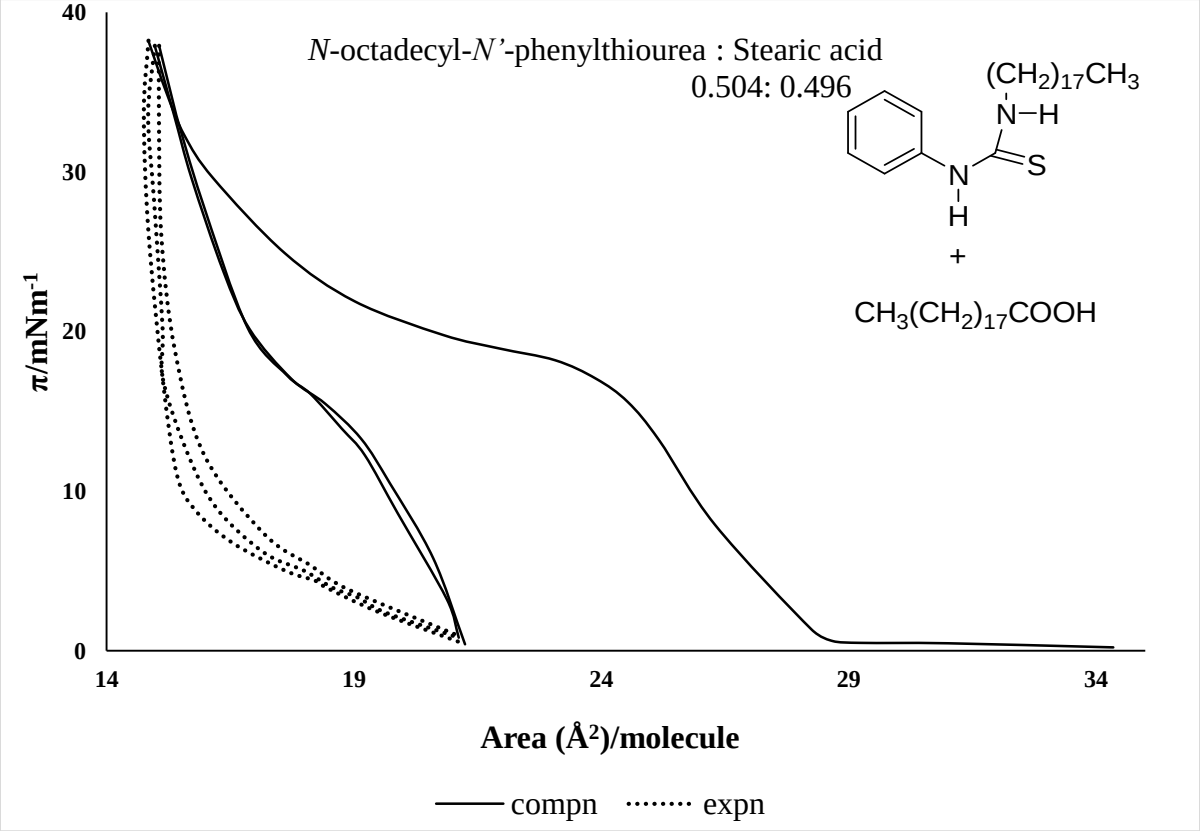

Figure 3.2.4: Surface pressure-area hysteresis isotherms of premixed OPT/SA monolayers of approximately equimolar composition over air/water interface at 25 °C.

The behaviour of the monolayer formed by spreading a 0.6:0.4 (OPT:SA) mixture is similar, as shown in Figure 3.2.5. The monolayers formed by spreading mixtures containing a mole fraction of SA 0.4 and above showed a plateau region around 14 – 17 mN/m. One possible explanation is that this results from an intermolecular proton transfer from the carboxylic acid to thiocarboxamide functional groups of an adjacent molecule [Eq. 13].

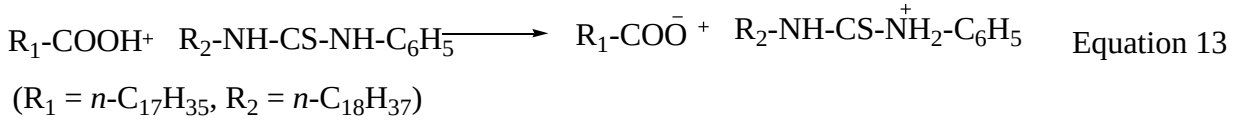

Equation 13

(R_1 = *n*-$C_{17}H_{35}$, R_2 = *n*-$C_{18}H_{37}$)

The attraction between the resulting ions draws them closer reducing the area, which shows as the flat region. This proton transfer can lead to a new monolayer phase, the behaviour of which does not correspond to either a pure OPT or pure SA monolayer. Figure 3.2.6 represents the behaviour of the monolayer formed by spreading 0.7:0.3 mixture. The behaviour is almost similar except that the initial surface pressure is ~ 4 mN/m, and no flat plateau was observed. The isotherms coincide after several cycles. Figure 3.2.7 shows the isotherm formed by spreading a 0.9:0.1 (OPT:SA) mixture. In this case also the initial pressure was high but the isotherms do not coincide completely.

.

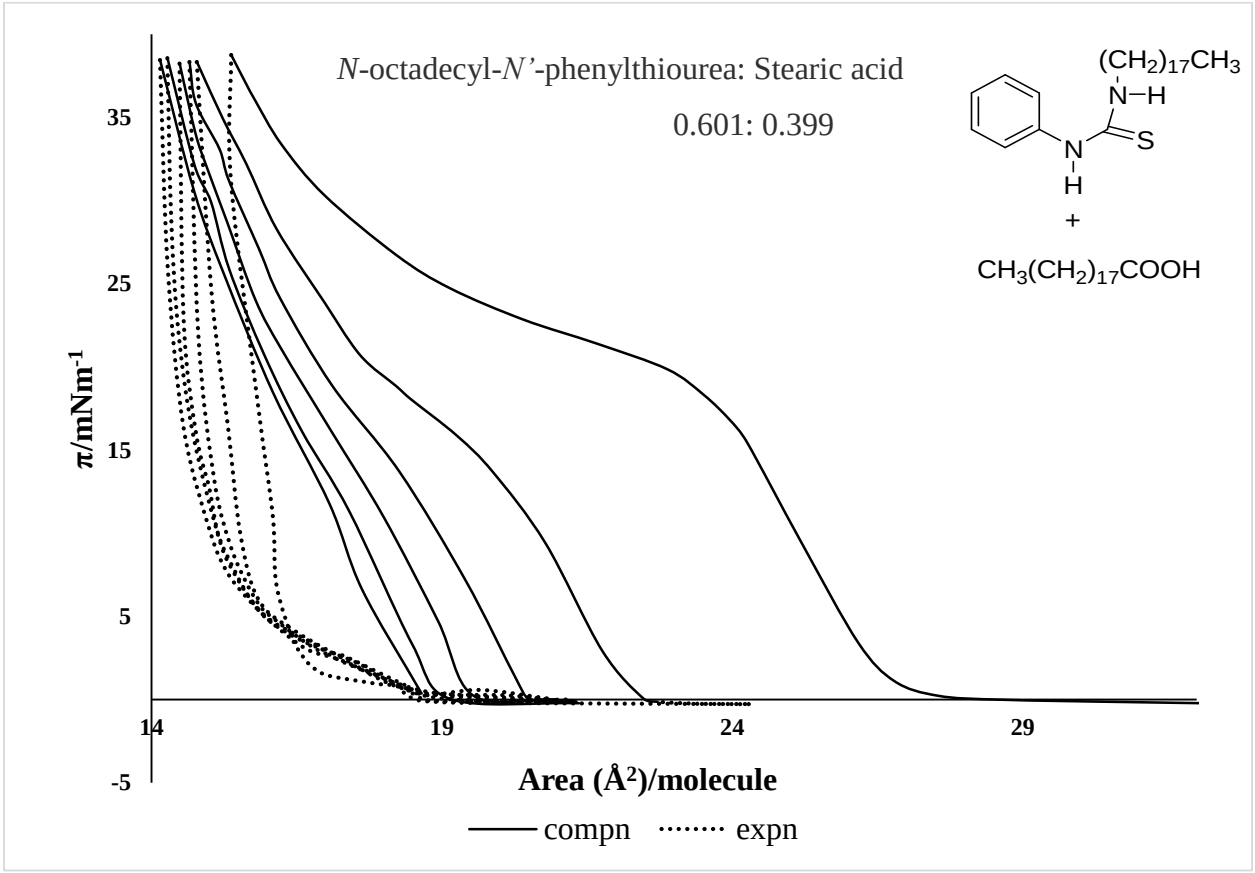

Figure 3.2.5: Surface pressure-area hysteresis isotherms of premixed OPT/SA monolayers with mole fraction ratio 0.601:0.399 over air/water interface at 25 °C.

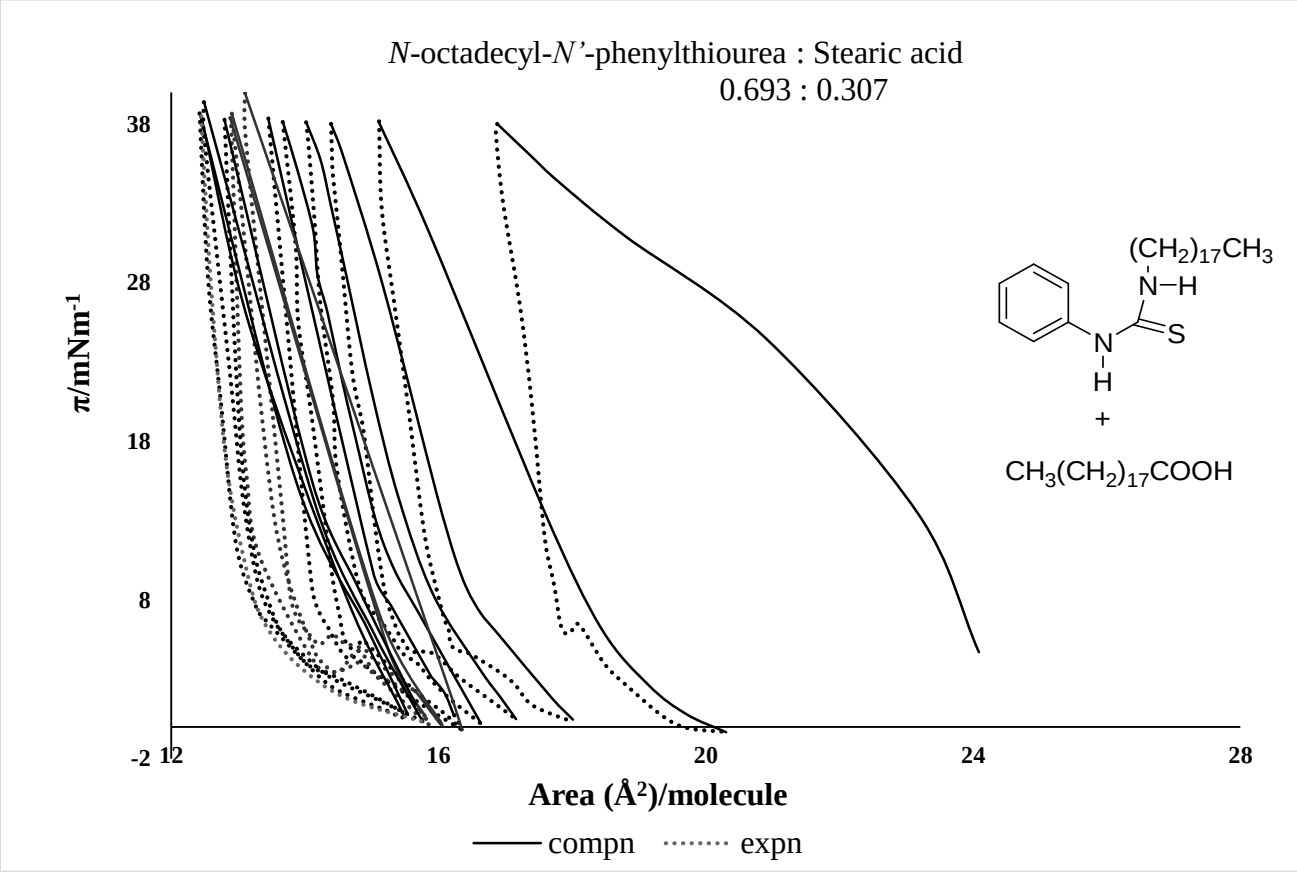

Figure 3.2.6: Surface pressure-area hysteresis isotherms of premixed OPT/SA monolayers with mole fraction ratio about 0.693:0.307 over air/water interface at 25 °C.

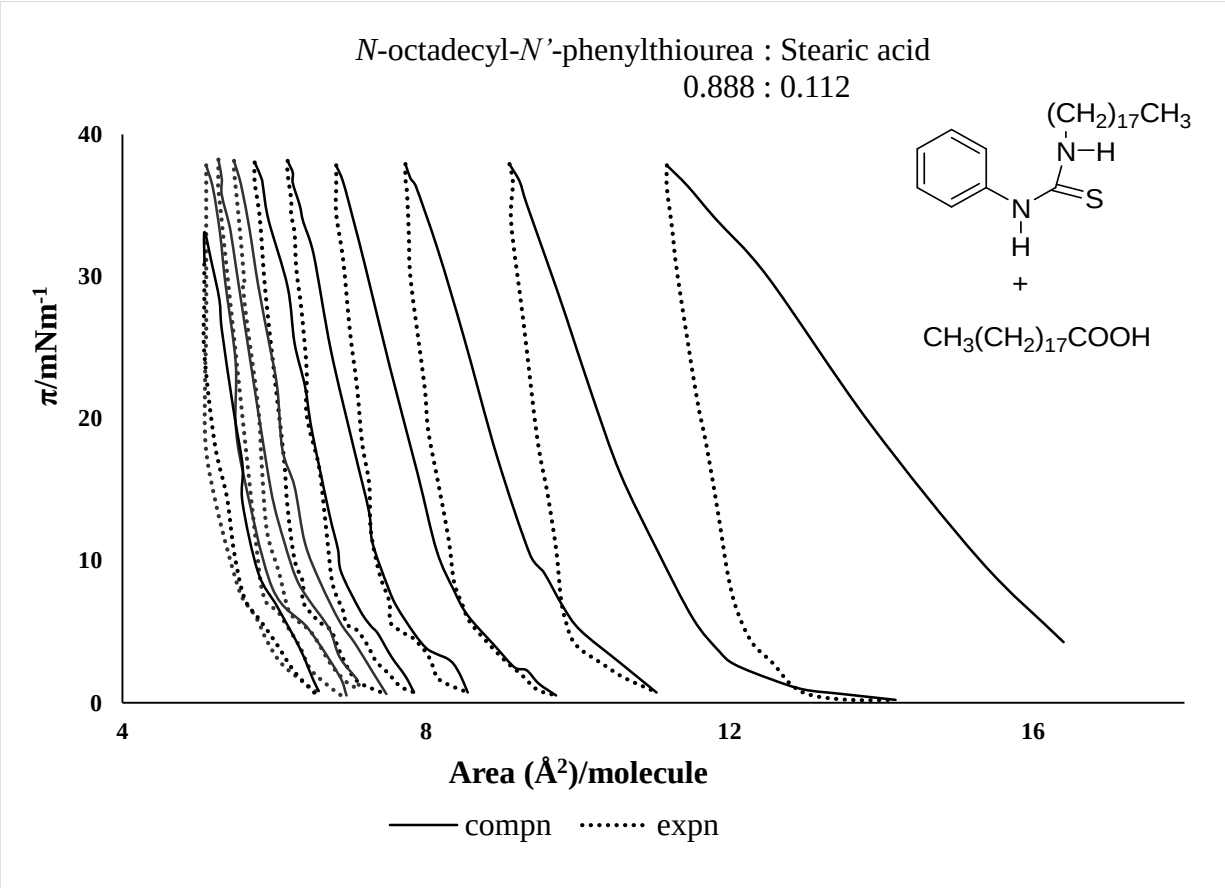

Figure 3.2.7: Surface pressure-area hysteresis isotherms of premixed OPT/SA monolayers with mole fraction ratio about 0.888:0.112 over air/water interface at 25 °C.

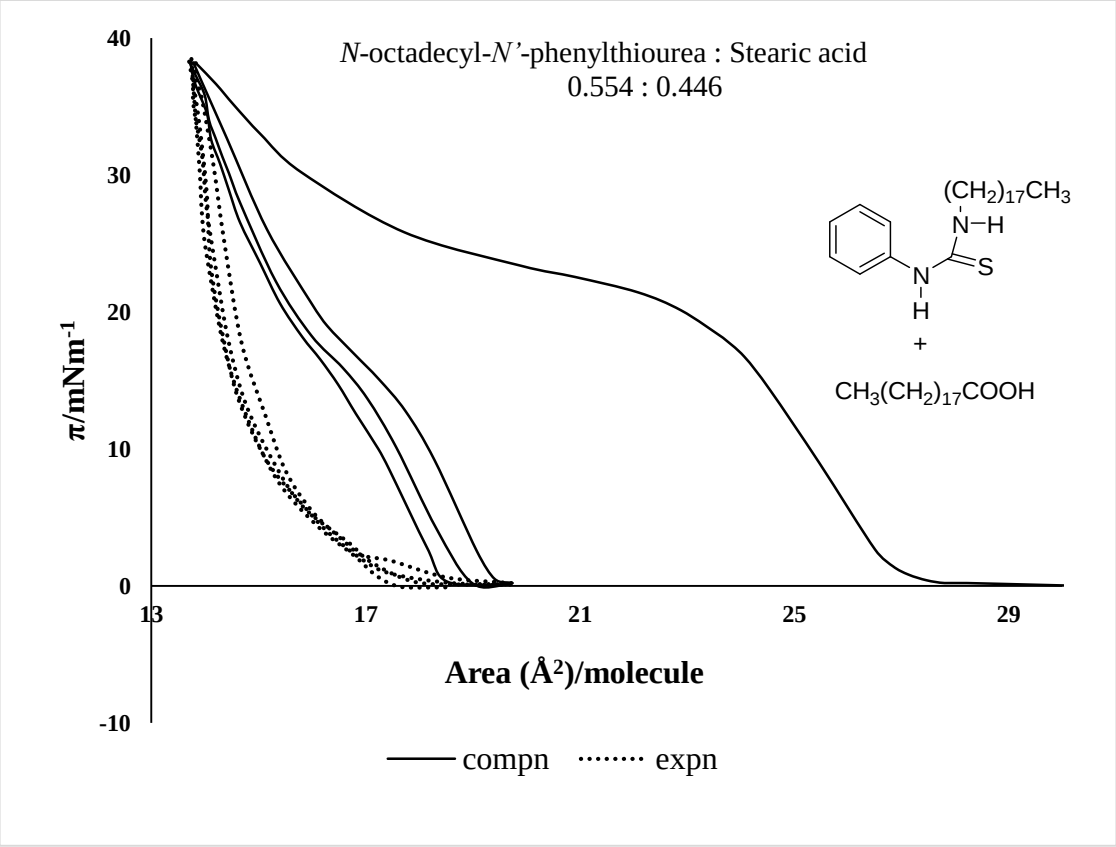

Figure 3.2.8: Surface pressure-area hysteresis isotherms of premixed OPT/SA monolayers with mole fraction ratio 0.554:0.446 over air/water interface at 25 °C.

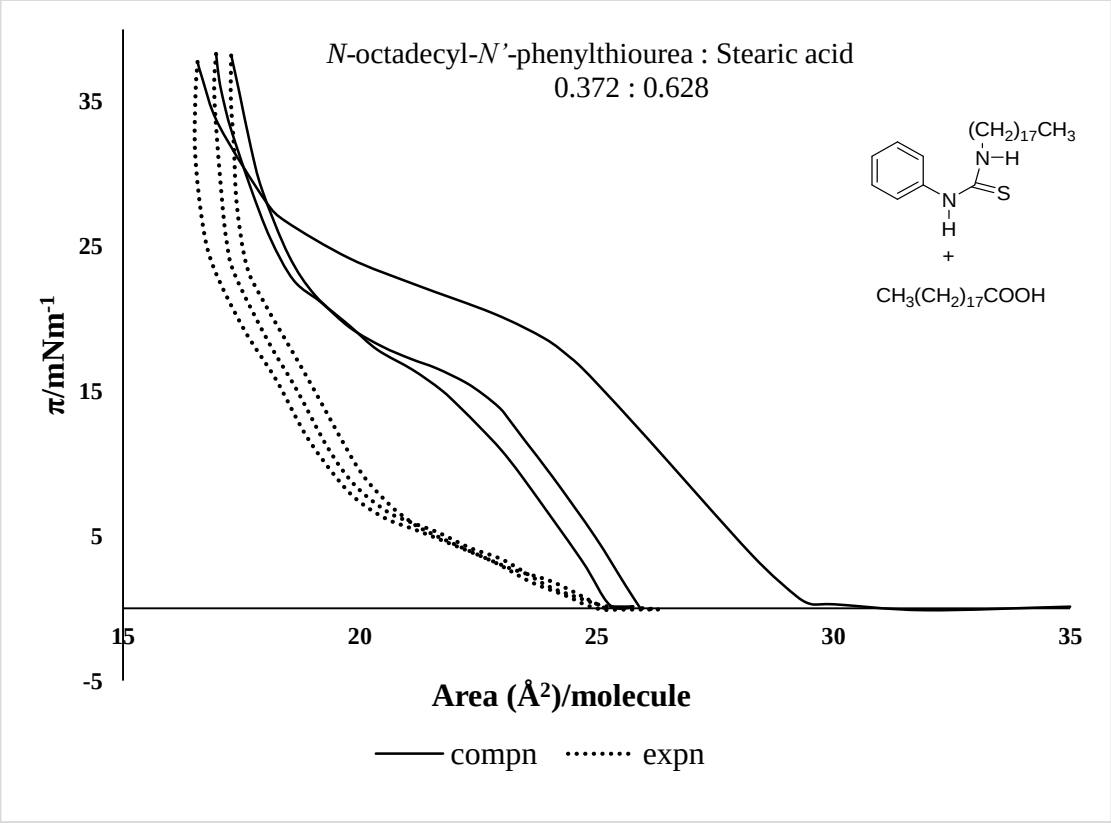

Figure 3.2.9: Surface pressure-area hysteresis isotherms of premixed OPT/SA monolayers with mole fraction ratio about 0.372:0.628 over air/water interface at 25 °C.

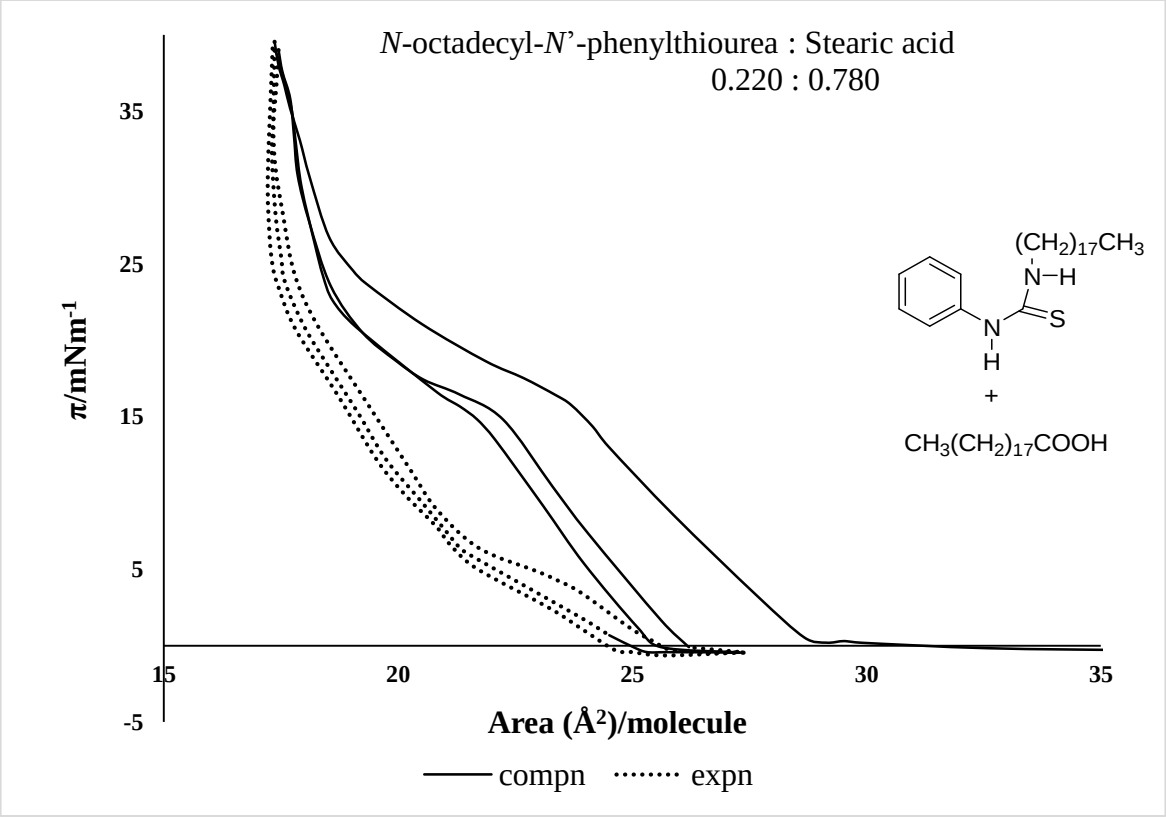

Figure 3.2.10: Surface pressure-area hysteresis isotherms of premixed OPT/SA monolayers with mole fraction ratio about 0.220:0.780 over air/water interface at 25 °C.

When OPT in the spreading mixture is in excess, however, the isotherms do not fully coalesce even after several cycles. In such monolayers, successive compression-expansion cycles progressively shift towards a lower area, indicating that the monolayer is continuously losing film material. By noting that this loss does not take place when SA is in excess, we can conclude that it is OPT which is being squeezed out of the interface. The difference between the positions of the isotherms for successive cycles, however, becomes smaller with each new cycle till the curves nearly coincide as shown in Figure 3.2.7.

Figure 3.2.8, Figure 3.2.9 and Figure 3.2.10 show the isotherms formed by spreading mixtures of 0.55:0.45, 0.4:0.6 and 0.2:0.8 (OPT:SA) respectively. These isotherms are similar to the one obtained when equimolar amount of OPT and SA are spread (Figure 3.2.4). These isotherms show that there is negligible loss of monolayer material, and in all three cases the isotherms coincide completely after the first cycle.

The limiting area of the composite film is obtained by extrapolating the straight line portion of the coinciding isotherm to zero pressure. Three quantities were calculated: total limiting area per molecule deposited, total limiting area per SA molecule deposited, and total limiting area per OPT molecule deposited. A comparison of these three quantities allows the estimation of the relative amount of each of the components in the monolayer, assuming that all the SA deposited remains in the monolayer. The monolayer formed by depositing equimolar mixture of the two components gives coinciding curves after the first compression, indicating that there is negligible loss of film material through repeated compression-expansion cycles. This shows that all the material deposited on the interface remains incorporated in the monolayer in this case and the equilibrium state of the monolayer is achieved just after the first compression. Since the area per molecule is known for stearic acid in a monolayer of pure stearic acid, the total area occupied by

stearic acid in the mixed monolayer can be calculated by multiplying the area/molecule of pure SA monolayer with the number of molecules of SA in the mixed monolayer. The area per molecule of OPT can then be calculated by subtracting this value from the total area occupied by the mixture of stearic acid and OPT. The value of the area per molecule allows us to calculate the amount of OPT remaining on the surface for those mixed films where some of OPT is squeezed out of the monolayer before a stable monolayer is formed. In the equimolar mixed film, the limiting area per molecule is found to be close to the area/molecule of a pure SA monolayer. Moreover the limiting area of the mixed equimolar film divided by the number of molecules of SA alone is found to be twice the area/molecule in the pure SA film. This indicates that half the area in the mixed film is occupied by the molecules of each component. This is as to be expected since both the molecules have similar hydrophobic chains.

Thus, total area/molecule OPT = total area/molecule SA = 2[area / (molecule SA + OPT)].

This leads us to conclude that the composition of the film is 1:1 and all OPT molecules are incorporated in the monolayer in the equimolar film.

This 1:1 composition is confirmed by the behaviour of the monolayer spread from solutions of other compositions. Table 3.2.1 shows the observed limiting areas per molecule for other compositions. The values of area/molecule shown in the last column are about constant for all monolayers that achieve a stable reproducible form when subjected to several compression-expansion cycles. Deviation from the constant value sets in for those mixtures where OPT is in large excess. It is noteworthy that for these monolayers, hysteresis curves do not coincide. The values for area/molecule for mixtures where SA is equal to or less than OPT are half of the area/molecule of SA, as excess OPT is squeezed out. For systems where SA is in excess the area/molecule is not exactly half because excess SA exists in the monolayer. Figure 3.2.11

depicts this deviation graphically; the solid line in the figure represents constant value of the area/molecule obtained on the basis of those monolayers where SA was in excess.

Table 3.2.1: Limiting area/molecule of OPT/SA premixed monolayer for coinciding curves.

Mole fraction of OPT:SA in the spreading mixtures	Area/total deposited OPT and SA molecules ($Å^2$)	Area/SA molecules added ($Å^2$)	Area/molecule remaining in monolayer, assuming a 1:1 complex plus any excess SA ($Å^2$)
0.888 : 0.112	5.70	50.6	25.3
0.693 : 0.307	14.8	48.1	24.1
0.601 : 0.399	17.1	42.7	21.4
0.530 : 0.470	20.3	43.2	21.6
0.504 : 0.496	19.0	38.4	19.2
0.372 : 0.628	19.9	31.8	19.9
0.220 : 0.780	19.7	25.2	19.7

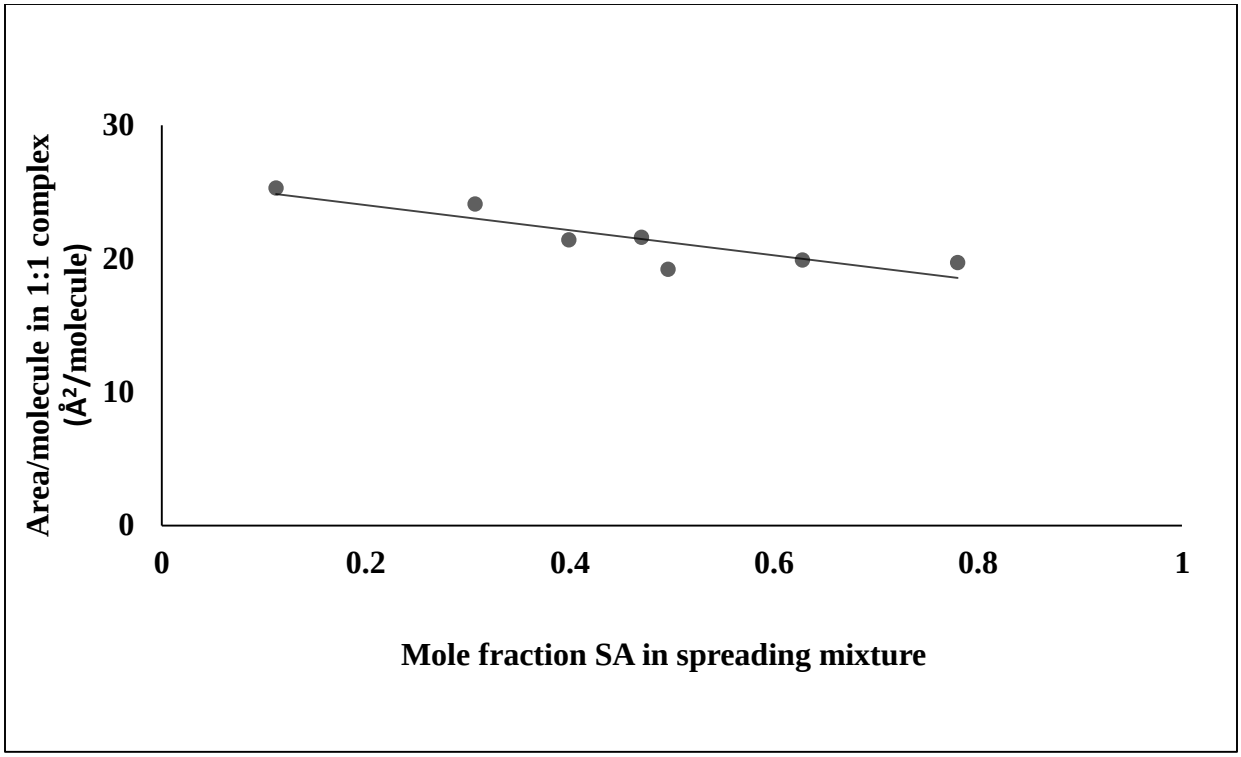

Figure 3.2.11: Area per molecule assuming the monolayer comprises 1:1 complex and excess SA versus mole fraction of SA in the spreading mixture. Any excess OPT is assumed removed from the monolayer. The solid line indicates constant area/molecule. At low mole fractions of SA deviation sets in from the constant value obtained at mole fractions of SA 0.4 or higher.

3.2.3.1 OPT excess

For a monolayer formed by spreading OPT and SA in the ratio 0.8:0.2 mole fractions only as many molecules of OPT are expected to be incorporated into the 1:1 complex as are the molecules of SA. The excess OPT will be removed from the film, since OPT alone does not form a stable film. What will result is a monolayer containing 0.2: 0.2 mole fraction of OPT and SA. Thus with repeated cycles of the hysteresis curves, excess OPT is progressively removed. A stage is reached when successive hysteresis curves coincide and the remaining monolayer remains stable. The observed area/molecule at this equilibrium stage should be about one half of the available area divided by the number of SA molecules. As Table 3.2.1 shows, this is what is observed experimentally for the spread mixtures with an excess of OPT. For the mixtures in which OPT is vastly in excess (0.693:0.307 and 0.888:0.112), successive curves do not fully coincide even after several cycles, though they get closer. This explains why the values of area per molecule start deviating from the values for other compositions as the excess of OPT becomes large, as shown in Figure 3.2.11. Keeping in view the fact that for 0.9:0.1 mixture the calculation assumes that only one-ninth of the amount of OPT deposited remains in the film as part of the 1:1 complex, the closeness of the area per molecule is remarkable. This is further confirmation of 1:1 complex.

3.2.3.2 SA excess

The result of the film formed by spreading mixtures in which SA is in excess is in accordance with the conclusions outlined above. When SA is in excess, the hysteresis curves show a reversible behaviour after the first compression as shown in Figure 3.2.4. The value of the limiting area per molecule can only be explained by assuming that all OPT remains in the

monolayer. This value is also consistent with all OPT molecules being incorporated in a 1:1 complex with excess SA molecules remaining at the surface.

In conclusion, OPT does not form a stable monolayer on air/water interface but when spread together with SA, it can get incorporated into the monolayer. Hysteresis measurements on such mixed monolayers show that the area/molecule is consistent with the monolayer having a 1:1 composition of the two components in addition to any excess SA deposited. For monolayers which are formed by spreading mixtures containing excess of the thiourea, the values correspond to a simple 1:1 mixture with excess thiourea not remaining in the monolayer.

3.3 Hysteresis of mixed monolayers of ODIMP and ODA at air/water interface

In this section mixed monolayers of ODIMP, a Schiff base, and ODA are reported. In recent years a number of papers on Schiff bases as amphiphiles and their derivatives have been studied for their film forming and interesting optical and electrical properties [71; 72; 73]. Schiff bases are biologically important compounds, with anticancer [277; 278], antibacterial [279; 280; 281], antifungal [281; 282; 283], antileishmanial [284]**,** and antiviral activity [285]. So far the LB films of amphiphilic Schiff base compounds, especially for those Schiff bases from salicylaldehyde, have been investigated and their interesting features were revealed [74; 75; 76]. Salicylaldehyde imines have been reported recently to have antioxidant activity [286]. In addition, they have extensive applications in polymer ultraviolet stabilizers [68], and laser dyes [70] as well as molecular switches in logic or memory circuits [287]. In view of these applications, studies of pure and mixed monolayers of Schiff bases are of considerable interest.

3.3.1 Surface pressure-area hysteresis isotherm of ODIMP

Surface pressure-area (π-A) hysteresis curves of ODIMP over water subphase are shown in Figure 3.3.1. The isotherm shows the onset of surface pressure at 30.2 $Å^2$/molecule and experiences a spike at 7.8 mN/m followed by a decrease in surface pressure. This is followed by a relatively flat region in which the surface pressure starts increasing much less steeply than the initial pre-spike increase. The appearance of the spike can be considered as collapse, a constant area collapse, not strictly speaking a traditional collapse, since a new phase is formed after the spike region where π starts increases only slowly.

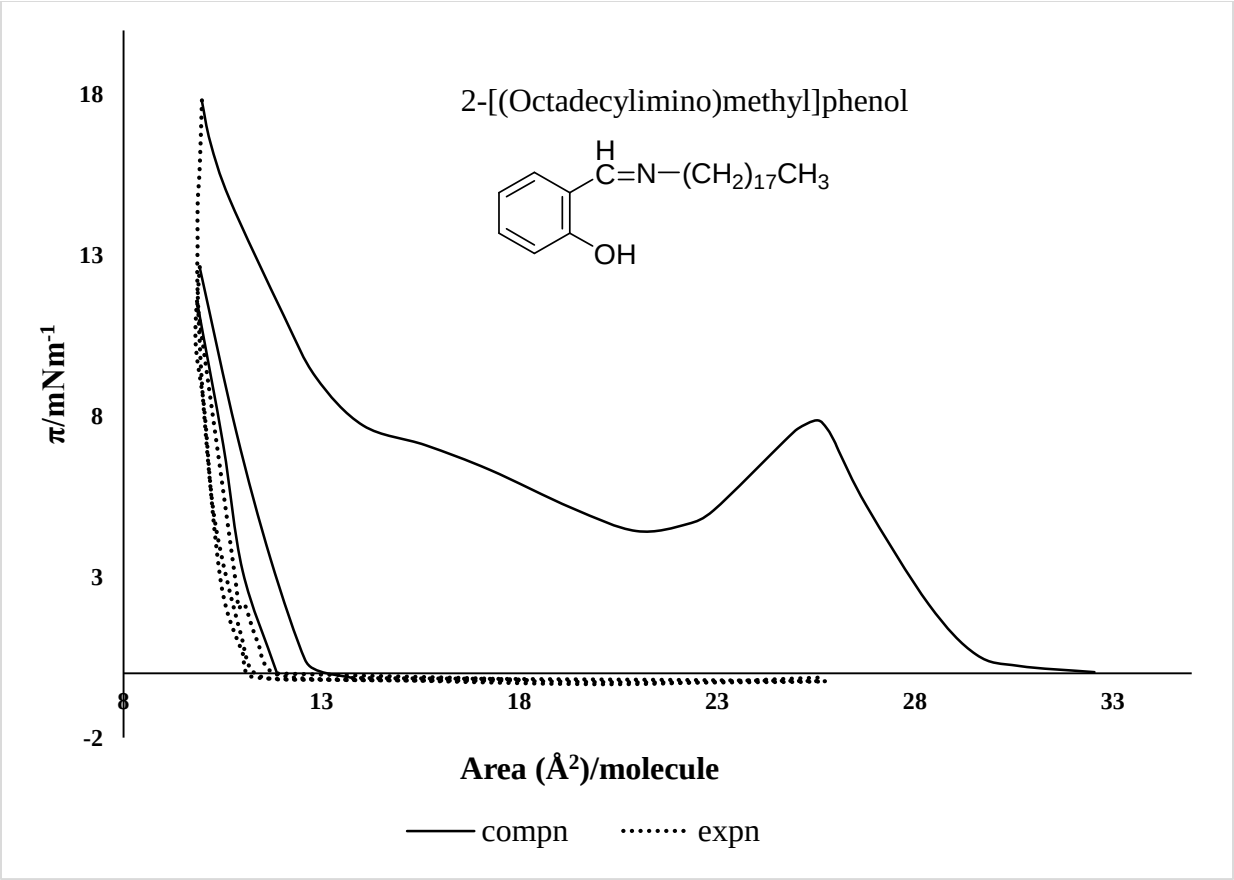

Figure 3.3.1: Surface pressure-area hysteresis isotherm of ODIMP monolayer over air/water interface at 25 °C.

Stability and hysteresis effects have been studied by means of three consecutive compression expansion cycles. The initial compression is the right-most trace in the diagram. When the monolayer is expanded the surface pressure decreases precipitously. The second compression curve does not exhibit the spike or the plateau region and it shifts slightly to the left side. This indicates that the processes occurring at the spike and the plateau are irreversible. Subsequent compression-expansion curves almost coincide. The hysteresis behaviour shows that first compression curve deviates considerably from the subsequent compression-expansion cycles. This indicates the loss of the material from the interface due to compression. Therefore, the subsequent isotherms do not coincide with the first one.

This type of behaviour has been observed for films of some fatty acids, including SA, heptacosa-10,12-diynoic acid [288] and 1-acyl-1,2,4-triazoles [136], which display a spike in their compression isotherms, followed by a trough of constant surface pressure, as they are compressed beyond monolayers. The spike was interpreted to indicate the buckling and subsequent folding of the monolayer, and the plateau was interpreted as a region where a multilayer forms by a roll-over mechanism of the previously existent monolayer [288]. The irreversible behaviour of ODIMP is similar to the result reported for 1-acyl-1,2,4-triazoles [136] while SA has been reported [288] to show some reversibility when expanded.

For the ODIMP monolayer in the current study, a comparison of the area/molecule at the peak, 25.6 $Å^2$/molecule, with the corresponding area/molecule at the subsequent point when the surface pressure attains the same value as at the peak, 13.8 $Å^2$/molecule, showed that molecules occupy roughly half the area (Figure 3.3.1). This indicates that after the collapse, a bilayer is formed, which on further compression gives an isotherm characteristic of a condensed film. This observation is in agreement with the conclusion reached by Chen and coworkers [217] and Ferreira and coworkers [227] about bilayer formation in the surface films of a simple fluorinated hydroxyl fatty acid methyl ester and an aromatic carboxylic acid respectively. The isotherm of ODIMP and its interaction with barbituric acid in the subphase have been investigated by Jiao and Liu [85] and the results interpreted as indicating multilayer formation after the collapse of ODIMP at air/water interface.

3.3.2 Surface pressure-area hysteresis isotherms of mixed monolayers of ODIMP and ODA

The hysteresis curves of the mixed films of ODIMP and ODA allow us to make inferences about the nature of surface films and how the individual components behave in the film. The characteristic of the mixed film depends on whether the components were individually spread on the surface or a pre-mixed solution of the two components was spread. Shapes of the curves and the values of areas per molecules can give us an indication of how each component behaves in the mixed film.

Thus, on the basis of the observed areas per molecule and the observed shape of the hysteresis curves, we can conclude that the monolayer of pure ODIMP collapses and forms a bilayer above a certain surface pressure. If in a mixed ODIMP/ODA monolayer, a similar pattern is repeated, yielding the expected values of area/molecule, that would indicate that ODIMP retains its

individuality and the part of the monolayer containing it collapses and forms a bilayer. This is indeed the case for the two components individually spread on the surface (Figure 3.3.2-Figure 3.3.5). The spike, which is a characteristic feature of the pure ODIMP, is still there in the mixed film, showing that ODIMP retains its individuality in the mixed film. As the film is compressed, a certain surface pressure is reached, where the ODIMP parts of the film collapses and doubles up. The spike becomes less pronounced as the proportion of ODIMP decreases. The hysteresis isotherms showed the continuous loss of the monolayer material even in the equimolar composition. This shows that the mixed monolayers prepared by this method does not form a homogeneous film, and the mixed monolayer preserves the individual characteristics of the components. This behaviour is similar to the one shown by mixed monolayers of SA and ODA [28]. Values of the limiting area/molecule for each composition of the individually spread and pre-mixed film were calculated to confirm the validity of the conclusions stated above that the individually spread mixed films do not form homogeneous monolayers at the molecular level.

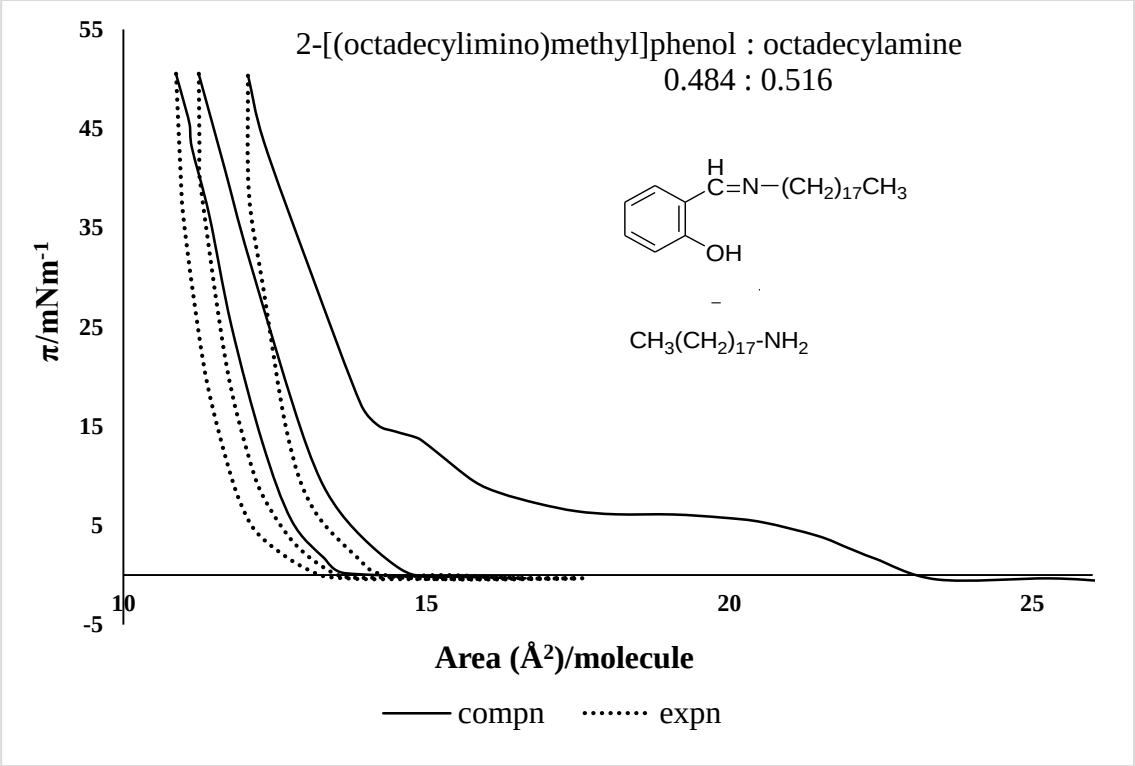

Figure 3.3.2: Surface pressure-area hysteresis isotherms of monolayer prepared by spreading individual solutions of ODIMP/ODA with approximately equimolar composition over air/water interface at 25 °C**.**

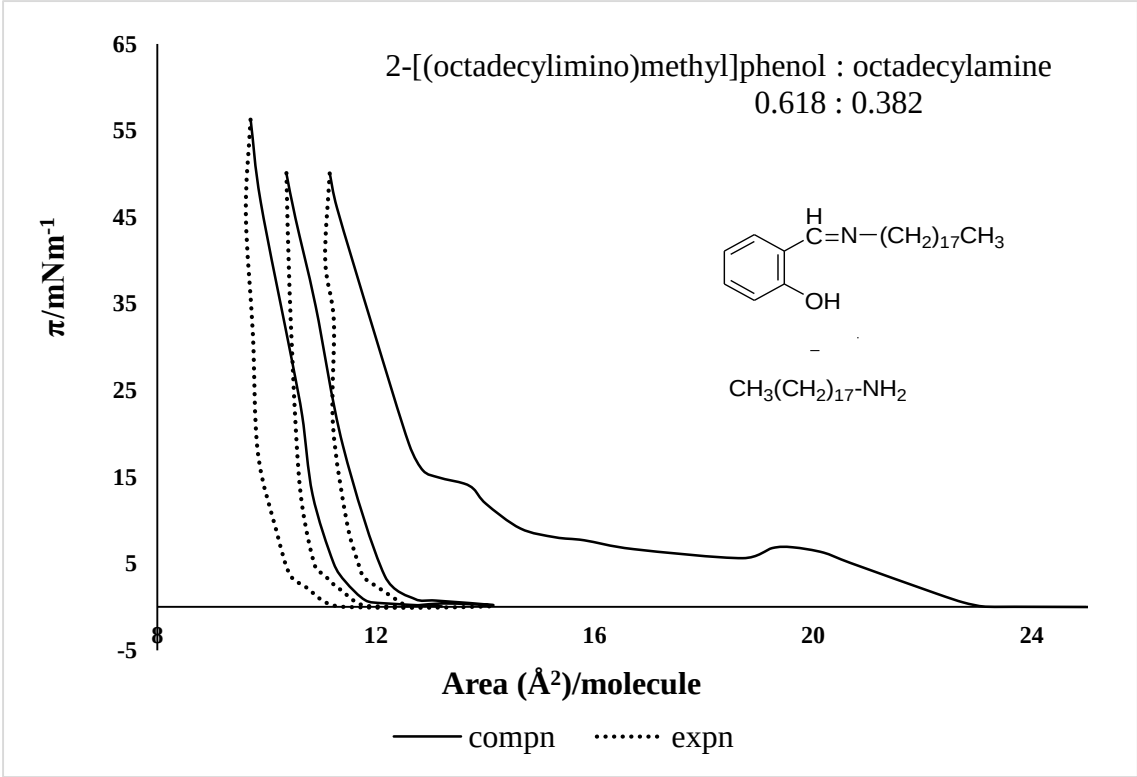

Figure 3.3.3: Surface pressure-area hysteresis isotherms of monolayer prepared by individually spreading ODIMP/ODA solutions over air/water interface at 25 °C. Mole fraction ratio ODIMP:ODA = 0.618:0.382.

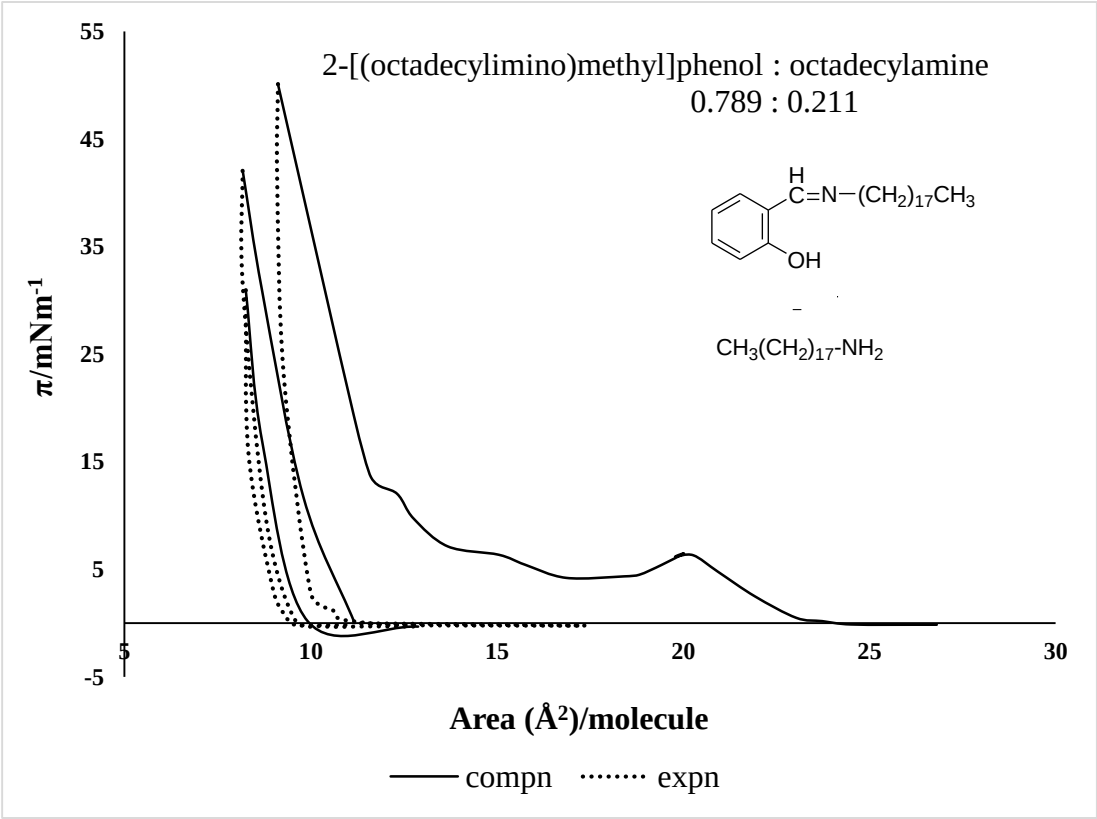

Figure 3.3.4: Surface pressure-area hysteresis isotherms of monolayer prepared by individually spreading ODIMP/ODA solutions over air/water interface at 25 °C. Mole fraction ratio ODIMP:ODA = 0.789:0.211.

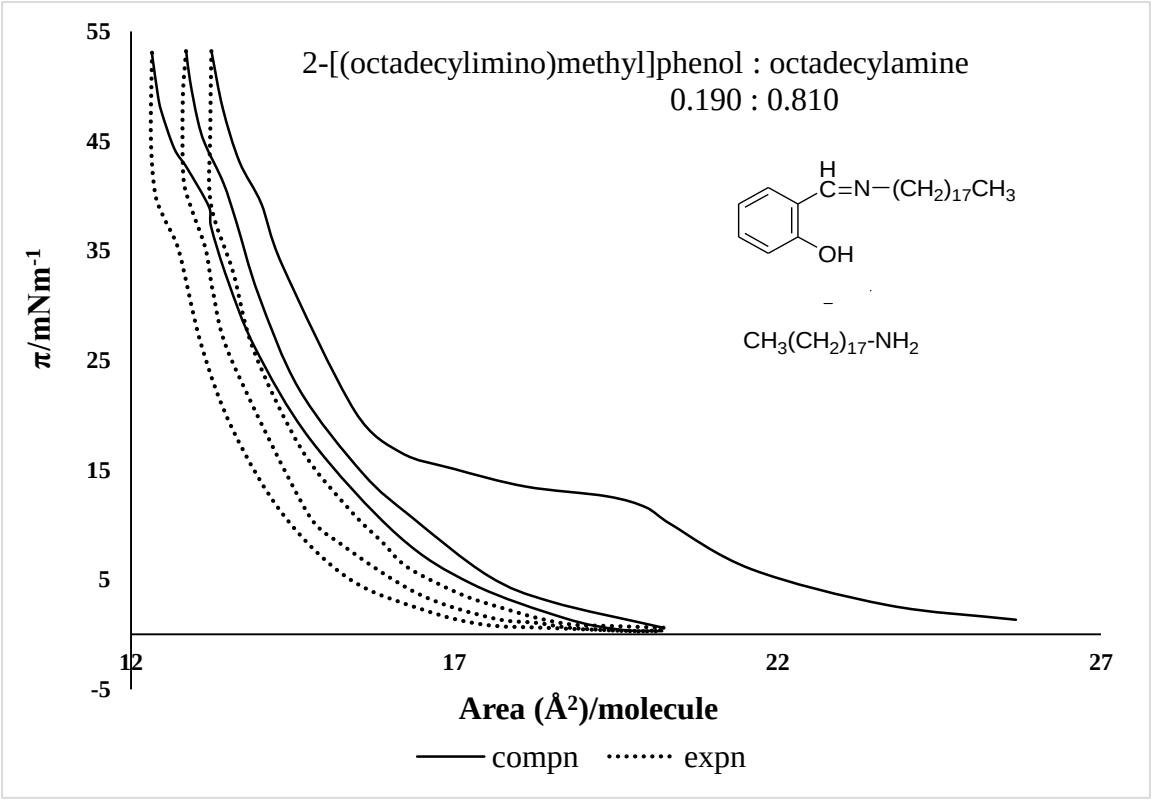

Figure 3.3.5: Surface pressure-area hysteresis isotherms of monolayer prepared by individually spreading ODIMP/ODA solutions over air/water interface at 25 °C. Mole fraction ratio ODIMP:ODA = 0.190:0.810.

3.3.2.1 Mixed films obtained by individually spreading the components

The limiting area of the mixed film (individually spread) is obtained by extrapolating the straight line portion of the first compression isotherm to zero pressure. The hysteresis isotherms showed the continuous loss of the monolayer material even in the equimolar composition. This might be due to the bilayer formation of ODIMP. Then the limiting area/molecule that the film finally reaches should be given by the following expression, if we assume that all the molecules of ODIMP form a bilayer, and the amine remains in monolayer state:

$$A_{film} = X_1.A_1 + ½\ X_2.\ A_{2.} \qquad \text{Equation 14}$$

Here A_{film} = Calculated area/molecule of the film.

A_1 and A_2 are the measured areas/molecule of pure ODA and ODIMP respectively, and X_1 and X_2 are the mole fractions of the two components in the surface film. The measured area/molecule for ODIMP is taken at the apex of the spike for the pure monolayer, since that is when a bilayer is formed. For ODA, it is the limiting area obtained from its isotherm. Table 3.3.1 shows the observed and calculated (by assuming the bilayer formation of ODIMP) limiting areas per molecule for various compositions.

Table 3.3.1: Limiting area/molecule of individually spread ODIMP/ODA film.

X_{ODA}	X_{ODIMP}	Experimental Area ($Å^2$) per molecule	Calculated Area ($Å^2$) per molecule assuming all ODIMP is in bilayer form	Area ($Å^2$) per molecule of ODA assuming no ODIMP remains
0.810	0.190	16.0	17.3	19.7
0.616	0.384	15.9	16.2	25.8
0.516	0.484	14.3	15.6	27.7
0.382	0.618	13.3	14.9	34.8
0.211	0.789	12.1	14.0	57.3

The experimental values calculated using Eq. (14) (Table 3.3.1) follow a similar trend and are mostly within around 10% of each other. Considering the loss of material on compression, as also seen in pure ODIMP monolayer, this agreement is significant.

3.3.2.2 Monolayers obtained from premixed solution

Films obtained by spreading a pre-mixed solution show quite different force-area isotherms; the characteristic spike of the pure ODIMP is now missing (Figure 3.3.6-Figure 3.3.11). This behaviour would be in line with the absence of aggregates of ODIMP molecules in a film that is homogeneous at the molecular level; the ODIMP molecules, not being together cannot form a bilayer. Another difference from the individually spread components is that in this case the isotherm obtained from the first compression has a flat region with remarkably constant surface pressure over a considerable range of area. This would indicate that as the surface pressure increases ODIMP begins to get squeezed out preventing any increase in surface pressure. The width of the flat region in the isotherm decreases as the proportion of ODIMP in the mixture being spread is reduced, further confirming that the plateau results from the material being squeezed out. In the mixed films with larger proportion of ODIMP, there is a greater amount of the material to be squeezed out, resulting in a wider plateau. Table 3.3.2 shows these calculated values for the various mixtures. The value is remarkably constant for most of the mixtures except for the one with the largest percentage of ODIMP, where it would seem that not all molecules are squeezed out.

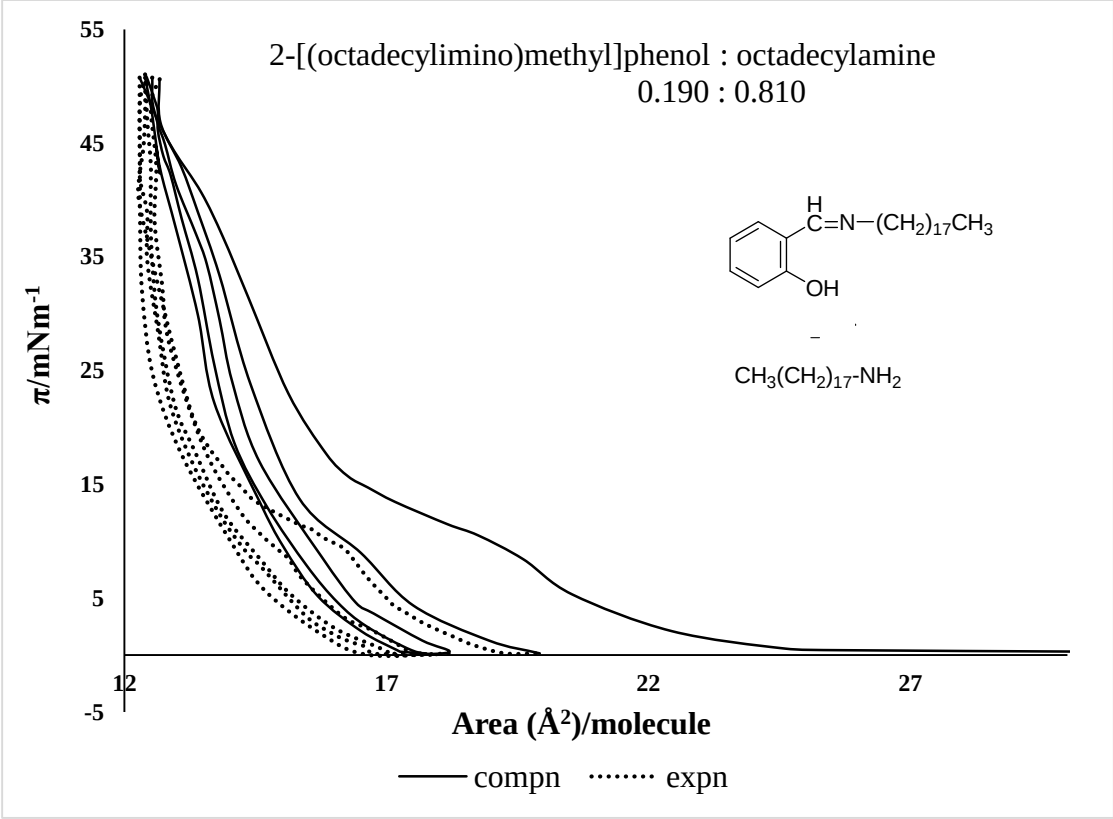

Figure 3.3.6: Surface pressure-area hysteresis isotherms of premixed ODIMP/ODA monolayers over air/water interface at 25 °C.

Mole fraction ratio ODIMP:ODA = 0.190:0.810.

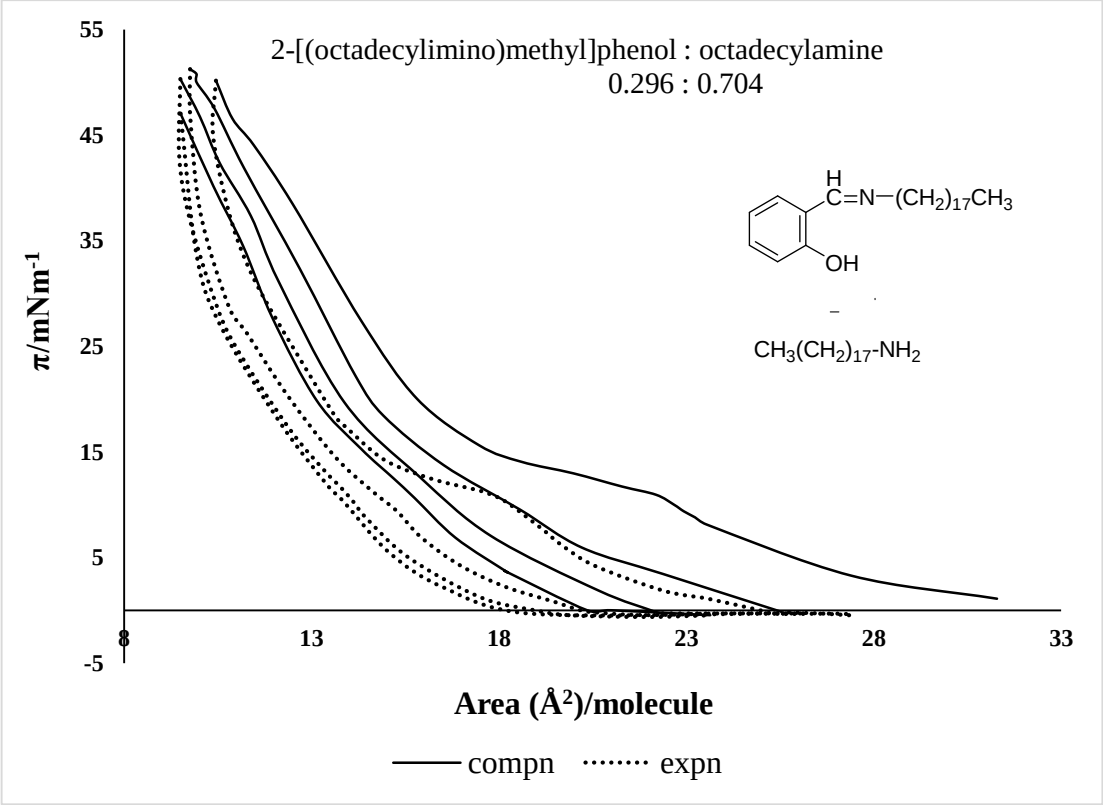

Figure 3.3.7: Surface pressure-area hysteresis isotherms of premixed ODIMP/ODA monolayers over air/water interface at 25 °C.

Mole fraction ratio ODIMP:ODA = 0.296:0.704.

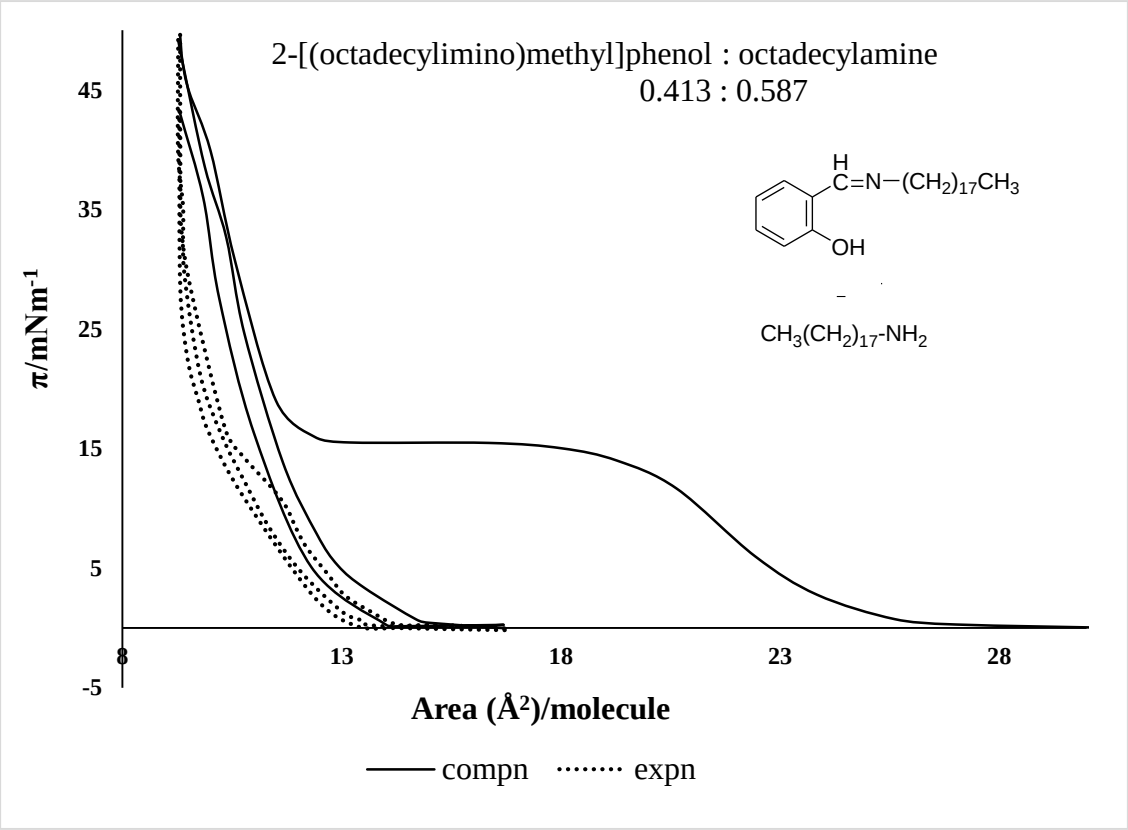

Figure 3.3.8: Surface pressure-area hysteresis isotherms of premixed ODIMP/ODA monolayers over air/water interface at 25 °C.

Mole fraction ratio ODIMP:ODA = 0.413:0.587.

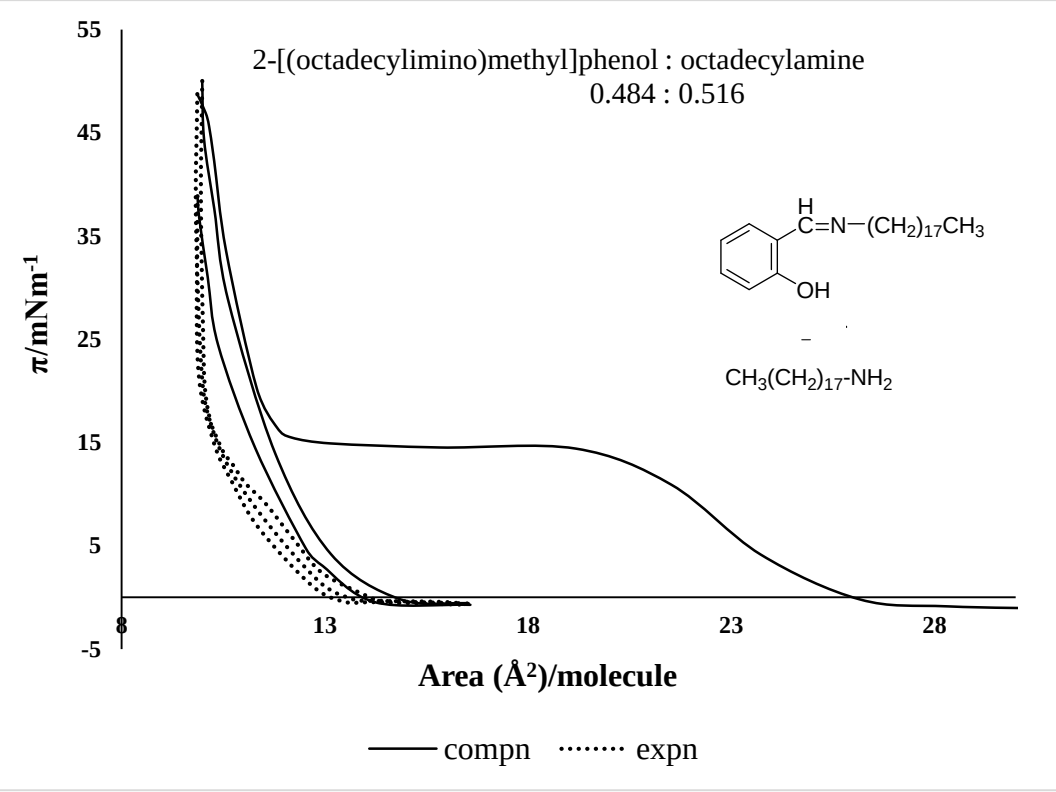

Figure 3.3.9: Surface pressure-area hysteresis isotherms of premixed ODIMP:ODA monolayers over air/water interface at 25 °C.

Mole fraction ratio ODIMP:ODA = 0.484:0.516.

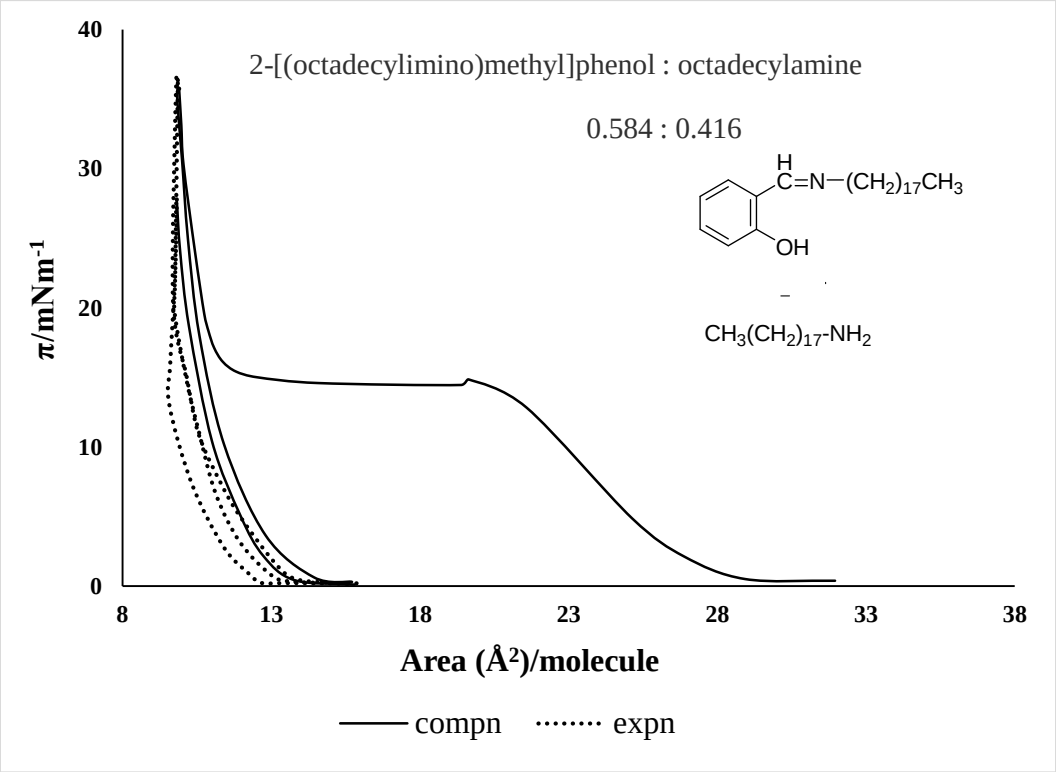

Figure 3.3.10: Surface pressure-area hysteresis isotherms of premixed ODIMP:ODA monolayers over air/water interface at 25 °C.

Mole fraction ratio ODIMP:ODA = 0.584:0.416.

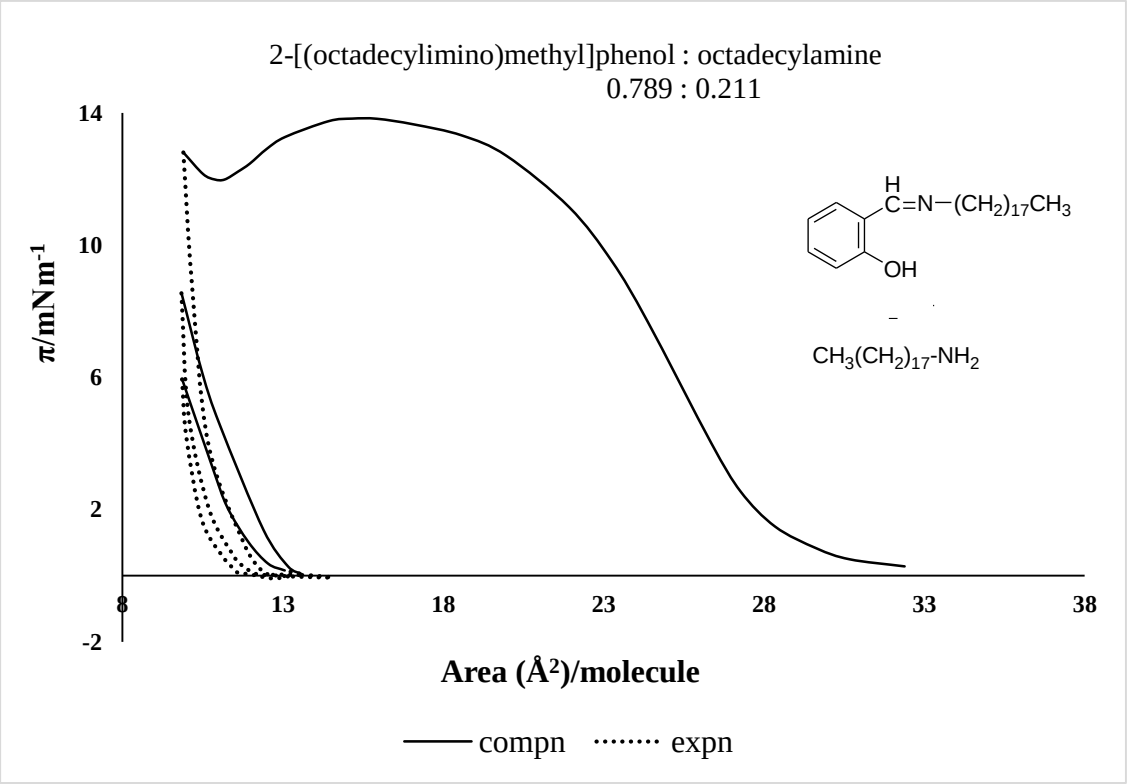

Figure 3.3.11: Surface pressure-area hysteresis isotherms of premixed ODIMP/ODA monolayers over air/water interface at 25 °C.

Mole fraction ratio ODIMP:ODA = 0.789:0.211.

Table 3.3.2: Limiting area/molecule of premixed spread ODIMP/ODA film.

X_{ODA}	X_{ODIMP}	Experimental Area ($Å^2$) per molecule	Area ($Å^2$) per molecule of ODA assuming no ODIMP remains in monolayer
0.810	0.190	17.2	21.2
0.704	0.296	16.7	23.7
0.587	0.413	13.1	22.3
0.516	0.484	11.9	23.1
0.416	0.584	11.4	27.4

If we assume that in the end all ODIMP is squeezed out, the limiting area will be due to the ODA part of the originally spread film. Knowing the proportion of the ODA in the mixture spread and hence the number of its molecules, we can calculate the area/molecule. The area per molecule obtained this way is generally constant for films of different composition as seen in Table 3.3.2. This is additional evidence that what remains in the film after first compression of the premixed film is a pure component. In contrast a similar calculation for the individually spread films shows widely different limiting areas per molecules (Table 3.3.1), showing that after first compression, there is a presence of ODIMP along with the ODA in the film. This remaining

ODIMP is the bilayer, which resists expulsion from the film as stated above. Compared to a bilayer, a monolayer is expected to be easier to be expelled from the film. The bilayer would comprise hydrophobic chains shielded between the hydrophilic groups on both sides. These hydrophilic head groups will not find the hydrophobic chains of the other component of the film energetically hospitable environment, which would oppose the bilayer from being squeezed out of the film.

3.3.2.2.1 Quantitative treatment of the width of the plateau in the isotherms:

If the plateau region of the film formed by spreading the pre-mixed solution is caused by progressive expulsion of ODIMP from the surface film, its width should be proportional to the amount of the component originally in the film. This is indeed the case as depicted in Figure 3.3.12, which gives the graph between the width of the plateau (expressed as the reduction in surface area for the duration of which the surface pressure remains constant) and the mole fraction of ODIMP in each solution spread. The linear dependence is evidence of the expulsion of ODIMP from the mixed film.

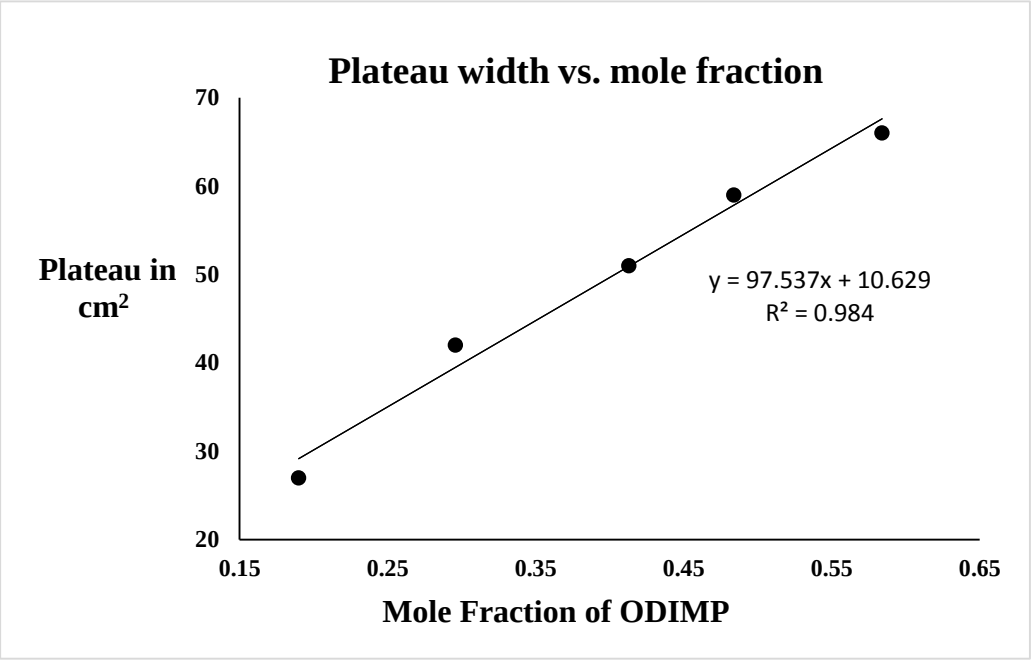

Figure 3.3.12: Plateau width as a function of composition for mixed ODIMP/ODA monolayers.

3.3.2.3 Hysteresis behaviour of monolayers prepared by spreading ODIMP and ODA individually

For mixed monolayers of ODIMP and ODA, the hysteresis curves show an irreversible behaviour for both individually spread and the pre-mixed films. The expansion curve of the film displaced towards lower areas than the compression curves. This shift in behaviour, that establishes the new path followed by the expansion sector, is a consequence of the new structural arrangements that molecules undergo after the first compression and not returning to their original state before compression. The shape of the loop after the first cycle is roughly the same in the successive cycles. This implies that after a complete expansion the molecules relax back to their original state. Since the hysteresis of ODA is negligible, the observed behaviour must be assigned to the ODIMP molecules in the mixed film. This explanation for the observed hysteresis phenomenon also supports the irreversible bilayer formation of ODIMP molecules in the case of individually spread films and the irreversible squeezing out of the ODIMP molecules from the premixed films.

The observed isotherms and hysteresis behaviour of the monolayer of ODIMP spread on air/water interface reveal that the monolayer irreversibly changes to a condensed bilayer on the first compression. When the phenol is mixed with ODA prior to spreading, and the monolayer compressed, the bilayer is not formed. Instead, the phenol is irreversibly squeezed out progressively till all of it leaves the monolayer during the first compression. During this process of being squeezed out the surface pressure does not increase. During the subsequent compression-expansion cycles, the film behaves as a condensed film with areas per molecule corresponding to that of pure ODA. When the phenol and the amine solutions are individually spread on the surface, the isotherms indicate that, unlike the premixed

solution, now the phenol is not homogeneously mixed with the amine and retains its individual characteristics. The phenol portion of the film irreversibly changes to a bilayer on the first compression. The results of this study have implications for work where bilayers might be used to mimic biological cell membranes. In this case, for example, the bilayer forming property of ODIMP is disrupted by the presence of ODA. These results suggest further investigations of the structure of the monolayer-bilayer mixture described here, possibly by Brewster angle microscopy.

3.4 Monolayer characteristics of mixed MODIMP and SA at air/water interface

Molecular assembly and molecular recognition through a noncovalent intermolecular action is one of the central topics in supramolecular chemistry [289; 290; 291]. Inter/intramolecular hydrogen bonding is one of the most fascinating noncovalent interactions for constructing artificial molecular assemblies due to its directionality and strong matching between different molecules [292; 293], and important work has been done by Ariga, Kunitake and coworkers at the air/water interface [294; 295; 296; 297]. They have explained the intermolecular hydrogen bonding in oligoglycine amphiphiles. The air/water interface provides a crucial environment for different molecules to react with each other, and many supramolecular assemblies were fabricated through the interaction at the air/water interface.

Many aromatic Schiff bases exhibit hydrogen bonding interactions, which are promoted by intramolecular or intermolecular proton transfer between the hydroxyl oxygen (O–H) and the imino nitrogen atoms (RC=NR). Several studies have shown that this process is responsible for the photochromic or thermochromic properties observed in the solid and solution states for imine derivatives of salicylaldehyde [298; 299]. Schiff bases exhibiting photochromism are of interest due to their potential applications in single molecule photochromism [300] optical switching devices [301] and data storage devices [302]. The hydrogen bonding interaction of Schiff base with barbituric acid has been reported both in solution [303] and at air/water interface [85]. Molecular recognition through the hydrogen bond was observed for these Schiff bases both in situ in the spreading film and ex situ in transferred multilayers. Mixed monolayers of the Schiff bases and fatty acids are of interest due to their potential applications.

Figure 3.4.1 shows the surface pressure-area hysteresis isotherm of MODIMP at the air/water interface. It forms an expanded type monolayer. When spreading on the subphase of water, the onset of surface pressure appeared in a larger molecular area, and the extrapolated molecular area was 43.6 $Å^2$ /molecule. In the hysteresis isotherms the successive compression-expansion cycles shift to the lower molecular area, which shows the continuous loss of the monolayer material. This might be due to the squeezing out of the rigid aromatic head groups from the interface due to compression. Hemakanthi and coworkers [87] reported an area per molecule of 44.0 $Å^2$ /molecule for a Schiff base prepared from hexadecylamine and *O*-vaniline. The area/molecule obtained in this study is consistent with this value. Hemakanthi and coworkers also suggested [87] the same behaviour, squeezing out of the monolayer material, that is responsible for the lesser area/molecule, 44.0 $Å^2$ /molecule compared to the area for the head group plane, 54.0 $Å^2$ /molecule obtained from the molecular modelling using ALCHEMIE.

3.4.1 Mixed monolayers of MODIMP and SA

The surface pressure-area per molecule (π-A) isotherms for mixed MODIMP/SA monolayers at various compositions are shown in Figure 3.4.2. The monolayers have low compressibility like that of SA but the phase transition point of the pure SA monolayer is not observed. Mixed monolayers showed higher collapse pressures than those of pure monolayers, when $X_{SA} > 0.3$.

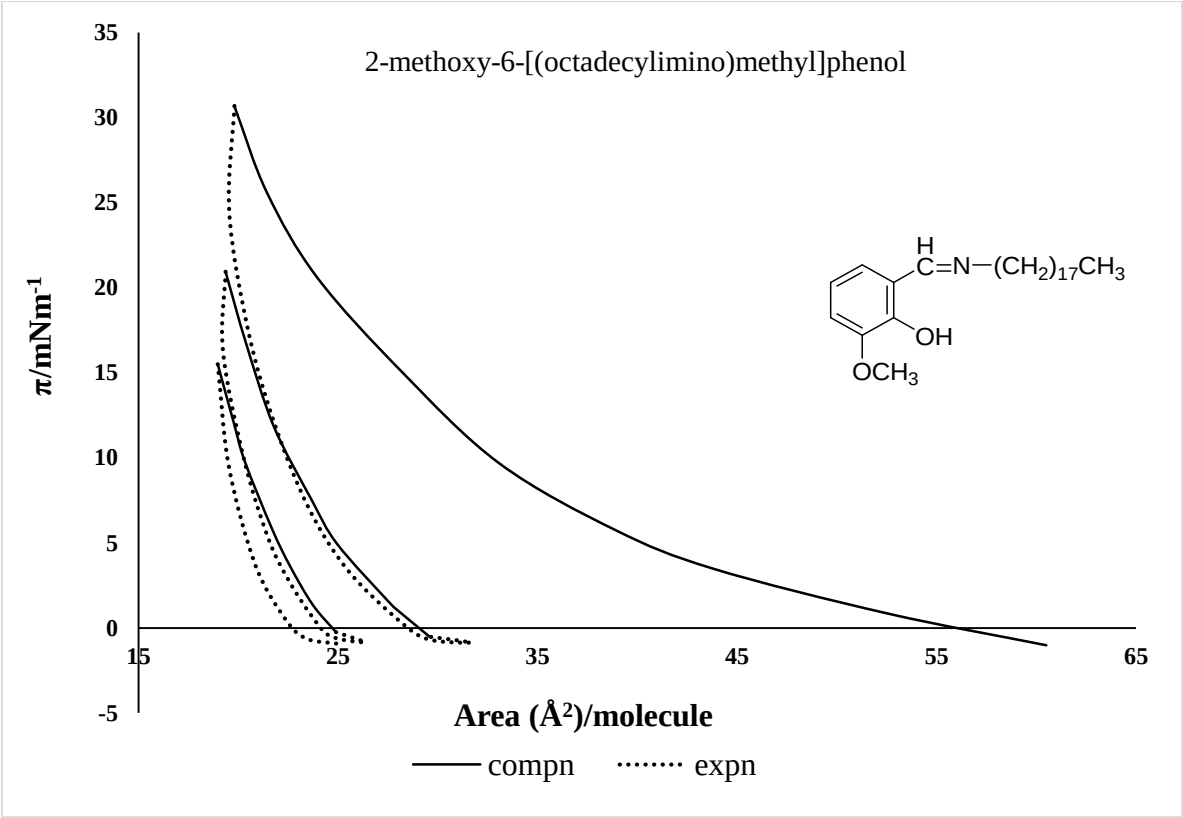

Figure 3.4.1: Surface pressure-area hysteresis isotherms of MODIMP spread over air/water interface at 25 °C.

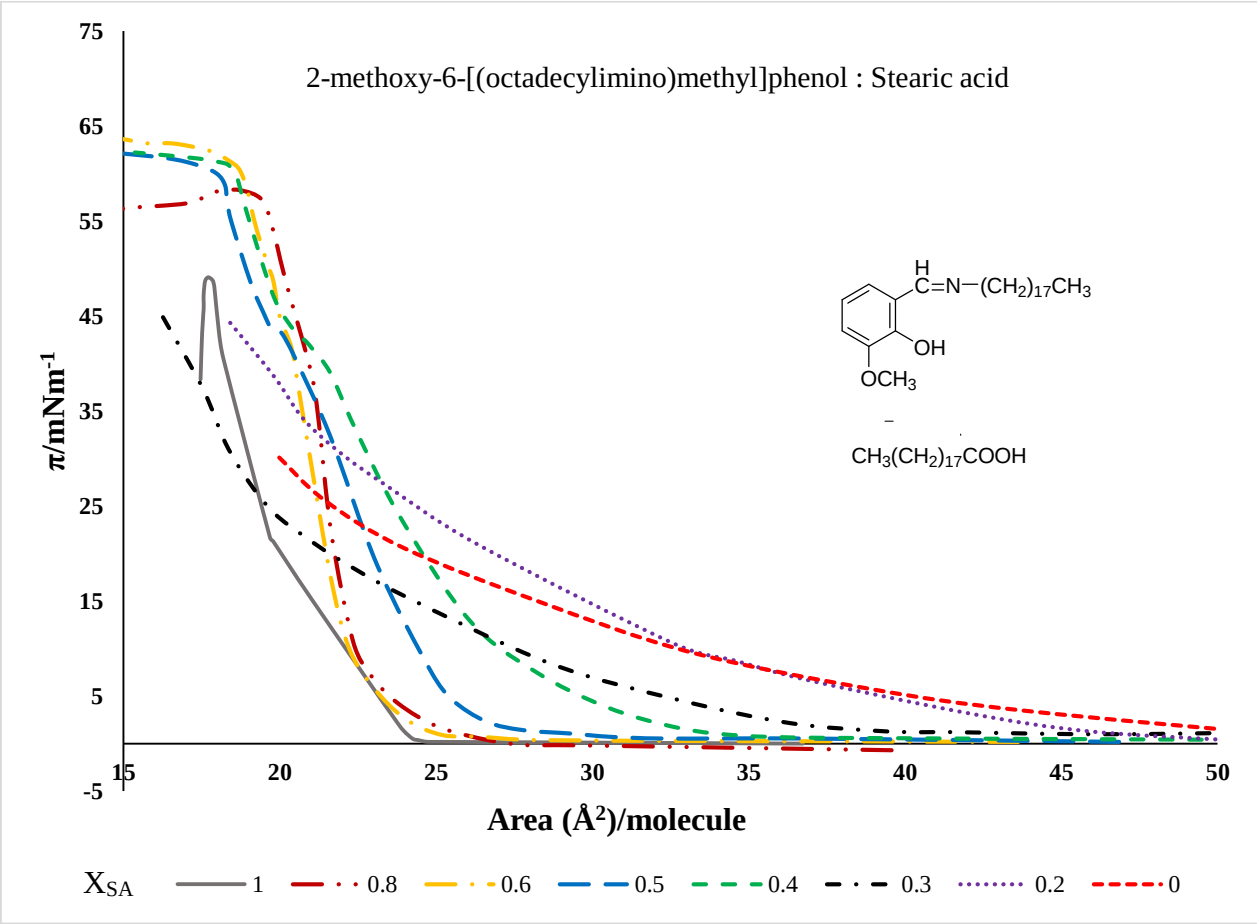

Figure 3.4.2: Surface pressure-area per molecule isotherms of mixed MODIMP/SA monolayers prepared by spreading the premixed solutions over air/water interface at 25 °C.

Table 3.4.1: Limiting area/molecule of premixed spread MODIMP/SA mixed film.

Composition of MODIMP:SA	Area/molecule ($Å^2$/molecule)
0.202: 0.798	23.16
0.403: 0.597	23.5
0.503: 0.497	24.6
0.594: 0.406	25.6
0.692: 0.308	23.4
0.797: 0.203	19.0

The area/molecule values of the MODIMP/SA monolayers are listed in Table 3.4.1. The values are almost constant. There is a large variation in the area/molecule values of the mixed monolayers compared to the pure MODIMP monolayer, indicating that there is an interaction between MODIMP and SA. This interaction may be due to the complex formation by hydrogen bond formation between the carboxyl group of the SA and the OH and imine functional groups of MODIMP of adjacently located molecules (Figure 3.4.3) [304]. The same kind of hydrogen bond formation of Schiff bases with barbituric acid has been reported by Jiao and coworkers [85; 86]. The large decrease in the area/molecule values of the mixed film compared to that of the pure MODIMP may be due to the change in the orientation plane of the molecules at the air/water interface [305]. This possibly happens due to the formation of a ring structure with an OH group in the second position. This is reported for the Cu^{2+} complexes of a Schiff base prepared from hexadecylamine and *O*-vaniline [87] and for a number of other Schiff bases [306].

From the dimensions of molecule determined from stacking of benzene rings, the calculated area for the plane of the benzene in side view is about 24 $Å^2$. Therefore an orientation of the head group nearly normal to the water surface is possible in the close packed region similar to stacking of benzene rings.

There was a decrease in surface pressure as MODIMP content increases, indicating that stability of the mixed films decrease with increasing MODIMP content. The observed trend suggests that the interactions between the MODIMP and SA are more favorable when a small amount of MODIMP is present. The characteristic behaviour of mixed films is entirely different from the pure ones, this rules out the possibility of self-association of MODIMP.

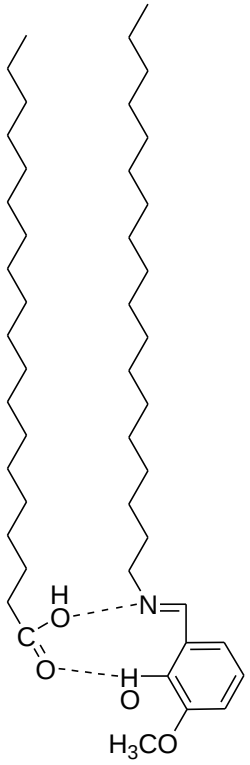

Figure 3.4.3: Possible structure of MODIMP/SA complex.

3.4.2 Miscibility of mixed monolayers

According to Gibbs phase rule, if the monolayers are miscible, the collapse pressures are dependent on the composition. Nevertheless, the isotherm of a monolayer consisting of two immiscible components will show two distinct collapse pressures corresponding to pure components, which are independent of the composition [307]. The isotherms in Figure 3.4.2 show only one collapse pressure, which varies with composition. Thus it can be concluded that MODIMP and SA were miscible at the air/water interface. It is also evident from the figure that collapsing of mixed monolayers occur at higher surface pressures than those of pure MODIMP and SA. This certainly is the evidence for the interaction between the MODIMP and SA.

Additional information on the miscibility of the components of the mixed monolayers and the interactions between them can be drawn from the excess area calculation (A_{ex}). The mean area per molecule of a mixed monolayer consisting of components 1 and 2 can be compared with that of the ideal mixed monolayer at a given surface pressure to obtain the excess area [1; 308]

$$A_{ex} = A_{12} - A_{id} = A_{12} - (X_1A_1 + X_2A_2) \qquad \text{Equation 7}$$

Where A_{12} is the mean area per molecule in the mixed monolayer at a given surface pressure, A_1 and A_2 are the areas per molecule of the pure monolayers at the same surface pressure. X_1 and X_2 are the mole fractions of components 1 and 2 respectively in the mixed monolayer. For an ideal mixed monolayer or when the components in the mixed monolayer are immiscible, the excess area will be zero and A_{12} will be linear in X_1. This arises from Eq. (7).

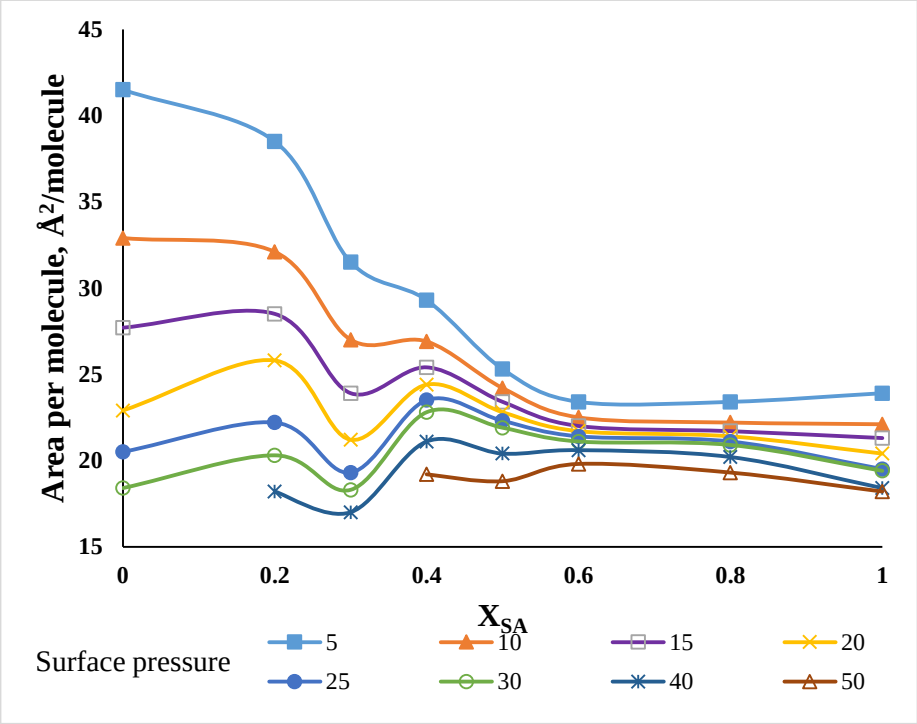

Figure 3.4.4: The mean area per molecule (A_{12}) as a function of composition for mixed MODIMP/SA monolayers at various surface pressures.

If $A_{ex}= 0$, $A_{12}= (X_1A_1 + X_2A_2)$;

but since $X_2 = 1- X_1$,

then $A_{12}= X_1A_1 + (1-X_1) A_2$;

$A_{12}= X_1(A_1 – A_2) + A_2$

Thus A_{12} will vary linearly with X_1 for an ideally mixed monolayer, or for a monolayer made of totally immiscible components. The values of A_{12} for the mixed monolayers investigated herein as a function of the film composition (X_{SA}) at various surface pressures are presented in Figure 3.4.4. The plots $A_{12} = f (X_{SA})$ for all of the investigated monolayers show deviation from linearity, which proves that the components of the mixed films are miscible.

Figure 3.4.5 shows the A_{ex}/A_{id} of the mixed monolayer system versus the mole fraction of SA at various surface pressures. From the Figure it is clear that the deviation depends on the monolayer composition and the surface pressure. The areas of monolayers exhibited negative deviations from the ideal values at all compositions for lower surface pressures. However, at higher surface pressures, distinctively positive deviation from ideality were observed. The positive deviation from linearity suggests that the interactions between the monolayer components are less attractive (or more repulsive) than those in the one-component monolayer. On the other hand, the negative deviations prove stronger attractions (weaker repulsion) between molecules in the mixed films than in the pure monolayers.

At higher surface pressures ($\pi > 15$), the values of A_{ex}/A_{id} were positive except for $X_{SA} = 0.3$ with the maxima at $X_{SA} = 0.4$, which increased with surface pressure. These data suggest that the interactions between SA and MODIMP are weaker at higher surface pressure than the interactions between similar molecules. Mixed monolayers always exhibit a negative A_{ex}/A_{id} if

attractive intermolecular forces are strong when geometric accommodation occurs. In fact, the negative values of A_{ex}/A_{id} at lower surface pressures show that, SA may produce a condensing effect in the MODIMP monolayer through the intermolecular hydrogen bond. But with increase in the MODIMP content and surface pressure, the A_{ex}/A_{id} tends to become positive indicating existence of repulsive interaction between MODIMP and SA. This may be due to the disruption of the preferential hydrogen-bonding network between the MODIMP and SA headgroups when more MODIMP molecules are present [304]. A common intersection point was found at X_{SA} = 0.3, indicating that at this point miscibility is independent of the composition and surface pressure. The same behaviour was reported in bovine lung surfactant/palmitic acid mixed monolayer [309] .

Mixed monolayers of DPPC/cholesterol [310] $C_{60}Br_{24}$ and SA [107] and ODA and SA[28] showed repulsive interaction at higher surface pressures.

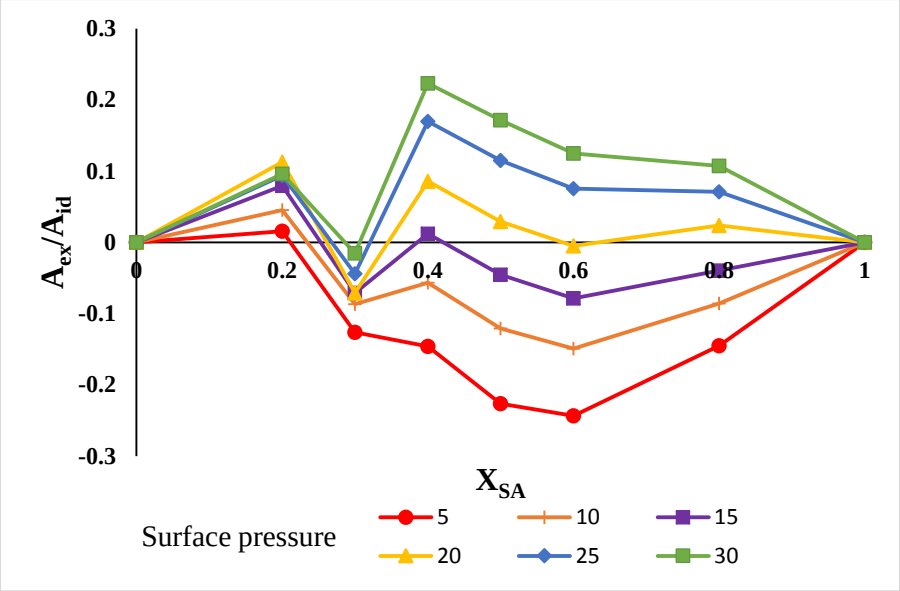

Figure 3.4.5: A_{ex}/A_{id} as a function of composition for mixed MODIMP/SA monolayers at various surface pressures.

3.4.3 Stability of mixed monolayers

Quantitative information on the interaction between the components in a mixed monolayer and the thermodynamic stability of a mixed monolayer compared with pure components can be investigated from the evaluation of Gibbs free energy of mixing, ΔG_{mix} [311]. For a mixing process of two pure monolayers to form a mixed monolayer at a constant surface pressure and temperature, the expression for Gibbs free energy of mixing (ΔG_{mix}) is given as

$$\Delta G_{mix} = \Delta G_{exc} + \Delta G_{id} \qquad \text{Equation 10}$$

$$\text{where } \Delta G_{exc} = \int_0^{\pi} [A_{12} - (X_1 A_1 + X_2 A_2)] d\pi \qquad [310] \qquad \text{Equation 9}$$

$$\Delta G_{id} = RT\,(X_1 \ln X_1 + X_2 \ln X_2) \qquad \text{Equation 11}$$

where R is the gas constant and T is the temperature. By this means, the ΔG_{exc} for various compositions of mixed MODIMP/SA monolayers at different surface pressures were calculated. From the dependence of ΔG_{mix} on composition (Figure 3.4.6), one can see that all the values of ΔG_{mix} were negative and there was a minimum in each curve, which corresponded to $X_{SA} = 0.5$ or 0.6. The negative values of ΔG_{mix} imply attractive interactions and compatibility, and the existence of a minimum indicates a mixture composition of greatest thermodynamic stability relative to the pure components. A similar trend showing a minimum at $X_{SA} = 0.5$ or 0.6 has been reported for DPPC/cholesterol [310], DPPC/cholestanol and DPPC/stigmasterol [312]. The values of ΔG_{mix} became less negative with increase in surface pressure, which again suggests that the thermodynamic stability of the mixed monolayer decreases at higher surface pressure. The common intersection point is at $X_{SA} = 0.3$, indicates the miscibility as mentioned earlier.

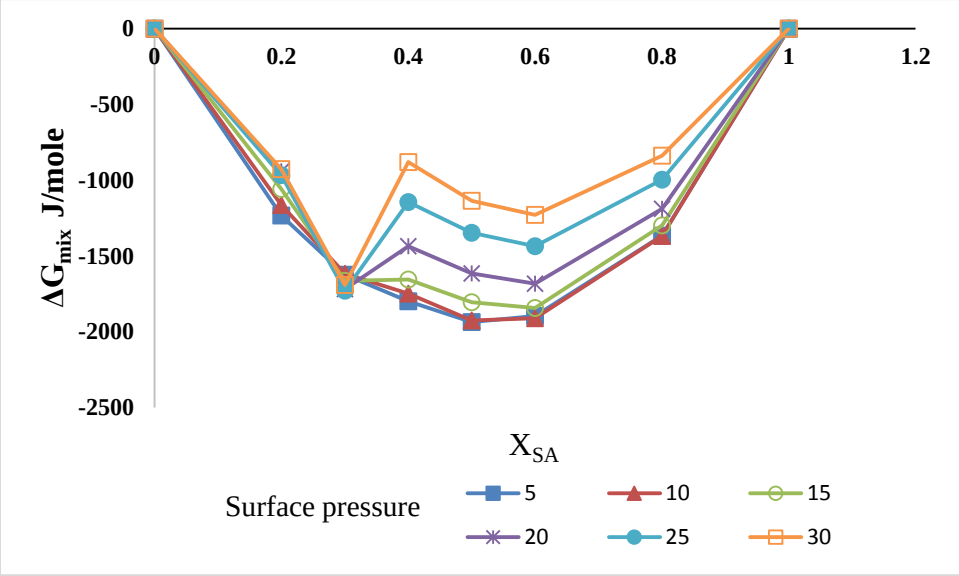

Figure 3.4.6: The free energy of mixing (ΔG_{mix}) as a function of composition for mixed MODIMP/SA monolayers at various surface pressures.

3.4.4 Hysteresis of mixed monolayers

Stability and hysteresis effects in mixed monolayers of MODIMP and SA have been studied by means of consecutive compression-expansion cycles. When MODIMP in the spreading mixture is in excess, the successive compression-expansion cycles progressively shift towards a lower area, indicating that the monolayer is losing film material. It is worth mentioning that this loss does not take place when SA is in excess; the compression-expansion curves coincide with each other (Figure 3.4.7). When $X_{MODIMP} > 0.6$, the isotherms shift to the lower side (Figure 3.4.8). This may be due to the formation of the bulk aggregates which may arise due to the rigid nature of the MODIMP/SA complex [87].

The mixed films of MODIMP and SA show a non-ideal behaviour. The values of the free energies of mixing indicate that the mixed monolayer with $X_{SA} = 0.5$ or 0.6 are the most stable compositions. The interaction between SA and MODIMP molecules in the mixed monolayer can be attributed to the hydrogen bonding interaction between the MODIMP and SA molecules. This study provides a new hydrogen bonding system at air/water interface. The hydrogen bond as an important class of molecular interactions is particularly useful in constructing artificial molecular assemblies due to its directionality and strong matching between different molecules. Further investigations on this work may need to be carried out, to transfer these hydrogen bonded films to the solid surface and their characterization by various methods such as UV-vis and FT-IR spectroscopies.

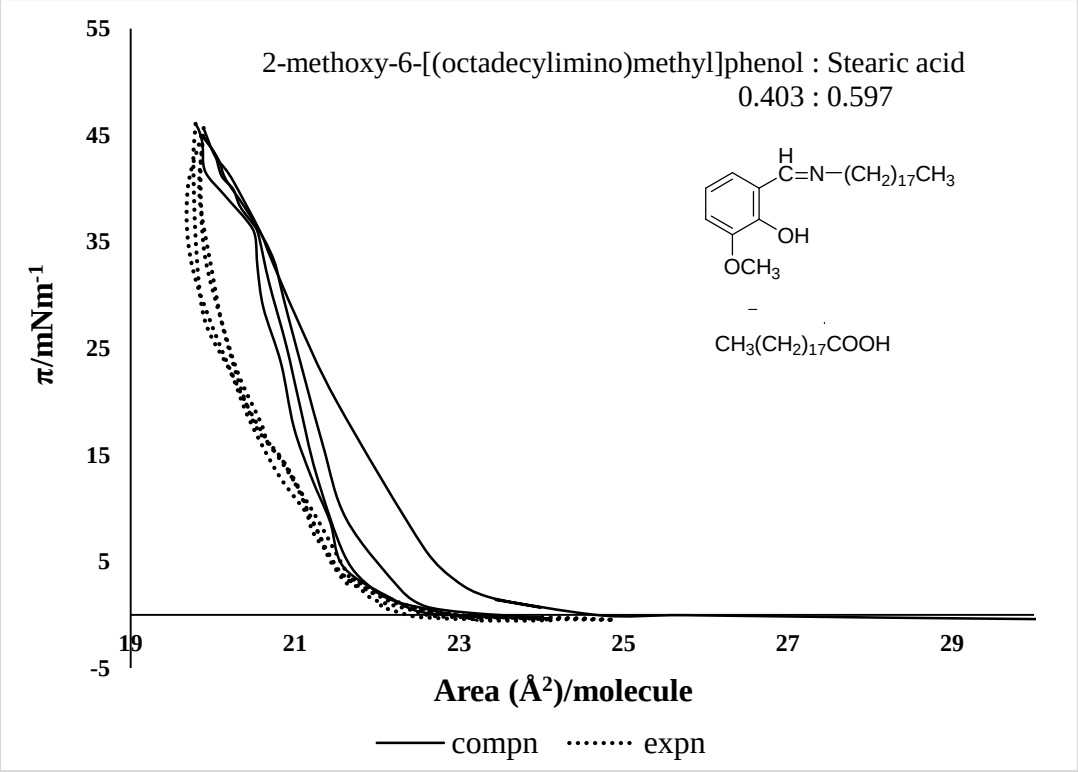

Figure 3.4.7: Surface pressure-area hysteresis isotherms of premixed MODIMP/SA monolayers over air/water interface at 25 °C.

Mole fraction ratio MODIMP:SA = 0.403:0.597.

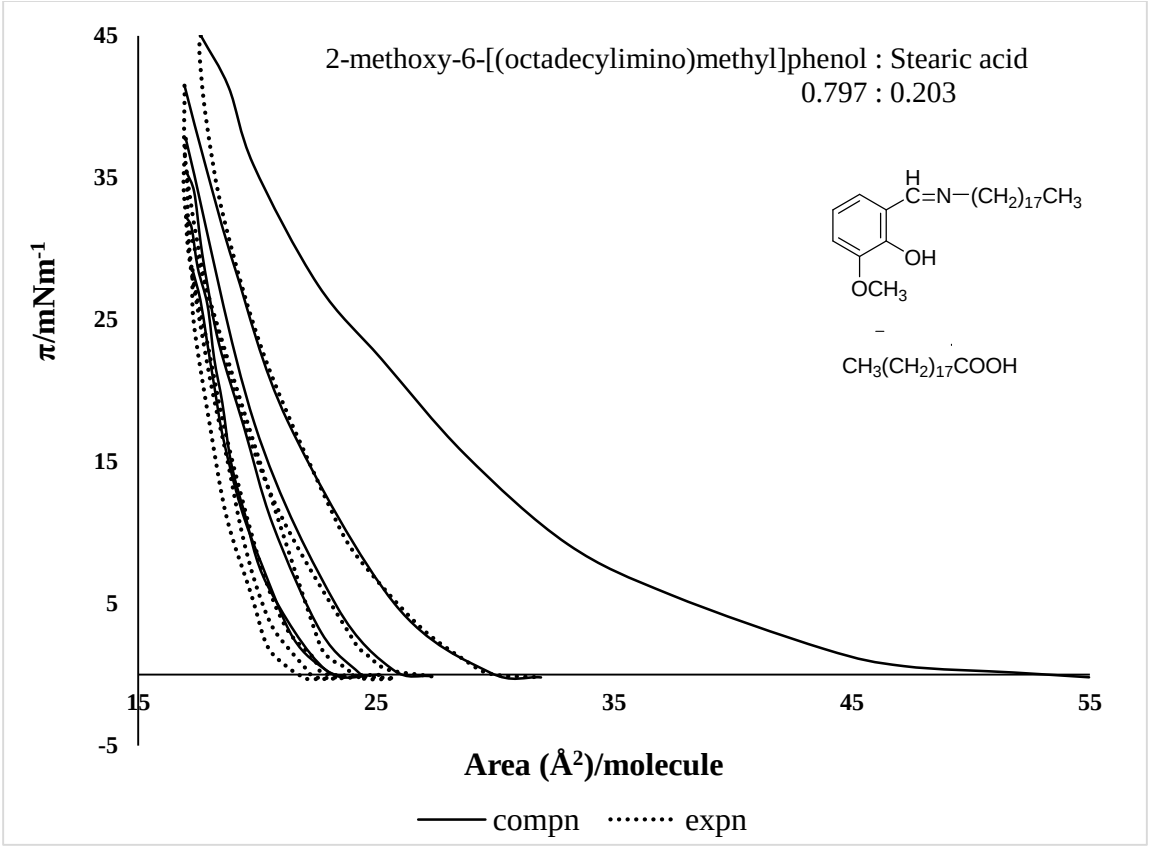

Figure 3.4.8: Surface pressure-area hysteresis isotherms of premixed MODIMP/SA monolayers over air/water interface at 25 °C.

Mole fraction ratio MODIMP:SA = 0.797:0.203.

3.5 Langmuir monolayers modulated by known chemical reactions: Behaviour of OPT over copper-containing subphase

Transition metal complexes of organic ligands containing N, S, and O have attracted attention as models for metal enzymes and electro active catalysts [313; 314]. Among the metal ions, copper is an essential co-factor for many enzymes, and complexation of Cu with sulphur of proteins facilitates the transportation of the metal ions to cellular sites [315]. It is of interest to investigate what effect such complexation would have if copper ions were present in aqueous bulk phase over which an unstable surface film of sulphur containing amphiphile is spread. Due to the similarity of the monolayers with lipid bilayers which make up cell membranes [316] the unusual Langmuir film formation by complexation of the copper subphase with sulphur of the amphiphile can serve as an effective tool to probe the copper sulphur interaction in living cells.

In addition, the Cu-S bond is involved in simultaneous oxidation of thiol ligands to the corresponding disulfides and reduction of Cu (II) ions to Cu (I) [317; 318]. This selective and reversible oxidation of thiols/thiolates to organo-disulfides (cysteine to cystine) is one of the most important biological reactions resulting in the formation of disulfide bridges within peptides and proteins. The reaction system thiol-disulfide is an important electron source for a number of redox processes in biological systems, making it an indispensable component of basic regulatory processes during signal transduction and enzyme activity. The effect of this conversion on the stability of a Langmuir film stabilized by Cu-S bond is of interest too.

Finally the amino group has the well-known property of being protonated in acidic media. It is of interest to see how the three reactions, complexation of Cu to S, the reversible oxidation of thiolate to disulfide and the protonation of the amino group, when taking place between the same

amphiphile, OPT, and the subphase (aqueous $CuSO_4$) modifies the behaviour of a Langmuir film of the amphiphile.

In this section the effect of the above well-known chemical behaviour in a Langmuir film spread is described.

3.5.1 Surface pressure-area isotherms of OPT

3.5.1.1 OPT over acidic $CuSO_4$ solutions

As mentioned in section 3.2.1, OPT does not form a stable monolayer over pure water (Figure 3.2.1), but if spread over aqueous subphase containing $CuSO_4$, it forms a stable monolayer. Figure 3.5.1 shows the surface pressure-area isotherm measured by spreading 0.010 mL solution of OPT over 0.5 mM $CuSO_4$, with limiting area of 53.7 $Å^2$/molecule. The monolayer remains stable and can be compressed to a surface pressure of 4.5 mN/m, after which it starts collapsing. The stabilization of the film by $CuSO_4$ can be explained by the coordination of OPT with copper (II) through the sulphur atoms [319]. Such behaviour has been reported for certain Schiff bases that do not form stable monolayers on water surface, but addition of metal ions such as Ag(I) or Cu(II) in the subphases causes an *in situ* coordination and leads to the formation of stable monolayers [72; 90; 91; 320].

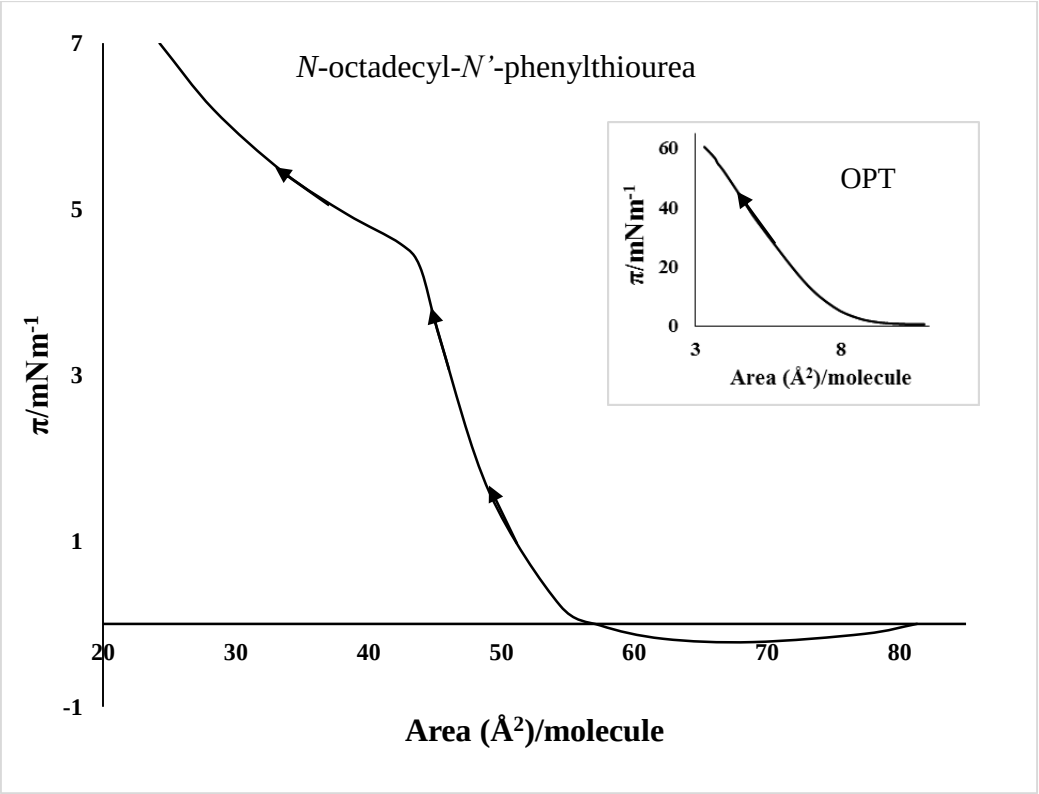

Figure 3.5.1: Surface pressure-area isotherm of OPT spread over $CuSO_4$ (0.5 mM) subphase at 25 °C. The inset represents surface pressure-area isotherm of OPT spread over air/water subphase at 25 °C.

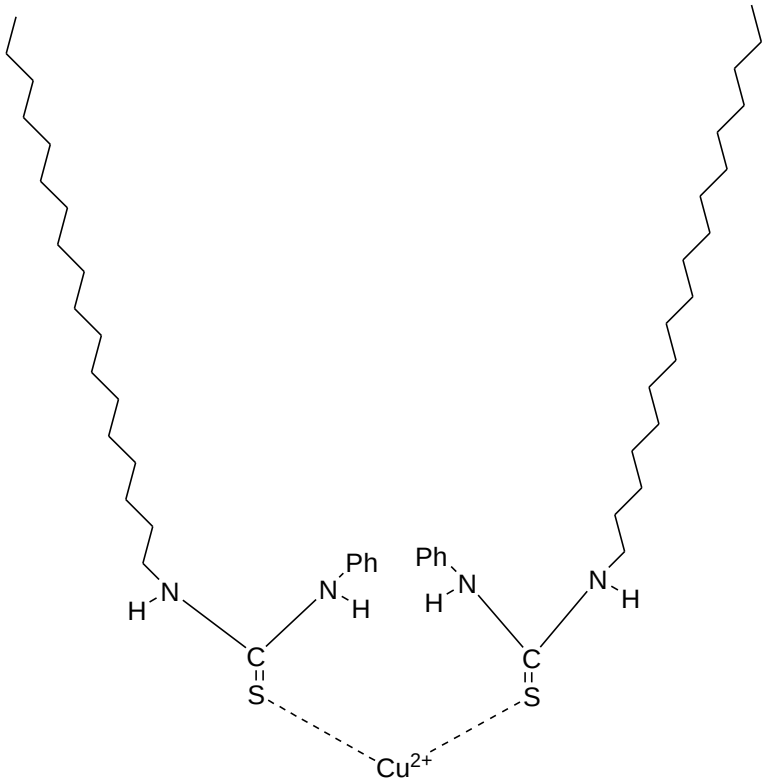

Figure 3.5.2: Possible structure of Cu (II) complex of OPT.

When the copper subphase is acidified with sulphuric acid, the isotherm is as in Figure 3.5.3. It shows that, the presence of acid in the copper subphase leads to a more stable film. After an initial slower increase to about 7 mN/m, the surface pressure increased greatly. By extrapolating the linear part of the isotherm of the monolayer film, a molecular area of 38.7 $Å^2$/molecule is obtained. This area/molecule is comparatively smaller than that of the film formed over copper subphase without the acid.

If, however, the subphase containing Cu^{2+} is made basic by the addition of NaOH, the film does not remain stable. When the OPT solution is spread on this basic solution, the surface pressure reaches an initially high value, but immediately starts decreasing and becomes zero. Compression of the surface does not result in increased surface pressure, indicating that OPT does not form a Langmuir film over a basic solution of $CuSO_4$.

In bulk, coordination between Cu and OPT is known to take place in both acidic and basic solution of $CuSO_4$, although the species in each case is different. It is known that equilibrium exists between the two species as depicted in Figure 3.5.4.

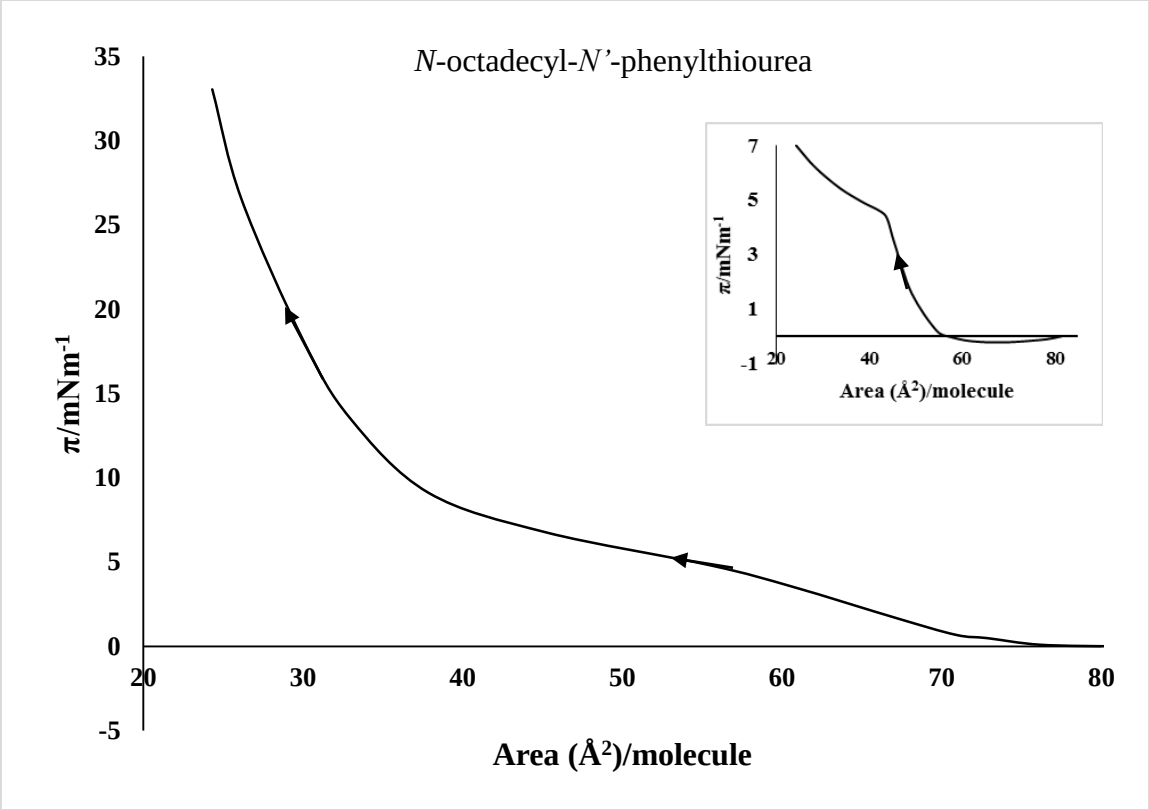

Figure 3.5.3: Surface pressure-area isotherm of OPT spread over acidic solution of $CuSO_4$ (1 mM) at 25 °C.

The inset shows surface pressure-area isotherm of OPT spread over un-acidified $CuSO_4$ (0.5 mM) subphase at 25 °C.

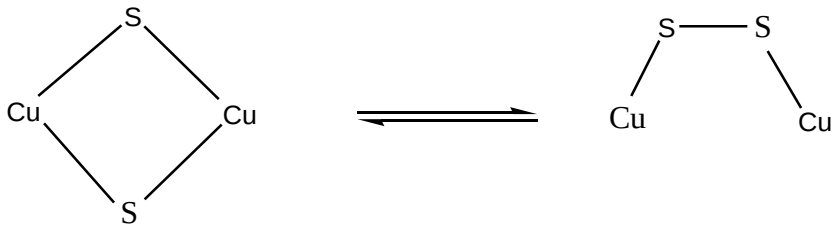

Cu(II): Basic solution

Cu(I) Acidic solution

Figure 3.5.4: Equilibrium between dimeric μ-thiolato Cu(II)Cu(II) state and its redox isomeric μ-disulphido Cu(I)Cu(I). Addition or removal of two equivalents of protons gives one or the other form.

This process is based on the redox isomerization of copper ligated by sulfur via proton coupled intermolecular shift of two electrons from the thiolates to Cu (II) atoms, resulting in the formation of the disulfide complex. The intramolecular shift of the electrons from the thiolates to the Cu (II) ion is common [59; 320; 321; 322]. In the bulk solution Cu(II) thiolate/Cu(I) disulfide interconversion can be controlled by simple addition or removal of protons [322; 323]. A solvent–dependent equilibrium exists between the dimeric μ-thiolato Cu(II)Cu(II) state (structure on the left in Figure 3.5.4) and its redox isomeric μ-disulfido Cu(I)Cu(I) form, given on the right. [59].

Both the films (over acidic and basic solution) are unstable, as indicated by a drop in their surface pressure with time (Figure 3.5.5 and Figure 3.5.6). The film over the acidic subphase, however, shows an increase in surface pressure with time, while the one over the basic subphase shows no such increase. One can conclude that a protonation reaction is responsible for the stability of the film and the increase in its surface pressure over the acidified subphase. The part of the amphiphile molecules susceptible to protonation is the NH groups, which because of the protonation, leading to the formation of NH_2^+, causes a gradual increase in the surface pressure. Such a possibility is absent in the basic solution.

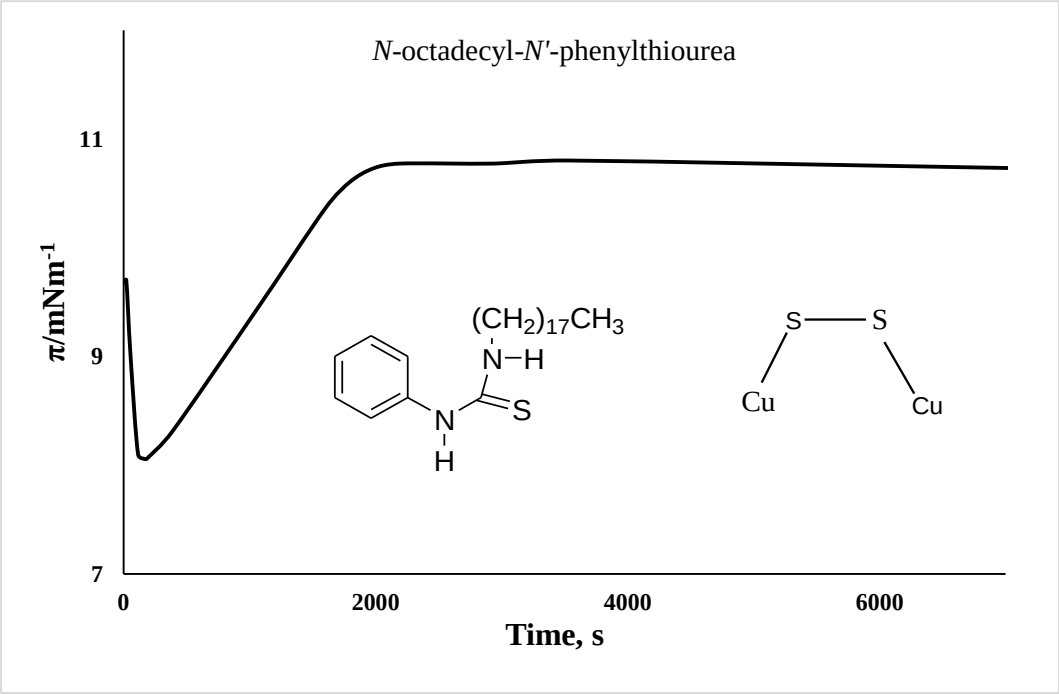

Figure 3.5.5: Surface pressure relaxation with time at constant area for 0.030 mL of OPT spread over acidic solution of $CuSO_4$ subphase (5 mM) at 25 °C.

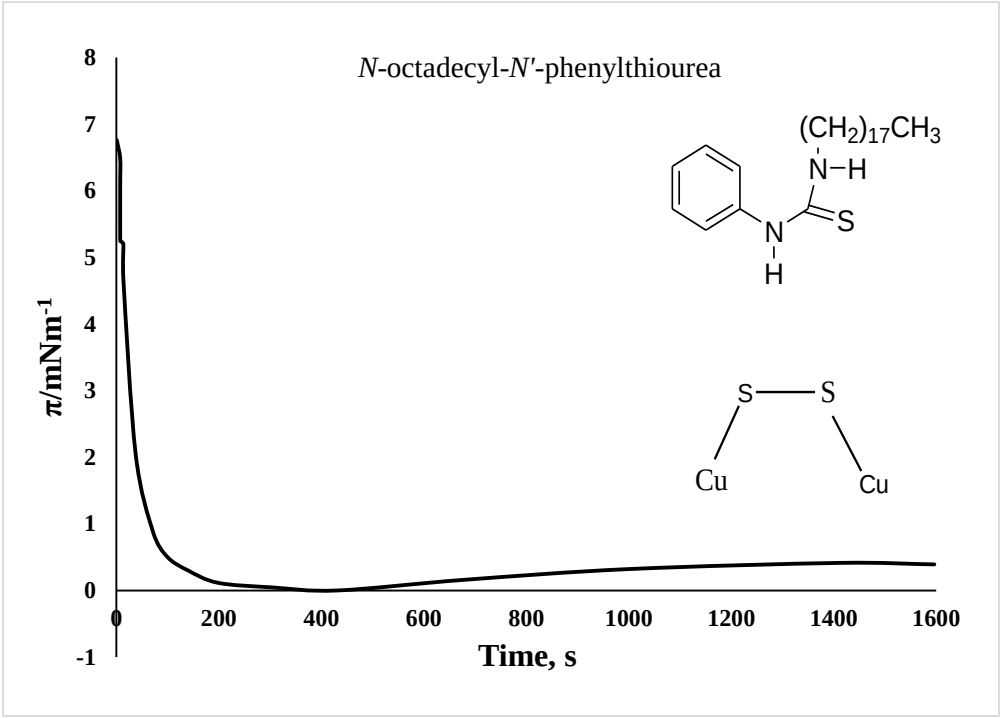

Figure 3.5.6: Surface pressure relaxation with time at constant area for 0.030 Ml of OPT spread over basic solution of $CuSO_4$ subphase at 25 °C.

The structures in Figure 3.5.4 explain why the area with acid in the subphase is smaller. In the system without the acid there is an equilibrium between the two structures, and both the structures are present. Cu (II) thiolate complex has shorter and longer Cu-S bonds, due to the distortion from the ideal tetrahedral geometry. Their bond lengths are 2.29 and 2.32 Å respectively [59]. Therefore, by assuming right angle, the S↔S distance will be around 3.26 Å. In the acidic solution, the structure predominant is the one shown on the right. The S-S bond length of Cu (I) disulfide complex is 2.04 Å. This distance is small compared to the S↔S distance of Cu (II) complex, hence the smaller area per molecule observed for the acidic subphase.

In acidic medium the thiourea is expected to exist as thiol. Oxidative coupling of the thiolate groups of two molecules leads to the formation of disulfide, while Cu^{2+} is reduced to Cu^{+} and the corresponding Cu (I)-disulfide complexes are formed [Eq. (15)] [317; 318; 324; 325].

$$2Cu^{2+} + 2RSH \longrightarrow 2Cu^{1+} + RS\text{-}SR + 2H^{+}$$

Equation 15

In contrast to this, if the solution of the amphiphile is spread on a subphase made basic by adding NaOH, it does not form a stable film. After an initial spike, the surface pressure falls and becomes zero. The addition of the base removes the protons, which inhibits the disulfide formation and reinforces the Cu (II) coordination.

3.5.2 Evolution of OPT monolayer over different subphases

To study the stability evolution of the OPT monolayer, surface pressure-time isotherms were measured. After spreading the OPT solution, the position of the barrier was fixed. The area of the monolayer was thus kept constant and the surface pressure was recorded against time. Figure 3.5.7-Figure 3.5.8 depict these isotherms for various systems. When the subphase contains $CuSO_4$ along with acid, surface pressure increases with time, and eventually reaches a steady value. In contrast, when the OPT was spread on $CuSO_4$ along with NaOH solution (Figure 3.5.6), the surface pressure decreased drastically from 8 mN/m to 0 mN/m indicating that the film was not stable. There was also no increase in surface pressure with time. When spread on $CuSO_4$ alone, the surface pressure dropped initially and then increases to a steady value (Figure 3.5.8). The initial surface pressure is high when OPT is spread over neutral or basic subphase, but over acidic subphase it is much lower. This is because over neutral and basic subphases Cu (II) thiolate molecules are formed while over acidic subphase the formation of Cu (I)-disulfide complexes takes place. The lower surface pressure of Cu (I) complex is due to the small S-S bond length compared to that of the Cu (II) complex. Figure 3.5.4 shows the Cu-S bonds part of the complexes.

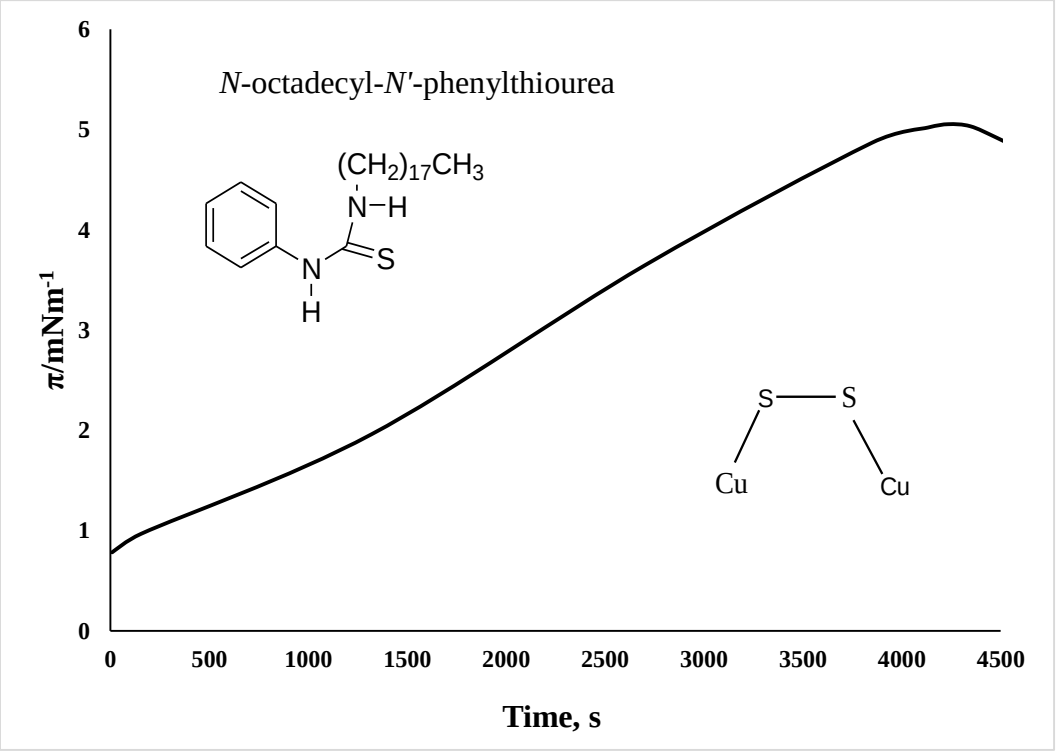

Figure 3.5.7: Surface pressure relaxation with time at constant area for 0.015 mL of OPT spread over acidic solution of $CuSO_4$ subphase (0.5 mM) at 25 °C.

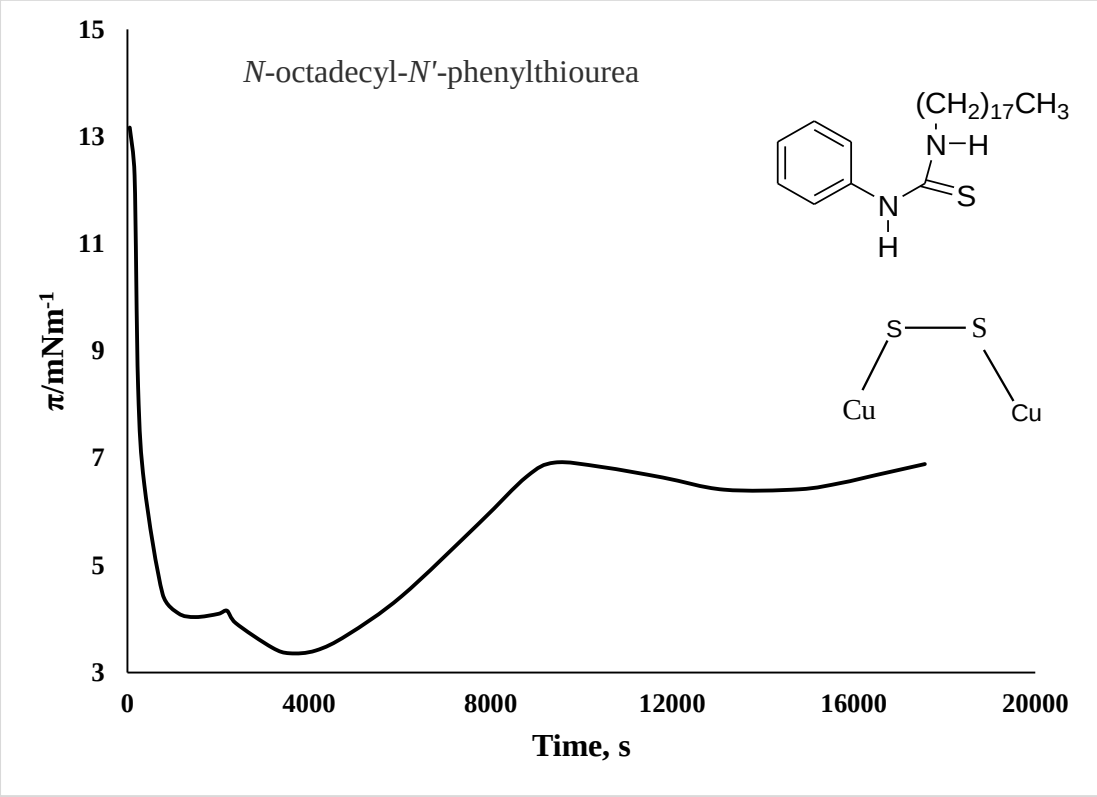

Figure 3.5.8: Surface pressure relaxation with time at constant area of OPT over 1 mM $CuSO_4$ solution at 25 °C.

3.5.3 Effect of OPT concentration

When a lower volume is spread, 0.013 mL of OPT over 0.5 mM Cu (II) concentration, there was an initial lag period of 1100 s, during which the surface pressure did not increase measurably (Figure 3.5.9). This lag period did not appear with 0.015 mL of OPT (Figure 3.5.7). This initial lag phase is described as a diffusion-limited regime (T_{lag}), where the interface is lacking sufficient quantity of complex for noticeable change in π. T_{lag} can thus be defined as the time required for attaining the minimum monolayer coverage for an effective and measurable surface pressure [326]. Similar observation has also been reported earlier in case of bovine serum albumin (BSA) [327]. During the lag period the complex molecules formed at the air/water interface are insignificant in number, and being on the average well apart, they are in gaseous phase. In course of time, the number of complex molecules at the interface increases. As a result, the surface pressure starts increasing after the period of T_{lag}. As the interface becomes populated, the surface pressure increases slowly with time and approaches a constant value. To confirm this effect, the effect of available area on these monolayers was studied, which is discussed in the next section.

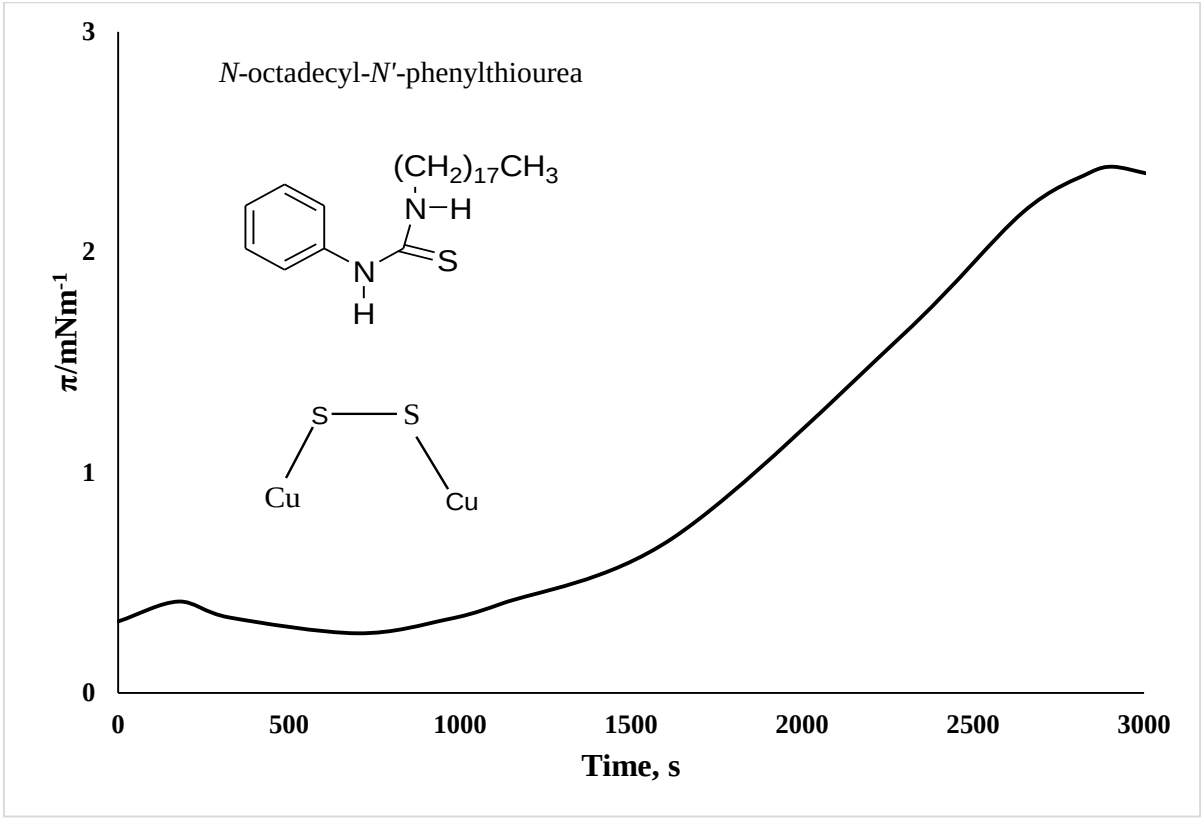

Figure 3.5.9: Surface pressure relaxation with time at constant area for 0.013 mL of OPT spread over acidic solution of $CuSO_4$ subphase (0.5 mM) at 25 °C.

3.5.4 Effect of available area on π-t isotherm

When a volume of 0.010 mL of OPT spread onto acidic solution of 0.5 mM $CuSO_4$ the surface pressure did not increase when the available area was 200 cm^2 (Figure 3.5.10). But when the area is reduced, surface pressure increased (Figure 3.5.11). The maximum surface pressure of the monolayers at various available areas of the monolayers are as shown in Table 3.5.1.

Table 3.5.1: Variation of maximum surface pressures with area of the OPT monolayers.

Available area for the monolayer(cm^2)	Maximum π (mN/m)	Area/molecule at maximum π ($Å^2$) by area calculation	Area/molecule at maximum π ($Å^2$)
168	1.41	69.4	69.3
156	1.70	64.4	66.9
144	3.18	59.5	62.3
134	5.90	55.4	47.1
124	7.65	51.2	44.5
110	4.40	45.5	53.4

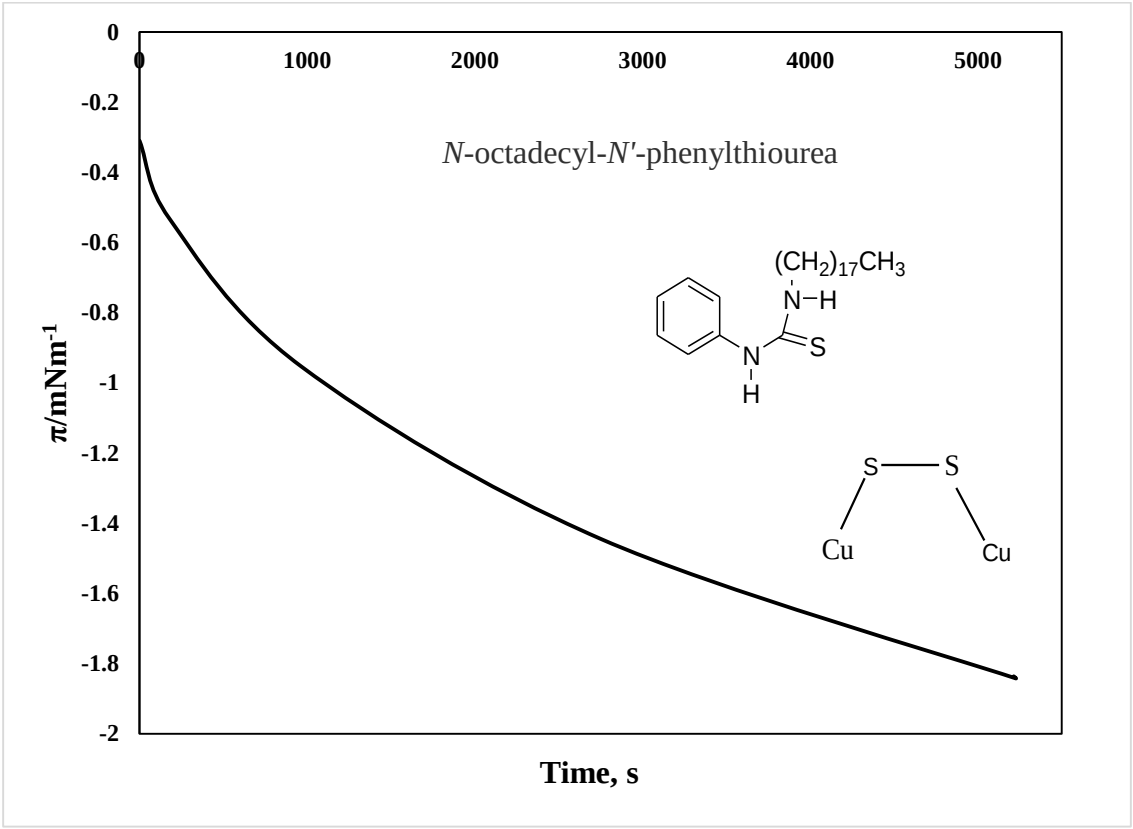

Figure 3.5.10: Surface pressure relaxation with time at constant area for 0.010 mL of OPT spread over acidic solution of $CuSO_4$ subphase (0.5 mM) at 25 °C. Available area is 200 cm^2.

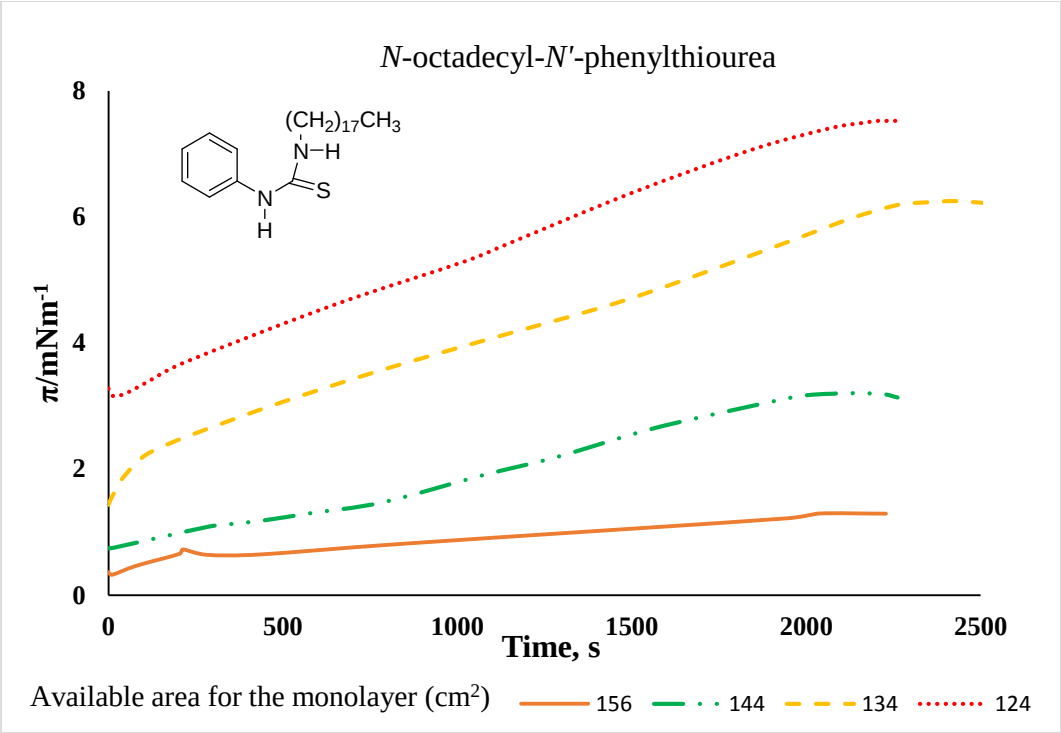

Figure 3.5.11: Surface pressure relaxation with time at constant area for 0.010 mL of OPT spread over acidic solution of $CuSO_4$ subphase (0.5 mM) at 25 °C at different available areas.

With a decrease in the available area for the monolayer, the maximum surface pressure increases and reaches a maximum before decreasing. Figure 3.5.12 shows the plot of available area of the monolayer versus π_{max}. This behaviour demonstrates that, when a very small amount of OPT is spread, the formation of complex (I) and the protonation of the NH groups occurs slowly.

3.5.5 Effect of $CuSO_4$ and H_2SO_4 concentration

The effects of the concentrations of the $CuSO_4$ and H_2SO_4 subphases were investigated. It is clear from Figure 3.5.13 and Figure 3.5.14, that within the range studied, the amount or concentrations of $CuSO_4$ and H_2SO_4 do not affect the area or the behaviour of the OPT monolayer. This is because their concentrations in the subphases are in excess, and don't change during the course of the reaction. Since the concentration of the monolayer is so small that any amount of $CuSO_4$ and H_2SO_4 will be in excess.

These results show that the nature of the OPT complex over aqueous solution of $CuSO_4$ depends on whether the subphase is acidic or not. The results presented clearly emphasize the unique potential of copper as a redox mediator in biomimetic systems, because Langmuir monolayers are excellent model systems for membrane biophysics.

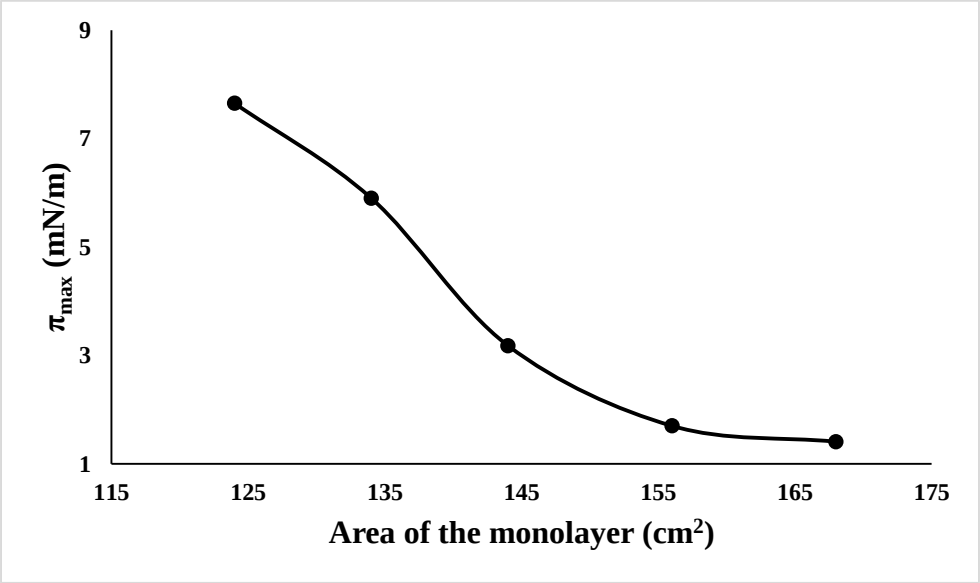

Figure 3.5.12: Plot of area of the monolayer versus maximum saturation pressure.

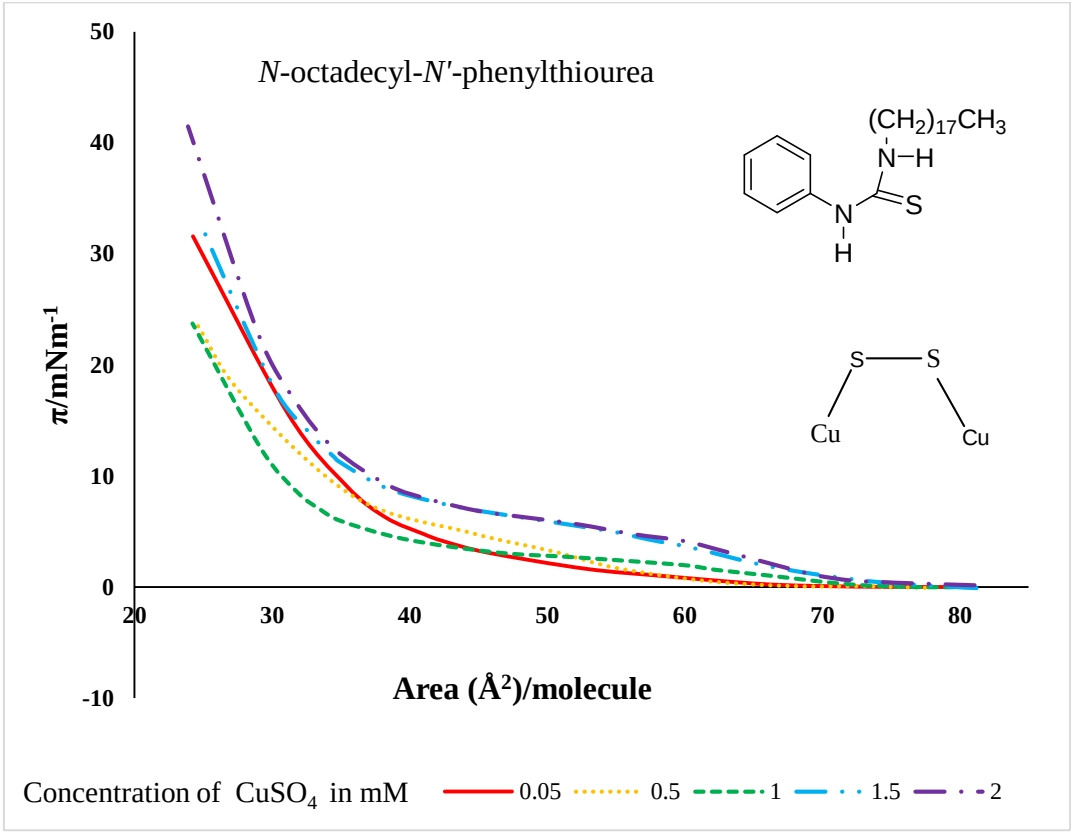

Figure 3.5.13: Surface pressure-area isotherms of OPT spread over acidic subphases with various concentrations of $CuSO_4$ at 25 °C.

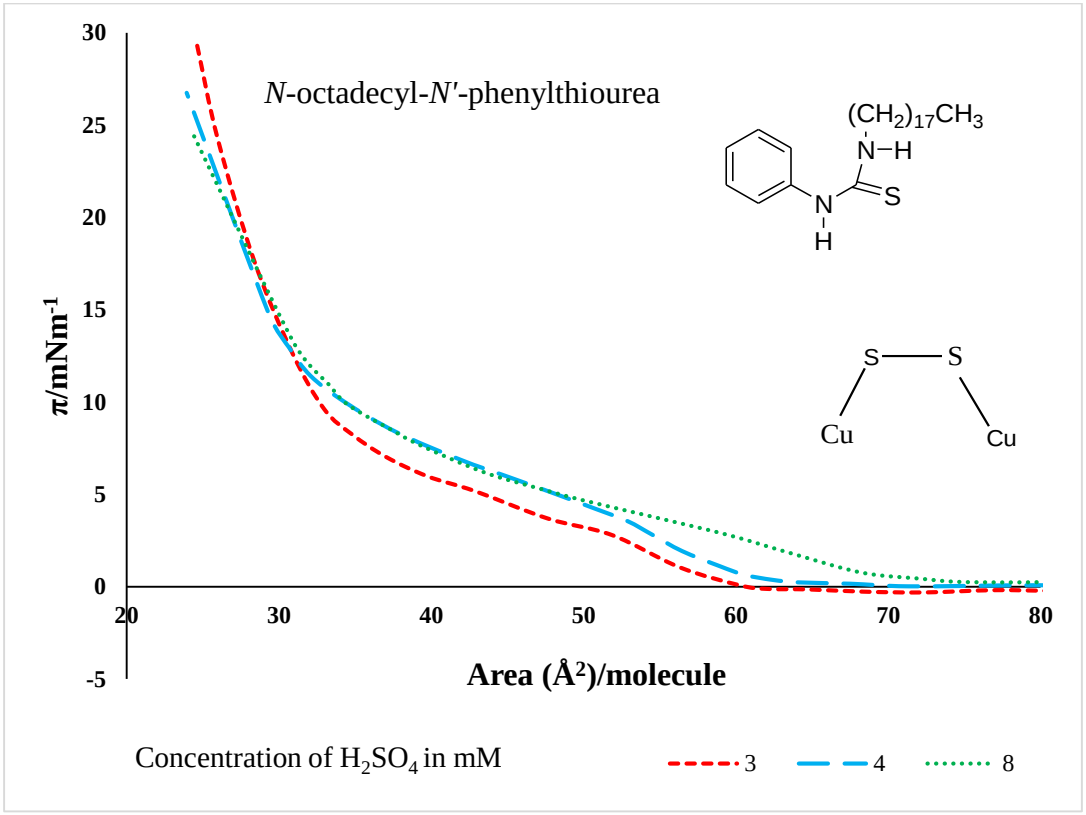

Figure 3.5.14: Surface pressure-area isotherm of OPT spread over $CuSO_4$ subphases with various concentrations of H_2SO_4 at 25 °C.

CHAPTER 4
CONCLUSIONS AND SUGGESTIONS FOR FURTHER WORK

In this study interactions between the components of the mixed monolayer systems *N*-octadecyl-*N'*-phenylthiourea/stearic acid, 2-[(octadecylimino)methyl]phenol/octadecylamine and 2-methoxy-6-[(octadecylimino)methyl]phenol/stearic acid (MODIMP/SA) and the effect of Cu ion in the aqueous subphase on Langmuir isotherms have been carried out.

In the thiourea-stearic acid mixed film, a 1:1 complex is formed, with excess stearic acid, if any remaining on the surface. On the other hand, calculation of the area/molecule shows that if thiourea has the larger mole fraction in the mixture being spread, any excess of it over what is required for a 1:1 complex is removed from the monolayer. Further studies like UV-vis spectroscopy can confirm the intermolecular interaction between thiourea and stearic acid.

When mixed films of 2-[(octadecylimino)methyl]phenol and octadecylamine are formed by spreading the two components separately, the film formed is non-homogeneous, and a calculation of the area per molecule shows that the phenol forms a bilayer. If, on the other hand the solutions of the two components are pre-mixed and then spread, calculations of the area/molecule show that the phenol does not form a bilayer, leading to the conclusion that the presence of the amine prevents the bilayer formation of the phenol. The results of this study have implications for work where bilayers might be used to mimic biological cell membranes, since the bilayers resemble the structure of the natural membranes. These results suggest further investigations of the structure of the monolayer bilayer mixture described here, possibly by Brewster angle microscopy.

In the case of 2-methoxy-6-[(octadecylimino)methyl]phenol/stearic acid mixed monolayers, the Gibbs free energy of mixing has been determined . The negative values of free energies of mixing indicated the thermodynamic stability of the mixed monolayers, and the monolayer with X_{SA} = 0.5 and 0.6 appeared to be the most stable. The interaction between the component molecules in the mixed monolayer is attributed to the hydrogen bonding interaction. Further investigations on this work may need to be carried out to transfer these hydrogen bonded films to the solid surface and their characterization by various methods such as UV-vis and FT-IR spectroscopies.

The effect of Cu ions in the aqueous subphase on Langmuir isotherms was investigated. For this, the complex formation of *N*-octadecyl-*N'*-phenylthiourea over aqueous solution of $CuSO_4$ with and without the presence of protons has been studied. The acid promotes the electron transfer from thiolate to Cu (II) resulting in the oxidation of thiolates to disulfide, and the corresponding reduction of Cu (II) to Cu (I). This leads to formation of Cu (I)-disulfide complexes. Suggested further work to this study is the comparison of the UV-vis absorption spectra of the LB films of OPT and the spectra of the chloroform solution of OPT to confirm the complex formation. The present study demonstrated that the redox interaction between copper ion and the thiourea can be controlled by the addition of protons, which should provide an insight into the copper-thiolate chemistry at interfaces, which is relevant to biological systems. These results underline the unique potential of copper as a redox mediator in biomimetic systems, Langmuir monolayers being excellent model systems for membrane biophysics.

REFERENCES

[1] G. Gaines Jr, Insoluble monolayers at gas-liquid interfaces. Interscience, New York 144 (1966).

[2] V.M. Kagnar, H. Mohwald, P. Dutta, Structure and phase transitions in Langmuir monolayers. Rev. Mod. Phys. 71 (1999) 779-819.

[3] R.A. Luz, R.M. Iost, F.N. Crespilho, Nanobioelectrochemistry, Springer-Verlag Berlin Heidelberg, (2013), 32.

[4] P. Dynarowicz-Latka, K. Kita, Molecular interaction in mixed monolayers at the air/water interface. Adv. Colloid Interface Sci. 79 (1999) 1-17.

[5] L. Rayleigh, Measurements of the amount of oil necessary in order to check the motions of camphor upon water. Proc. R. Soc. London 47 (1889) 364-367.

[6] A. Pockels, On the relative contamination of the water-surface by equal quantities of different substances. Nature 46 (1892) 418-419.

[7] H. Devaux, Journal of Physics Radium 699 (1912) 891-898.

[8] W. Hardy, The influence of chemical constitution upon interfacial tension. Proc. R. Soc. London 88 (1913) 303-313.

[9] I. Langmuir, Constitution and fundamental properties of solids and liquids. II. Liquids. J. Am. Chem. Soc. 39 (1917) 1848-1906.

[10] A.W. Adamson, A.P. Gast, Physical chemistry of surfaces, Wiley New York, (1990).

[11] J. Kim, K.C. Chou, G.A. Somorjai, Structure and dynamics of acetonitrile at the air/liquid interface of binary solutions studied by infrared-visible sum frequency generation. J. Phys. Chem. B 107 (2003) 1592-1596.

[12] P.B. Miranda, Y.R. Shen, Liquid interfaces: A study by sum-frequency vibrational spectroscopy. J. Phys. Chem. B 103 (1999) 3292-3307.

[13] I. Kuzmenko, H. Rapaport, K. Kjaer, J. Als-Nielsen, I. Weissbuch, M. Lahav, L. Leiserowitz, Design and characterization of crystalline thin film architectures at the air/liquid interface: Simplicity to complexity. Chem. Rev. 101 (2001) 1659-1696.

[14] K.Y.C. Lee, Collapse mechanisms of Langmuir monolayers. Annu. Rev. Phys. Chem. 59 (2008) 771-791.

[15] S.R. Carino, H. Tostmann, R.S. Underhill, J. Logan, G. Weerasekera, J. Culp, M. Davidson, R.S. Duran, Real-time grazing incidence X-ray diffraction studies of polymerizing n-octadecyltrimethoxysilane Langmuir monolayers at the air/water interface. J. Am. Chem. Soc. 123 (2001) 767-768.

[16] K. Kjaer, J. Als-Nielsen, C.A. Helm, L.A. Laxhuber, H. Moehwald, Ordering in lipid monolayers studied by synchrotron X-ray diffraction and fluorescence microscopy. Phys. Rev. Lett. 58 (1987) 2224-2227.

[17] Y.-L. Lee, Y.-C. Yang, Y.-J. Shen, Monolayer characteristics of mixed octadecylamine and stearic acid at the air/water interface. J. Phys. Chem. B 109 (2005) 4662-4667.

[18] O. Albrecht, H. Matsuda, K. Eguchi, Main and tilt transition in octadecylamine monolayers. Colloids Surf. A Physicochem. Eng. Asp. 284 (2006) 166-174.

[19] P. Pedraz, F.J. Montes, R.L. Cerro, M.E. Diaz, Characterization of Langmuir biofilms built by the biospecific interaction of arachidic acid with bovine serum albumin. Thin Solid Films 525 (2012) 121-131.

[20] A.P. Girard-Egrot, L.J. Blum, Langmuir-Blodgett technique for synthesis of biomimetic lipid membranes, in, Nanobiotechnology of biomimetic membranes, Springer, (2007), 23-74.

[21] A. Ulman, An introduction to ultrathin organic films, Academic Press New York (1991) 237-245.

[22] M.C. Petty, Langmuir-Blodgett films: an introduction, Cambridge University Press, (1996).

[23] N.R. Pallas, B.A. Pethica, The liquid–vapour transition in monolayers of n-pentadecanoic acid at the air/water interface. J. Chem. Soc., Faraday Trans.1 83 (1987) 585-590.

[24] P. Winch, J. Earnshaw, A light scattering study of phase transitions in monolayers of n-pentadecanoic acid. J. Phys.: Condens. Matter 1 (1989) 7187.

[25] J.F. Baret, H. Hasmonay, J.L. Firpo, J.J. Dupin, M. Dupeyrat, The different types of isotherm exhibited by insoluble fatty acid monolayers. A theoretical interpretation of phase transitions in the condensed state. Chem. Phys. Lipids 30 (1982) 177-187.

[26] G.G. Roberts, Langmuir-Blodgett films, Plenum press New York, (1990).

[27] I.S. Costin, G.T. Barnes, Two-component monolayers. II. Surface pressure-area relations for the octadecanol-docosyl sulfate system. J. Colloid Interface Sci. 51 (1975) 106-121.

[28] Y.-L. Lee, Y.-C. Yang, Y.-J. Shen, Monolayer characteristics of mixed octadecylamine and stearic acid at the air/water interface. J. Phys. Chem. B 109 (2005) 4662-4667.

[29] A. Pal, B.K. Mishra, R.K. Nath, S. Deb, S. Panigrahi, T.P. Sinha, Study of miscibility and aggregate formation in nano-dimensional Langmuir-Blodgett films of p-quaterphenyl with stearic acid. Nanosci. Nanotechnol. Lett. 3 (2011) 328-334.

[30] D. Crisp, Surface chemistry. T. Butterworth, London (1949) 65.

[31] K.P. De, P. Joos, Desorption at constant surface pressure from slightly soluble monolayers. J. Colloid Interface Sci. 91 (1983) 131-137.

[32] M. Alsina, C. Mestres, J. Garcia Anton, M. Espina, I. Haro, F. Reig, Interaction energies of cholesterol, phosphatidylserine, and phosphatidylcholine in spread mixed monolayers at the air/water interface. Langmuir 7 (1991) 975-977.

[33] L. Amaral, O.S. Filho, G. Taddei, N. Vila-Romeu, Change in micelle form induced by cosurfactant addition in nematic lyotropic phases. Langmuir 13 (1997) 5016-5021.

[34] C.L. Feng, Y.J. Zhang, J. Jin, Y.L. Song, L.Y. Xie, G.R. Qu, L. Jiang, D.B. Zhu, Reversible wettability of photoresponsive fluorine-containing azobenzene polymer in Langmuir-Blodgett films. Langmuir 17 (2001) 4593-4597.

[35] R. Tredgold, C. Winter, Langmuir-Blodgett monolayers of preformed polymers. J. Phys. D: Appl. Phys. 15 (1982) 15-55.

[36] S. Ducharme, T.J. Reece, C.M. Othon, R.K. Rannow, Ferroelectric polymer Langmuir-Blodgett films for nonvolatile memory applications. IEEE Trans. Device Mat. Rel. 5 (2005) 720-735.

[37] N.C. Maliszewskyj, P.A. Heiney, D.R. Jones, R.M. Strongin, M.A. Cichy, A.B. Smith III, Langmuir films of fullerene C_{60}, fullerene epoxide $C_{60}O$, and dihydrofulleroid $C_{61}H_2$. Langmuir 9 (1993) 1439-1441.

[38] Y.S. Obeng, A.J. Bard, Langmuir films of C_{60} at the air/water interface. J. Am. Chem. Soc. 113 (1991) 6279-6280.

[39] Y. Tomioka, M. Ishibashi, H. Kajiyama, Y. Taniguchi, Preparation and structural characterization of fullerene C_{60} Langmuir film. Langmuir 9 (1993) 32-35.

[40] R.C. Ahuja, P.-L. Caruso, D. Mobius, D. Philp, J.A. Preece, H. Ringsdorf, J.F. Stoddart, G. Wildburg, Langmuir films and Langmuir-Blodgett multilayers incorporating mechanically-threaded molecules-pseudorotaxanes. Thin Solid Films 284 (1996) 671-677.

[41] C.L. Brown, U. Jonas, J.A. Preece, H. Ringsdorf, M. Seitz, J.F. Stoddart, Introduction of [2] catenanes into Langmuir films and Langmuir-Blodgett multilayers. A possible strategy for molecular information storage materials. Langmuir 16 (2000) 1924-1930.

[42] S.S. Jang, Y.H. Jang, Y.-H. Kim, W.A. Goddard, J.W. Choi, J.R. Heath, B.W. Laursen, A.H. Flood, J.F. Stoddart, K. Norgaard, Molecular dynamics simulation of amphiphilic bistable [2] rotaxane Langmuir monolayers at the air/water interface. J. Am. Chem. Soc. 127 (2005) 14804-14816.

[43] A.P. Schenning, C. Elissen-Roman, J.-W. Weener, M.W. Baars, S.J. van der Gaast, E. Meijer, Amphiphilic dendrimers as building blocks in supramolecular assemblies. J. Am. Chem. Soc. 120 (1998) 8199-8208.

[44] D. Janietz, R.C. Ahuja, D. Mobius, Langmuir monolayers of sheet-shaped multialkyne amphiphiles. Langmuir 13 (1997) 305-309.

[45] C.M. Knobler, Recent developments in the study of monolayers at the air/water interface. Adv. Chem. Phys. 77 (1990) 397-449.

[46] E.C. Griffith, E.M. Adams, H.C. Allen, V. Vaida, Hydrophobic collapse of a stearic acid film by adsorbed l-Phenylalanine at the air/water interface. J. Phys. Chem. B 116 (2012) 7849-7857.

[47] J.W. Munden, D.W. Blois, J. Swarbrick, Surface pressure relaxation and hysteresis in stearic acid monolayers at the air/water interface. J. Pharm. Sci. 58 (1969) 1308-1312.

[48] E. Okamura, N. Fukushima, S. Hayashi, Molecular dynamics simulation of the vibrational spectra of stearic acid monolayers at the air/water interface. Langmuir 15 (1999) 3589-3594.

[49] M. Moller, D. Tildesley, K. Kim, N. Quirke, Molecular dynamics simulation of a Langmuir–Blodgett film. J. Chem. Phys. 94 (1991) 8390-8401.

[50] A. Brzozowska, M. Duits, F. Mugele, Stability of stearic acid monolayers on artificial sea water. Colloids Surf. A Physicochem. Eng. Asp. 407 (2012) 38-48.

[51] M. Muro, Y. Itoh, T. Hasegawa, A conformation and orientation model of the carboxylic group of fatty acids dependent on chain length in a Langmuir monolayer film studied by polarization-modulation infrared reflection absorption spectroscopy. J. Phys. Chem. B 114 (2010) 11496-11501.

[52] R. Vijayalakshmi, A. Dhathathreyan, M. Kanthimathi, V. Subramanian, B.U. Nair, T. Ramasami, Penetration of DNA into mixed monolayers of 1, 3-bis (salicylideneamino) propanechromium (III) perchlorate and octadecylamine at an air/water interface. Langmuir 15 (1999) 2898-2900.

[53] P. Ganguly, D. Paranjape, F. Rondelez, Role of tail-tail interactions versus head-group/subphase interactions in the pressure-area isotherms of fatty amines at the air/water interface. 1. Influence of subphase acid counterions. Langmuir 13 (1997) 5433-5439.

[54] P. Ganguly, D. Paranjape, K. Patil, M. Sastry, F. Rondelez, Role of tail-tail interactions versus head-group-subphase interactions in pressure-area isotherms of fatty amines at the air/water interface. 2. Time dependence. Langmuir 13 (1997) 5440-5446.

[55] M. Bardosova, R. Tredgold, Z. Ali-Adib, Langmuir-Blodgett films of docosylamine. Langmuir 11 (1995) 1273-1276.

[56] A.-F. Mingotaud, C. Mingotaud, L.K. Patterson, Handbook of monolayers. (1993).

[57] Y.-L. Lee, Surface characterization of octadecylamine films prepared by Langmuir-Blodgett and vacuum deposition methods by dynamic contact angle measurements. Langmuir 15 (1999) 1796-1801.

[58] A. Bibo, C. Knobler, I. Peterson, A monolayer phase miscibility comparison of long-chain fatty acids and their ethyl esters. J. Phys. Chem. 95 (1991) 5591-5599.

[59] A.M. Thomas, B.-L. Lin, E.C. Wasinger, T.D.P. Stack, Ligand noninnocence of thiolate/disulfide in dinuclear copper complexes: Solvent-dependent redox isomerization and proton-coupled electron transfer. J. Am. Chem. Soc. 135 (2013) 18912-18919.

[60] M. Broniatowski, I. Sandez Macho, J. Minones, P. Dynarowicz-Latka, Langmuir monolayers characteristic of (perfluorodecyl)-alkanes. J. Phys. Chem. B 108 (2004) 13403-13411.

[61] M.N. De Mul, J.A. Mann Jr, Multilayer formation in thin films of thermotropic liquid crystals at the air/water interface. Langmuir 10 (1994) 2311-2316.

[62] A. Itaya, M. Van der Auweraer, F. De Schryver, Preparation of monolayers and stacked layers of 1-octadecanethiol. Langmuir 5 (1989) 1123-1126.

[63] R. Bilewicz, M. Majda, Monomolecular Langmuir-Blodgett films at electrodes. Formation of passivating monolayers and incorporation of electroactive reagents. Langmuir 7 (1991) 2794-2802.

[64] J. Ahmad, N. Silavwe, Behaviour of 1-octadecanethiol film spread over silver nitrate solution. Asian J. Chem. 14 (2002) 1282-1286.

[65] W. Zhao, M.W. Kim, D.B. Wurm, S.T. Brittain, Y.-T. Kim, Silver n-octadecanethiolate Langmuir monolayers mimicking self-assembled monolayers on silver. Langmuir 12 (1996) 386-391.

[66] R.K. Gupta, K. Suresh, R. Guo, S. Kumar, Langmuir–Blodgett films of octadecanethiol–properties and potential applications. Anal. Chim. Acta 568 (2006) 109-118.

[67] I. Rousso, N. Friedman, M. Sheves, M. Ottolenghi, pKa of the protonated Schiff base and aspartic 85 in the bacteriorhodopsin binding site is controlled by a specific geometry between the two residues. Biochemistry 34 (1995) 12059-12065.

[68] K. Das, N. Sarkar, A.K. Ghosh, D. Majumdar, D.N. Nath, K. Bhattacharyya, Excited-state intramolecular proton transfer in 2-(2-hydroxyphenyl) benzimidazole and-benzoxazole: Effect of rotamerism and hydrogen bonding. J. Phys. Chem. 98 (1994) 9126-9132.

[69] M. Fores, M. Duran, M. Sola, M. Orozco, F.J. Luque, Theoretical evaluation of solvent effects on the conformational and tautomeric equilibria of 2-(2-hydroxyphenyl)benzimidazole and on its absorption and fluorescence spectra. J. Phys. Chem. A 103 (1999) 4525-4532.

[70] A.U. Acuna, F. Amat-Guerri, A. Costela, A. Douhal, J.M. Figuera, F. Florido, R. Sastre, Proton-transfer lasing from solid organic matrixes. Chem. Phys. Lett. 187 (1991) 98-102.

[71] T. Jiao, X. Li, Q. Zhang, P. Duan, L. Zhang, M. Liu, X. Luo, Q. Li, F. Gao, Interfacial assembly of a series of trigonal Schiff base amphiphiles in organized molecular films. Colloids Surf., A 407 (2012) 108-115.

[72] P. Guo, M. Liu, In situ coordination and supramolecular chirality of some achiral benzothiazole-derived schiff bases fabricated at air/water interface. Chem. Lett. 41 (2012) 1199-1200.

[73] P.J. Lebanon, M. Prakash, A. Dhathathreyan, Role of chain length and spacers in the organization of long chain Schiff base compounds at air/water and solid/liquid interfaces. Thin Solid Films 519 (2011) 5616-5622.

[74] S. Collins, A. Dhathathreyan, T. Ramasami, H. Mohwald, Langmuir and Langmuir–Blodgett films of octadecylaminodihydroxysalicylaldehyde. Thin Solid Films 358 (2000) 229-233.

[75] J. Nagel, U. Oertel, P. Friedel, H. Komber, D. Moebius, Langmuir-Blodgett layers from Schiff base copper(II) complexes. Langmuir 13 (1997) 4693-4698.

[76] S.S. Sundari, A. Dhathathreyan, M. Kanthimathi, B.U. Nair, Langmuir-Blodgett films of Schiff base complexes of copper(II). Langmuir 13 (1997) 4923-4925.

[77] J. Nagel, U. Oertel, P. Friedel, H. Komber, D. Mobius, Langmuir-Blodgett layers from Schiff base copper (II) complexes. Langmuir 13 (1997) 4693-4698.

[78] Y. Liang, L. Wu, Y. Tian, Z. Zhang, H. Chen, Structure control of synthetic bilayer membranes from single-chain amphiphiles containing the Schiff base segment. I. Conformation control and spectral characterization. J. Colloid Interface Sci. 178 (1996) 703-713.

[79] Y. Liang, Z. Zhang, L. Wu, Y. Tian, H. Chen, Structure control of synthetic bilayer membranes from single-chain amphiphiles containing the Schiff base segment. I. Conformation control and spectral characterization. J Colloid Interface Sci 178 (1996) 714-719.

[80] Y. Liu, M. Liu, Langmuir–Blodgett film and acidichromism of a long chain carbazole-containing Schiff base. Thin Solid Films 415 (2002) 248-252.

[81] T. Jiao, M. Liu, Supramolecular nano-architectures and two-dimensional/three-dimensional aggregation of a bolaamphiphilic diacid at the air/water interface. Thin Solid Films 479 (2005) 269-276.

[82] T. Jiao, J. Zhou, L. Zhang, M. Liu, Supramolecular assembly and headgroup effect in interfacial organized films (I): A study of some bolaamphiphiles. J. Dispersion Sci. Technol. 32 (2011) 1592-1598.

[83] T. Jiao, M. Liu, Substitution controlled molecular orientation and nanostructure in the Langmuir–Blodgett films of a series of amphiphilic naphthylidene-containing Schiff base derivatives. J Colloid Interface Sci 299 (2006) 815-822.

[84] T. Jiao, Y. Xing, J. Zhou, X. Zhu, L. Zhang, M. Liu, Supramolecular assembly and headgroup effect in interfacial organized films (I): A study of some bolaamphiphiles. J. Dispersion Sci. Technol. 32 (2011) 1599-1604.

[85] T. Jiao, M. Liu, Supramolecular assemblies and molecular recognition of amphiphilic Schiff bases with barbituric acid in organized molecular films. J. Phys. Chem. B 109 (2005) 2532-2539.

[86] T.F. Jiao, J.X. Zhou, Research on hydrogen bonding interaction of trigonal Schiff base compound with barbituric acid in organized molecular Films. Mater. Sci. Forum (2011) 528-532.

[87] G. Hemakanthi, B. Unni Nair, A. Dhathathreyan, Langmuir films of amphiphilic schiff base of O-Vaniline and its metal complexes. Chem. Phys. Lett. 341 (2001) 407-411.

[88] G. Hemakanthi, A. Dhathathreyan, D. Mobius, Complexation of metal ions in monolayers of amphiphilic schiff bases at liquid/air interface. Colloids Surf. A Physicochem. Eng. Asp. 198 (2002) 443-452.

[89] M. Lakshmanan, S. Sundar Raman, A. Dhathathreyan, Langmuir films of nitro substituted N-benzylidene hexadecylamine Schiff bases at air/water interface—Phase transitions and molecular dynamics simulation. Appl. Surf. Sci. 255 (2008) 3381-3387.

[90] J. Cai, M. Liu, G. Yu, Y. Liu, Coordination induced monolayer formation and fabrication of a novel conductive Langmuir–Schaefer film of benzimidazole-containing Schiff bases without a substituted alkyl chain. J. Mater. Chem. 11 (2001) 1924-1927.

[91] P. Guo, M. Liu, Chiral supramolecular assemblies from some achiral Schiff bases without alkyl chain through the organization at the air/water interface. Colloids Surf., A 284-285 (2006) 70-73.

[92] A.M. Goncalves da Silva, M.I. Viseu, C.S. Campos, T. Rechena, Effect of the spreading procedure on the formation of cationic-anionic mixed monolayers. Thin Solid Films 320 (1998) 236-240.

[93] H.-D. Dorfler, C. Koth, W. Rettig, Complete and partial miscibility in binary monolayers of phosphatidylethanolamines with different lengths of acyl groups. Langmuir 11 (1995) 4803-4810.

[94] Y.-L. Lee, K.-L. Liu, Relaxation behaviors of monolayers of octadecylamine and stearic acid at the air/water Interface. Langmuir 20 (2004) 3180-3187.

[95] R. Stosch, H.K. Cammenga, Molecular interactions in mixed monolayers of octadecanoic acid and three related amphiphiles. J. Colloid Interface Sci. 230 (2000) 291-297.

[96] A. Teixeira, A. Goncalves da Silva, A. Fernandes, Phase behaviour of stearic acid-stearonitrile mixtures: A thermodynamic study in bulk and at the air/water interface. Chem. Phys. Lipids 144 (2006) 160-171.

[97] A.C. Teixeira, A.C. Fernandes, A.R. Garcia, L.M. Ilharco, P. Brogueira, A.M. Goncalves da Silva, Microdomains in mixed monolayers of oleanolic and stearic acids: Thermodynamic study and BAM observation at the air–water interface and AFM and FTIR analysis of LB monolayers. Chem. Phys. Lipids 149 (2007) 1-13.

[98] A.C. Teixeira, P. Brogueira, A.C. Fernandes, A.M. Goncalves da Silva, Phase behaviour of binary mixtures involving tristearin, stearyl stearate and stearic acid: Thermodynamic study and BAM observation at the air/water interface and AFM analysis of LB films. Chem. Phys. Lipids 153 (2008) 98-108.

[99] A.C. Teixeira, A.R. Garcia, L.M. Ilharco, A.M. Goncalves da Silva, A.C. Fernandes, Phase behaviour of oleanolic acid/stearyl stearate binary mixtures in bulk and at the air/water interface. Chem. Phys. Lipids 160 (2009) 45-57.

[100] M. Kuramori, T. Ishikawa, T. Narita, Y. Oishi, Phase separation for langmuir monolayer in binary system based on a π-A isotherm measurement. Prog. Colloid Polym. Sci. 138 (2011) 103-107.

[101] S. Chakraborty, D. Bhattacharjee, S.A. Hussain, Formation of nanoscale aggregates of a coumarin derivative in Langmuir–Blodgett film. Appl. Phys. A 111 (2013) 1037-1043.

[102] A. Brzozowska, F. Mugele, M. Duits, Stability and interactions in mixed monolayers of fatty acid derivatives on artificial sea water. Colloids Surf. A Physicochem. Eng. Asp. 433 (2013) 200-211.

[103] R. Li, Q. Chen, D. Zhang, H. Liu, Y. Hu, Mixed monolayers of Gemini surfactants and stearic acid at the air/water interface. J Colloid Interface Sci 327 (2008) 162-168.

[104] S. Hussain, S. Deb, S. Biswas, D. Bhattacharjee, Langmuir–Blodgett films of 9-phenyl anthracene molecules incorporated into different matrices. Spectrochim. Acta, Part A 61 (2005) 2448-2454.

[105] R. Azumi, M. Matsumoto, S.-I. Kuroda, M.J. Crossley, Orientation control of porphyrin in the mixed monolayer at the air/water interface by adding long-chain N-alkanes. Mol. Cryst. Liq. Cryst. Sci. Technol., Sect. A 295 (1997) 469-472.

[106] B.M.D. O'Driscoll, J.L. Ruggles, I.R. Gentle, Mixed thin films of a cationic amphiphilic porphyrin and n-alkanes. Langmuir 20 (2004) 6246-6251.

[107] S.S. Gayathri, A. Patnaik, Interfacial behaviour of brominated fullerene ($C_{60}Br_{24}$) and stearic acid mixed Langmuir films at air/water interface. Chem. Phys. Lett. 433 (2007) 317-322.

[108] A. Asnacios, D. Langevin, J.-F. Argillier, Complexation of cationic surfactant and anionic polymer at the air/water interface. Macromolecules 29 (1996) 7412-7417.

[109] J.M. Berg, L.G.T. Eriksson, Mixed monolayers and Langmuir-Blodgett films consisting of a fatty amine and a bipolar substance. Langmuir 10 (1994) 1213-1224.

[110] B. Gur, K. Meral, Preparation and characterization of mixed monolayers and Langmuir− Blodgett films of merocyanine 540/octadecylamine mixture. Colloids Surf. A Physicochem. Eng. Asp. 414 (2012) 281-288.

[111] M.N. Islam, D. Bhattacharjee, S.A. Hussain, Monolayer characteristics of pyrene mixed with stearic acid at the air/water interface. Surf. Rev. Lett. 15 (2008) 287-293.

[112] P. Paul, S. Hussain, D. Bhattacharjee, Photophysical characterizations of 2-(4-biphenylyl)-5 phenyl-1, 3, 4-oxadiazole in restricted geometry. J. Lumin. 128 (2008) 41-50.

[113] S. Acharya, D. Bhattacharjee, G. Talapatra, Monolayer characteristics and spectroscopic study of benz (b) fluoranthene assembled in Langmuir Blodgett films mixed with stearic acid. J. Phys. Chem. Solids 64 (2003) 651-657.

[114] A.M.G. da Silva, M.I. Viseu, R.I. Romao, S.M. Costa, Behaviour of the water-soluble meso-tetra (4-methylpyridyl) porphine in mixed monolayers and in Langmuir–Blodgett films. Phys. Chem. Chem. Phys. 4 (2002) 4754-4762.

[115] A.R. Merrill, P. Proulx, A. Szabo, Effects of exogenous fatty acids on calcium uptake by brush-border membrane vesicles from rabbit small intestine. Biochim. Biophys. Acta 855 (1986) 337-344.

[116] F. Messineo, M. Rathier, C. Favreau, J. Watras, H. Takenaka, Mechanisms of fatty acid effects on sarcoplasmic reticulum. III. The effects of palmitic and oleic acids on sarcoplasmic reticulum function--a model for fatty acid membrane interactions. J. Biol. Chem. 259 (1984) 1336-1343.

[117] M. Dahim, H. Brockman, How colipase-fatty acid interactions mediate adsorption of pancreatic lipase to interfaces. Biochemistry 37 (1998) 8369-8377.

[118] A. Ortiz, J.C. Gomez-Fernandez, A differential scanning calorimetry study of the interaction of free fatty acids with phospholipid membranes. Chem. Phys. Lipids 45 (1987) 75-91.

[119] M. Langner, T. Isac, S.W. Hui, Interaction of free fatty acids with phospholipid bilayers. Biochim. Biophys. Acta 1236 (1995) 73-80.

[120] J. Beno, M. Weis, E. Dobrocka, D. Hasko, Mixed 2D molecular systems: Mechanic, thermodynamic and dielectric properties. Appl. Surf. Sci. 254 (2008) 6370-6375.

[121] C.A. Andrade, N.S. Santos-Magalhaes, C.P. de Melo, Thermodynamic characterization of the prevailing molecular interactions in mixed floating monolayers of phospholipids and usnic acid. J Colloid Interface Sci 298 (2006) 145-153.

[122] A.M. Goncalves da Silva, R.I. Romao, Mixed monolayers involving DPPC, DODAB and oleic acid and their interaction with nicotinic acid at the air/water interface. Chem. Phys. Lipids 137 (2005) 62-76.

[123] R.I. Romao, A.M. Goncalves da Silva, Phase behaviour and morphology of binary mixtures of DPPC with stearonitrile, stearic acid, and octadecanol at the air/water interface. Chem. Phys. Lipids 131 (2004) 27-39.

[124] A.D. Petelska, Z.A. Figaszewski, The equilibria of phosphatidylcholine–fatty acid and phosphatidylcholine–amine in monolayers at the air/water interface. Colloids Surf., B 82 (2011) 340-344.

[125] R.K. Gupta, K.A. Suresh, Stabilization of Langmuir monolayer of hydrophobic thiocholesterol molecules. Colloids Surf., A 320 (2008) 233-239.

[126] T.E. Goto, A. Sakai, R.M. Iost, W.C. Silva, F.N. Crespilho, L.O. Peres, L. Caseli, Langmuir–Blodgett films based on poly(p-phenylene vinylene) and protein-stabilised palladium nanoparticles: Implications in luminescent and conducting properties. Thin Solid Films 540 (2013) 202-207.

[127] A. Sakai, S.H. Wang, L.O. Peres, L. Caseli, Controlling the luminescence properties of poly(p-phenylene vinylene) entrapped in Langmuir and Langmuir-Blodgett films of stearic acid. Synth. Met. 161 (2011) 1753-1759.

[128] Y.-L. Lee, A. Dudek, T.-N. Ke, F.-W. Hsiao, C.-H. Chang, Mixed polyelectrolyte-surfactant Langmuir monolayers at the air/water interface. Macromolecules 41 (2008) 5845-5853.

[129] T.C.F. Santos, L.O. Peres, S.H. Wang, O.N. Oliveira, Jr., L. Caseli, Mixing alternating copolymers containing fluorenyl groups with phospholipids to obtain Langmuir and Langmuir-Blodgett Films. Langmuir 26 (2010) 5869-5875.

[130] I. Watanabe, K. Hong, M.F. Rubner, Fabrication of novel electrically conductive Langmuir-Blodgett thin films of the poly(3-alkylthiophenes). Thin Solid Films 179 (1989) 199-206.

[131] G. Xu, Z. Bao, J.T. Groves, Langmuir-Blodgett films of regioregular poly (3-hexylthiophene) as field-effect transistors. Langmuir 16 (2000) 1834-1841.

[132] J.Z. Niu, G. Cheng, Z. Li, H. Wang, S. Lou, Z. Du, L.S. Li, Poly (3-dodecylthiophene) Langmuir–Blodgett films: Preparation and characterization. Colloids Surf. A Physicochem. Eng. Asp. 330 (2008) 62-66.

[133] Y. Yang, C.-S. Song, R.-Q. Ye, B.-Z. Mu, Hysteresis behavior of surfactin monolayer at the air/water interface. Acta Phys-Chim. Sin. 27 (2011) 2217-2221.

[134] K.-H. Wang, M.-J. Syu, C.-H. Chang, Y.-L. Lee, Immobilization of glucose oxidase by Langmuir–Blodgett technique for fabrication of glucose biosensors: Headgroup effects of template monolayers. Sens. Actuators, B 164 (2012) 29-36.

[135] J. Chovelon, K. Wan, N. Jaffrezic-Renault, Influence of the surface pressure on the organization of mixed Langmuir-Blodgett films of octadecylamine and butyrylcholinesterase. 1. Film preparation at the air/water interface. Langmuir 16 (2000) 6223-6227.

[136] S. Reuter, K. Busse, U. Radics, H.-J. Niclas, J. Kressler, Langmuir monolayers and Langmuir-Blodgett films of 1-acyl-1,2,4-triazoles. J. Colloid Interface Sci. 340 (2009) 276-284.

[137] T. Lopes-Costa, F. Gamez, S. Lago, J.M. Pedrosa, Adsorption of DNA to octadecylamine monolayers at the air/water interface. J Colloid Interface Sci 354 (2011) 733-738.

[138] M. Perez-Morales, J.M. Pedrosa, M.T. Martin-Romero, D. Mobius, L. Camacho, Reversible trilayer formation at the air/water interface from a mixed monolayer containing a cationic lipid and an anionic porphyrin. J. Phys. Chem. B 108 (2004) 4457-4465.

[139] V. Alvarez-Venicio, M. Gutierrez-Nava, O. Amelines-Sarria, E. Alvarez-Zauco, V. Basiuk, M. Carreon-Castro, Incorporation in Langmuir–Blodgett films of an amphiphilic derivative of fullerene C_{60} and oligo-*para*-phenylenevinylene. Thin Solid Films 526 (2012) 246-251.

[140] F. Cardinali, J.-L. Gallani, S. Schergna, M. Maggini, J.-F. Nierengarten, An amphiphilic C_{60} derivative with a tris(2,2′-bipyridine)ruthenium(II) polar head group: Synthesis and incorporation in Langmuir films. Tetrahedron Lett. 46 (2005) 2969-2972.

[141] J. Sanchez-Gonzalez, J. Ruiz-Garcıia, M.J. Galvez-Ruiz, Langmuir–Blodgett films of biopolymers: a method to obtain protein multilayers. J Colloid Interface Sci 267 (2003) 286-293.

[142] M. Haro, P. Cea, I. Gascon, F.M. Royo, M.C. Lopez, Mixed Langmuir and Langmuir-Blodgett films of a proton sponge and a fatty acid: Influence of the subphase nature on the interactions between the two components. J. Phys. Chem. B 111 (2007) 2845-2855.

[143] J. Ahmad, K.B. Astin, Conformer selection by monolayer compression. J. Am. Chem. Soc. 108 (1986) 7434-7435.

[144] J. Ahmad, K.B. Astin, Influencing reactivity by monolayer compression: An alcohol dehydration. J. Am. Chem. Soc. 110 (1988) 8175-8178.

[145] J. Ahmad, K.B. Astin, Reactions in monolayers: The oxidation of thiols to disulfides. Colloids Surf. 49 (1990) 281-287.

[146] J. Ahmad, K.B. Astin, Oxidation of alcohol monolayers by chromic acid. Langmuir 4 (1988) 780-781.

[147] S.J. Valenty, Chemical reactions in monolayer films. Chromatography, a multicompartment trough, and the hydrolysis of surfactant ester derivatives of tris(2,2'-bipyridine)ruthenium(II)2+. J. Am. Chem. Soc. 101 (1979) 1-8.

[148] I. Gascon, C. Patrascu, J.-D. Marty, C. Mingotaud, Example of an organic reaction in a Langmuir film: Reduction of an amphiphilic ketone by $NaBH_4$. J Colloid Interface Sci 289 (2005) 574-580.

[149] B. Liu, H.-X. Huang, C.-F. Zhang, M. Chen, D.-J. Qian, Monolayers, Langmuir-Blodgett films of bimetallic coordination polymers of 4'-(4-pyridyl)-2,2':6',2''-terpyridine. Thin Solid Films 516 (2008) 2144-2150.

[150] Y. Zhang, P. Chen, M. Liu, A general method for constructing optically active supramolecular assemblies from intrinsically achiral water-insoluble free-base porphyrins. Chem. - Eur. J. 14 (2008) 1793-1803.

[151] J.K. Kumar, J.S. Oliver, Kinetic analysis of amide bond formation at the air/water interface using ^1H NMR spectroscopy. J. Am. Chem. Soc. 124 (2002) 11307-11314.

[152] C.-F. Zhang, M. Chen, D.-J. Qian, Characterization and electrochemistry of interfacial self-assembled multi-manganese(III)-porphyrin arrays. Thin Solid Films 517 (2009) 3760-3765.

[153] P. Duan, L. Qin, M. Liu, Langmuir-Blodgett films and chiroptical switch of an azobenzene-containing dendron regulated by the in situ host-guest reaction at the air/water Interface. Langmuir 27 (2011) 1326-1331.

[154] S. Biswas, S.A. Hussain, S. Deb, R.K. Nath, D. Bhattacharjee, Formation of complex films with water-soluble CTAB molecules. Spectrochim. Acta, Part A 65 (2006) 628-632.

[155] S. Biswas, D. Bhattacharjee, R.K. Nath, S.A. Hussain, Formation of complex Langmuir and Langmuir–Blodgett films of water soluble rosebengal. J Colloid Interface Sci 311 (2007) 361-367.

[156] S.A. Hussain, M.N. Islam, D. Bhattacharjee, Reaction kinetics of organo-clay hybrid films: in-situ IRRAS and AFM studies. arXiv.org. (2011) 1-11.

[157] M. Saha, S.A. Hussain, D. Bhattacharjee, Interaction of a laser dye with a floating phospholipid monolayer. Journal of Macromolecular Science, Part A: Pure and Applied Chemistry 50 (2013) 607-614.

[158] L. Zhong, T. Jiao, M. Liu, Synthesis and assembly of gold nanoparticles in organized molecular films of gemini amphiphiles. Langmuir 24 (2008) 11677-11683.

[159] L. Zhang, Y.H. Shen, A.J. Xie, S.K. Li, L.G. Qiu, Y.M. Li, Assembly of gold composite thin films by spontaneous reduction of subphase chloroaurate anions beneath vitamin E Langmuir monolayers. Mater. Chem. Phys. 105 (2007) 25-30.

[160] R. Pasricha, A. Singh, M. Sastry, Shape and size selective separation of gold nanoclusters by competitive complexation with octadecylamine monolayers at the air/water interface. J. Colloid Interface Sci. 333 (2009) 380-388.

[161] J. Ahmad, Reactions in monolayers: Oxidation of 1-octadecanethiol catalyzed by octadecylamine. Langmuir 12 (1996) 963-965.

[162] A. Pasc-Banu, C. Sugisaki, T. Gharsa, J.-D. Marty, I. Gascon, M. Kraemer, G. Pozzi, B. Desbat, S. Quici, I. Rico-Lattes, C. Mingotaud, Monolayers of salen derivatives as catalytic planes for alkene oxidation in water. Chem. - Eur. J. 11 (2005) 6032-6039.

[163] M.S. Chandra, T.P. Radhakrishnan, Polyelectrolyte templated polymerization in Langmuir films: Nanoscopic control of polymer chain organization. Chem. - Eur. J. 12 (2006) 2982-2986.

[164] J. Zhao, H. Akiyama, K. Abe, Z. Liu, F. Nakanishi, Studies on the molecular environment and reaction kinetics of photo-oligomerization in Langmuir-Blodgett films of 4-(4-(2-(octadecyloxycarbonyl)vinyl)- cinnamoylamino)benzoic acid. Langmuir 16 (2000) 2275-2280.

[165] O. Fichet, D. Teyssie, A new type of spontaneous vinyl monomer polymerization in Langmuir films. Macromolecules 35 (2002) 5352-5354.

[166] L. Zhang, Y. Li, Y. Shen, A. Xie, One-step synthesis of poly(2-hexadecyloxyaniline)/selenium nanocomposite Langmuir-Blodgett film by in situ redox reaction. Mater. Chem. Phys. 125 (2011) 522-527.

[167] T.J.S. Viitala, J. Peltonen, M. Linden, J.B. Rosenholm, Spectroscopy, polymerization kinetics and topography of linoleic acid Langmuir and Langmuir-Blodgett films. J. Chem. Soc., Faraday Trans. 93 (1997) 3185-3190.

[168] S.A. Letts, T. Fort, Polymerization of oriented monolayers of octadecyl acrylate. Characterization of the reaction products. J. Colloid Interface Sci. 202 (1998) 341-347.

[169] Y. Xu, J. Li, W. Hu, G. Zou, Q. Zhang, Thermochromism and supramolecular chirality of the coumarin-substituted polydiacetylene LB films. J. Colloid Interface Sci. 400 (2013) 116-122.

[170] H.Y. Araghi, M.F. Paige, Deposition and photopolymerization of phase-separated perfluorotetradecanoic acid-10,12-pentacosadiynoic acid Langmuir-Blodgett monolayer films. Langmuir 27 (2011) 10657-10665.

[171] T. Koga, T. Taguchi, N. Higashi, β-Sheet peptide-assisted polymerization of diacetylene at the air/water interface and thermochromic property. Polym. J. 44 (2012) 195-199.

[172] M. Bardosova, P. Hodge, H. Matsuda, F. Nakanishi, R.H. Tredgold, Ultrathin films of polymerized smectic liquid crystals. A study of the polymerization process. Langmuir 15 (1999) 631-633.

[173] T. Kamilya, P. Pal, G.B. Talapatra, Incorporation of ovalbumin within cationic octadecylamine monolayer and a comparative study with zwitterionic DPPC and anionic stearic acid monolayer. J. Colloid Interface Sci. 315 (2007) 464-474.

[174] M. Mahato, P. Pal, B. Tah, G.B. Talapatra, Hemoglobin-phospholipid interaction and biocomposite formation at air/water interface. Colloids Surf., A 414 (2012) 375-383.

[175] T. Kamilya, P. Pal, G.B. Talapatra, Adsorption of pepsin in octadecylamine matrix at air/water interface. Biophys. Chem. 146 (2010) 85-91.

[176] D.K. Schwartz, Langmuir-Blodgett film structure. Surf. Sci. Rep. 27 (1997) 245-334.

[177] R. Ghaskadvi, S. Carr, M. Dennin, Effect of subphase ca^{2+} ions on the viscoelastic properties of langmuir monolayers. J. Chem. Phys. 111 (1999) 3675-3678.

[178] J. Zasadzinski, R. Viswanathan, L. Madsen, J. Garnaes, D. Schwartz, Langmuir-Blodgett films. Science 263 (1994) 1726-1733.

[179] S. Mann, Molecular tectonics in biomineralization and biomimetic materials chemistry. Nature 365 (1993) 499-505.

[180] J.M. Bloch, W. Yun, Condensation of monovalent and divalent metal ions on a Langmuir monolayer. Phys. Rev. A 41 (1990) 844-862.

[181] S. Mann, D.D. Archibald, J.M. Didymus, T. Douglas, B.R. Heywood, F.C. Meldrum, N.J. Reeves, Crystallization at inorganic-organic interfaces: biominerals and biomimetic synthesis. Science 261 (1993) 1286-1292.

[182] K.B. Blodgett, Films built by depositing successive unimolecular layers on a solid surface. J. Am. Chem. Soc. 57 (1935) 1007-1022.

[183] K.B. Blodgett, I. Langmuir, Built-up films of barium stearate and their optical properties. Phys. Rev. 51 (1937) 964-982.

[184] J.A. Spink, Transfer ratio of Langmuir-Blodgett monolayers for various solids. J. Colloid Interface Sci. 23 (1967) 9-26.

[185] J.E. Riegler, J.D. LeGrange, Observation of a monolayer phase transition on the meniscus in a Langmuir-Blodgett transfer configuration. Phys. Rev. Lett. 61 (1988) 2492-2495.

[186] H. Riegler, K. Spratte, Structural changes in lipid monolayers during the Langmuir-Blodgett transfer due to substrate/monolayer interactions. Thin Solid Films 210-211 (1992) 9-12.

[187] S. Kundu, D. Langevin, Fatty acid monolayer dissociation and collapse. Effect of pH and cations. Colloids Surf., A 325 (2008) 81-85.

[188] A. Gericke, H. Huehnerfuss, The effect of cations on the order of saturated fatty acid monolayers at the air/water interface as determined by infrared reflection-absorption spectrometry. Thin Solid Films 245 (1994) 74-82.

[189] J. Simon-Kutscher, A. Gericke, H. Huehnerfuss, Effect of bivalent Ba, Cu, Ni, and Zn cations on the structure of octadecanoic acid monolayers at the air/water interface as determined by external Infrared Reflection-Absorption Spectroscopy. Langmuir 12 (1996) 1027-1034.

[190] Y. Wang, X. Du, L. Guo, H. Liu, Chain orientation and headgroup structure in Langmuir monolayers of stearic acid and metal stearate (Ag, Co, Zn, and Pb) studied by infrared reflection-absorption spectroscopy. J. Chem. Phys. 124 (2006) 134706-134709.

[191] J.Y. Hyun, G.S. Lee, T.Y. Kim, D.J. Ahn, Selectivity of heavy metal ions at acidic supramolecular surfaces. Korean J. Chem. Eng. 14 (1997) 533-540.

[192] S. Kundu, A. Datta, S. Hazra, Effect of metal ions on monolayer collapses. Langmuir 21 (2005) 5894-5900.

[193] Y. Ren, K.-i. Iimura, T. Kato, Structure of barium stearate films at the air/water interface investigated by polarization modulation infrared spectroscopy and π-A isotherms. Langmuir 17 (2001) 2688-2693.

[194] Y. Ren, K.-i. Iimura, T. Kato, Crystal lattice of the cadmium alkanoate monolayer at the air/water interface investigated by polarization modulation infrared spectroscopy. J Chem. Phys. 114 (2001) 1949-1951.

[195] Y. Ren, K.-i. Iimura, T. Kato, Crystal lattice transition of behenic acid monolayer on pure water surface observed by polarization modulation infrared spectroscopy. J. Chem. Phys. 114 (2001) 6502-6504.

[196] F. Al-Ali, C. Dejugnat, G. Etemad-Moghadam, I. Rico-Lattes, Langmuir films of (α-amino) phosphorus amphiphiles on various ion-containing subphases. J. Colloid Interface Sci. 273 (2004) 512-516.

[197] Q. Lu, Y. Luo, L. Li, M. Liu, Self-assembled supramolecular architecture of a bolaamphiphilic diacid on the subphases containing Ag(I) and Eu(III) metal ions. Langmuir 19 (2003) 285-291.

[198] S. Yoshida, Y. Okawa, T. Watanabe, S. Inokuma, T. Kuwamura, Ion sensitive tin oxide electrodes carrying amphiphilic crown ether Langmuir-Blodgett films. Chem. Lett. (1989) 243-246.

[199] H. Matsumura, T. Watanabe, K. Furusawa, S. Inokuma, T. Kuwamura, Electrical double layer formed on the monolayer of crown ether compounds. Bull. Chem. Soc. Jpn. 60 (1987) 2747-2750.

[200] I.K. Lednev, M.C. Petty, Langmuir-Blodgett films of chromoionophores containing a crown ether ring: Complex formation with Ag+ cations in water. J. Phys. Chem. 98 (1994) 9601-9605.

[201] I.K. Lednev, M.C. Petty, Complex formation of an amphiphilic benzothiazolium styryl chromoionophore with metal cations in a monolayer at the air/water interface. J. Phys. Chem. 99 (1995) 4176-4180.

[202] Y. Ishikawa, T. Kunitake, T. Matsuda, T. Otsuka, S. Shinkai, Formation of calixarene monolayers which selectively respond to metal ions. J. Chem. Soc., Chem. Commun. (1989) 736-738.

[203] J.H. Van Esch, A.L.H. Stols, R.J.M. Nolte, Surfactants containing imidazole ligands. Spontaneous formation of vesicles by addition of metal ions. J. Chem. Soc., Chem. Commun. (1990) 1658-1660.

[204] J.H. van Esch, R.J.M. Nolte, H. Ringsdorf, G. Wildburg, Monolayers of chiral imidazole amphiphiles: Domain formation and metal complexation. Langmuir 10 (1994) 1955-1961.

[205] P.J. Werkman, A.J. Schouten, M.A. Noordegraaf, P. Kimkes, E.J.R. Sudhoelter, Morphological changes of monolayers of two polymerizable pyridine amphiphiles upon complexation with Cu(II) Ions at the air/water interface. Langmuir 14 (1998) 157-164.

[206] D.R. Shnek, D.W. Pack, D.Y. Sasaki, F.H. Arnold, Specific protein attachment to artificial membranes via coordination to lipid-bound copper(II). Langmuir 10 (1994) 2382-2388.

[207] W. Budach, R.C. Ahuja, D. Moebius, Metal ion complexation and electron donor properties of dioctadecyldithiocarbamate in monolayers at the gas/water interface and in organized monolayer systems. Langmuir 9 (1993) 3093-3100.

[208] P.J. Werkman, A. Schasfoort, R.H. Wieringa, A.J. Schouten, Langmuir-Blodgett films of a polymerizable N,N'-disubstituted dithiooxamide coordination compound. Thin Solid Films 323 (1998) 243-250.

[209] P.J. Werkman, R.H. Wieringa, A.J. Schouten, The formation of copper sulfide semiconductors inside Langmuir-Blodgett films of Cu(II) ion complexes. Thin Solid Films 323 (1998) 251-256.

[210] P.J. Werkman, H. Wilms, R.H. Wieringa, A.J. Schouten, Formation of mono- and multilayers of metal complexes of 4-(((10,12-pentacosadiynoyl)oxy)methyl)pyridine. Thin Solid Films 325 (1998) 238-245.

[211] P.J. Werkman, R.H. Wieringa, E.J. Vorenkamp, A.J. Schouten, Langmuir-Blodgett films of metal complexes of 4-(10,12-penta-cosadiynamidomethyl)pyridine: A structural investigation. Langmuir 14 (1998) 2119-2128.

[212] P.J. Werkman, A.J. Schouten, Langmuir monolayer formation of metal complexes from polymerizable amphiphilic ligands. Thin Solid Films 284-285 (1996) 24-26.

[213] B. Kesimli, A. Topacli, C. Topacli, G. Guemues, I. Guerol, V. Ahsen, Langmuir monolayers with some vic-dioxime ligands and their complexation behaviour. Colloids Surf., A 256 (2005) 137-143.

[214] I. Kuzmenko, R. Buller, W.G. Bouwman, K. Kjaer, J. Als-Nielsen, M. Lahav, L. Leiserowitz, Formation of chiral interdigitated multilayers at the air/liquid interface through acid-base interactions. Science 274 (1996) 2046-2049.

[215] I. Kuzmenko, M. Kindermann, K. Kjaer, P.B. Howes, J. Als-Nielsen, R. Granek, G. von Kiedrowski, L. Leiserowitz, M. Lahav, Crystalline films of interdigitated structures formed via amidinium-carboxylate interactions at the air/water interface. J. Am. Chem. Soc. 123 (2001) 3771-3783.

[216] J. Xue, C.S. Jung, M.W. Kim, Phase transitions of liquid-crystal films on an air/water interface. Phys. Rev. Lett. 69 (1992) 474-477.

[217] X. Chen, S. Wiehle, M. Weygand, G. Brezesinski, U. Klenz, H.-J. Galla, H. Fuchs, G. Haufe, L. Chi, Unconventional air-stable interdigitated bilayer formed by 2,3-disubstituted fatty acid methyl esters. J. Phys. Chem. B 109 (2005) 19866-19875.

[218] M. Ibn-Elhaj, H. Riegler, H. Moehwald, Layering transitions and reentrant-like phenomenon in thin films of three-block organosiloxane smectogens at the air/water interface. J. Phys. I 6 (1996) 969-980.

[219] B. Rapp, H. Gruler, Phase transitions in thin smectic films at the air/water interface. Phys. Rev. A 42 (1990) 2215-2218.

[220] S.G.J. Mochrie, M. Sutton, R.J. Birgeneau, D.E. Moncton, P.M. Horn, Multilayer adsorption of ethylene on graphite: Layering, prewetting, and wetting. Phys. Rev. B: Condens. Matter 30 (1984) 263-273.

[221] P.C. Ball, R. Evans, Structure and adsorption at gas-solid interfaces: layering transitions from a continuum theory. J. Chem. Phys. 89 (1988) 4412-4423.

[222] C. Bernardini, S.D. Stoyanov, M.A. Cohen Stuart, L.N. Arnaudov, F.A.M. Leermakers, PMMA Highlights the layering transition of PDMS in Langmuir films. Langmuir 27 (2011) 2501-2508.

[223] J.L. Gallani, C. Bourgogne, S. Nakatsuji, Layering transitions and schlieren textures in Langmuir films of two organic radicals. Langmuir 20 (2004) 10062-10067.

[224] A.M. Gonzalez-Delgado, M. Perez-Morales, J.J. Giner-Casares, E. Munoz, M.T. Martin-Romero, L. Camacho, Reversible collapse of insoluble monolayers: New insights on the influence of the anisotropic line tension of the domain. J. Phys. Chem. B 113 (2009) 13249-13256.

[225] H.E. Ries, Stable ridges in a collapsing monolayer. Nature 281 (1979) 287-289.

[226] M. Ibn-Elhaj, H. Riegler, H. Mohwald, M. Schwendler, C.A. Helm, X-ray reflectivity study of layering transitions and the internal multilayer structure of films of three-block organosiloxane amphiphilic smectic liquid crystals at the air/water interface. Phys. Rev. E 56 (1997) 1844-1852.

[227] M. Ferreira, P. Dynarowicz-Latka, J. Minones, Jr., W. Caetano, K. Kita, M. Schalke, M. Loesche, O.N. Oliveira, Jr., On the origin of the plateau in surface-pressure isotherms of aromatic carboxylic acids. J. Phys. Chem. B 106 (2002) 10395-10400.

[228] M.C. Friedenberg, G.G. Fuller, C.W. Frank, C.R. Robertson, Formation of bilayer disks and two-dimensional foams on a collapsing/expanding liquid-crystal monolayer. Langmuir 10 (1994) 1251-1256.

[229] H.E. Ries, Jr., H. Swift, Twisted double-layer ribbons and the mechanism for monolayer collapse. Langmuir 3 (1987) 853-855.

[230] C. Gourier, C.M. Knobler, J. Daillant, D. Chatenay, Collapse of monolayers of 10,12-pentacosadiyonic acid: Kinetics and structure. Langmuir 18 (2002) 9434-9440.

[231] Q. Huo, S. Russev, T. Hasegawa, J. Nishijo, J. Umemura, G. Puccetti, K.C. Russell, R.M. Leblanc, A Langmuir monolayer with a nontraditional molecular architecture. J. Am. Chem. Soc. 122 (2000) 7890-7897.

[232] J.-L. Gallani, S. Mery, Y. Galerne, D. Guillon, Organization of a polar molecule at the air/water interface. J. Phys. Chem. B 108 (2004) 11627-11632.

[233] P. Dynarowicz-Latka, A. Dhanabalan, O.N. Oliveira, Modern physicochemical research on Langmuir monolayers. Adv. Colloid Interface Sci. 91 (2001) 221-293.

[234] V.M. Kaganer, H. Mohwald, P. Dutta, Structure and phase transitions in Langmuir monolayers. Rev. Mod. Phys. 71 (1999) 779.

[235] S.-M. Yuan, H. Yan, K. Lv, C.-B. Liu, S.-L. Yuan, Surface behavior of a model surfactant. A theoretical simulation study. J. Colloid Interface Sci. 348 (2010) 159-166.

[236] H. Rapaport, I. Kuzmenko, M. Berfeld, K. Kjaer, J. Als-Nielsen, R. Popovitz-Biro, I. Weissbuch, M. Lahav, L. Leiserowitz, From nucleation to engineering of crystalline architectures at air-liquid interfaces. J. Phys. Chem. B 104 (2000) 1399-1428.

[237] H. Lin, H. Sakamoto, W. Seo, K. Kuwabara, K. Koumoto, Crystal growth of lepidocrocite and magnetite under Langmuir monolayers. J. Cryst. Growth 192 (1998) 250-256.

[238] J.P. Santos, M.E.D. Zaniquelli, C. Batalini, W.F. De Giovani, Palmitic acid and aquo-ruthenium complex monolayers at the liquid-air interface and electroactive Langmuir-Blodgett films. Thin Solid Films 349 (1999) 238-243.

[239] D. Vollhardt, Supramolecular organisation in monolayers at the air/water interface. Mater. Sci. Eng., C C22 (2002) 121-127.

[240] S. Siegel, M. Kindermann, M. Regenbrecht, D. Vollhardt, G. Von Kiedrowski, Molecular recognition of a dissolved carboxylate by amidinium monolayers at the air/water interface. Prog. Colloid Polym. Sci. 115 (2000) 233-237.

[241] D. Vollhardt, V.B. Fainerman, Penetration of dissolved amphiphiles into two-dimensional aggregating lipid monolayers. Adv. Colloid Interface Sci. 86 (2000) 103-151.

[242] K. El Kirat, F. Besson, A.-F. Prigent, J.-P. Chauvet, B. Roux, Role of calcium and membrane organization on phospholipase D localization and activity. Competition between a soluble and an insoluble substrate. J. Biol. Chem. 277 (2002) 21231-21236.

[243] M. Higuchi, T. Koga, K. Taguchi, T. Kinoshita, Substrate-induced conformation of an artificial receptor with two receptor sites. Langmuir 18 (2002) 813-818.

[244] A. Girard-Egrot, J.-P. Chauvet, G. Gillet, M. Moradi-Ameli, Specific interaction of the antiapoptotic protein Nr-13 with phospholipid monolayers is prevented by the BH3 domain of bax. J. Mol. Biol. 335 (2003) 321-331.

[245] M.E. Hayes, A.V. Gorelov, K.A. Dawson, DNA-induced fusion of phosphatidylcholine vesicles. Prog. Colloid Polym. Sci. 118 (2001) 243-247.

[246] R.C. MacDonald, A. Gorbonos, M.M. Momsen, H.L. Brockman, Surface properties of dioleoyl-sn-glycerol-3-ethylphosphocholine, a cationic phosphatidylcholine transfection agent, alone and in combination with lipids or DNA. Langmuir 22 (2006) 2770-2779.

[247] G.B. Khomutov, Interfacially formed organized planar inorganic, polymeric and composite nanostructures. Adv. Colloid Interface Sci. 111 (2004) 79-116.

[248] A.P. Girard-Egrot, S. Godoy, L.J. Blum, Enzyme association with lipidic Langmuir-Blodgett films: Interests and applications in nanobioscience. Adv. Colloid Interface Sci. 116 (2005) 205-225.

[249] S. Hou, J. Wang, C.R. Martin, Template-synthesized protein nanotubes. Nano Lett. 5 (2005) 231-234.

[250] Z. Siwy, L. Trofin, P. Kohli, L.A. Baker, C. Trautmann, C.R. Martin, Protein biosensors based on biofunctionalized conical gold nanotubes. J. Am. Chem. Soc. 127 (2005) 5000-5001.

[251] C. Leger, P. Bertrand, Direct electrochemistry of redox enzymes as a tool for mechanistic studies. Chem. Rev. 108 (2008) 2379-2438.

[252] H. Moehwald, Phospholipid and phospholipid-protein monolayers at the air/water interface. Annu. Rev. Phys. Chem. 41 (1990) 441-476.

[253] Y. Ren, C.W. Meuse, S.L. Hsu, H.D. Stidham, Reflectance infrared spectroscopic analysis of monolayer films at the air/water interface. J. Phys. Chem. 98 (1994) 8424-8430.

[254] W. Miao, X. Du, Y. Liang, Molecular recognition of 1-(2-octadecyl oxy carbonylethyl) cytosine monolayers to guanosine at the air/water interface investigated by infrared reflection-absorption spectroscopy. J. Phys. Chem. B 107 (2003) 13636-13642.

[255] X. Du, Y. Liang, Detection of NH stretching signals from the monolayers of amino acid amphiphiles at the air/water interface and change of hydrogen bond depending on metal ion in the subphase: Infrared reflection-adsorption spectroscopy. J. Phys. Chem. B 108 (2004) 5666-5670.

[256] P. Atkins, J. de Paula, Physical chemistry, Oxford University Press, 2014.

[257] L.J. Wilson, S.R. Klopfenstein, M. Li, A traceless linker approach to the solid phase synthesis of substituted guanidines utilizing a novel acyl isothiocyanate resin. Tetrahedron Lett. 40 (1999) 3999-4002.

[258] S. Pang, D. Zhu, Studies on molecular structure of Schiff base derivatives in LB films. J. Colloid Interface Sci. 265 (2003) 65-69.

[259] G. Hemakanthi, A. Dhathathreyan, Synthesis of nickel sulfide using Langmuir-Blodgett films of nickel complex of 2-hydroxy-5-nitro-N-benzylidene hexadecylamine monolayers at air/water interface. Chem. Phys. Lett. 334 (2001) 245-249.

[260] V. Ramakrishnan, M. D'Costa, K.N. Ganesh, M. Sastry, PNA-DNA hybridization at the air/water interface in the presence of octadecylamine Langmuir monolayers. Langmuir 18 (2002) 6307-6311.

[261] Y.S. Kang, D.K. Lee, P. Stroeve, FTIR and UV-vis spectroscopy studies of Langmuir–Blodgett films of stearic acid/γ-Fe_2O_3 nanoparticles. Thin Solid Films 327–329 (1998) 541-544.

[262] M. Broniatowski, Long-chain alkyl thiols in Langmuir monolayers. J Colloid Interface Sci 337 (2009) 183-190.

[263] J.B. Peng, G.T. Barnes, I.R. Gentle, The structures of Langmuir–Blodgett films of fatty acids and their salts. Adv. Colloid Interface Sci. 91 (2001) 163-219.

[264] A. Esteves-Souza, K. Pissinate, M.d. Graça Nascimento, N.F. Grynberg, A. Echevarria, Synthesis, cytotoxicity, and DNA-topoisomerase inhibitory activity of new asymmetric ureas and thioureas. Bioorg Med Chem 14 (2006) 492-499.

[265] R. Ziessel, L. Bonardi, P. Retailleau, G. Ulrich, Isocyanate-, isothiocyanate-, urea-, and thiourea-substituted boron dipyrromethene dyes as fluorescent probes. J. Org. Chem. 71 (2006) 3093-3102.

[266] D.E. Fuerst, E.N. Jacobsen, Thiourea-catalyzed enantioselective cyanosilylation of ketones. J. Am. Chem. Soc. 127 (2005) 8964-8965.

[267] A.G. Wenzel, E.N. Jacobsen, Asymmetric catalytic Mannich reactions catalyzed by urea derivatives: enantioselective synthesis of β-aryl-β-amino acids. J. Am. Chem. Soc. 124 (2002) 12964-12965.

[268] Y. Tang, L. Deng, Y. Zhang, G. Dong, J. Chen, Z. Yang, Thioureas as ligands in the Pd-catalyzed intramolecular Pauson-Khand reaction. Org Lett 7 (2005) 1657-1659.

[269] A.R. Katritzky, M.F. Gordeev, New 1H-benzotriazole-mediated synthesis of N,N'-disubstituted thioureas and carbodiimides. J. Chem. Soc., Perkin Trans. 1 (1991) 2199-2203.

[270] H.-Q. Li, P.-C. Lv, T. Yan, H.-L. Zhu, Urea derivatives as anticancer agents. Anticancer Agents Med. Chem. 9 (2009) 471-480.

[271] J. Stefanska, D. Szulczyk, A.E. Koziol, B. Miroslaw, E. Kedzierska, S. Fidecka, B. Busonera, G. Sanna, G. Giliberti, C.P. La, M. Struga, Disubstituted thiourea derivatives and their activity on CNS: synthesis and biological evaluation. Eur J Med Chem 55 (2012) 205-213.

[272] S. Van Poecke, H. Munier-Lehmann, O. Helynck, M. Froeyen, S. Van Calenbergh, Synthesis and inhibitory activity of thymidine analogues targeting Mycobacterium tuberculosis thymidine monophosphate kinase. Bioorg. Med. Chem. 19 (2011) 7603-7611.

[273] A. Saeed, U. Shaheen, A. Hameed, S.Z.H. Naqvi, Synthesis, characterization and antimicrobial activity of some new 1-(fluorobenzoyl)-3-(fluorophenyl)thioureas. J. Fluorine Chem. 130 (2009) 1028-1034.

[274] H. Arslan, N. Kuelcue, U. Floerke, Synthesis and characterization of copper(II), nickel(II) and cobalt(II) complexes with novel thiourea derivatives. Transition Met. Chem. 28 (2003) 816-819.

[275] H. Arslan, N. Duran, G. Borekci, O.C. Koray, C. Akbay, Antimicrobial activity of some thiourea derivatives and their nickel and copper complexes. Molecules 14 (2009) 519-527.

[276] H. Ali Dondas, Y. Nural, N. Duran, C. Kilner, Synthesis, crystal structure and antifungal/antibacterial activity of some novel highly functionalized benzoylaminocarbothioylpyrrolidines. Turk. J. Chem. 30 (2006) 573-583.

[277] S.B. Desai, P.B. Desai, K.R. Desai, Synthesis of some Schiff bases, thiazolidinones and azetidinones derived from 2,6-diaminobenzo[1,2-d:4,5-d'] bisthiazole and their anticancer activities. Heterocycl. Commun. 7 (2001) 83-90.

[278] P. Przybylski, A. Huczynski, K. Pyta, B. Brzezinski, F. Bartl, Biological properties of Schiff bases and azo derivatives of phenols. Curr. Org. Chem. 13 (2009) 124-148.

[279] A.A. Abdel Aziz, A.N.M. Salem, M.A. Sayed, M.M. Aboaly, Synthesis, structural characterization, thermal studies, catalytic efficiency and antimicrobial activity of some M(II) complexes with ONO tridentate Schiff base N-salicylidene-o-aminophenol (saphH2). J. Mol. Struct. 1010 (2012) 130-138.

[280] D. Sinha, A.K. Tiwari, S. Singh, G. Shukla, P. Mishra, H. Chandra, A.K. Mishra, Synthesis, characterization and biological activity of Schiff base analogues of indole-3-carboxaldehyde. Eur. J. Med. Chem. 43 (2008) 160-165.

[281] G.S. Singh, Y. MSA Al-kahraman, D. Mpadi, M. Yasinzai, Antimicrobial, crown gall tumor inhibitory and cytotoxicity assays of N-[(1-methyl-1H-indole-3-yl) methylene] amines synthesized by an improved protocol. Med. Chem 10 (2014) 382-387.

[282] P. Panneerselvam, R.R. Nair, G. Vijayalakshmi, E.H. Subramanian, S.K. Sridhar, Synthesis of Schiff bases of 4-(4-aminophenyl)morpholine as potential antimicrobial agents. Eur. J. Med. Chem. 40 (2005) 225-229.

[283] P. Rathelot, P. Vanelle, M. Gasquet, F. Delmas, M.P. Crozet, P. Timon-David, J. Maldonado, Synthesis of novel functionalized 5-nitroisoquinolines and evaluation of in vitro antimalarial activity. Eur. J. Med. Chem. 30 (1995) 503-508.

[284] G.S. Singh, Y.M. Al-Kahraman, D. Mpadi, M. Yasinzai, Synthesis of N-(1-methyl-1H-indol-3-yl)methyleneamines and 3,3-diaryl-4-(1-methyl-1H-indol-3-yl)azetidin-2-ones as potential antileishmanial agents. Bioorg. Med. Chem. Lett. 22 (2012) 5704-5706.

[285] A. Jarrahpour, D. Khalili, E. De Clercq, C. Salmi, J.M. Brunel, Synthesis, antibacterial, antifungal and antiviral activity evaluation of some new bis-Schiff bases of isatin and their derivatives. Molecules 12 (2007) 1720-1730.

[286] E.M. Yeboah, T.H. Tabane, L.L. Masutlha, G.S. Singh, Evaluation of the DPPH radical scavenging activity of N-salicylideneanilines and their reduction products synthesized by a green protocol. SOAJ Org. Biomol. Chem 1 (2013) 201-210.

[287] T. Nishiya, S. Yamauchi, N. Hirota, M. Baba, I. Hanazaki, Fluorescence studies of intramolecularly hydrogen-bonded o-hydroxyacetophenone, salicylamide, and related molecules. J. Phys. Chem. 90 (1986) 5730-5735.

[288] C. McFate, D. Ward, J. Olmsted, III, Organized collapse of fatty acid monolayers. Langmuir 9 (1993) 1036-1039.

[289] J.-M. Lehn, Supramolecular chemistry. Concepts and Perspectives (1995).

[290] J.-M. Lehn, Toward self-organization and complex matter. Science 295 (2002) 2400-2403.

[291] J.M. Lehn, Perspectives in supramolecular chemistry-from molecular recognition towards molecular information processing and self-organization. Angew. Chem. Int. Ed. Engl. 29 (1990) 1304-1319.

[292] J.C. MacDonald, G.M. Whitesides, Solid-state structures of hydrogen-bonded tapes based on cyclic secondary diamides. Chem. Rev. 94 (1994) 2383-2420.

[293] P. Jonkheijm, F.J. Hoeben, R. Kleppinger, J. van Herrikhuyzen, A.P. Schenning, E. Meijer, Transfer of π-conjugated columnar stacks from solution to surfaces. J. Am. Chem. Soc. 125 (2003) 15941-15949.

[294] K. Ariga, T. Kunitake, Molecular recognition at air/water and related interfaces: complementary hydrogen bonding and multisite interaction. Acc. Chem. Res. 31 (1998) 371-378.

[295] H. Koyano, P. Bissel, K. Yoshihara, K. Ariga, T. Kunitake, Syntheses and interfacial hydrogen-bonded network of hexaalkyl tris (melamine) amphiphiles. Langmuir 13 (1997) 5426-5432.

[296] V. Marchi-Artzner, F. Artzner, O. Karthaus, M. Shimomura, K. Ariga, T. Kunitake, J.-M. Lehn, Molecular recognition between 2, 4, 6-triaminopyrimidine lipid monolayers and complementary barbituric molecules at the air/water interface: effects of hydrophilic spacer, ionic strength, and pH. Langmuir 14 (1998) 5164-5171.

[297] K. Ariga, A. Kamino, X. Cha, T. Kunitake, Multisite recognition of aqueous dipeptides by oligoglycine arrays mixed with guanidinium and other receptor units at the air/water interface. Langmuir 15 (1999) 3875-3885.

[298] M. Ziolek, G. Burdzinski, J. Karolczak, Influence of intermolecular hydrogen bonding on the photochromic cycle of the aromatic Schiff base N, N′-bis (salicylidene)-p-phenylenediamine in solution. J. Phys. Chem. A 113 (2009) 2854-2864.

[299] A. Jimenez-Sanchez, M. Rodriguez, R. Metivier, G. Ramos-Ortiz, J.L. Maldonado, N. Reboles, N. Farfan, K. Nakatani, R. Santillan, Synthesis and crystal structures of a series of Schiff bases: A photo-, solvato-and acidochromic compound. New J. Chem 38 (2014) 730-738.

[300] M. Irie, Photochromism of diarylethene single molecules and single crystals. Photochem. Photobiol. Sci. 9 (2010) 1535-1542.

[301] M. Sliwa, S. Letard, I. Malfant, M. Nierlich, P.G. Lacroix, T. Asahi, H. Masuhara, P. Yu, K. Nakatani, Design, synthesis, structural and nonlinear optical properties of photochromic crystals: Toward reversible molecular switches. Chem. Mater. 17 (2005) 4727-4735.

[302] S. Prashanthi, P.H. Kumar, D. Siva, S.R. Lanke, V.J. Rao, S. Basak, P.R. Bangal, Photochemical E (trans)–Z (cis)–E isomerization of an amphiphilic cholest-5-en-3β-yl (E)-9-anthraceneprop-2-enoate on solid substrate. J. Phys. Chem. C 115 (2011) 20682-20688.

[303] Y. Kim, C. Chung, Cyclic polyether Schiff base as molecular container for barbituric acid. Synth. Met. 117 (2001) 301-303.

[304] E.M. Adams, H.C. Allen, Palmitic acid on salt subphases and in mixed monolayers of cerebrosides: Application to atmospheric aerosol chemistry. Atmosphere 4 (2013) 315-336.

[305] W.R. Barger, A.W. Snow, H. Wohltjen, N.L. Jarvis, Derivatives of phthalocyanine prepared for deposition as thin films by the Langmuir-Blodgett technique. Thin Solid Films 133 (1985) 197-206.

[306] A.D. Garnovskii, A.L. Nivorozhkin, V.I. Minkin, Ligand environment and the structure of Schiff base adducts and tetracoordinated metal-chelates. Coord. Chem. Rev. 126 (1993) 1-69.

[307] S. Wu, J.R. Huntsberger, Intermolecular interaction in some mixed polymer monolayers at the air/water interface. J. Colloid Interface Sci. 29 (1969) 138-147.

[308] K. Birdi, Lipid and biopolymer monolayers at liquid interfaces, Plenum Press New York, 1989.

[309] A. Panda, K. Nag, R. Harbottle, F. Possmayer, N. Petersen, Thermodynamic studies on mixed molecular langmuir films: Part 2. Mutual mixing of DPPC and bovine lung surfactant extract with long-chain fatty acids. Colloids Surf. A Physicochem. Eng. Asp. 247 (2004) 9-17.

[310] T.H. Chou, C.H. Chang, Thermodynamic behavior and relaxation processes of mixed DPPC/cholesterol monolayers at the air/water interface. Colloids Surf., B 17 (2000) 71-79.

[311] R. Pagano, N. Gershfeld, Physical chemistry of lipid films at the air/water interface. II. Binary lipid mixtures. Principles governing miscibility of lipids in surfaces. J. Phys. Chem. 76 (1972) 1238-1243.

[312] M. Kodama, O. Shibata, S. Nakamura, S. Lee, G. Sugihara, A monolayer study on three binary mixed systems of dipalmitoyl phosphatidyl choline with cholesterol, cholestanol and stigmasterol. Colloids Surf., B 33 (2004) 211-226.

[313] S.N. Oseback, S.W. Shim, M. Kumar, S.M. Greer, S.R. Gardner, K.M. Lemar, P.R. DeGregory, E.T. Papish, D.L. Tierney, M. Zeller, Crowded bis ligand complexes of TtzPh, Me with first row transition metals rearrange due to ligand field effects: Structural and electronic characterization (TtzPh, Me= tris (3-phenyl-5-methyl-1, 2, 4-triazolyl) borate). Dalton Trans. 41 (2012) 2774-2787.

[314] S.V. Kryatov, B.S. Mohanraj, V.V. Tarasov, O.P. Kryatova, E.V. Rybak-Akimova, B. Nuthakki, J.F. Rusling, R.J. Staples, A.Y. Nazarenko, Nickel (II) complexes with tetra- and pentadentate aminopyridine ligands: Synthesis, structure, electrochemistry, and reduction to nickel (I) species. Inorg. Chem. 41 (2002) 923-930.

[315] J.T. Rubino, K.J. Franz, Coordination chemistry of copper proteins: how nature handles a toxic cargo for essential function. J. Inorg. Biochem. 107 (2012) 129-143.

[316] H.M. McConnell, Structures and transitions in lipid monolayers at the air/water interface. Annu. Rev. Phys. Chem. 42 (1991) 171-195.

[317] T. Ottersen, L.G. Warner, K. Seff, Synthesis and crystal structure of a dimeric cyclic copper (I)-aliphatic disulfide complex cyclo-di-. mu.-[bis [2-(N, N-dimethylamino) ethyl] disulfide]-dicopper (I) tetrafluoroborate. Inorg. Chem. 13 (1974) 1904-1911.

[318] L.G. Warner, T. Ottersen, K. Seff, Synthesis and crystal structure of a polymeric copper (I) aliphatic disulfide complex.[Bis [2-(2-pyridyl) ethyl] disulfide] copper (I) perchlorate. Inorg. Chem. 13 (1974) 2819-2826.

[319] B.H. Abdullah, Y.M. Salh, Synthesis, characterization and biological activity of N-phenyl-Ñ-(2-phenolyl) thiourea (PPTH) and its metal complexes of Mn (II), Co (II), Ni (II), Cu (II), Zn (II), Cd (II), Pd (II), Pt (II) and Hg (II). Orient. J. Chem. 26 (2010) 763.

[320] A. Neuba, R. Haase, W. Meyer-Klaucke, U. Florke, G. Henkel, A halide-induced copper (I) disulfide/copper (II) thiolate interconversion. Angew. Chem. Int. Ed. Engl. 51 (2012) 1714-1718.

[321] R. Pulukkody, S.J. Kyran, R.D. Bethel, C.-H. Hsieh, M.B. Hall, D.J. Darensbourg, M.Y. Darensbourg, Carbon monoxide induced reductive elimination of disulfide in an N-heterocyclic carbene (NHC)/ thiolate dinitrosyl iron complex (DNIC). J. Am. Chem. Soc. 135 (2013) 8423-8430.

[322] M. Tamura, N. Matsuura, T. Kawamoto, T. Konno, Thiolato-bridged Ru (II)Ag(I)Ru(II) Trinuclear complex composed of bis(bipyridine)ruthenium(II) units with chelating

2-aminoethanethiolate: Conversion to a disulfide-bridged Ru(II)Ru(II) dinuclear complex. Inorg. Chem. 46 (2007) 6834-6836.

[323] W.-F. Liaw, C.-K. Hsieh, G.-Y. Lin, G.-H. Lee, Syntheses, reactivity, and π-donating ligand metathesis reaction of five-coordinate sixteen-electron Manganese(I) complexes: Crystal structures of $[Mn(CO)_3(\text{-}TeC_6H_4\text{-}o\text{-}NH\text{-})]$-, $[(Mn(CO)_3)_2(\mu\text{-}SC_6H_4\text{-}o\text{-}S\text{-}S\text{-}C_6H_4\text{-}o\text{-}\mu\text{-}S\text{-})]$, $[(CO)_3Mn(\mu\text{-}SC_6H_4\text{-}o\text{-}NH_2\text{-})]_2$, and $[(CO)_3Mn(\mu\text{-}SC_8N_2H_4\text{-}o\text{-}S\text{-})]_{22}$. Inorg. Chem. 40 (2001) 3468-3475.

[324] M. Krunks, T. Leskela, R. Mannonen, L. Niinisto, Thermal decomposition of copper (I) thiocarbamide chloride hemihydrate. J. Therm. Anal. Calorim. 53 (1998) 355-364.

[325] C.J. Simmons, M. Lundeen, K. Seff, A centric organic disulfide (CSSC= 180. degree.): crystal and molecular structures of chloro [bis (2-pyrimidyl) disulfide] copper (I) monohydrate and of bis (2-pyrimidyl) disulfide. Inorg. Chem. 18 (1979) 3444-3452.

[326] P. Pal, T. Kamilya, M. Mahato, G.B. Talapatra, The formation of pepsin monomolecular layer by the Langmuir-Blodgett film deposition technique. Colloids Surf., B 73 (2009) 122-131.

[327] C. Ybert, J.M. di Meglio, Study of protein adsorption by dynamic surface tension measurements: Diffusive regime. Langmuir 14 (1998) 471-475.

APPENDIX

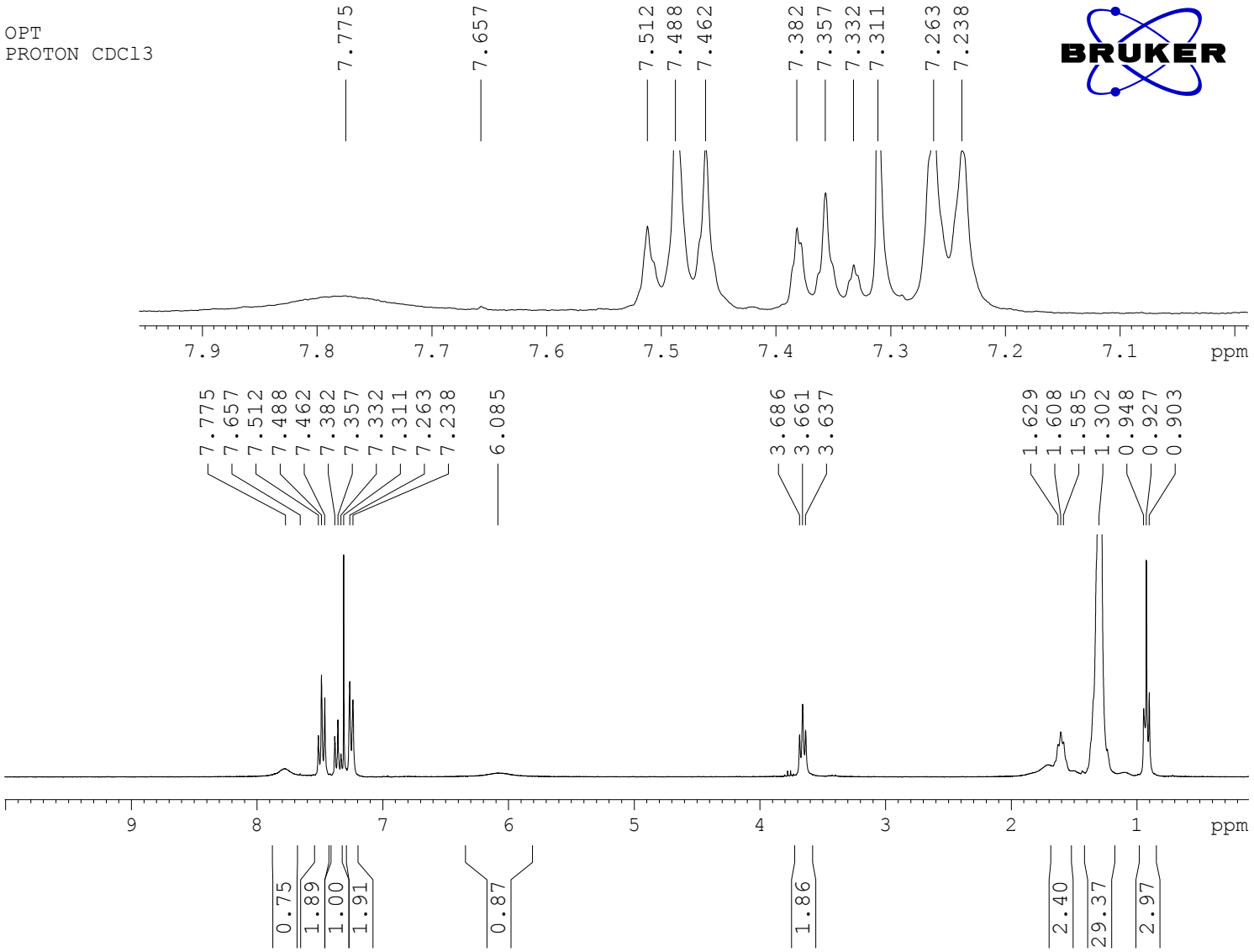

A1: ^{1}H NMR spectrum of *N*-octadecyl-*N'*-phenylthiourea.

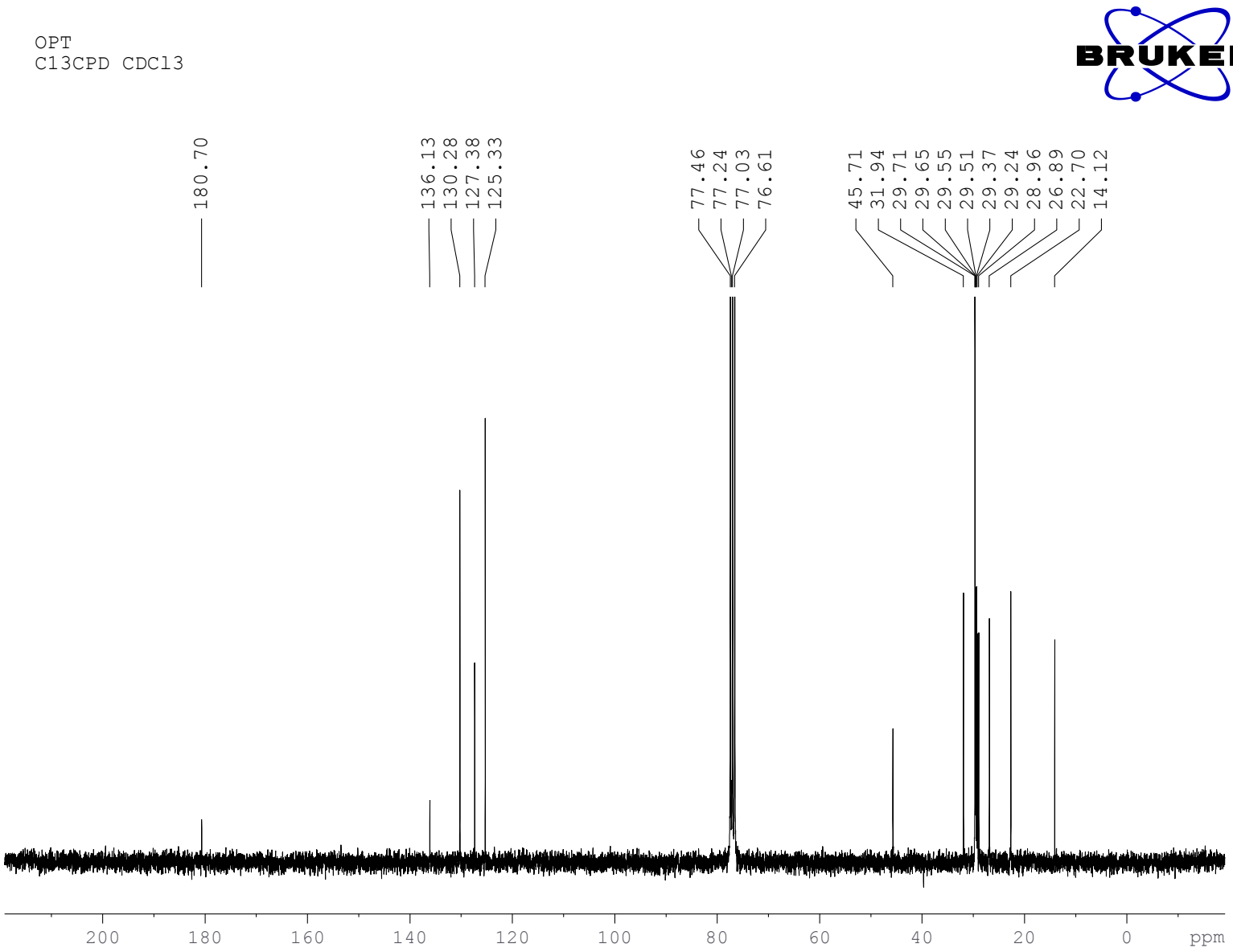

A2: ^{13}C NMR spectrum of *N*-octadecyl-*N'*-phenylthiourea.

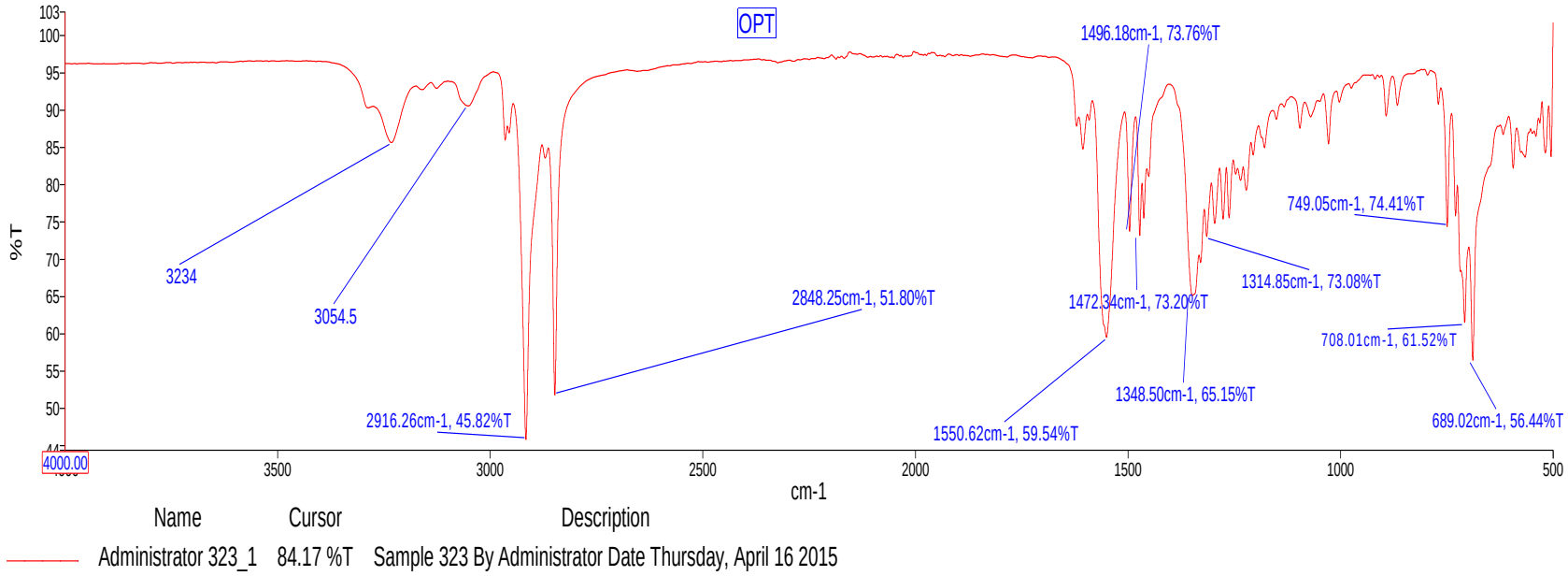

A3: IR spectrum of *N*-octadecyl-*N'*-phenylthiourea.

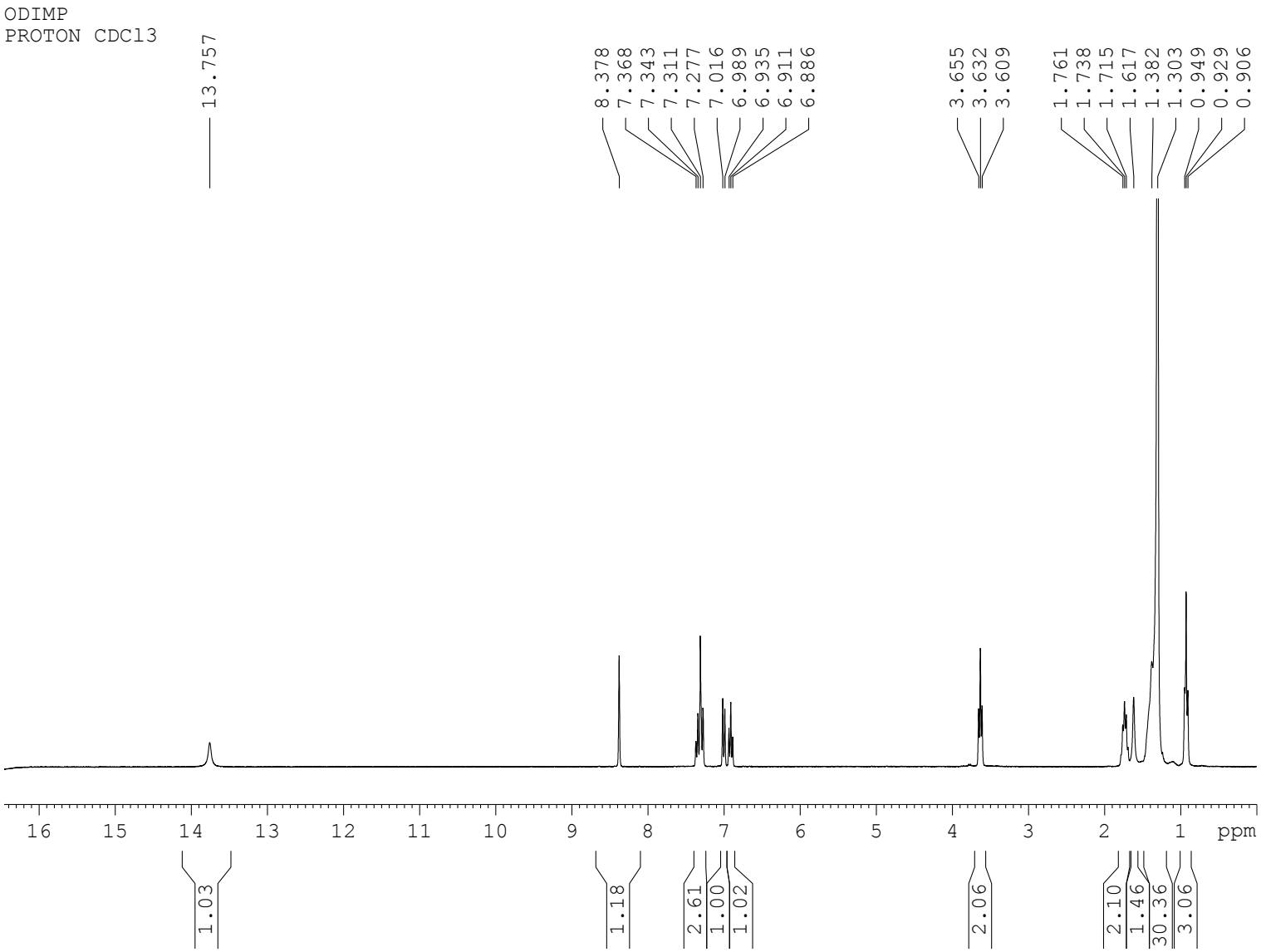

A4: ^{1}H NMR spectrum of 2-[(Octadecylimino)methyl]phenol.

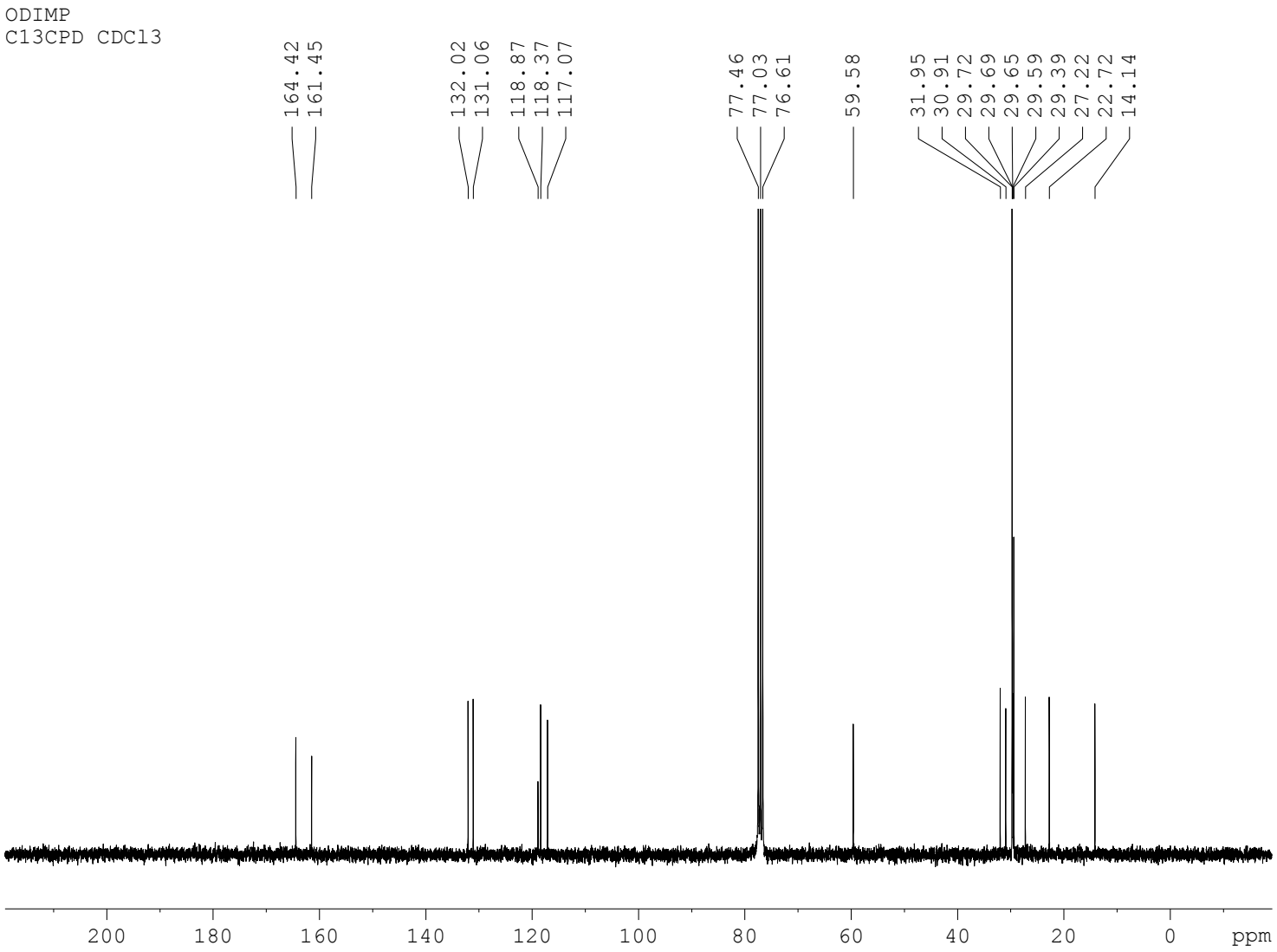

A5: ^{13}C NMR spectrum of 2-[(Octadecylimino)methyl]phenol.

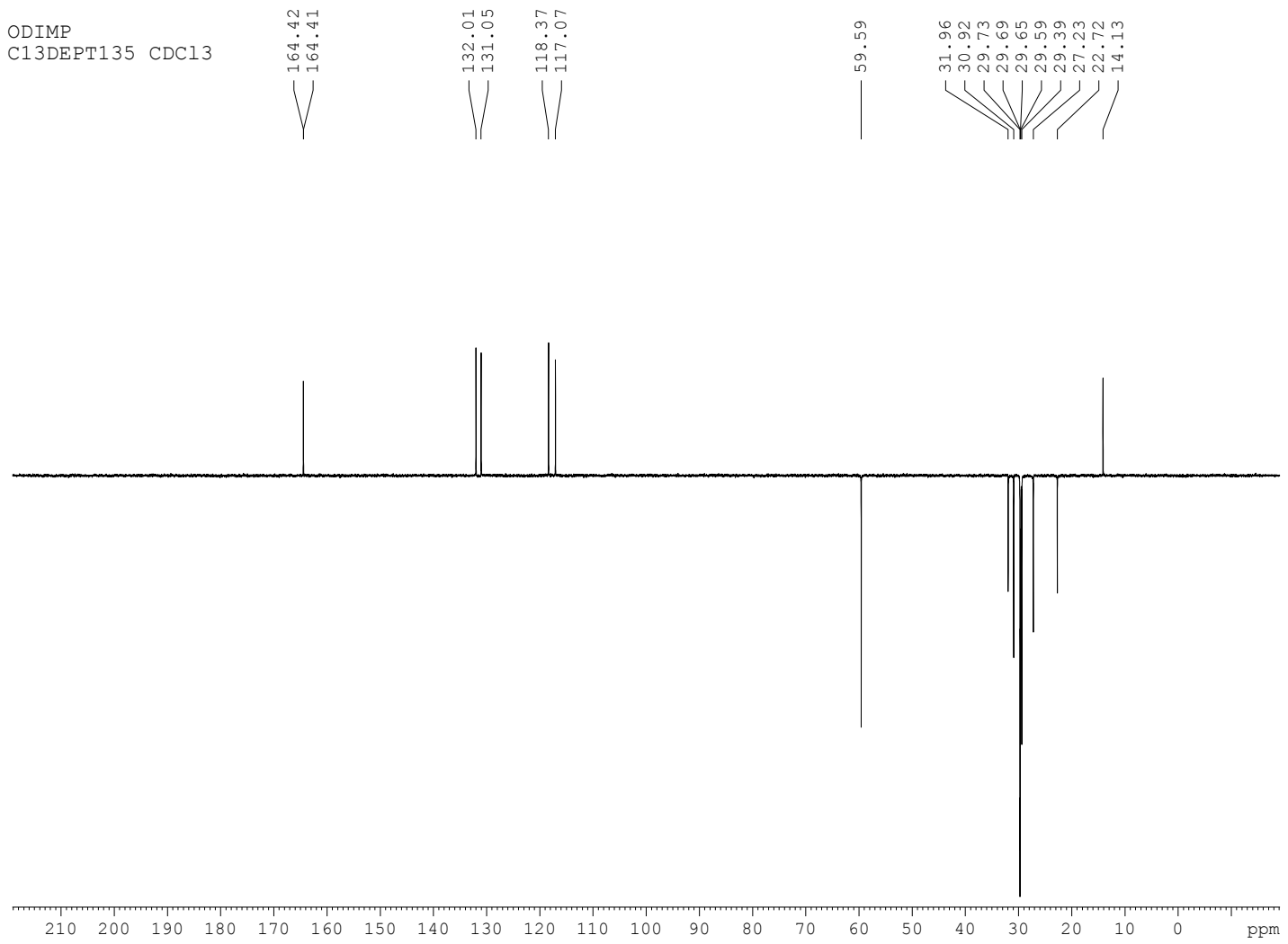

A6: DEPT NMR spectrum of 2-[(Octadecylimino) methyl]phenol.

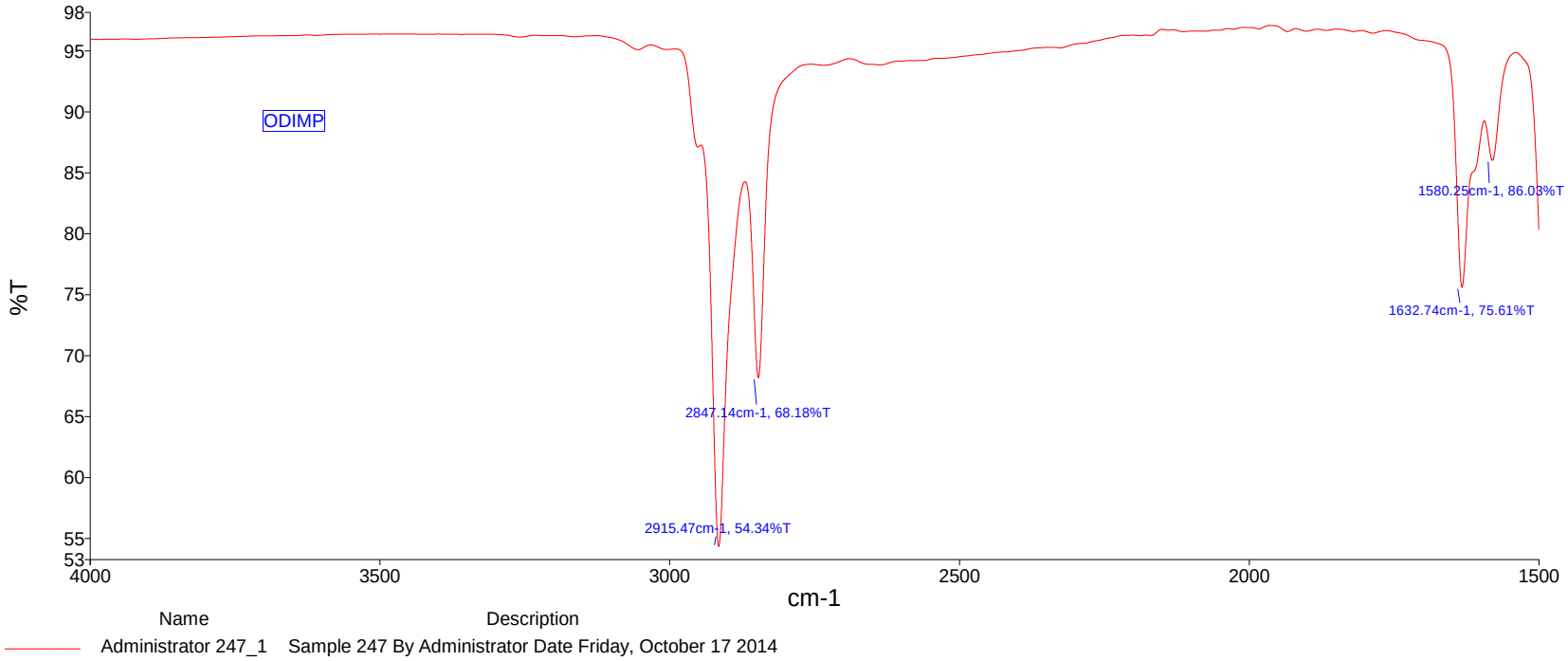

A7: IR spectrum of 2-[(Octadecylimino)methyl]phenol.

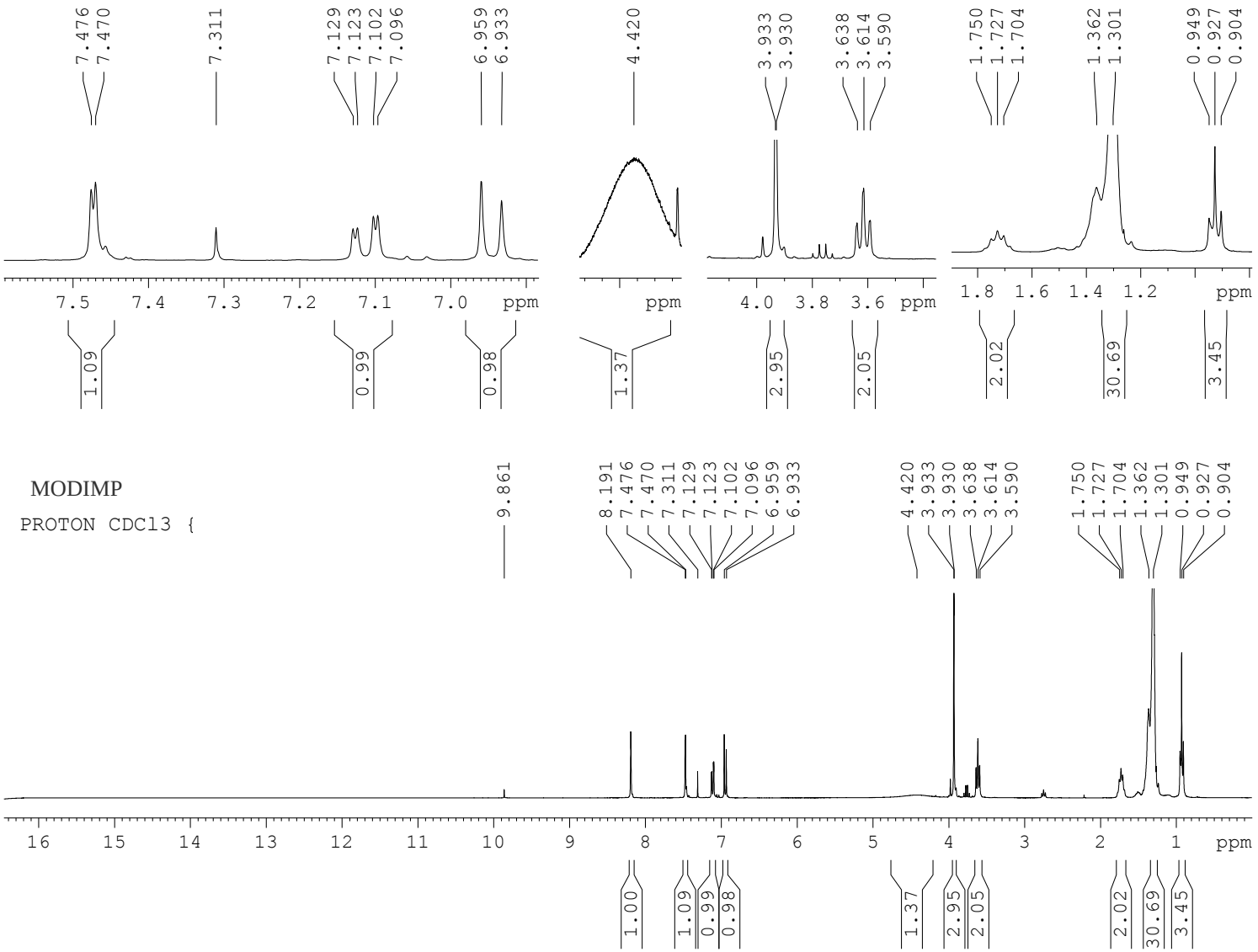

A8: ^{1}H NMR spectrum 2-methoxy-6-[(octadecylimino)methyl]phenol.

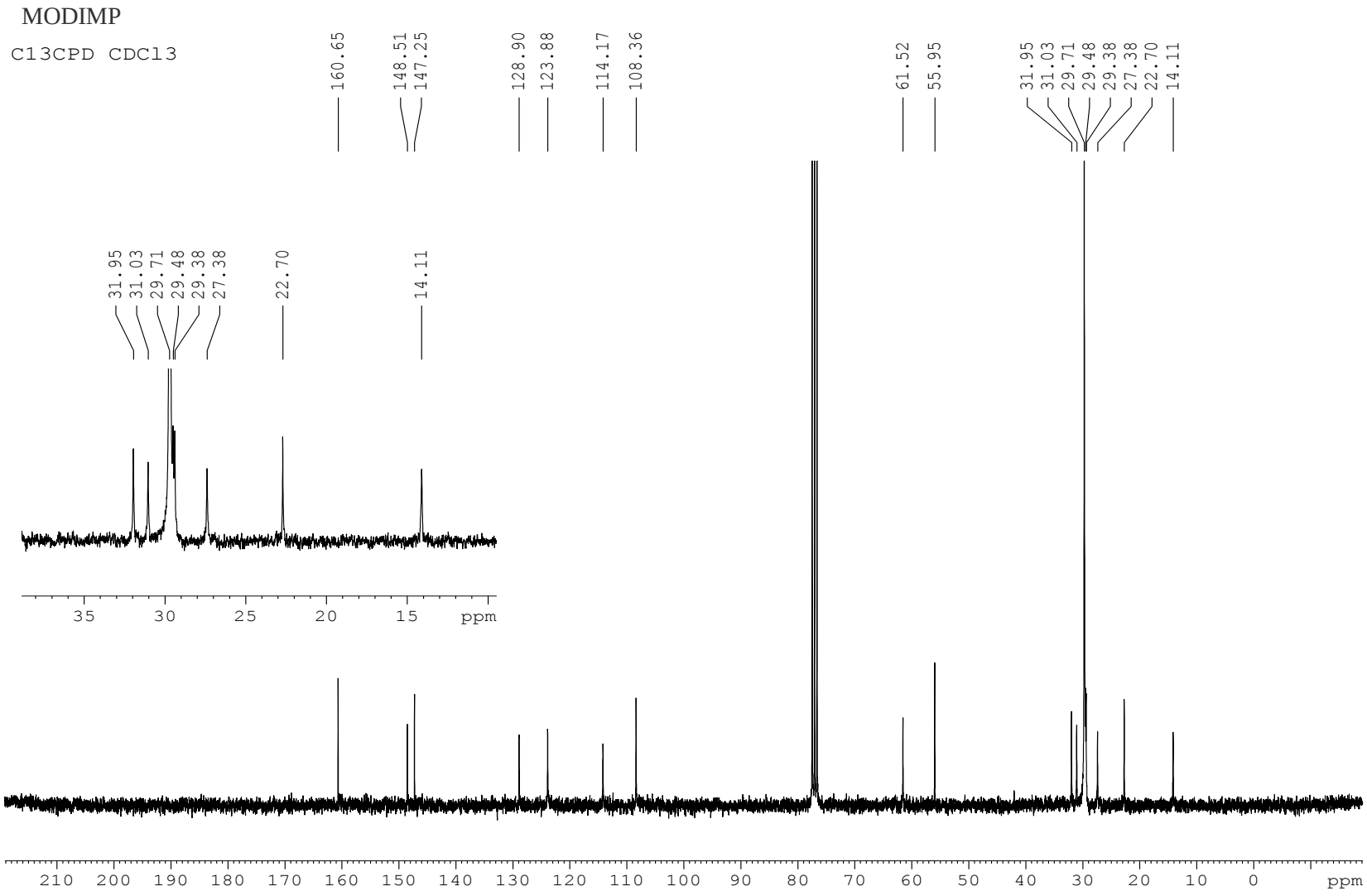

A9: ^{13}C NMR spectrum 2-methoxy-6-[(octadecylimino)methyl]phenol.

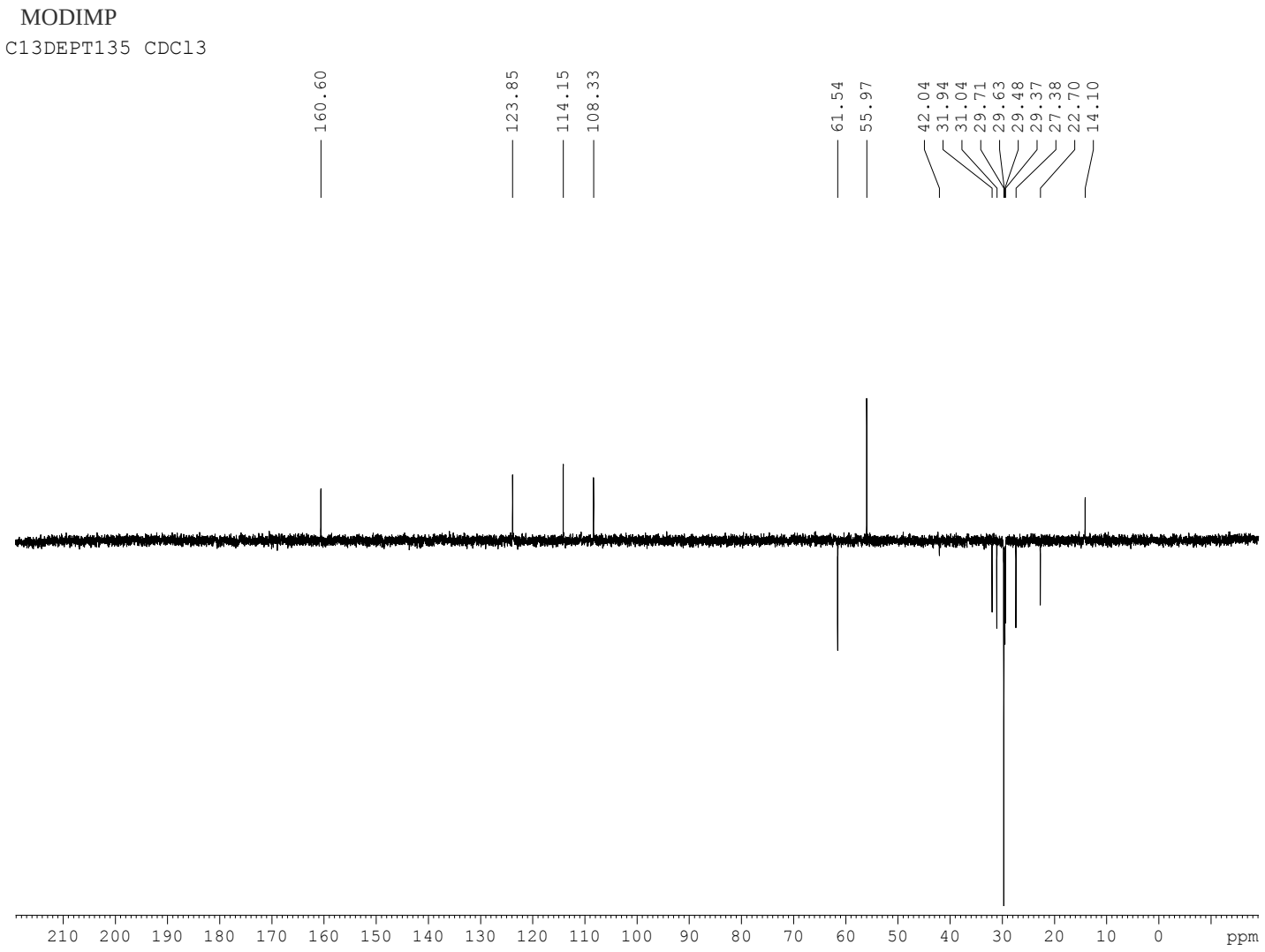

A10: DEPT NMR spectrum 2-methoxy-6-[(octadecylimino)methyl]phenol.

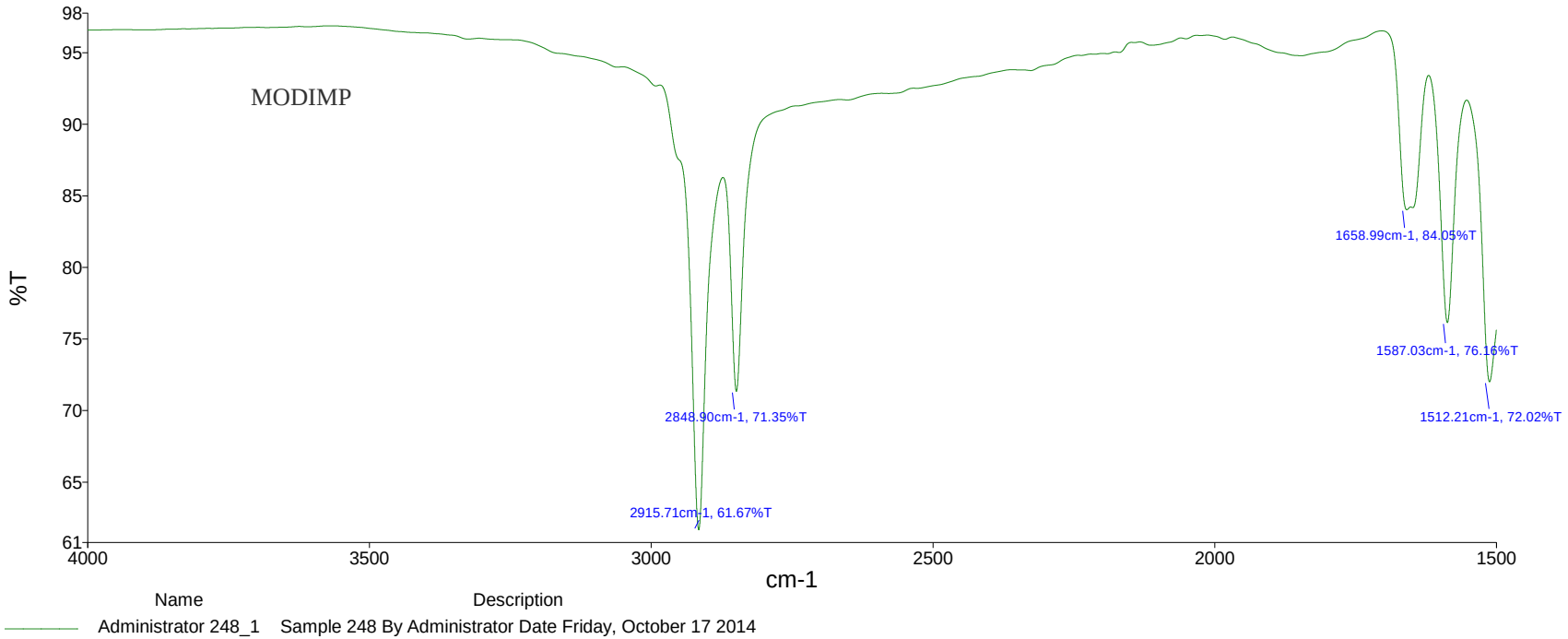

A11: IR spectrum of 2-methoxy-6-[(octadecylimino)methyl]phenol (MODIMP)